Geology of the loch Ailsh complex, Assynt

Ian Parsons

Abstract.

The Loch Ailsh intrusion, Assynt, was interpreted by Phemister (1926) as a stratified laccolite, the basal ultrabasic, intermediate, and upper leucocratic portions being differentiated at depth and intruded separately. The whole complex rested on a thrust plane.

The leuco-syenites are here divided into three intrusions, S1, S2 and S3. S3 is latest and roofs S1-2. Their contacts are sharp or gradational, when feldspars of S1-2 type are enclosed as xenocrysts in S3. Basic alkaline rocks form a discontinuous zone at the top of S2; calc-silicate rocks occur at the same horizon. Similar basic types grade into limestone xenoliths in the north of the intrusion.

A magnetometer survey showed anomalies corresponding to the outcrop of the ultrabasic rocks allowing their continuation to be traced. The magnetic properties of these rocks require that the induced component of the magnetization be used in interpretation of the anomalies. They are caused by a steeply inclined sheet. Further ultrabasic masses were proved by excavation.

Brief petrographic description of the rock types is made with modal data. Cell dimensions of pyroxenes from metamorphosed limestones and basic and ultrabasic types are identical. The mafic aggregates in the basic rocks represent the remains of material of metamorphic origin.

The alkali feldspars are described in terms of their appearance in thin section, optic axial angle, bulk composition and X-ray powder and single-crystal properties. They are low albite-microcline and low albite-orthoclase perthites in the compositional range Or_{27}-Or_{41}. Only S1 and S2 have monoclinic material in the potassium phase. There may be a systematic distribution of microcline obliquities with locality. Little modification of feldspars was found at contacts between syenites and xenocrysts preserve

higher temperature features than host material. Minimum crystallization temperatures are suggested. The variation depended on concentration of volatiles during cooling. A mechanism is suggested for the metastable preservation of orthoclase.

The ultrabasic rocks are a skarn between limestone and syenite. The basic alkaline rocks are hybrids of feldspathic magma contaminated by metamorphic material, and represent the remains of a roof to S2, disrupted by S3. The mass does not have a major thrust at its contacts and is a stock like body with stoping its mode of emplacement.

GEOLOGY OF THE LOCH AILSH COMPLEX, ASSYNT.

Ian Parsons, B.Sc.

Thesis submitted for the degree of Doctor of Philosophy in the University of Durham.

Hatfield College. Oct. 1963.

P. 161

Frontispiece:

General view of the area of the Loch Ailsh complex from the eastern shore of Loch Ailsh, looking north in early April. The snow-covered hills forming the skyline are, from the west, Conival, Ben More Assynt and Meall an Aonaich. The syenites extend to the base of the latter hill which is largely of Lewisian rocks.

The rocky hill in the left-hand middle distance is Black Rock. The dark overhang on its southern side is weathered in along a crush containing basic alkaline rocks, whilst the remainder of the hill is leuco-syenite. The undulating ridge with three clear summits is Sail an Ruathair, the most easterly summit being the melanite bearing syenite of the South Top.

The rough ground immediately behind the farmhouse is Durness limestone. The low cliff beneath the sheep exposes Moine rocks.

Preface and Acknowledgements.

This work was carried out in the years 1960-1963 under a D.S.I.R. Research Studentship. Five months were spent in the field, of which a month was devoted to making geophysical measurements.

Each chapter of this thesis is intended to be as coherent as possible on its own whilst avoiding undue repetition. Thus an individual table of contents and bibliography is presented with each chapter. The final chapter brings together the main conclusions of each aspect of the work.

The writer wishes to thank Prof. K.C. Dunham, F.R.S., for allowing him to use the facilities of the department and for his interest and encouragement during the work.

He would also especially like to thank Dr. C.H. Emeleus for his supervision of the work, for suggesting the project and for continual help and advice throughout the period of research;

Mr. R. Phillips for help during the X-ray work;

Dr. D. Hirst for assistance in the wet chemical analysis;

Dr. M.H.P. Bott for suggesting and helping throughout the geophysical work;

Dr. R.W. Girdler for supervision of the palaeo-magnetic work;

Mr. R. Stacey for the use of his computer programme and for assistance at all stages of the geophysical interpretation;

Mr. W.G. Hancock for help with the pyroxenes;

Messrs. P. Scott, A.R. Ramsden, G. Vago and A.A. Parsons who acted as assistants in the field geophysical survey;

Mr. P. Bradshaw, for finding the best limestone xenolith in the Black Rock Burn.

Mr. C. Chaplin and the technical staff of the Geology Dept. at Durham for preparing 340 thin sections and carrying out much of the photographic work in this thesis.

Miss J.I. Norcott for her rapid and accurate typing of the manuscript.

CONTENTS.

LIST OF ILLUSTRATIONS.

LIST OF TABLES.

Abstract.

The Loch Ailsh intrusion, Assynt, was interpreted by Phemister (1926) as a stratified laccolite, the basal ultrabasic, intermediate, and upper leucocratic portions being differentiated at depth and intruded separately. The whole complex rested on a thrust plane.

The leuco-syenites are here divided into three intrusions, S1, S2 and S3. S3 is latest and roofs S1-2. Their contacts are sharp or gradational, when feldspars of S1-2 type are enclosed as xenocrysts in S3. Basic alkaline rocks form a discontinuous zone at the top of S2; calc-silicate rocks occur at the same horizon. Similar basic types grade into limestone xenoliths in the north of the intrusion.

A magnetometer survey showed anomalies corresponding to the outcrop of the ultrabasic rocks allowing their continuation to be traced. The magnetic properties of these rocks require that the induced component of the magnetization be used in interpretation of the anomalies. They are caused by a steeply inclined sheet. Further ultrabasic masses were proved by excavation.

Brief petrographic description of the rock types is made with modal data. Cell dimensions of pyroxenes from metamorphosed limestones and basic and ultrabasic types are identical. The mafic aggregates in the basic rocks represent the remains of material of metamorphic origin.

The alkali feldspars are described in terms of their appearance in thin section, optic axial angle, bulk composition and X-ray powder and single-crystal properties. They are low albite-microcline and low albite-orthoclase perthites in the compositional range Or_{27}-Or_{41}. Only S1 and S2 have monoclinic material in the potassium phase. There may be a systematic distribution of microcline obliquities with locality. Little modification of feldspars was found at contacts between syenites and xenocrysts preserve

higher temperature features than host material. Minimum crystallization temperatures are suggested. The variation depended on concentration of volatiles during cooling. A mechanism is suggested for the metastable preservation of orthoclase.

The ultrabasic rocks are a skarn between limestone and syenite. The basic alkaline rocks are hybrids of feldspathic magma contaminated by metamorphic material, and represent the remains of a roof to S2, disrupted by S3. The mass does not have a major thrust at its contacts and is a stock like body with stoping its mode of emplacement.

CHAPTER 1.

INTRODUCTION.

Contents:

1) Location of area studied.

2) Previous work.

3) Summary of the structure of the mass according to Phemister (1926).

4) Relationship to the Assynt District.

5) Age of the intrusion.

1) Location of area studied.

The intrusion described in this study lies at the most easterly extension of the Assynt Culmination, near the top of the intricate pile of nappes revealed in that area, and immediately below the overthrust Moine series.

The area is included entirely by the square given by the National Grid coordinates NC 355118 - 355160 - 310160 - 310118. Names of localities are those used on the Ordnance Survey 6" : 1 mile sheets of the area.

For a general picture of the geology of the region the Geological Survey 1" : 1 mile sheet of the Assynt District is available, and a much simplified picture of the structural setting of the Loch Ailsh mass is given as fig. 1.1.

2) Previous work.

Igneous rocks in the eastern part of Assynt, north of Loch Ailsh, were recognized by Murchison (1860), who described them as syenite. In his section across the Assynt district he showed the igneous rock as being enclosed in limestone. Prior to 1926 only general descriptions had been made of the exposed rocks, by Peach, Horne and Teall (1907). Callaway (1883) traced the outcrop of the Loch Ailsh intrusion but considered it

Fig.I.I.

Simplified structural map of the Assynt culmination , to show the location of the major alkaline plutons, the area mapped in this study, and the major nature of the Ben More-Glencoul thrust plane as evidenced by the distribution of felsites of grorudite type. (Sabine, 1953). The map and section are from the Geological Survey I" sheet of the Assynt District.

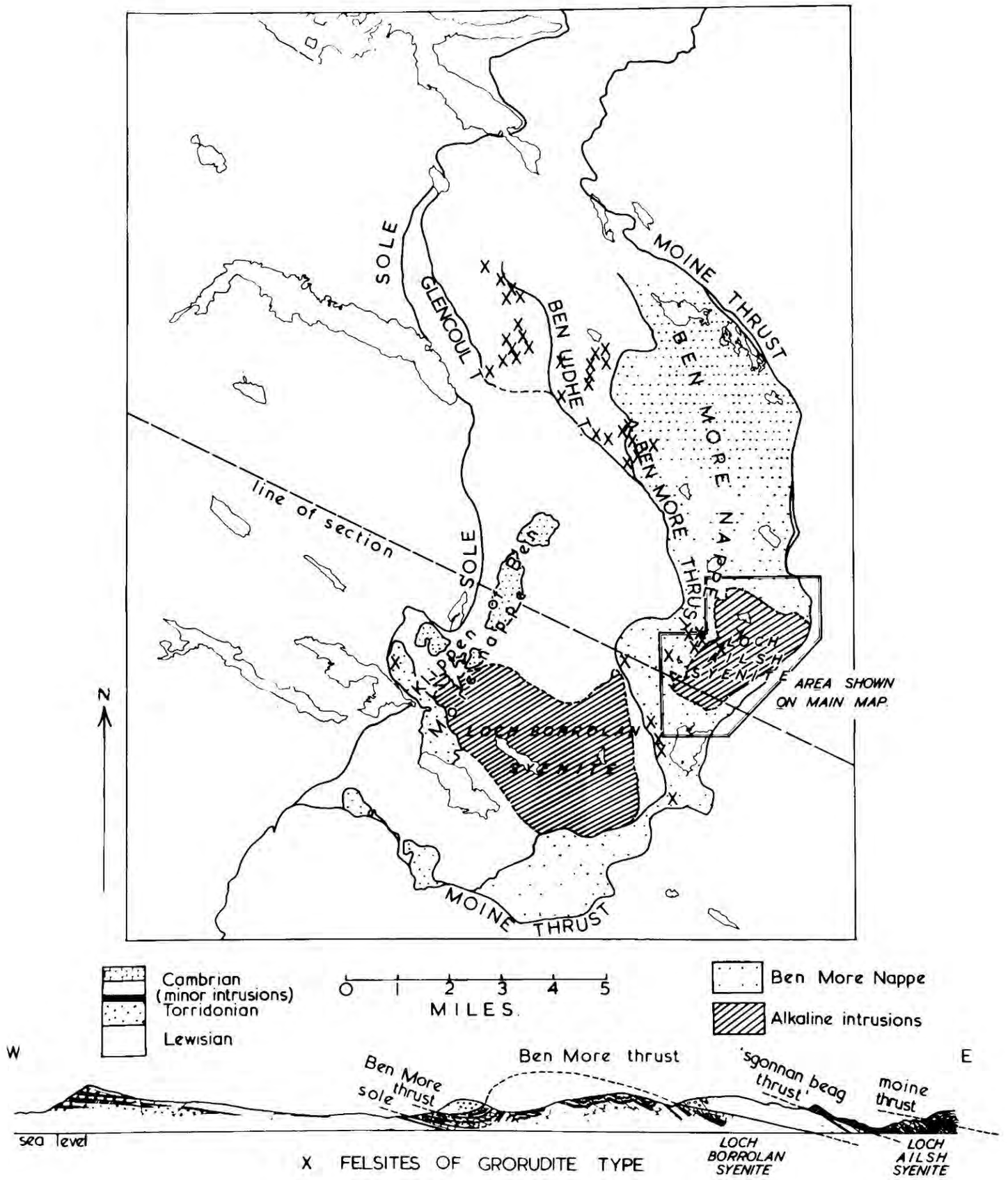
SOLE
GLENCOUL T
BEN UIDHE T
MOINE THRUST
BEN MORE NAPPE
BEN MORE THRUST
line of section
SOLE
Upper Limestone of Ben More
LOCH BORROLAN SYENITE
LOCH AILSH SYENITE
AREA SHOWN ON MAIN MAP
MOINE THRUST
N
Cambrian (minor intrusions)
Torridonian
Lewisian
0 1 2 3 4 5
MILES
Ben More Nappe
Alkaline intrusions
W
E
Ben More sole thrust
Ben More thrust
'sgonnan beag thrust'
moine thrust
sea level
LOCH BORROLAN SYENITE
LOCH AILSH SYENITE
X FELSITES OF GRORUDITE TYPE

continuous with the Loch Borralan mass from which it is now known to be separated by at least one mile and very probably by a major thrust plane. In 1926, however, Phemister published a map and a detailed petrological account of the Loch Ailsh syenite. This remains the only published source of detailed information on the intrusion, although comments on its field relations were made by Bailey (1935), and on its relationship to the minor intrusions of Assynt by Sabine (1953). A brief résumé of Phemister's main conclusions and of Bailey's comments will now be made.

3) Summary of the structure of the mass according to Phemister (1926).

Phemister followed previous workers (Peach and Horne) in that the intrusion was supposed to be carried forward on a plane of dislocation, which he called the Sgonnan Beag Thrust. The intrusion thus constituted a distinct nappe, between the Ben More nappe and the Moine rocks (fig. 1.1).

Within the mass itself he recognised a number of different rock types which are tabulated below (table 1.1) with the present writer's equivalents.

He considered that the intrusion had a laccolithic form, being stratified in the sequence given in table 1.1 (fig. 1.2). The aegirine-melanite-syenite occupied a pipe through which it was supposed the remainder of the intrusion had come. The base of the laccolite was in the Pipe-rock, the top in the Durness Limestone.

The layering did not, however, demonstrate gravitative differentiation in place, but was the result of separate phases of intrusion of already differentiated and progressively more leucocratic alkaline magmas, (op. cit. p.91). Since the differentiation had undoubtedly taken place at depth the hypothesis of assimilation of limestone to account for the alkaline nature of the rocks (as proposed by Shand (1910) for the

Table 1.1.

Rock types of Phemister (1926) and the present writer's equivalents.

Phemister (1926)	Equivalent	
Perthosite	S3	Leuco-syenites
Aegirine-Melanite Syenite	Melanite bearing S3	
Nordmarkite	S1 and S2	
Pulaskite		
Riebeckite syenite		
Basic Pulaskites	Intermediate and basic alkaline types (Hybrids)	
Shonkinites		
Hybrid Rocks		
Biotite-pyroxenite	Ultrabasics of Cathair Bhàn type. (Skarn rocks).	
Hornblendite		

Fig.I.2.

Sections of the Loch Ailsh mass as postulated by Phemister, (1926).

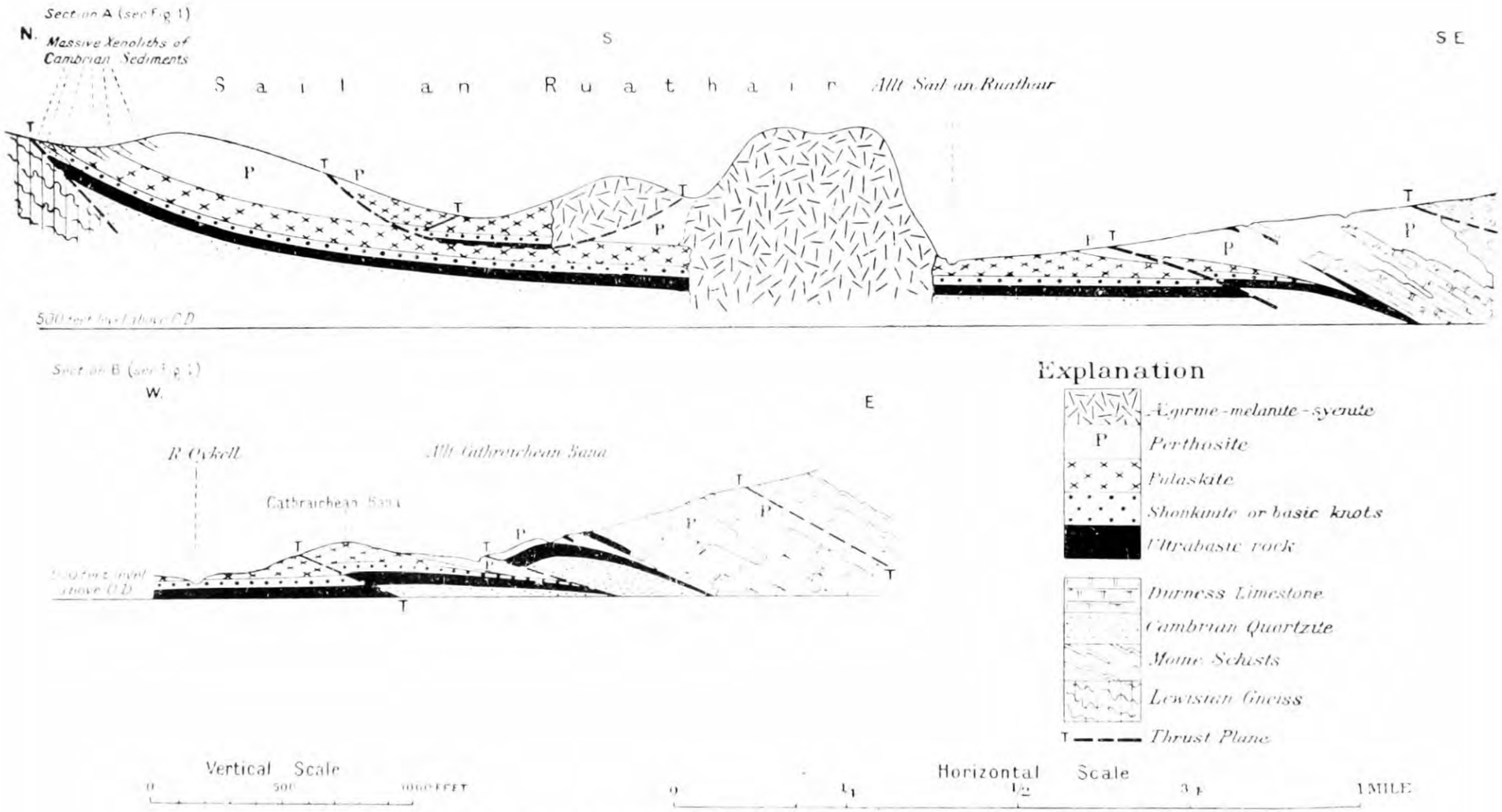

FIG. 2. —*Diagrammatic Sections to illustrate the Structure of the Loch Ailsh Mass.*

Section A.— *Vertical section along the line* AA *on sketch-map p.* 23.
Section B.— *Vertical section along the line* BB *on sketch-map p.* 23.

neighbouring Loch Borralan intrusion) was considered untenable.

Phemister noted the existence of numerous xenoliths of Cambrian sediments and observed that at certain localities abnormal types of contaminated syenite and modified sediment were produced, often very similar to the ultrabasic and "shonkinitic" rocks observed at other localities. He discounted the possibility that all of these latter rocks were hybrids formed by contamination of syenite by sediment, or that the ultrabasic rocks were altered sediments, on the grounds that the intruded sheet was not thick enough to produce the necessary volume of derivatives. He further believed that he could recognise differences between rocks which had sedimentary associations, and the normal basic rocks of the intrusion.

The main syenites were broadly divided into two groups on the basis of obvious field differences, and the more mafic types were then subdivided on the basis of the nature of the chief mafic constituent and the presence or absence of quartz, into pulaskite (quartz poor or quartz free alkali-feldspar rich rock with 3 to 30 per cent. of pyroxene or biotite), riebeckite-pulaskite, and nordmarkite (2 or more per cent. quartz). To the later, extremely feldspathic syenite he gave the name "perthosite". This rock graded into the aegirine-melanite-syenite, the youngest part of the intrusion.

4) Relationship to the Assynt District.

Bailey (1935) suggested a modification of the structural relationships proposed by Peach and Horne (1907) and accepted by Phemister (1926). Lugeon (in 1912, quoted by Bailey (1935)) had suggested that if the Sgonnan Beag thrust revealed the Loch Ailsh rocks through a window, it would be simply a reappearance of the Ben More thrust. No major dislocation would then separate the L. Ailsh and L. Borralan intrusions, which

could be one mass. Bailey, however, observed that, despite strong shearing at the margins, the syenite mapped across the whole of the Cambrian quartzite of the Ben More nappe with the outline of an intrusion.

The writer agrees with Bailey's notion that the intrusion can be regarded as being emplaced in the Ben More nappe. There are comparatively minor marginal dislocations, which, as will be demonstrated later, are not consistent with the existence of the Sgonnan Beag thrust as a major plane of movement.

5) Age of the intrusion.

Clearly the age of the intrusion is post-Cambrian and pre-Moine-thrusting. At L. Borralan evidence was found by Eskola (Bailey and McCallien, 1934), that the deformation and intrusion overlapped somewhat in time. This was in the form of unsheared pegmatite veins cutting sheared borolanite. Despite search for relationships of this type, no evidence has been found at L. Ailsh for intrusive activity younger than the thrusting.

Bibliography to Chapter 1.

BAILEY, E.B., 1935. 'The Glencoul Nappe and the Assynt culmination.' Geol. Mag. 72. pp. 151-165.

BAILEY, E.B. and McCALLIEN, W.J., 1934. Pre-Cambrian Association. Second excursion to Scotland. Geol. Mag. 71, pp. 549-557.

CALLAWAY, C., 1883. 'The Age of the Newer Gneissic Rocks of the Northern Highlands.' Quart. Journ. Geol. Soc. 34. p.409.

GEOLOGICAL SURVEY OF SCOTLAND. 1923, reprinted 1959. Special sheet for the Assynt District; parts of sheets 107, 108, 101, 102. 1" : 1 ml.

MURCHISON, R.I., 1860. 'Supplemental Observations on the Order of the Ancient Stratified Rocks of the North of Scotland and their associated Eruptive Rocks.' Quart. Journ. Geol. Soc., 16. pp.232-233.

PEACH, B.N., HORNE, J., TEALL, J.J.H., 1907 in 'The Geological Structure of the North-West Highlands of Scotland.' Mem. Geol. Surv., pp.435-437.

PHEMISTER, J., 1926. in 'The Geology of Strath Oykell and Lower Loch Shin.' Mem. Geol. Surv. Scotland. (Explanation of sheet 102).

SABINE, P.A., 1953. 'The petrography and geological significance of the post-Cambrian minor intrusions of Assynt and the adjoining districts of North-West Scotland.' Quart. Journ. Geol. Soc. 109, pp.137-171.

SHAND, S.J., 1910. 'On Borolanite and its Associates in Assynt.' Trans. Geol. Soc. Edin. 9 pt. 5, pp.202-216.

CHAPTER 2.

FIELD DATA.

Contents:

Introduction.

The data obtained by normal mapping methods could be considerably amplified by data obtained by geophysical means (Chapter 3), which, in turn, suggested reassessment of field data and worthwhile excavations.

The structure of the mass as a whole is suggested by consideration of ten critical areas where contacts or transitions between the rock types are exposed.

A geological map is given as Map 1, at the back of this thesis. The localities described in the following sections are named thereon.

1) North Top of Sail an Ruathair.

This area was chosen as a first example as it shows most clearly the relationships between two of the leucocratic syenites. The upper part of the Northern summit of the Sail an Ruathair spur consists of moderately coarse grained grey or brown feldspar rock, the 'perthosite' of Phemister (1926), which makes up the greater part of the exposed rock of the L. Ailsh mass. This will be known as S3. Occasionally at this locality small bright red feldspars can be discerned in the grey-brown feldspar matrix. At the base of the cliffs, and just above the top of the grassed-over scree (see photograph and explanatory sketch , Fig. 2.1) is a zone, usually not more than 3 m. in height, in which a coarse grained rock appears, with tabular red feldspars up to 5 cms. in length. Above, it is enclosed as xenoliths in S3, below, it is intimately veined by S3. This rock will be known as S1. (Pulaskite of Phemister (1926)). In this rock dark green mafics are usually obvious in hand specimen; in S3 they cannot normally be seen.

The line of contact can be traced through the gullies to the south of the North Top, on to the base of the cliffs below the 2nd Top of Sail an Ruathair. The contacts are always sharp, with no apparent chilling of S3. Crystals of S1 feldspars can be seen broken across. At locality 'D' (Fig. 2.4) rounded or somewhat angular S1 xenoliths can be seen (Fig. 2.2) from more than a metre across to small groups of a few crystals, and in some places (Fig. 2.3) individual red feldspar xenocrysts can be seen broken off and incorporated in the massive S3.

The S1 rocks are frequently quite strongly foliated. The dip of this igneous lamination is here generally steeply to the west, (Fig. 2.4). Often S3 veins appear simply to have dilated the S1 rock, the foliation

Fig.2.I.

Photograph and explanatory sketch showing the domal form of the S1-S3 contacts on the North and 2nd tops of Sail an Ruathair. View taken from the E.N.E. approx.

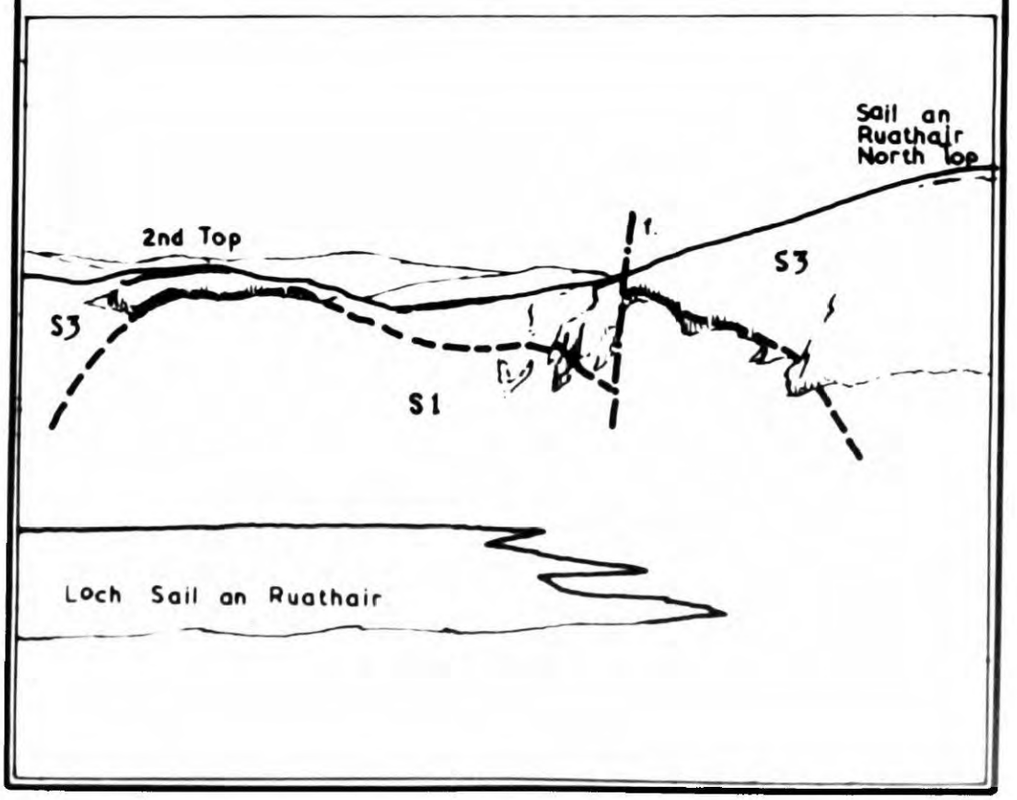
Sail an
Ruathair
North top
2nd Top
S3
S3
S1
Loch Sail an Ruathair

being conformable on both sides of the vein, (locality 'C', Fig. 2.4). When the proportion of S3 to S1 material increases S1 blocks can be shown to conform no longer to the prevailing dip (locality 'C', above previous position).

At locality 'A' (Fig. 2.4), on the 2nd Top, narrow (15 to 30 cms.) 6 m. long sheets of S1 are held in S3. The S1 feldspars are aligned parallel to the sides of these sheets. The S1 lamination in massive blocks below dips steeply to the west. A tendency for lenticular masses of S1 to form, or for xenoliths to wedge out at one end, is also seen on the North Top, (Fig. 2.3), but more equidimensional rounded blocks are also common (Fig. 2.2).

On the west side of the Sail an Ruathair ridge S1 outcrops over a limited area only, and is taken to represent a large xenolith removed from the main mass. Analogous masses are seen in the Metamorphic Burn and Cathair Bhan areas.

2) The 'Metamorphic Burn.'

This was the name given by Phemister (1926) to the largest of the streams feeding Loch Sail an Ruathair from the north. Since it represents an excellent locality for inspection of a range of contact metamorphic rocks, a sketch exposure map is shown (Fig. 2.5). This is simply a copy of a field sketch measured by pacing, and should not be regarded as accurate.

There are certain differences between Phemister's (1926, p.77) interpretation of this area and that of the present writer. In summary, the succession up the stream from the first exposures above the lower obscured area (where the stream flows through drift), can be described as follows:

Fig.2.2.

SI-S3 contact relationships, North Top, Sail an Ruathair. A rounded SI xenolith (the pale rock above the hammer head) is also cut by a fine S3 vein.

Fig.2.3.

SI/S3 contact relationships, North Top, Sail an Ruathair. Massiveveins of S3 (the dark, smooth textured rock to which the pencil is stuck) cutting SI. A thin wedge of SI is seen pinching out near the pencil point.

In detail (below) individual red SI feldspar xenocrysts can be seen being incorporated in the S3 matrix.

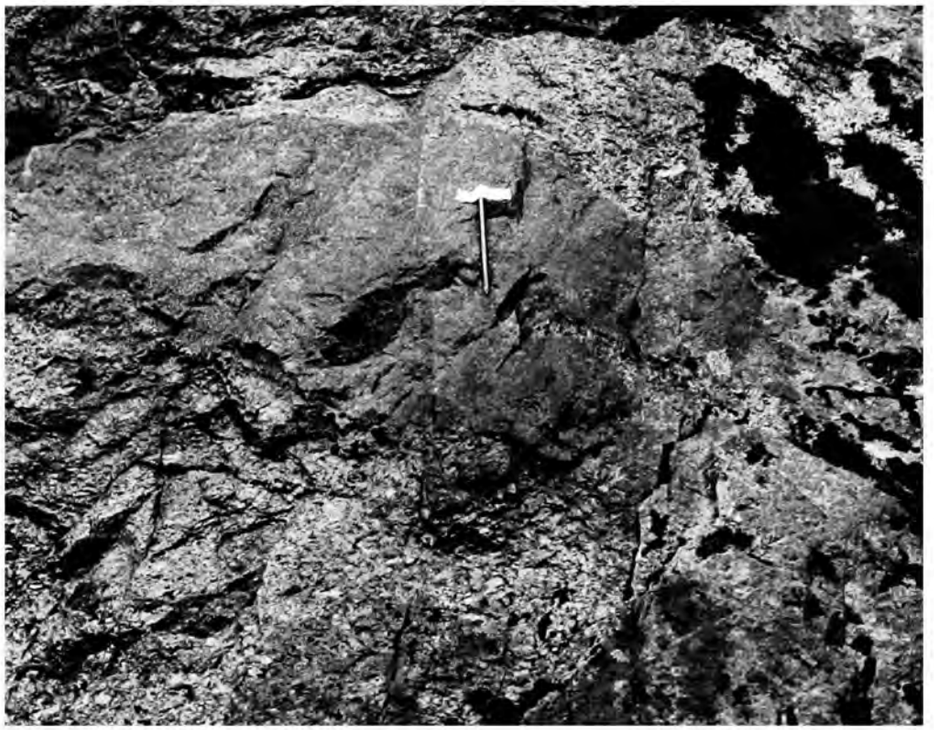


Transition zone

Fig .2.4.

Map of Coire Sail an Ruathair to show localities mentioned in text, dip of lamination of SI, and the area considered in the section on the Metamorphic Burn.

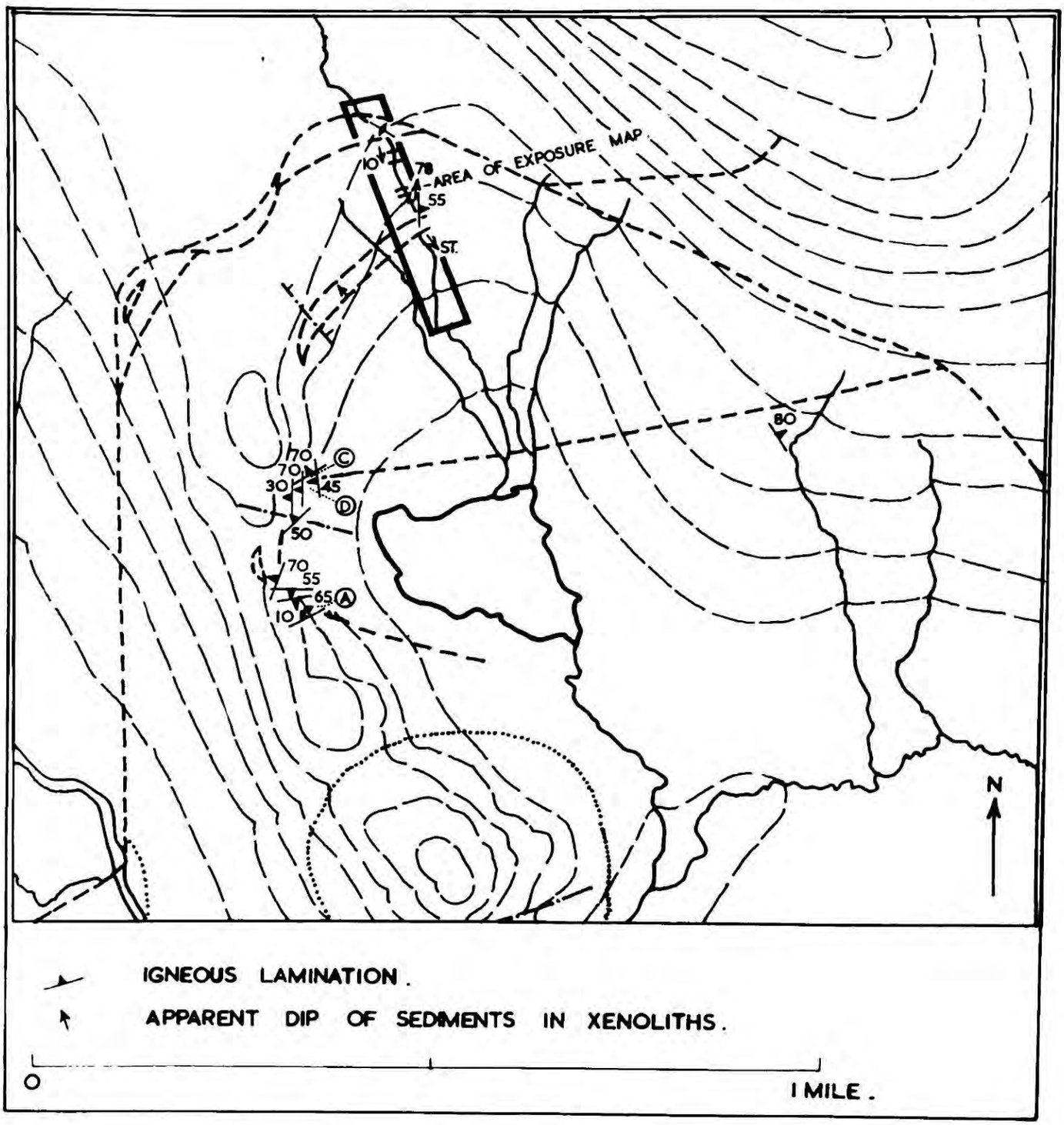
AREA OF EXPOSURE MAP
10
70
55
ST.
80
70
70
30
45
C
D
50
70
55
65
A
10
N
IGNEOUS LAMINATION.
APPARENT DIP OF SEDIMENTS IN XENOLITHS.
O
1 MILE.

a) S3, with sparse red feldspars in an otherwise grey or brown medium grained feldspar matrix, with numerous lenses of micaceous or pyroxenic rock clearly representing metamorphosed Durness Limestone.
(Specimens 200-215). 0 - 180 yards.

b) Large mass of limestone with apparent dip downstream, in contact with a pale white feldspathic rock with obvious small black grains of melanite.
(Spec. 216, 462). 180 - 182 yards.

On the west side of the stream normal brown S3 with included red feldspars is seen. This extends a little above the melanite-syenite exposure.
(Spec. 218). 190 yards.

c) S3 is seen in sharp contact with a coarse red feldspathic rock identical in hand specimen to the S1 of the North Top of Sail an Ruathair. This type (S1) continues for about 35 yards.
(Spec. 219, 229, 230, 237, 238). 190 - 225 yards.

d) S1 gives way sharply to a foliated more mafic type. The vertical contact runs parallel to the sides of the stream, in the middle of the stream, for a short distance. The foliation of the mafic minerals dips 55° E. Occasionally clots of dark minerals may be seen. This rock is very similar to the basic rocks outcropping in the River Oykel and Black Rock Burn areas. It is presumed to correspond with the lower of Phemister's "shonkinites."
(Spec. 231-235). 225 - 230 yards.

e) Brown S3 with coarse red crystals included at intervals, occasional basic patches and Limestone xenoliths.
(Spec. 236, 239-243). 230 - 275 yards.

Fig.2.5.

Sketch exposure map of the Metamorphic Burn. Specimen localities are shown with numbers as given in the text.

SKETCH EXPOSURE MAP OF THE METAMORPHIC BURN

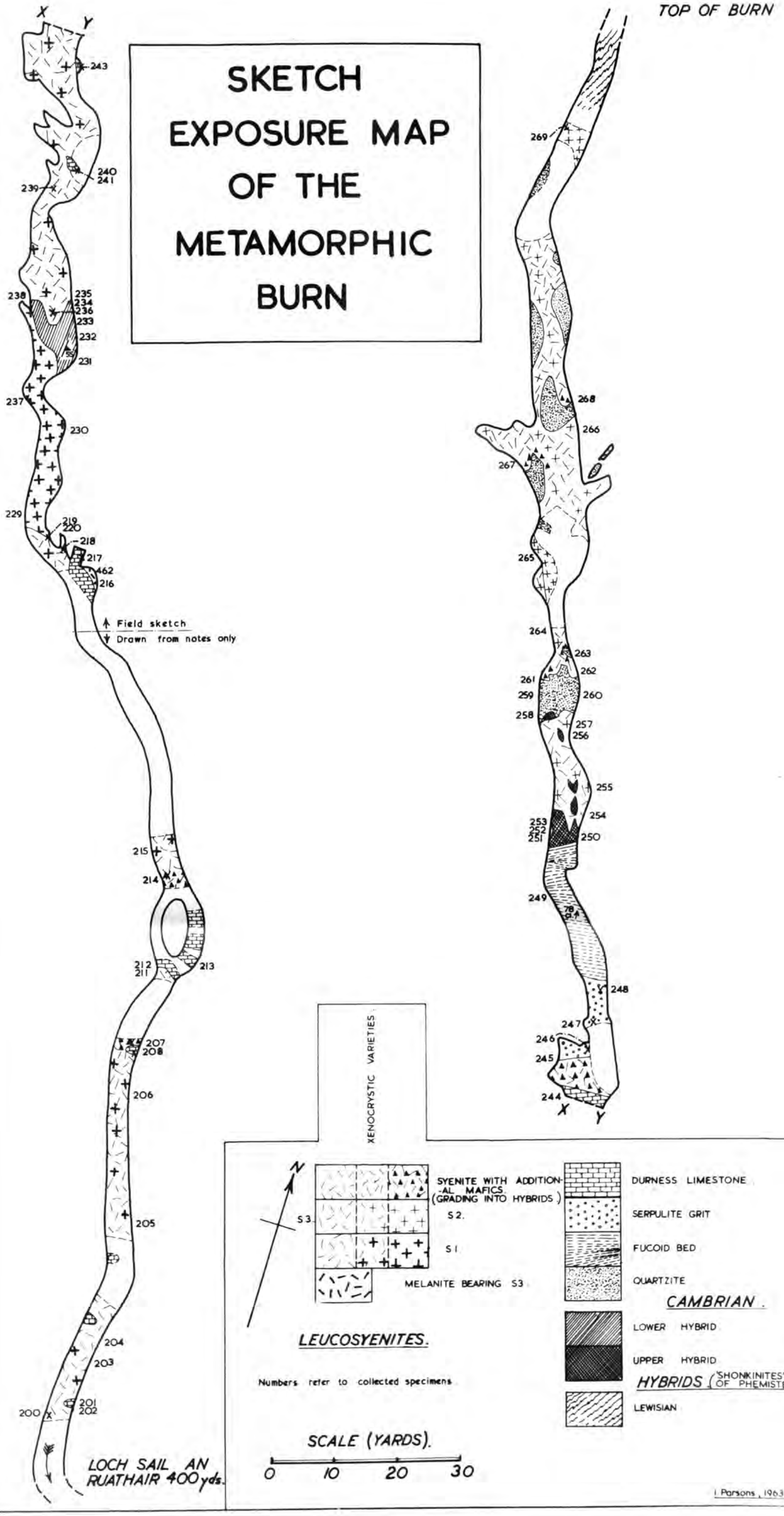

f) Limestone xenoliths, in contact with fine flinty dark green rock, with conspicuous pink feldspars and mafics (3 yards), in contact upstream, with hard white or dark grey quartzite. This is supposed to represent the Serpulite Grit, by comparison to this horizon exposed in the River Oykel a little south of its confluence with the Black Rock Burn.

(Spec. 244-248). 275 - 295 yards.
(Grit occupies 13 yards).

g) Hard baked fine grained cleaved shaley rock, with black streaks. The cleavage dips upstream. This rock is clearly part of the Fucoid Bed (Spec. 249). The fine grey rock continues for some 20 yards, when it gives way to dark green pyroxenite (Spec. 250-253) and micaceous xenoliths (255) of a type similar to those produced from the Durness Limestone lower down the stream. Further smaller basic xenoliths (256) are enclosed in grey S3 with occasional conspicuous red feldspars enclosed. A further basic type (258) rims the exposures above. In terms of distance from the base of the burn this group appears to correspond to the upper "shonkinite" of Phemister, but he does not mention the coarse pyroxenite or micaceous material (which is identical to types produced downstream at the horizon of Durness Limestone) which are associated with the fine grained types.

(Spec. 250-258). 295 - 335 yards.

h) Splintery white or glassy green quartzite (5 yards) gives way to fine grained dark green syenite with occasional conspicuous pink feldspars. This type borders numerous massive quartzite xenoliths which occur above this point. ("Syenite with additional mafics", on fig. 2.5). Otherwise the syenite is pale grey S3 with conspicuous red feldspars

included, their long axes aligned in places (near specimen 268). (Spec. 261-268). 335 - 407 yards.

i) At the 357 yard point (Spec. 265) blocks of a bright red variety of syenite are enclosed in S3. Although similar to S1 in appearance, it is called S2 on petrographic grounds.

j) The last solid rock seen is a red S2 type, with obvious dark blue riebeckite (Spec. 269). Above this point is obscured, but there are many boulders of Lewisian gneiss and a contact (of unknown type) with this rock is presumed to be close.

420 yards.

The syenite in the Burn is thus believed to be mainly S3, earlier generations only occurring over limited extents as massive rock. The Cambrian succession is straight-forward. Making allowance for apparent downstream dip the relative thickness of the various horizons is of comparable order to those given in the stratigraphical column appended to the 1" Geological map of Assynt (Geol. Surv. Scotland, 1923).

The writer cannot see the repetition of sequence by thrusting or apparent reversal of Fucoid Bed and Serpulite Grit as described by Phemister (1926). Furthermore leucocratic syenite with quartzite inclusions is the last ("lowest") rock seen and it appears to continue up the burn a greater distance than was believed, by Phemister. Discussion of the status of his "shonkinitic" types and the detailed structure of this part of the mass will be made after the petrography of the rocks has been considered. They are referred to as "hybrids" on the exposure map.

3) Northern Margin of the Mass.

At various localities along the northern and north-eastern sides of Coire Sail an Ruathair, S3 rocks, sometimes crushed, enclose calc-silicate xenoliths of types similar to those in the lower part of the Metamorphic Burn. In the stream E of the Metamorphic Burn feldspar-pyroxene rocks similar to the hybrid types of the latter locality are found in close association with metamorphosed Durness Limestone.

4) Sròn Sgàile.

A series of specimens were taken from base to top of this enigmatic mass. About halfway up the broken S. facing cliff there is a zone in which the rock has a pronounced roughly horizontal banding, (Fig. 2.6). This does not especially correspond to the change from very basic to less basic types, because mixed basic and more leucocratic types extend above and below this zone (see Chapter 3, section 4). The thin sections of rocks from this banded zone show obvious evidence of cataclasis, and it appears that the banding is nothing more than a cleavage induced by thrusting which happens to be developed in part of the basic-intermediate transition zone on this hill.

Beautiful net veining by narrow white and pink feldspathic veins, which contain dark minerals visible in hand specimen, is well seen at numerous horizons (Fig. 2.6).

The writer can see no evidence for the multiplicity of thrusts supposed previously to surround the Sron Sgaile rocks.

5) Central area, around the confluence of the River Oykel and Allt Sail an Ruathair.

The area considered here is that part of the mass ¼ mile downstream from the waterfall in the River Oykel (the first waterfall above Loch Ailsh) to about ½ mile upstream in the Oykel and Allt Sail an Ruathair,

Fig 2.6.ABOVE

Photograph to show the "banded" zone on the S. face of Srôn Sgàile.

Fig 2.6. BELOW

Intricate net veining of Srôn Sgàile basic rocks by feldspathic veins. Unlike other feldspathic veins in basic rocks of the mass, they contain conspicuous dark minerals which may be seen in the photograph.

above the confluence of these two streams.

In this area a transition is seen between a coarse pink feldspathic syenite (called by the writer S2, the nordmarkites and pulaskites of Chemister, 1926) and grey-brown feldspathic S3 rocks identical to those described in the Coire Sail an Ruathair area. In addition a complex relationship between these two rock types and basic types is seen.

A traverse up the Oykel, from the 'S' bend N.W. of the south end of Cathair Bhàn shows the following sequence:

On the track above the E. bank of the river grey and pink syenite in a crushed condition is seen. In the river, at the northern limb of the bend, basic masses are enclosed in pale grey syenite with included pink feldspars. These basic masses continue upstream, become the predominant rock type near the waterfall, and then become progressively less abundant, the last representative being seen about 120 yards below the Oykel-Allt Sail an Ruathair confluence (Fig. 2.7(C)). The best exposures are around the waterfall and immediately upstream. Between this point and the bend lower down the stream, the basic rocks are veined by medium grained pale grey syenite. On the E. bank, 50 yards below the waterfall, a small eastward-dipping thrust carries pink, coarse syenite over the grey syenite with basic inclusions.

At the waterfall it is more correct to describe the basic rocks as being veined by leuco-syenite (Fig. 2.8 above). Northwards the basic types become xenolithic in leuco-syenite. The veining of the basic types is intricate, broad and narrow pale net veining dissecting the dark green basic rocks, and weathering out to stand above the basic material, (Fig. 2.8 below).

Diagram 2.7(B) shows the detailed relationships within a typical

Fig.2.7.

A: Form of massive basic inclusions in leuco-syenite . (Locality A, map C.) This shows a vertical cliff section on the E. bank of the river.

B: Detail of the mode of enclosure and veining (two generations) of a basic xenolith with ultrabasic clots. (Locality B, map C.)

C: General map of area around the Oykel falls, to show general zones exposed .

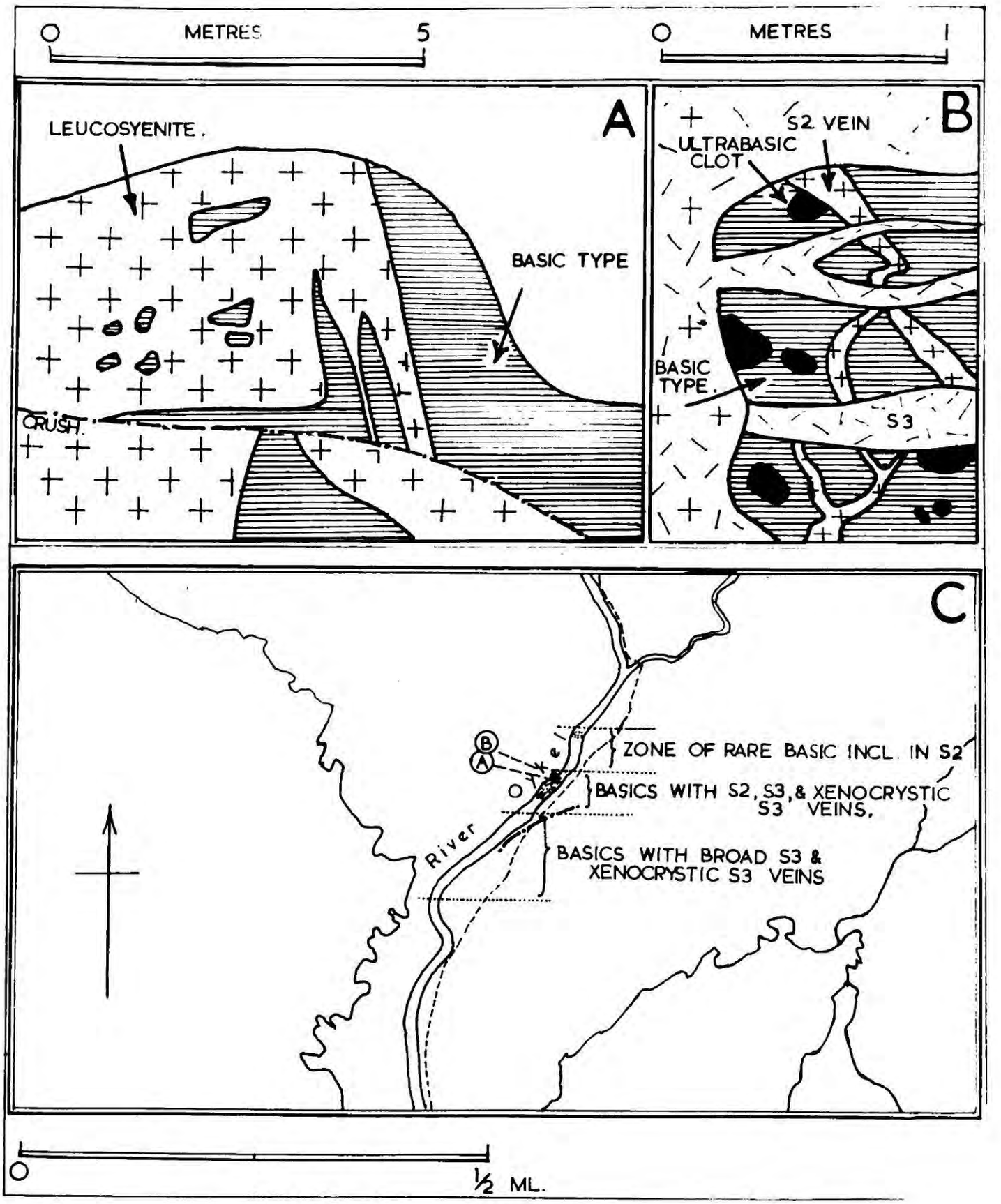
METRES 5
METRES 1
A
LEUCOSYENITE.
BASIC TYPE
CRUSH.
B
S2 VEIN
ULTRABASIC CLOT
BASIC TYPE.
S3
C
ZONE OF RARE BASIC INCL. IN S2
BASICS WITH S2, S3, & XENOCRYSTIC S3 VEINS.
BASICS WITH BROAD S3 & XENOCRYSTIC S3 VEINS
River
½ ML.

Fig.2.8.ABOVE.

Massive basic rocks veined by broad and fine feldspathic veins. (Out weathering). Falls, R. Oykel.

Fig.2.8. BELOW.

Detail of net veining.

Fig.2.9.

Detail of basic xenoliths to show feldspathic veining and ultramafic inclusions which sometimes show sharp margins to the normal basic material and to the enclosing leuco-syenite (above), or, in some cases grading into the basic material (below).

Both from the falls, R.Oykel.

basic xenolith in sketch form. Photographs of the variable basic xenoliths appear as Fig. 2.9. The most abundant basic rock has a pale white or pink feldspathic matrix with conspicuous patches of pyroxene and mica. Interspersed throughout the basic types are dark green ultrabasic patches in which little or no feldspar is visible. As demonstrated in Fig. 2.9 these may abut directly on the later leuco-syenite; they form neither rims nor cores to the basic rocks, but are distributed apparently randomly through it. They offer either sharp or gradational contacts to the enclosing basic types.

Intricately veining the basic masses are at least two generations of veins. The earlier are red in colour and are cut by both the later grey or brown generation of veins, and the massive enclosing leuco-syenite. It seems reasonable to suppose that the two generations of veining correspond to S1/S2 and S3 respectively.

In the area around the falls the basic rocks are massive and veined by sometimes broad sheets of syenite. South of the falls the syenite is predominantly a pale grey type, i.e. S3. At the falls a grey or brown feldspathic matrix encloses large pink feldspars and sometimes coherent blocks of a pink rock. This will be called S2. A little below the Oykel-Allt Sail an Ruathair confluence the leuco-syenite is entirely of this pink variety (S2). All gradations between the two types seem to be present, gradual increase in the number of pink S2 feldspars leading to a rock in which only a small amount of S3 material is present. By analogy with the exposures on the North Top of Sail an Ruathair the relationship is believed to be one in which the later invading S3 encloses S2 material as xenocrysts; at the latter exposures the xenocrystic relationship can be seen developing but the invasion and break-up of the

earlier material by S3 has not proceeded so far as in the central area.

Sometimes the xenocrysts have their long axes aligned parallel to the sides of veins. In the centre of the waterfall xenocrysts can be seen concentrated in embayments at the edge of a basic xenolith.

Upstream from the junction of the two rivers coarse red rocks of S2 type continue for about ½ mile. They are also exposed in the low ground between the two rivers, but on the valley sides, towards Black Rock and the head-waters of the Allt Cathair Bhàn, brown S3 is exposed. In the low undulating ground E. of Black Rock it is possible to map a zone of S3 with included red feldspars and masses of S2, above the S2 exposures in the river. These xenolithic masses are often elongate in form, but an attempt to map the directions of their long axes did not show any consistent pattern. The two types are also difficult to distinguish on the lichen-covered surfaces in this area. On the summit of the low ridge between the Allt Sail an Ruathair and the upper branch of the Allt Cathair Bhan, however, contrasting dark red S2 held as large veined masses in pale brown S3 is well seen.

The northern margin of S2 in the two rivers does not yield such a clear picture of the contact relationships, but a gradational contact, S2 being veined by and incorporated in S3, may be demonstrated.

6) Black Rock Burn.

This stream demonstrates similar relations between S2 and S3 and basic rocks as does the area around the falls in the Oykel. Basic masses occur at various localities up the stream where it falls most steeply down from the edge of Coire na Mang into the Oykel valley. Basic types with intricate feldspathic veining like the types exposed in the Oykel are seen (Fig. 2.10 above). Near the top some varieties occur

Fig.2.IO. ABOVE.

Intricate net veining of massive basic xenolith, Black Rock Burn.

Fig.2IO. BELOW.

Rusty coloured, in-weathering baked siliceous limestone xenolith, Black Rock Burn. The creamy colour of a fresh surface may be seen on the left of the photograph.

with rather more irregular basic patches and streaky feldspathic areas.

An important discovery at three localities (marked 'λ' on the main map) was of specimens which have clear affinities with metamorphosed limestone. At the two lower localities the xenoliths consist of soft, pale green powdery feeling rocks. The upper specimens are found as rusty weathering inclusions in the leuco-syenite, which on breaking open have hard, but clearly carbonate bearing creamy white interiors (Fig. 2.10 below). There are occasional siliceous bands visible, and also lenses of dark mica. There can be no doubt whatever that this xenolith is of a baked siliceous limestone.

The existence of these types, at the same horizon as the basic alkaline types, in the Black Rock Burn, an association observed in the Metamorphic Burn area and the streams on the north side of Coire Sail an Ruathair, has an important bearing on the revised picture of the structural relationships and origin of these basic rocks.

The enclosing leuco-syenite of the burn again illustrates a transition from grey and brown S3 to a red type grouped with S2. The leuco-syenite at the base of the steeper part of the stream is pale grey S3. Red feldspars are seen rarely, but, 30 yards above the base of the slope, bright red masses of S2 appear in the S3 material. The S3 in places becomes crowded with the red feldspars which are believed to be xenocrysts from S2. (This idea was also put forward by Phemister, 1926, p.79). A little above the lowest S2 xenolith the lowest basic xenolith appears. From this point on the massive leuco-syenite is progressively of red S2 type. For a considerable distance S2 is seen veined by S2. The veins are typically about 5 cm. across and cut off angular or slightly rounded masses of S2 usually a few feet in length. For some distance (near the

middle locality marked 'λ' on the map) the veins show preferred directions, either vertical or dipping at 20° upstream. Near the top of the stream S3 material becomes less frequent and the last exposures seen are of S2, which, although deep red in colour, is not so characteristically coarse-grained as below.

The writer's observations in the Black Rock Burn area thus suggest that much more S2 material is present than was believed by Phemister (1926). S2, rather than occurring rarely as blocks, makes up most of the exposed rock of the burn, and is presumed to continue to the edge of the mass.

7) Black Rock.

The greater part of this well exposed hill is made up of strikingly homogeneous even-textured pale brown S3. Very occasionally patches with numbers of red feldspars in a loose group are seen. In the flat area at the foot of Black Rock elongate veins of S3 material with included red phenocrysts are sometimes seen cutting the normal S3. These have coarsely crystalline rims, the matrix feldspars apparently growing inwards from the edge of the body, and they would seem to represent a late phase of S3 injection which had acquired S2 xenocrysts en route to its present level.

Also seen in this area are narrow (± 1 cm.) veinlets consisting of dark green coarsely crystalline pyroxene. The veins are really a succession of individual large pyroxene crystals, not necessarily in contact. They can be traced as dark lines, sometimes gently curving, over distances of at least 20 yards in some cases, although they often die out. A photograph of an entire thin section across a narrow example of one of these veins is given as Fig. 2.11 (above).

Fig.2.II. ABOVE.

Photograph of an entire thin section of a pyroxene veinlet from the base of the Black Rock.(Presented as a negative; the pyroxene appears white. Ord. Light, X5.)

Fig. 2. II. BELOW.

Crushed basic rocks beneath the conspicuous overhang on the S.W. side of Black Rock. The cross-cutting pinched out band passing justbelow the hammer head is a leuco-syenite vein which has beeh deformed but has not lost its coherency.

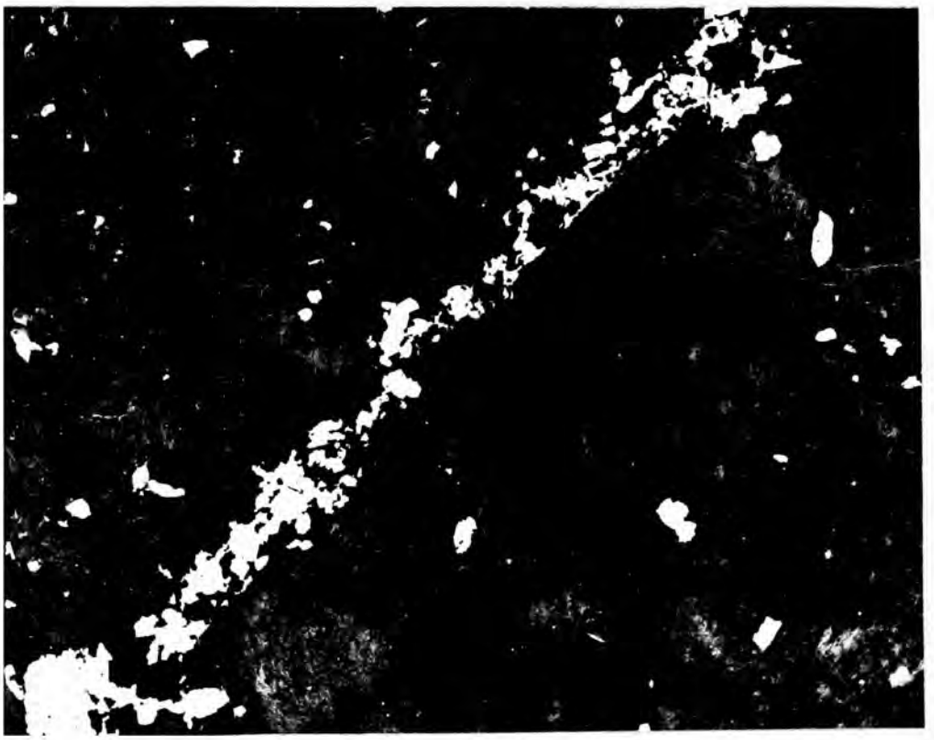

On the western side of Black Rock, a little below the summit, red S2 rocks are seen in contact with S3, with a similar veining relationship as is seen in the Black Rock Burn. This contact, which is dipping steeply to the E., can be traced around the line of crags forming the western edge of Black Rock. It is well exposed above the conspicuous overhang at the base of the south-west corner of Black Rock. East of this point it dips beneath the grassed over slopes of Black Rock, and strikes exactly towards its reappearance at the base of the Black Rock Burn.

The striking overhang beneath the south-west corner of Black Rock is weathered in along a crush belt. In the crush and immediately below are found basic rocks similar to those of the Black Rock Burn. They are veined by leuco-syenite, the veins being drawn out but nevertheless maintaining their coherency across the crush zone. This suggests that the magnitude of the displacement along this shear zone may be quite small, despite the quite broad band of crushed rock involved (Fig. 2.11, below). The S2 slightly above is veined by S3, and the zone of S3 alone is less than 10' above the basic rocks.

8) Sgonnan Beag.

This area is the only one in which syenite is actually seen in contact with country rock which is massive rather than as xenoliths. At the base of the cliffs forming the southern rim of Coire na Mang pink syenite is seen in contact with white quartzite. Between them is an extensive band of fine grained deep red mylonite, with a brittle fracture, the grain size of the normal leucosyenite being rather coarse above. This contact, however, clearly dips to the south-west. Further down the slopes of Sgonnan Beag, in the "Perthite Burn" (see map) a crush belt can

be traced in the syenite. This too dips to the south-west. The south-western margin of the intrusion is thus pushed over the main mass by a thrust (or perhaps reverse fault, as the plane of movement is steep), but there is no evidence pointing to the whole syenite mass being moved over the Cambrian quartzite by a major thrust. (The "Sgonnan Beag" thrust, of Phemister and predecessors).

At the extreme highest end of the crushed syenite exposed on the edge of Coire na Mang, (at about 1450'), a small (25 cms. in size) mass of quartzite was found enclosed in the mylonite. This had maintained its coherency but nevertheless proved, in thin section, to show evidence of recrystallization following shearing. It is possible that this represents a quartzite xenolith,in which case the syenite at the base of the lower end of the Coire na Mang crags (at about 900') could bear an intrusive relationship to the quartzite a little above.

9) Cathair Bhàn.

(Allt Cathraichean Bàna).

Most of the data on this poorly exposed area was obtained by geophysical means. The suggestion of Phemister (1926) was that a sheet of ultrabasic rocks lies beneath leucosyenite and that leucosyenite occurs between the ultrabasic rocks and the Durness limestone to the south-east. The geophysical data show this hypothesis to be untenable, so that a reassessment of the exposures considered critical by Phemister was made.

The lower of these is at the sharp bend in the Allt Cathair Bhàn 700 yards from its junction with the River Oykel. Here leucosyenite is supposed to be seen overlying ultrabasics. A small excavation to the west of the top of the exposure showed that all the

leucocratic material at this locality occurs as veins. One of these happens to be cut obliquely by the surface topography, and gives the impression of representing massive leuco-syenite. Detail of this locality is shown in Fig. 2.12.

In the upper branch of the Allt Cathair Bhàn, where the stream turns to the east, leuco-syenite forms a waterfall and appears to overlie ultrabasics. Above, ultrabasics are again seen. The magnetic anomaly suggests that this too is a minor sheet of leuco-syenite in the ultrabasic rock (see Chapter 3).

At no locality has massive syenite been seen between the Allt Cathair Bhan and the Durness Limestone to the east. An excavation in the ground between the exposed limestone and the Allt Cathair Bhan, at a point south-east of the southern end of the Cathair Bhan ridge, revealed many angular fragments of pale green calc-silicate rocks, apparently a buried scree. A belt of normally contact metamorphosed Durness limestone thus extends parallel to the dark blue ultrabasic exposures in the Allt Cathair Bhàn. One of these specimens contained a fine grained feldspathic vein, indicating that apophyses of the syenite extend beyond the ultrabasic exposures and invade normally metamorphosed limestones comparable to those of the Metamorphic Burn. At Kinlochailsh similar contact metamorphosed limestones can be seen, and marbling extends for some distance into the massive limestone.

The ultrabasic rocks are much veined by pink feldspathic material, and there is a certain amount of shearing visible at some localities. Both ultrabasics and leuco-syenite are sheared, although the veins maintain continuity. At the base of the south end of Cathair Bhàn intermediate basic types are seen veined by leuco-syenite in a similar

Fig.2.I2.

Diagram illustrating the veining of ultrabasics by leucosyenite in the Allt Cathair Bhân, 700 yards from its junction with the R. Oykel.

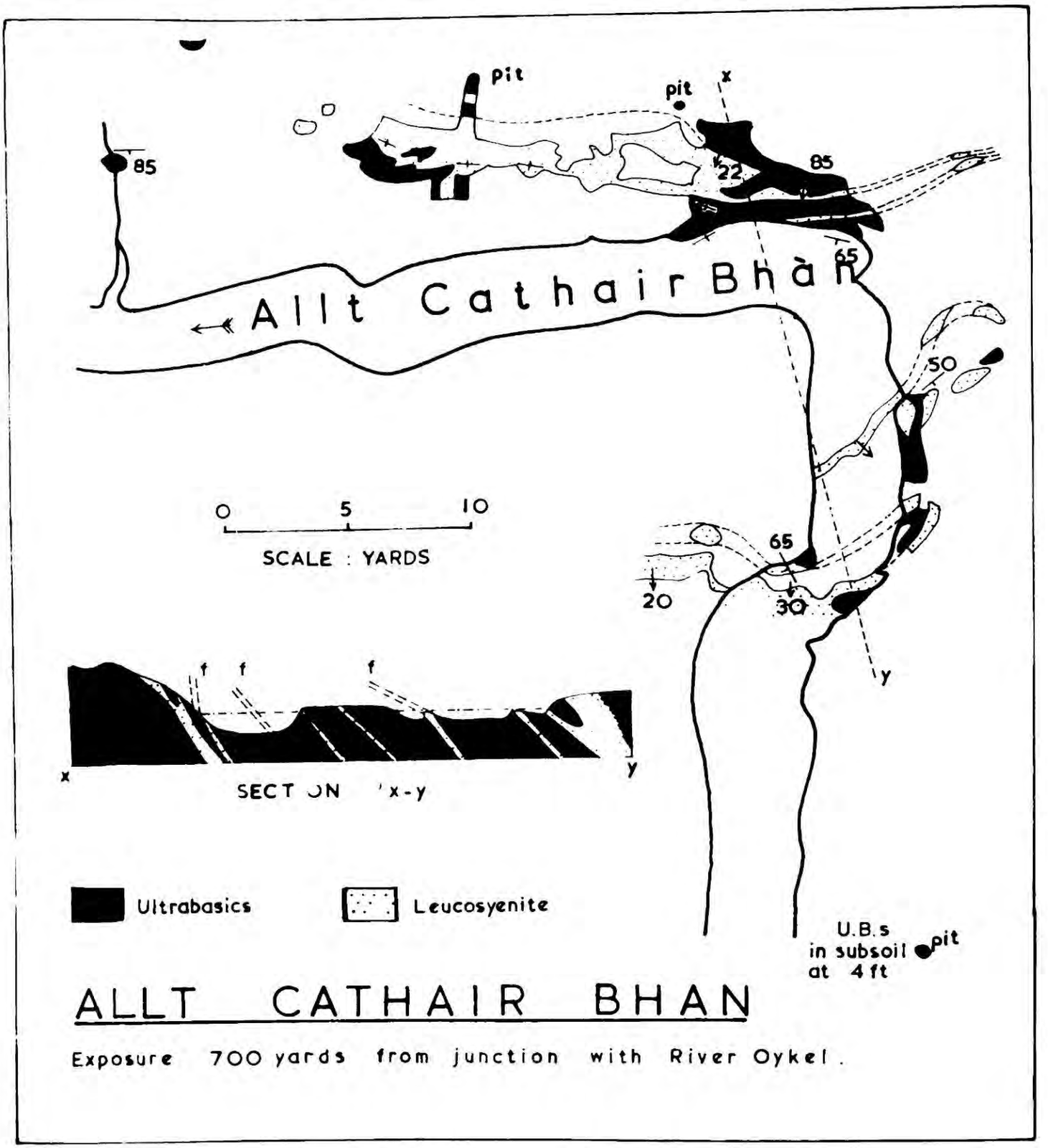

ALLT CATHAIR BHAN

Exposure 700 yards from junction with River Oykel.

relationship to their counterparts in the Oykel and Black Rock Burn areas. These lie between the ultrabasic rocks and the massive leuco-syenites.

10) South Top of Sail an Ruathair.

The entire mass of this hill consists of a melanite bearing variety of a rock otherwise indistinguishable from S3. The melanite is usually visible in hand specimen as dark brown equidimensional grains, usually not more than 2 mm. in size. If the amount is small, however, it is not easy to detect. Thus the nature of the transition between melanite bearing S3 and normal S3 between the South and 3rd Tops of Sail an Ruathair is uncertain. It appears to be lateral and continuous, although the disappearance of melanite takes place over a short distance.

At the southern base of the South Top the S3 contains both melanite and S2 xenocrysts, and it can thus be shown on the map (Map 1) intersecting the xenocrystic zone. Specimens for a short length of the Allt Sail an Ruathair also contain melanite, so that the melanite syenite can be shown extending a little further to the east than on the map of Phemister (1926).

Summary and Conclusions.

Having presented descriptive data for the areas showing best the inter-relations of the main rock types, some generalizations can now be made.

a) Contacts between the leuco-syenites.

The contact phenomena observed at various localities (North Top; Sail an Ruathair; Metamorphic Burn; Black Rock Burn; Oykel falls) clearly demonstrate the existence of two or more generations of leucocratic syenite. The contact relationships can clearly be seen because of the contrasting colours of the two phases of the intrusion - S1/S2 red

or pink, S3 grey or brown. Fig. 2.13 summarizes diagrammatically the contact relations observed. At all localities S3 can be said to overlie S1/S2. The relationship is clear on the North Top of Sail an Ruathair. On the S. side of the Black Rock the dip of the contact can be traced to the base of the Black Rock Burn, so that the mixed rocks exposed in a traverse upstream are progressively further from a contact dipping a little more steeply than the fall of the stream.

In the region around the Oykel falls one has only to climb a short distance above the low ground made up of S2 to come on to S3, which thus again overlies S2. Here the S2 seems to rise as a dome (as does S1 on the North Top of Sail an Ruathair), dipping under S3 again above the branching of the Oykel and Allt Sail an Ruathair. At the southern end of the intrusion S2 is thus seen as having an undulating surface, domed beneath the Oykel, and rising again beneath the S3 of Black Rock.

On the North Top of Sail an Ruathair S1 must have a steep domal form. It is massively veined by, and enclosed in, S3. Occasionally at this locality the breaking down of xenoliths can be observed yielding individual xenocrysts. The relationships here suggest that S3 is the later rock, and that S1 is roofed by S3. (Whether the whole of Coire Sail and Ruathair should be mapped as S1 is doubtful, but certainly identical rocks are exposed on both sides of the Coire at similar levels). The possibility that these contact effects are due to rheomorphism and that S3 is really the earlier rock, may be ruled out, since:

a) Xenocrysts are found far into S3, both around the S1 mass in the north, and the S2 in the south.

b) At other localities, i.e. Metamorphic Burn, west of the upper branches of Allt Cathair Bhàn, and on the Black Rock, xenolithic masses

of S1 or S2 are found hundreds of yards from massive S1 or S2, a scale of rheomorphism considered improbable.

On the North Top, Sail an Ruathair, most of the S1 exists as blocks in S3, and development of xenocrysts is only observed to a limited degree. The S3 of the lower part of the Black Rock Burn, and above the S2 of the central area, carries xenocrysts in profusion, and coherent masses of S2 are only rarely found at the latter locality. The junction here can be said to be gradational, since progressive increase of S2 and diminution of S3 material does not allow a true sharp contact to be mapped.

Thus the contact between the two main generations of leuco-syenite may be either sharp (North Top, Sail an Ruathair; Black Rock) or gradational (parts of Black Rock Burn, central area). In the first case easily recognizable masses of S1/2 are held in S3. In the second the S1/2 is broken up by the invading S3 and incorporated as xenocrysts. These gradually increase in amount towards the massive S1/2 until there is proportionally less S3 material.

At the S1/S3 contact on the North Top of Sail an Ruathair, S1 crystals along contacts may be seen broken across. The blocks of S1 are subangular or rounded and have been rotated in some cases by the S3 intrusion. At one locality flat sheets of S1 are seen, their feldspars orientated parallel to the sides of the sheets. There is no diminution of grain size of S3 at contacts. The conclusion is that S1 was in a fully consolidated state on intrusion of S3, but that at certain points some partial remobilization of S1 may have occurred.

Fig. 2.13.

Generalized columns illustrating the contact relationships between leucosyenites. The columns are drawn in their true way-up. The actual topographic top is marked 'T'. Limits of exposure are given with a dashed line, uncertain transitions witha dotted line.

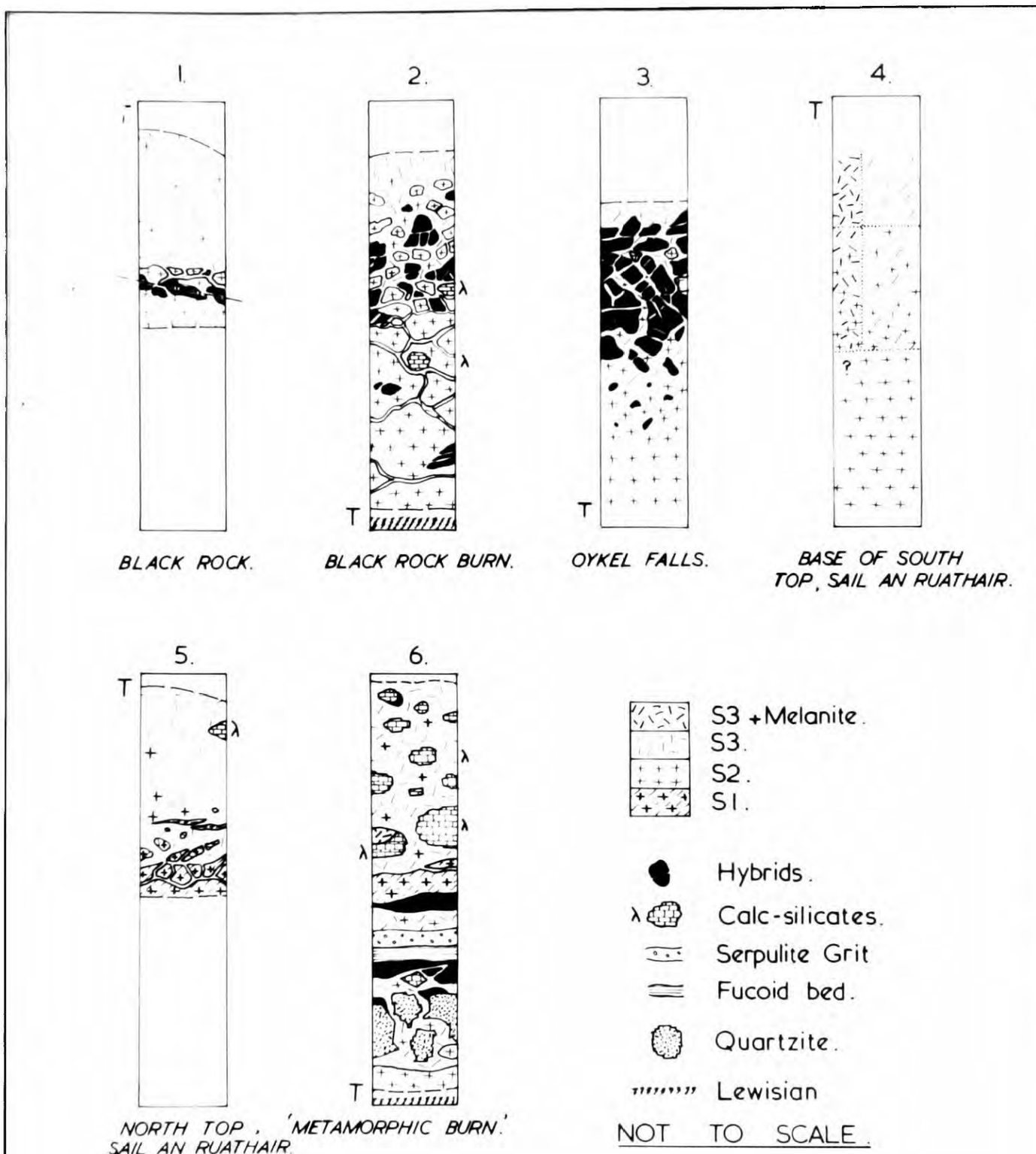
1.
2.
3.
4.
T
λ
λ
T
T
?
BLACK ROCK.
BLACK ROCK BURN.
OYKEL FALLS.
BASE OF SOUTH TOP, SAIL AN RUATHAIR.
5.
6.
T
λ
λ
λ
T
NORTH TOP, SAIL AN RUATHAIR.
'METAMORPHIC BURN.'
S3 + Melanite.
S3.
S2.
S1.
Hybrids.
λ Calc-silicates.
Serpulite Grit
Fucoid bed.
Quartzite.
Lewisian
NOT TO SCALE.

b) Relationships of the variable basic types, and of the ultrabasic rocks.

The S2-S3 contacts in the southern part of the central area, in the Black Rock Burn, and on the Black Rock are complicated by the presence of basic and ultrabasic inclusions. As represented on Fig. 2.13 these become more sparse downwards into S2 and, in the central area, eventually die out. They never extend into S3 above the zone of S2 xenoliths and xenocrysts.

Thus it may be seen that the basic rocks form a discontinuous zone always concentrated near the top of S2.

In the Black Rock Burn and in the Metamorphic Burn, basic rocks are at the same level as xenoliths obviously derived from Durness limestone. Any hypothesis as to the origin of the basic types must consider this fact, especially bearing in mind the undoubtedly upward relative position of the limestone. It seems reasonable to suggest that the basic rocks are the remains of a roof to S2, some portions of which sank into S2, others remaining in place until the intrusion of S3. This broke up the roof zone, and, in some cases, lifted fragments into its lower portion, with other fragments and xenocrysts from S2.

In the Cathair Bhan area the ultrabasic types exist between syenite and limestone. Syenite is not seen above them. Their attitude cannot be established from exposural evidence alone. Geophysical data offering a solution to this problem is given in Chapter 3.

Bibliography to Chapter 2.

GEOLOGICAL SURVEY OF SCOTLAND. 1923, reprinted 1959. Special sheet for the Assynt district; parts of sheets 107, 108, 101, 102. 1" : 1 ml.

PHEMISTER, J. 1926. in 'The Geology of Strath Oykell and Lower Loch Shin.' Mem. Geol. Surv. Scotland.
(Explanation of sheet 102).

CHAPTER 3.

GEOPHYSICAL DATA.

Contents:

General Introduction.

Determination of the relationships of the ultrabasic pyroxenites and hornblendites of the Allt Cathair Bhàn to the leuco-syenites in the west and the Cambrian sediments to the east is clearly vital in discussion of possible structures for the intrusion as a whole.

Since the ultrabasic rocks have a high magnetite content it seemed that the area lent itself to investigation by magnetic means. Models could be suggested to give rise to anomalies of the observed form. In addition some of the magnetic properties of orientated samples of the ultrabasic rocks were determined allowing interpretation of the observed anomalies with little fear of ambiguity.

The magnetic data suggests a radically different interpretation of the structure of this part of the mass to that suggested by Phemister (1926). Excavations have further substantiated the relationships determined geophysically.

Section 1.

Field Data and Techniques.

a) Field survey method.

Measurements of total magnetic intensity were made using an Elsec proton precession magnetometer. An assistant was always used when making the measurements. Traverses were made by pacing along a predetermined bearing, readings being taken at different intervals appropriate to the local magnetic gradient. Location was checked at intervals on air photographs. The instrument was read at each station three times to establish a steady reading. (An unsteady reading usually means either that the magnetic gradient is too high for the instrument or that the instrument requires re-tuning). Normally stations would be

20 yards apart, decreasing to 2.5 yard intervals when the magnetic gradient was steep. Time was noted at ½ hourly intervals, and the reading at the origin of each traverse recorded at the end as well as the beginning of most traverses.

b) Data.

Instrument readings were recorded at 1010 stations on the eastern side of the Loch Ailsh mass. The location of profiles made is shown on diagram 3.1. Work was concentrated on the Allt Cathair Bhàn area, with some profiles across the Sròn Sgàile body. The data is presented as contour maps of total magnetic intensity (Map 2, at back of thesis, and Fig. 3.3), and selected profiles (Fig. 3.2). These are plotted as raw equivalents in γ (gamma = 10^{-5} oersted) to the magnetometer scale readings using the relationship

$$H_{(\gamma)} = \frac{24050}{\text{count}}$$

The magnitude of the anomalies was such as to make corrections for daily variation and drift unnecessary.

c) Description of anomalies, Allt Cathair Bhan area.

As shown by Map 2 and the profiles of Fig. 3.2, an anomaly of considerable magnitude (up to 5000 γ) was found following the general course of the Allt Cathair Bhàn and corresponding to the exposures of ultrabasic rocks in this stream. The continuity of these rocks between the upper and lower parts of the Allt Cathair Bhàn is therefore proved.

Their extension to the south-west, where the anomaly passes across the River Oykel, strikingly turns westward when limestone appears in the river.

At the north-east end, beyond the highest exposures of ultrabasics in the stream, the anomaly can be traced until it turns a little to the

Fig.3.I.

Outline map of the intrusion showing location of proton magnetometer profiles, and the areas shown by the two contour maps of magnetic intensity. (Map 2 and Fig. 3.3.)

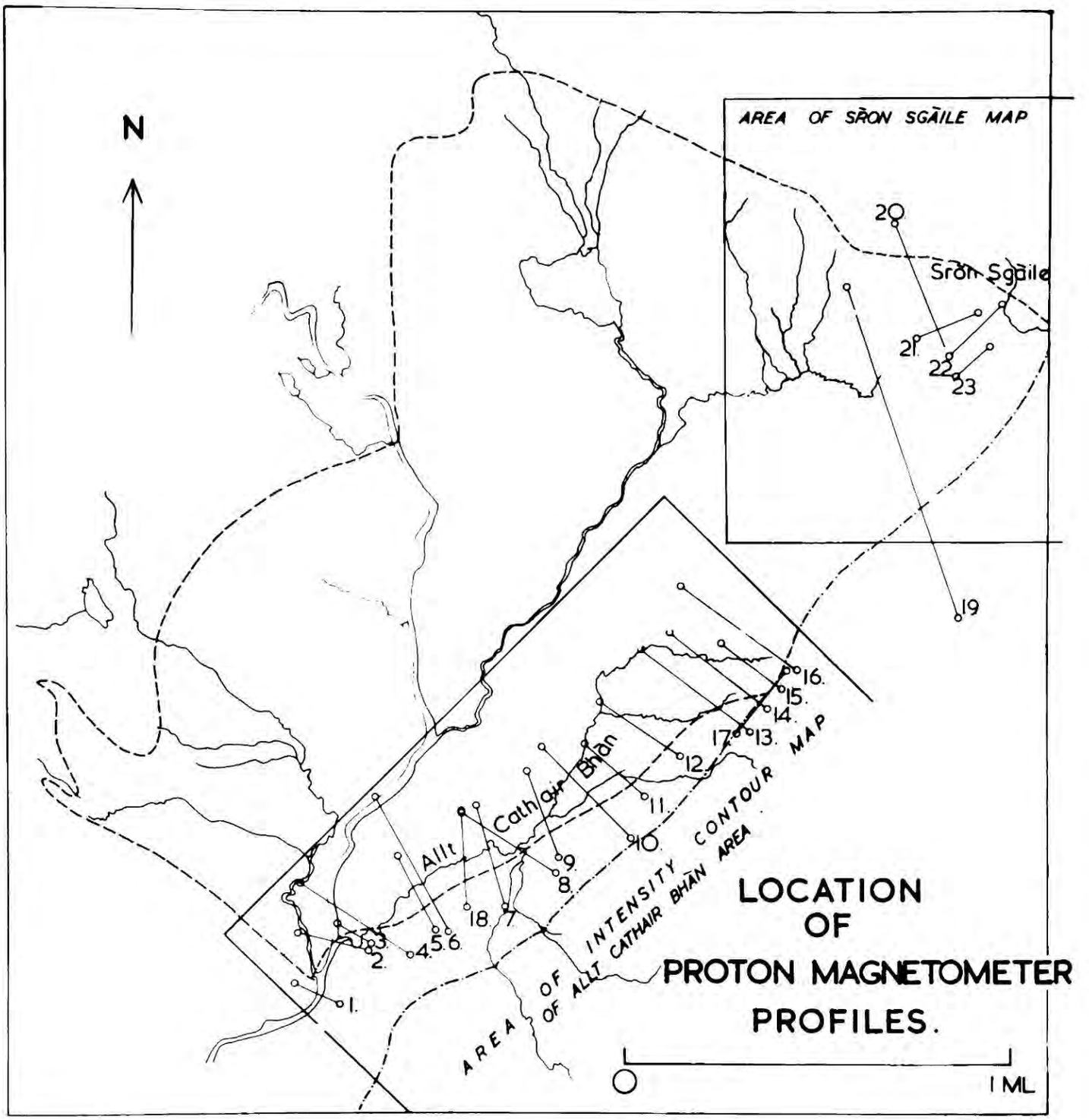
N
AREA OF SRON SGAILE MAP
Sron Sgaile
20
21
22
23
19
16.
15.
14.
13.
17
12.
11.
10.
9.
8.
7
18.
6.
5.
4.
3.
2.
1.
Allt Cathair Bhan
AREA OF INTENSITY CONTOUR MAP OF ALLT CATHAIR BHAN AREA
LOCATION OF PROTON MAGNETOMETER PROFILES.
1 ML

Fig.3.2.

Selected total magnetic intensity profiles across the ultrabasic rocks of the Allt Cathair Bhân. South is to the left of the diagram.

PROTON MAGNETOMETER PROFILES. (ALLT CATHAIR BHÃN.)

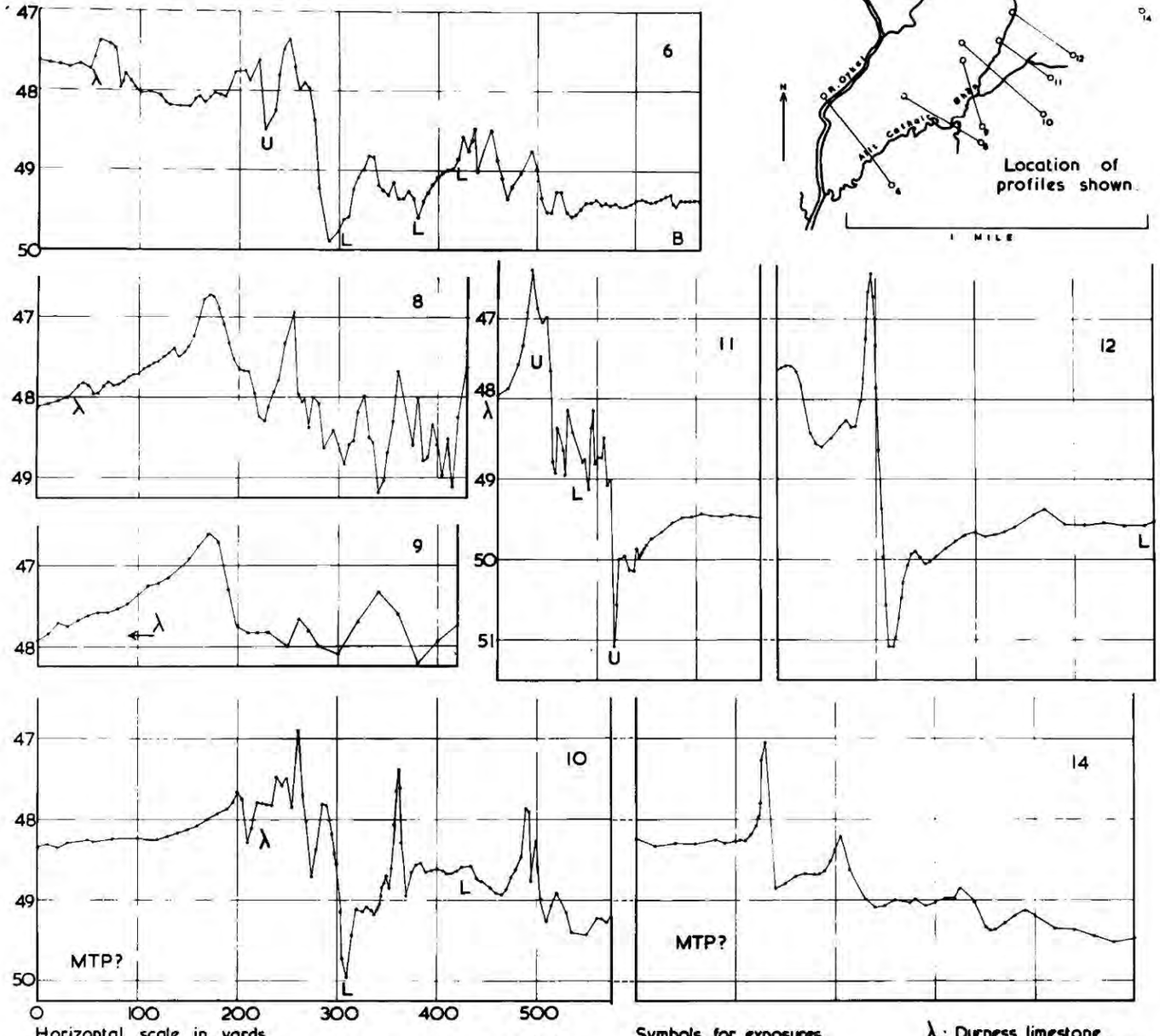

east and dies out at the base of the feature ascribed to the Moine Thrust.

On its southern side the main positive anomaly is sharply bounded by more or less constant values, and such values extend into the known Durness Limestone area. At no point was massive leuco-syenite found between limestone and the main anomaly. Indeed the anomaly follows perfectly the general area of the contact between limestone and intrusion. The form of the individual profiles will be discussed in the later section concerning their interpretation.

A surprising feature of many of the profiles in the Allt Cathair Bhàn area, particularly at the southern end, was the presence, in a wide belt to the north-west of the most pronounced anomaly, of numerous sharp irregularities in the magnetic field, often in the form of pronounced positive anomalies. Some attempt has been made on Map 2 to contour these irregularities when they seem to correspond, but their complexity makes this difficult and many subsidiary irregularities are smoothed out on the contour map.

The source of these not inconsiderable ($> 1500\ \gamma$) disturbances in the magnetic field was obscure, since only leucocratic syenites were exposed in most of the area concerned, with some intermediate and basic types at the south-eastern tip of the Cathair Bhàn ridge. Neither of these rock types would be expected to give such anomalies, particularly by comparison with the traverse including the zone of basic inclusions in the R. Oykel. (See the northern end of profile 6, Fig. 3.2).

An excavation was therefore undertaken at the point 'X' of Map 3, (see back of thesis), on traverse 18, at the station corresponding to the maximum of one of these anomalies. This was taken to a depth of

about 10' and passed mainly through weathered blue-grey crumbly material but revealed several unweathered feldspathic veins, up to 2" in width, exactly as seen in the ultrabasic rocks in the stream below. A thin section of a fresher portion of the dark weathered material showed it to be pyroxenite of the Allt Cathair Bhàn type.

Since it may safely be assumed that the other irregular anomalies observed in this area have similar sources, the importance of these observations in assessing the structure of this part of the intrusion must be far reaching, the presence of ultrabasic rocks on the ridge of Cathair Bhàn being hitherto unsuspected.

The form in depth of the ultrabasic rock masses can be deduced from the shape of the magnetic anomalies, using the techniques described in Section 3.

In an appendix comparison is made with strikingly similar anomalies discovered in a comparable geological setting at the southern boundary of the nearby Loch Borralan syenite.

d) Description of anomalies, Sròn Sgàile area.

A limited magnetometer survey was made of the enigmatic Sròn Sgàile area. No anomalies of comparable magnitude to those of the Allt Cathair Bhàn were found, and no southward connection with the latter anomalies is suggested. Diagram 3.3 shows the limited arcuate anomaly found. The long traverse (19) showed no sharp changes in magnetic intensity, but a distinct change of gradient towards its southern end suggests the position of the Moine Thrust.

The data suggests that the Sròn Sgàile rocks are limited in extend and are not in near surface connection with rocks of Cathair Bhàn type. They are neither sufficiently clearly defined nor the data adequate to offer possibilities of detailed interpretation.

Fig.3.3.

Contour map of total magnetic intensity of the Sròn Sgàile area, together with rock types exposed.

KEY TO ROCK TYPES: (Exposures indicated by appropriate letter.)

S: Leucosyenite.

B: Basic rocks of Sròn Sgàile type.

Q: Quartzite.

L: Limestone xenoliths.

M: Moine rocks.

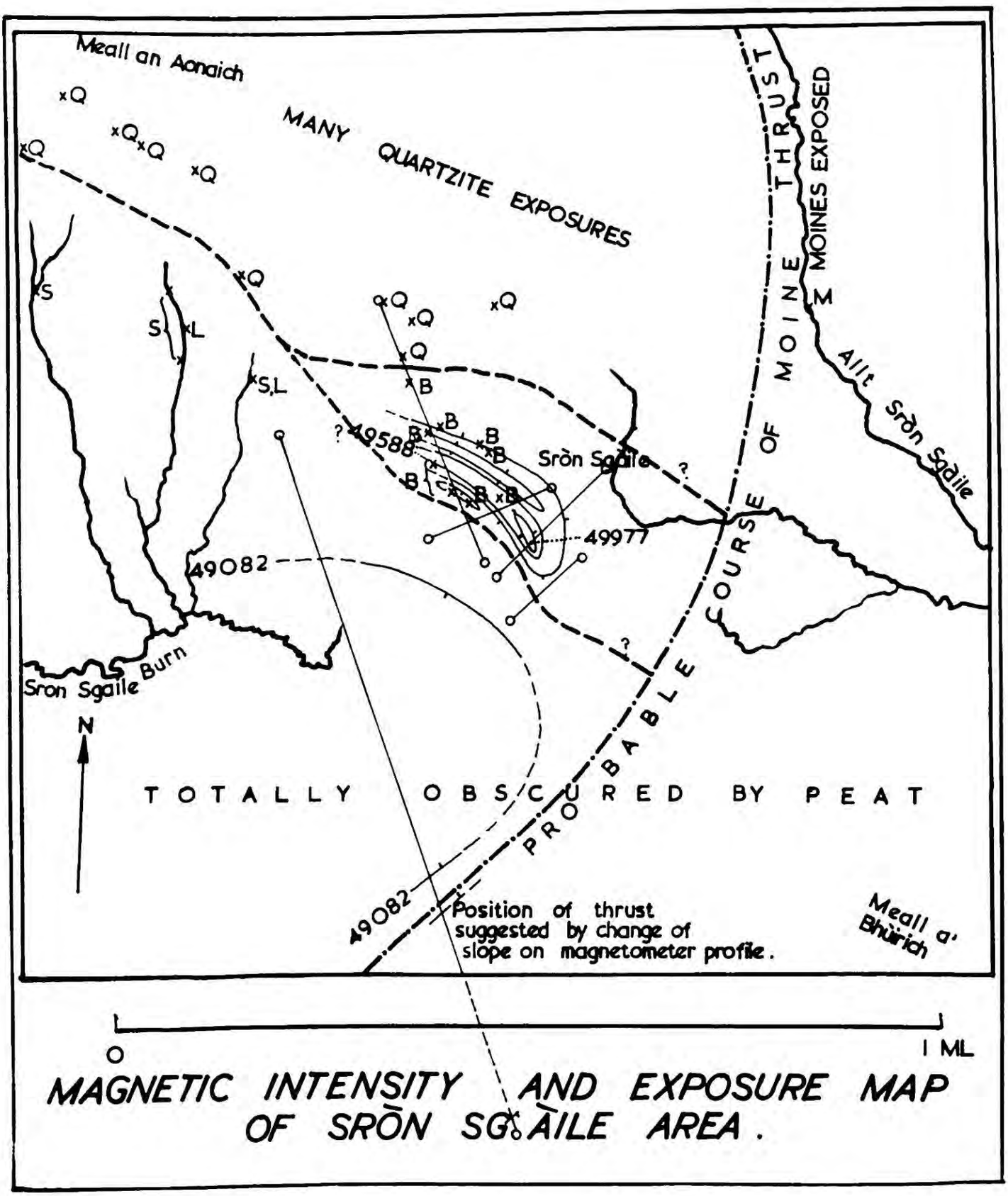

MAGNETIC INTENSITY AND EXPOSURE MAP OF SRÒN SGÀILE AREA.

Section 2.

Magnetic properties of the Allt Cathair Bhan ultrabasic rocks.

a) Introduction.

To obtain an unambiguous solution for the shape of a rock mass to give a magnetic anomaly of any observed form, it is necessary to know both the orientation and intensity of magnetization of the rocks forming the body.

In rocks such as those studied the effective direction of magnetization $\bar{I}_T$ and $\bar{D}_T$, and its magnitude J_T, is the vector sum of two components. One, the remanent magnetization, is acquired by the rock as it cools through the Curie temperatures of its magnetic components, and will usually reflect the orientation of the earth's magnetic field at the time the rock cooled. This direction can be represented by $\bar{D}_r$ (declination), $\bar{I}_r$ (inclination), and J_r (magnitude).

The other component is the result of magnetization induced by the present magnetic field of the earth. In a magnetic field strength H the induced intensity (in the direction of the field $\bar{I}_i$, $\bar{D}_i$) is given by

$$J_i = kH$$

where k is the magnetic susceptibility of the sample.

The effective direction of magnetization $\bar{I}_T$ and $\bar{D}_T$ is the vector sum of $\bar{I}_r$, $\bar{I}_i$, $\bar{D}_r$, and $\bar{D}_i$, and the intensity of magnetization:

$$J_T = J_r + kH$$

All these components may be determined experimentally. $\bar{I}_i$ and $\bar{D}_i$, of course, correspond to the orientation of the earth's field at the locality from which the samples are taken.

b) Orientated samples.

Orientated specimens of Allt Cathair Bhàn rocks were obtained using

a tripod device with built-in spirit level kindly lent by Dr. R.W. Girdler. Cylindrical specimens 1" in length by 1" in diameter, suitable for measurement were then cut using a special coring machine.

c) Measurement of remanent magnetization.

The measurements were made on the "igneous" astatic magnetometer in the Dept. of Physics, King's College, Newcastle-upon-Tyne. (See Runcorn, Collinson and Creer, in 1960, p.120 for details). The cylindrical specimens described above were used and the intensity of magnetization determined by comparison with a standard coil.

d) Results.

It was soon apparent that the specimens used were far from ideal for these measurements since they were frequently markedly inhomogeneous and did not approximate to the dipole required for the successful functioning of the instrument. Of the 22 specimens measured only ten gave significant results, a far from satisfactory sample. These are given in table 3.1, and in diagram 3.4 (left).

The considerable scatter is obvious. There is no correlation between specimen locality and orientation, except in so far as the specimens which could not be measured tended to come from areas wnere the rocks were notably deformed.

e) Measurement of susceptibility.

The second component of the magnetization depends on the susceptibility of the rock. This property was determined for all of the 22 available samples on an A.C. susceptibility bridge (see Collinson and Creer in Runcorn et al., op.cit., p.196) at the Physics Dept., King's College, Newcastle-upon-Tyne.

Table 3.1.

Orientation and intensity of remanent magnetization of specimens of Allt Cathair Bhān ultrabasic rocks.

Specimen No.	Declination. $\bar{D}_r$ (degrees)*	Inclination. $\bar{I}_r$ (degrees)*	Intensity. $\bar{J}_r$ (E.m.u.cm^{-3} x 10^3)
M2	6	- 4	1.72
M3	34	+ 5	1.82
M4	222	-50	0.54
M5	327	-34	0.57
M6	130	+37	0.79
M7	302	+42	1.67
M17/1	323	-18	0.27
M17/2	5	-28	0.25
M18	180	-64	1.70
M19	261	-18	1.72

* Measured relative to True North.

* Measured relative to the horizontal.

+ poles down, - poles up.

The values are plotted stereographically on figure 3.4.

Fig.3.4.

LEFT: Directions of remanent components of magnetization of Allt Cathair Bhàn ultrabasic rocks.

RIGHT: Directions of resultants of remanent and induced magnetizations.

Points linked by the broken line are cores from the same hand specimen.

DIRECTIONS OF REMANENT MAGNETIZATION .

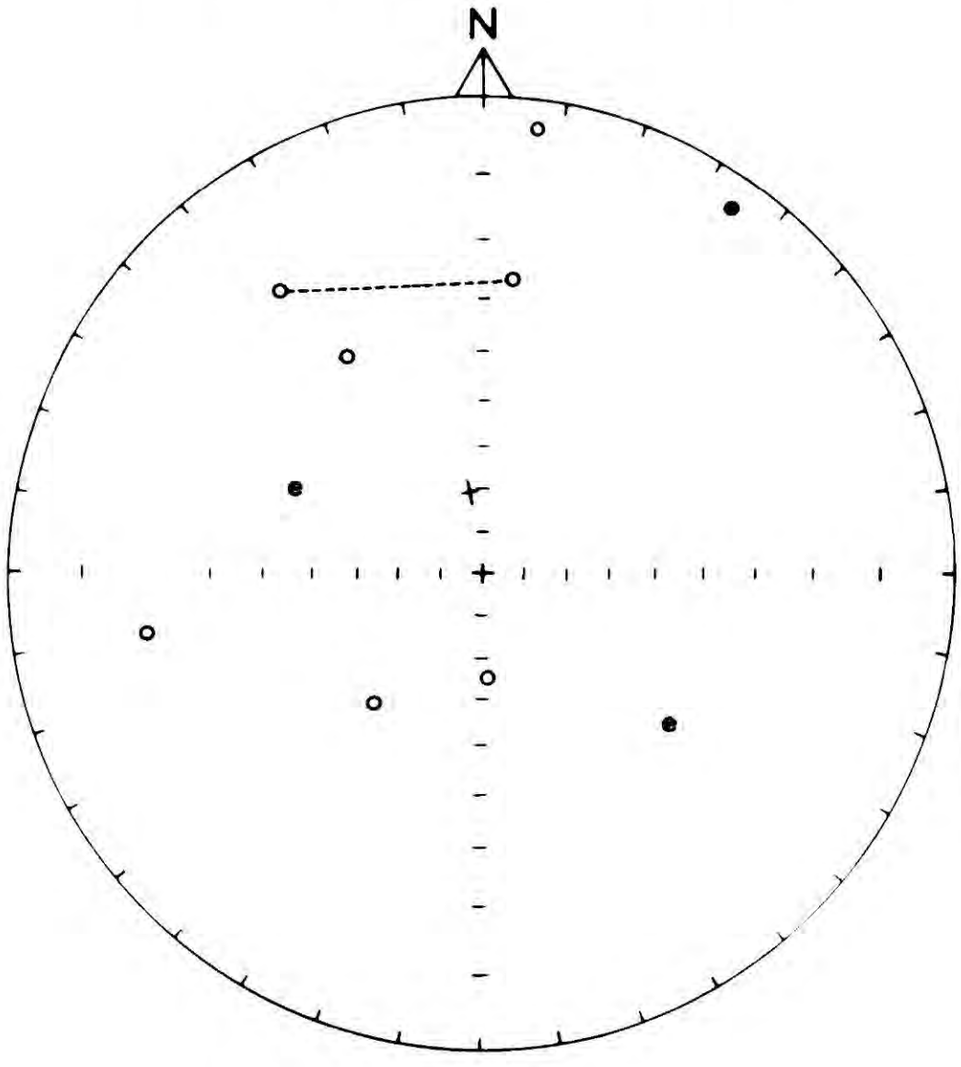

● VECTOR DOWN

○ VECTOR UP

DIRECTIONS OF RESULTANTS OF REMANENT AND INDUCED MAGNETIZATIONS.

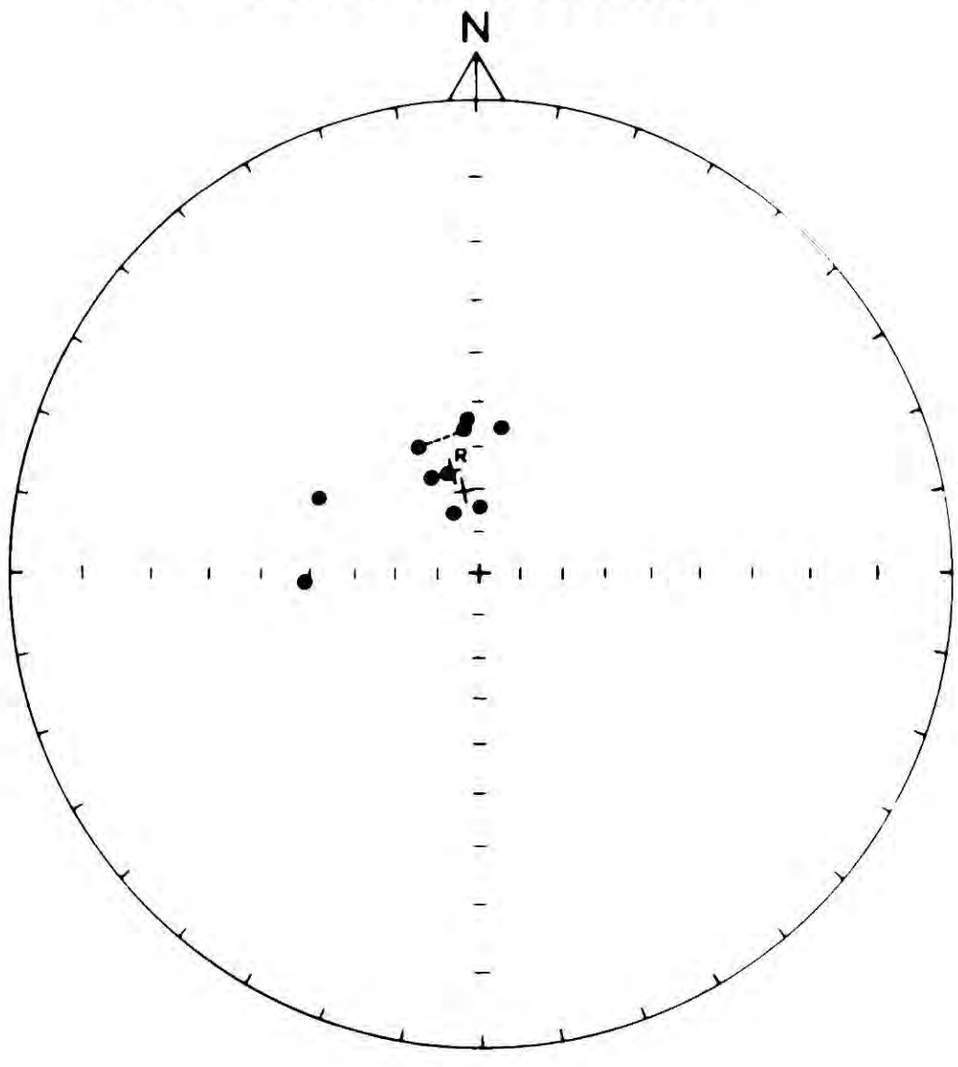

+ EARTH'S FIELD IN N.W. SCOTLAND

$+^{R}$ VECTOR SUM OF ENTIRE POPULATION

Table 3.2.

Susceptibility, intensity of induced component, and magnetite content of Allt Catheir Bhàn ultrabasic rocks.

Specimen No.	Susceptibility (K) e.m.u.cm^{-3}x10^{6}	Intensity in 0.5 oersted field (J_i) e.m.u.cm^{-3}x10^{3}	J_r/J_i (Königsberger Ratio)	Modal % magnetite (vol).
M2	10260	5.13	0.34	4.1
M3	11733	5.87	0.31	4.2
M4	1560	0.78	0.69	0.5
M5	10533	5.27	0.11	3.9
M6	10933	5.47	0.14	6.9
M7	13067	6.53	0.26	6.8
M17/1	2114	1.06	0.26	0.7
M17/2	1927	0.96	0.26	0.6
M18	8027	4.04	0.42	4.8
M19	6900	3.45	0.50	4.2
M8	9715	4.86	-	-
M9	12833	6.42	-	-
M10	13860	6.93	-	-
M11/1	4180	2.09	-	-
M11/2	3915	1.96	-	-
M13/1	4971	2.86	-	-
M13/2	6200	3.1	-	-
M13/3	7770	3.89	-	-
M22	2261	1.13	-	-
M24/1	5029	2.52	-	-
M24/2	4077	2.04	-	-
M25	3600	1.8	-	-

Table 3.3.

Orientation and magnitude of resultants of remanent and induced magnetizations of Allt Cathair Bhàn ultrabasic rocks.

Specimen No.	Declination D_t (degrees)*	Inclination I_t (degrees)*	Intensity J_t ($e.m.u.cm^{-3} \times 10^3$)
M2	357.5	55	5.79
M3	11	55.5	6.67
M4	88.5	49.5	0.426
M5	345	65	5.14
M6	4.5	74	5.79
M7	333	65.5	7.38
M17/1	335	57	1.09
M17/2	356	56.5	0.95
M18	337.5	75.5	2.33
M19	295.5	49.5	3.037

* Relative to true north.

* Relative to horizontal; all downwards.

Note that specimens M4 and M19, which depart furthest from the mean, have the highest Königsberger ratios. (See Table 3.2).

f) Results.

The results are tabulated in table 3.2, together with J_i calculated from $J_i = kH$, H being taken as 0.5 oersted, the approximate background intensity value observed in the Loch Ailsh area. Also shown are modal volume percentages of magnetite determined by point counting polished sections. (There was a little coarse ilmenite in some specimens). From the column showing J_r/J_i it may be seen that the induced component is always larger than the remanent component by, on average, a factor of 3, and in all but two cases a factor of 5. The mean value of J_i is 3.86×10^{-3} e.m.u.cm^{-3}.

There is a general, but not precise, correlation between the modal magnetite content and the susceptibility. Using the means of the magnetite content and susceptibility, the susceptibility (in e.m.u.cm^{-3} x 10^6) is approximately 2×10^3 x vol. per cent. magnetite. Thus specimen 46 (Table 4.5) with 11.6 per cent. magnetite would have a susceptibility of 23200 e.m.u.cm^{-3} x 10^6 and J_i of 11.6 e.m.u.cm^{-3} x 10^3, which represents the maximum probable for the Loch Ailsh samples.

g) Resultant directions of magnetization.

The comparitively large values of J_i mean that the effective direction of magnetization will lie near to the orientation of the earth's field at the present day. The resultant of two vectors as described here is given by:

$$N_r = J_r \cos I_r \cos D_r$$
$$E_r = J_r \cos I_r \sin D_r$$
$$Z_r = J_r \sin I_r$$

N_i, E_i and Z_i are calculated similarly and

$$N_t = N_r + N_i$$
$$E_t = E_r + E_i$$
$$Z_t = Z_r + Z_i$$

$$\text{Tan } D_t = \frac{E_t}{N_t}$$

$$\text{Sin } I_t = \frac{Z_t}{J_t}$$

$$J_t^2 = N_t^2 + E_t^2 + Z_t^2$$

The resultant directions calculated are tabulated as table 3.3, and plotted on diagram 3.4 (right). The earth's field was taken to be $D_h = 350^\bullet$, $I_h = 71^\circ$, $J_h = 0.5$ oersted. The vector sum of all the unit vectors in the sample is the best estimate of the true mean direction of the population (Fisher, 1953). This point is also plotted and falls at

$$D_m = 355.5^\circ, \; I_m = 65.25^\circ,$$

or rather close to the orientation of the earth's field.

h) General conclusions.

These results suggest that the anomaly must be interpreted in terms of the induced component which can be determined by direct measurement of susceptibility or estimated from the modal magnetite content of the rocks. This conclusion is reached bearing in mind the following points:

(i) The measurements of direction of remanent magnetization are widely scattered even in the ten measured specimens, and a further eleven specimens did not have a consistent direction of magnetization even over the short (1") distance of the cored samples. This suggests that the remanent magnetization is effectively random, probably as a result of the irregular deformation that the rocks have undergone.

(ii) The measurements of susceptibility show that in any case the induced component will be considerably the larger, and the calculated position of the vector sum of the entire group of samples is strikingly near to the position of the vector for the present day field of the earth.

This confirms the validity of assuming the latter direction as the direction of magnetization of the body as a whole.

i) Assumed values.

A mean value of susceptibility for the 22 measured specimens is 7.069×10^{-3} e.m.u.cm^{-3}, so that the average intensity of the rock will be 3.55×10^{-3} e.m.u.cm^{-3}. For the 10 specimens which could be fully measured the mean was 3.86×10^{-3} e.m.u.cm^{-3}. From this data the value used for the initial stages of computation was taken to be 0.004 e.m.u.cm^{-3}, Declination 350°, Inclination 71°.

j) Sources of deviation from the mean.

The most important factor influencing the form of the anomaly will be changes in the magnetite content of the rocks. The modal data show a considerable range of magnetite content which will be a major contributing factor in determining the magnitude of the anomaly. It is also possible that in a particularly undisturbed part of the mass, J_r/J_i could become such that the direction of magnetization approached more closely to the remanent than the induced magnetization.

Using the assumptions of section (i), and bearing in mind the above remarks, we can now turn to the interpretation of the magnetic anomalies.

Section 3.

Interpretation of magnetic anomalies.

a) Technique.

The magnetic intensity at a given point over a buried magnetic mass is given by: (Heiland, 1940.)

For the horizontal component:

$$\Delta H = 2kF_0 \sin i \left\{ \cos I \sin\alpha \left[\sin i(\varphi_1 - \varphi_2) - \cos i \log_e \frac{r_2}{r_1} \right] + \sin I \left[\sin i \log_e \frac{r_2}{r_1} + \cos i (\varphi_2 - \varphi_1) \right] \right\}$$

and for the vertical component:

$$\Delta Z = 2kF_0 \sin i \left\{ \cos I \sin\alpha \left[\sin i \log_e \frac{r_2}{r_1} + \cos i (\varphi_2 - \varphi_1) \right] + \cos I \left[\sin i (\varphi_2 - \varphi_1) - \cos i \log_e \frac{r_2}{r_1} \right] \right\}$$

The total intensity, which the proton magnetometer measures, is given by:

$$\Delta F = \Delta H \cos I' \sin\alpha' + \Delta Z \sin I'$$

where

kF_0 = Total magnetization J.

α = Strike of the body measured clockwise from the declination of the total magnetization.

I = Inclination of the total magnetization.

α' = Strike of body measured clockwise from the declination of the present earth's field.

I = Inclination of the present field.

All these factors have been measured either in the field (Section 1) or the laboratory (Section 2).

i, r and ϕ are functions of the shape of the body, which are calculated by the computer which is fed only xy coordinates. These are

the only unknowns in the problem considered here.

Since this rather lengthy equation must be solved for a large number of stations on any profile, it can only be solved in practice by use of an electronic computer.

The machine used was the Ferranti "Pegasus" computer, at King's College, Newcastle-upon-Tyne, using a program (2D Magnetic Simulator) devised by Mr. R.A. Stacey, M.Sc., Dept. of Geology, Durham University, whose assistance throughout the computing work is especially gratefully acknowledged.

The technique is to construct possible graphical models of cross sections of the mass giving rise to the anomaly, endow them with the appropriate magnetic properties and calculate the magnetic anomaly due to the model. This is compared to that observed in the field, and the model progressively refined until a good fit is achieved. To this end the computer is given:

(i) A series of coordinates expressing the vertical and horizontal positions of stations on a profile normal to the strike of the anomaly. For most work this is adequately taken with a constant vertical component (i.e. with a horizontal land surface) although for traverses with appreciable relief the topography may be defined.

(ii) α' (= about 65°)

and I' ($= 71^\circ$)

(iii) A series of xy coordinates expressing the proposed shape of the body, together with the <u>contrast</u> between the total magnetizations (J_t) at interfaces between the body and enclosing country rock, and the values α and I. In our case these orientation parameters have been shown to approximate to the present field of the earth, so that $\alpha = \alpha'$ and $I = I$. The value of J_t (dependent on the susceptibility of the rocks)

was established in the preceding section as being about 0.004 e.m.u.cm^{-3}.

b) Initial calculations.

Initially it was decided to see whether the previously held structural hypothesis, due to Phemister (1926) fitted with the new data. He believed that the ultrabasic rocks in the Allt Cathair Bhàn had a shallow anticlinal form. A simplified model based on his diagram (reproduced as Fig. 1.2, below) was used. This and the calculated anomaly are shown as Fig. 3.8 (left). The topography was used in the calculation. Comparison with the observed profile (traverse 11) shows a marked difference, both in amplitude and shape. It is considered that this diagram clearly demonstrates the need for a reassessment of the form in depth of these ill exposed rocks.

Diagram 3.5 shows a series of anomalies computed for the variously dipping sheets illustrated, made up of rock with the magnetic properties determined for that of the Allt Cathair Bhàn. These are shown in some cases with an additional curve for a body buried 5 m. below the surface - i.e. below 5m. of peat, which must be a maximum estimate for the area considered.

From these curves some general points emerge:

(i) Low angle structures, whether dipping northwards into the syenite or southwards beneath the limestone are unable to produce magnetic anomalies of sufficient magnitude, unless the rocks at depth have appreciably different magnetic properties to those observed. This would necessitate a high magnetite content, probably at least 25 per cent. in the case of the very low angle structures.

(ii) The most notable variation in the form of the anomalies on changing the dip of the structure, is in the relative magnitudes of the

Fig.3.5.

Magnetic anomalies computed for sheets of varying dip. The anomalies produced when the body has its top at the surface and at 5m. below are shown.

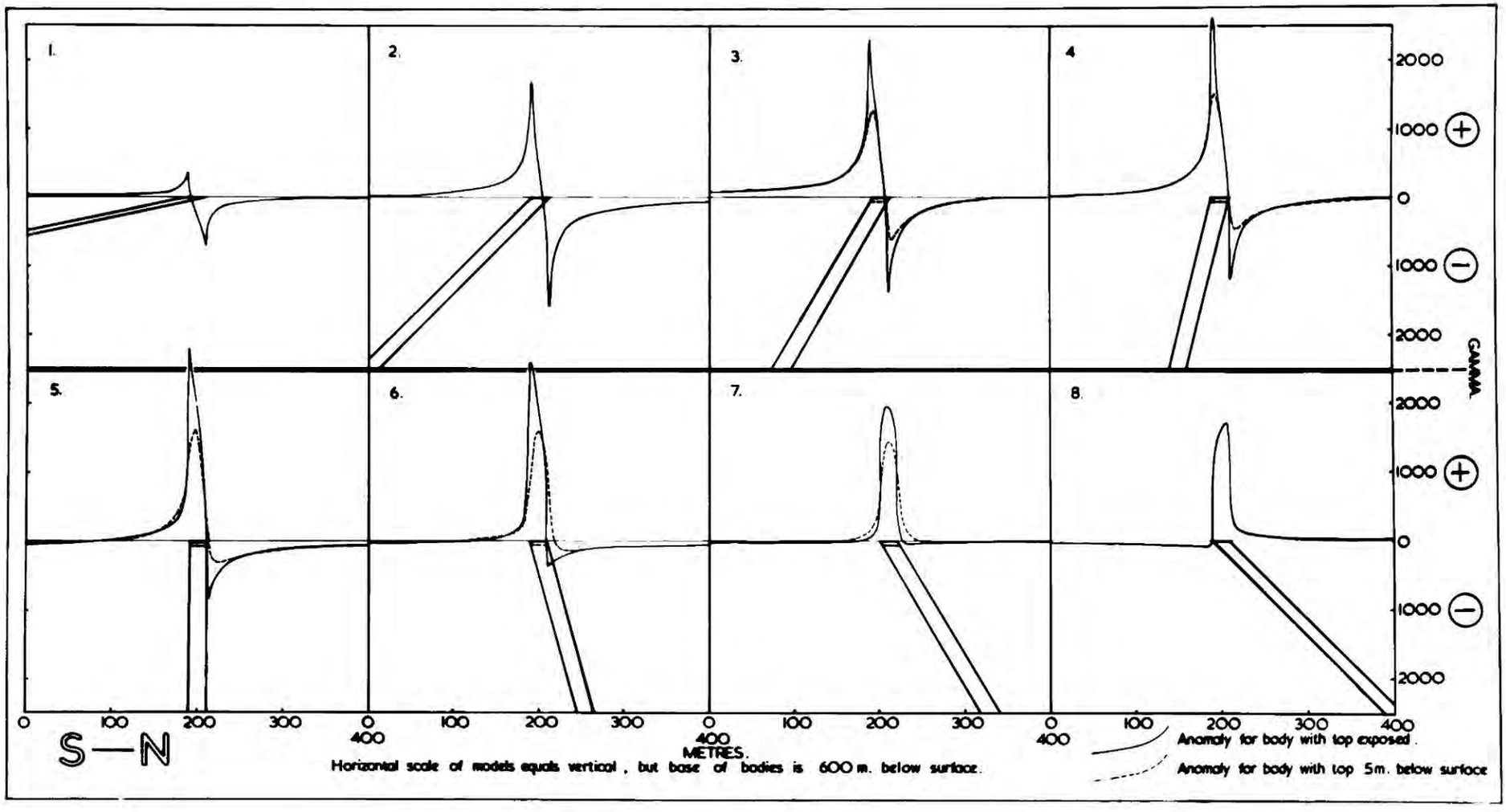
1.
2.
3.
4
5.
6.
7.
8.
2000
1000
0
1000
2000
GAMMA
0
100
200
300
400
METRES.
S—N
Horizontal scale of models equals vertical , but base of bodies is 600 m. below surface.
Anomaly for body with top exposed .
Anomaly for body with top 5m. below surface

positive and negative peaks of the anomaly. Since a very similar variation is seen in the Cathair Bhàn anomalies it seems likely that the structure has a variable, if steep, deep.

(iii) The effect of the peat cover is to depress the maxima and minima and generally to give a smoother, somewhat broader anomaly. The peat cover over the Allt Cathair Bhàn rocks is variable, ranging from zero in the exposed stream sections to moderate thicknesses in the peaty basin between the upper and lower parts of the stream, and in the area to the north of the stream exposures. It is in these areas that an appreciable smoothing-out of the anomaly is observed.

Fig. 3.6 shows two of the more steeply dipping models recalculated with their bases at varying depths. When the base becomes shallow, at less than 50 m. or 2.5 times the outcrop width, a small negative begins to develop on the south side of the still intense main positive peak. None of the Loch Ailsh anomalies show this feature, in a simple form, but there is a suggestion, although much more irregularly represented, in some profiles from the southern end of the body.

Diagram 3.7 illustrates the effect of increase in the magnitude of the total magnetization of a body, in this case from the value of 0.004 e.m.u.cm^{-3} used in previous sections to 0.007 e,m.u.cm^{-3}, well within the range encompassed by the modal magnetite content of the rocks.

In summary we can vary the following features of our simple sheet-form model:

(i) Angle of dip.

(ii) Depth of burial of top.

(iii) Depth to base.

(iv) Magnitude of total magnetization.

Fig.3.6.

Magnetic anomalies computed for two sheet-form bodies with various depths to their base.

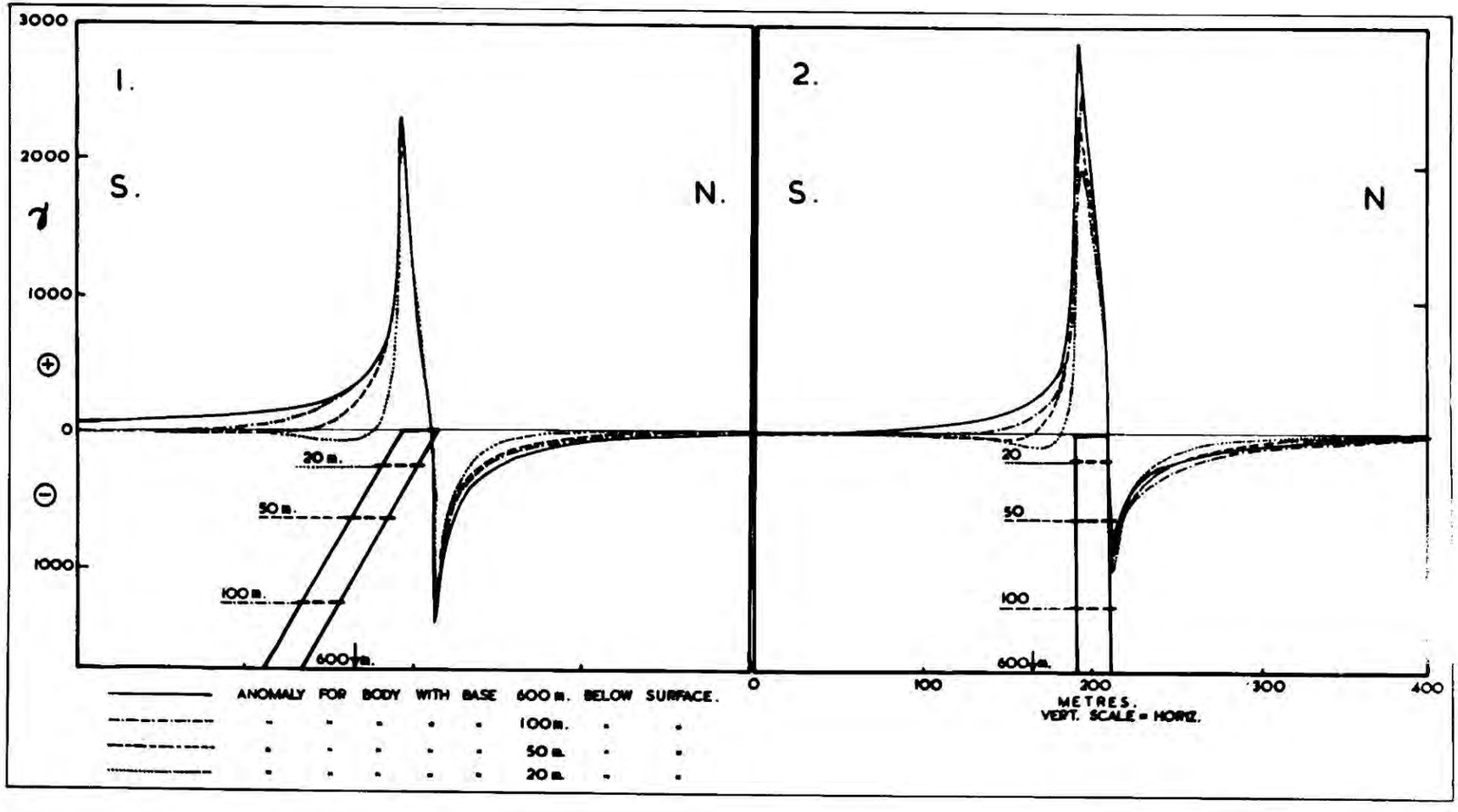
3000
2000
γ
1000
⊕
0
⊖
1000
1.
S.
N.
20 m.
50 m.
100 m.
600 m.
2.
S.
N
20
50
100
600 m.
0
100
200
300
400
METRES.
VERT. SCALE = HORIZ.
ANOMALY FOR BODY WITH BASE 600 m. BELOW SURFACE.
100 m.
50 m.
20 m.

Fig.3.7.

Magnetic anomalies calculated for deep and shallow based vertical sheets with two magnitudes of total magnetization in each case.

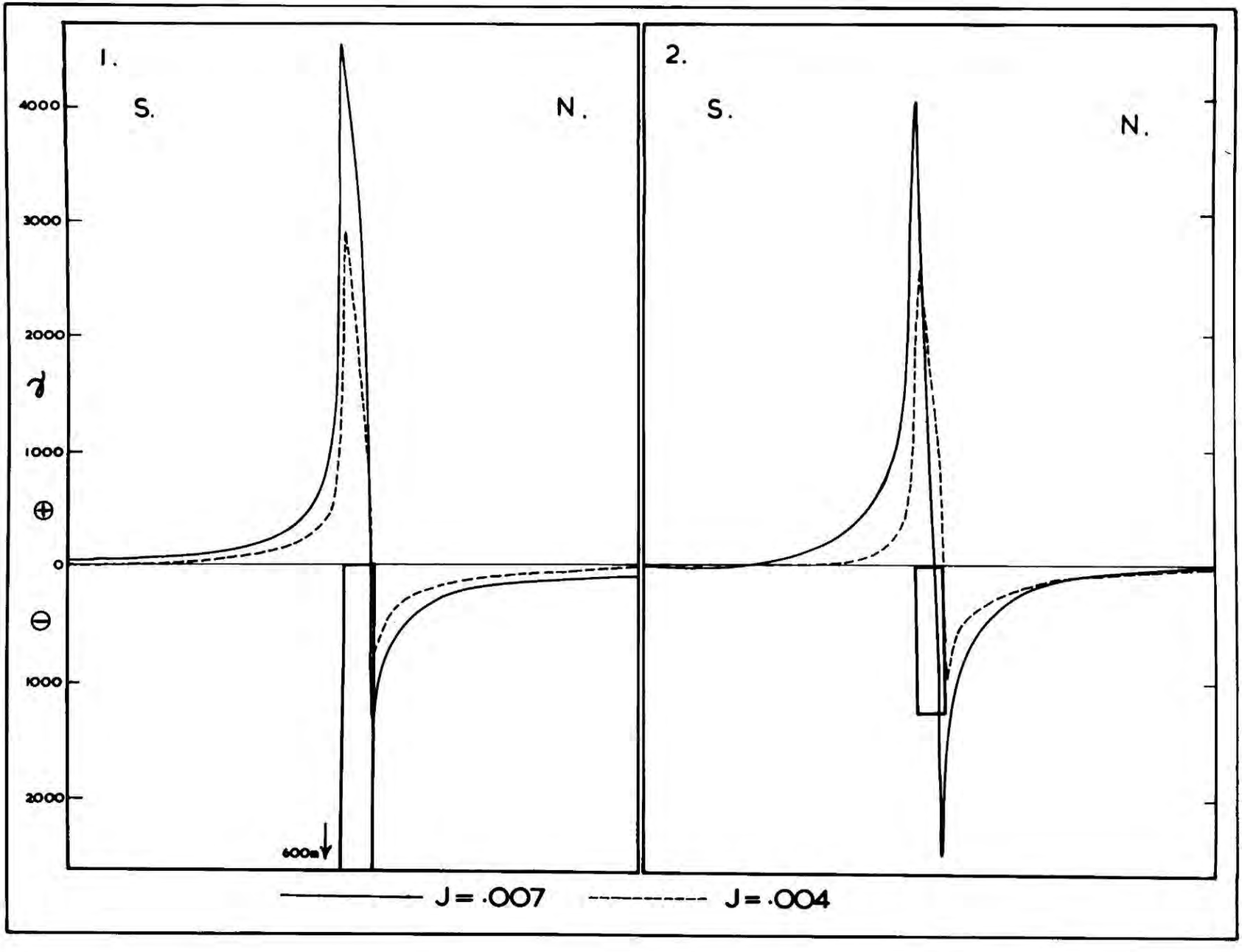
1.
S.
N.
2.
S.
N.
4000
3000
2000
1000
0
1000
2000
600m
J = .007
J = .004

c) Refinement.

With the computer there is little limit to the complexity of the models one can attempt to fit to the observed curves. Rounded parts of models must be expressed as a series of straight lines but such approximations have little effect as it is easy to show that the maxima of anomalies develop over the sharp corners of a given body.

In the time available it was decided to refine to a closer degree a model to approximate to one only of the observed profiles. Profile 11 (Fig. 32) was chosen for a number of reasons:

(i) It approximates to the section 'B' given by Phemister (1926, reproduced here as fig. 1.2) and thus comparison of observed and calculated profiles for both his body and other bodies fitting the exposures could be made.

(ii) Its basic form is comparitively simple.

(iii) There are numerous exposures along the length of the profile to which any model must be fitted.

As a further refinement the topography shown on the profile due to Phemister was incorporated. Sharp changes of slope, particularly when the body is near surface, can have a pronounced effect on the form of the anomaly.

In fig. 3.8 comparison is made between the observed profile 11 and the anomalies due to two complex models, one following Phemister, the other utilizing the same outcrop lengths but having a totally different form in depth.

The new model, whilst not in any way being a perfect fit, offers a good comparison of general form and amplitude. The ultrabasics form a vertical mass with a series of vertical syenite sheets within them.

Fig. 3.8.

Refinement of models.

The observed profile (11) is compared to a model based on the section of Phemister (1926), left, and a series of vertical sheets , right.

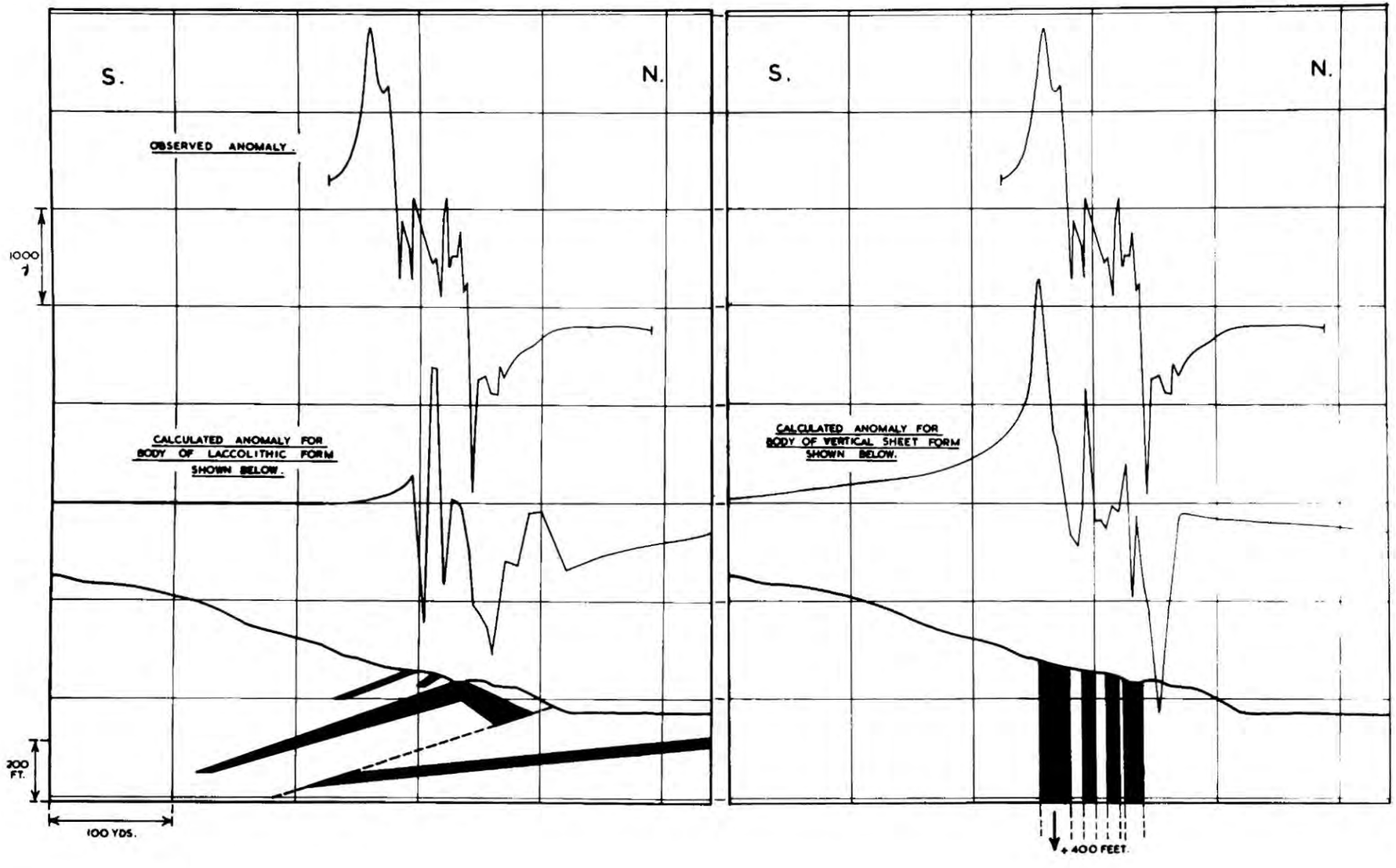
S.
N.
OBSERVED ANOMALY.
1000 ft
CALCULATED ANOMALY FOR BODY OF LACCOLITHIC FORM SHOWN BELOW.
200 FT.
100 YDS.
S.
N.
CALCULATED ANOMALY FOR BODY OF VERTICAL SHEET FORM SHOWN BELOW.
+400 FEET.

These are observed in the field when they are much more irregular in form than used for the model, but the general effect of producing an irregular zone between the maximum and the minimum of the overall anomaly may be seen.

When this model was originally tried the negative on the north side was much too large. A modification which brought the curve to its present equality in magnitude was the assumption that the syenite, both as the small dykes and as massive syenite to the north, contains some magnetite, whilst the limestone to the south was magnetite free. The contrast in total magnetization over the seven ultrabasic-leuco-syenite interfaces was taken as 0.002 e.m.u.cm^{-3} and that for the ultra-basic-limestone interface given as the normal 0.004 e.m.u.cm^{-3}.

No attempt was made to estimate the depth to the base of the body, since it has been established (Fig. 3.6) that only a very shallow base has an appreciable effect on the form of the anomaly, and this profile and adjacent ones did not show such a modification.

d) General conclusions.

It has been shown that magnetic anomalies of the correct general form can be obtained using the magnetic properties of the rocks, determined experimentally. The unknowns are solely those defining the form of the body. Comparison of observed and computed forms suggests that the body is steeply dipping and not a low angle structure, and follows the contact between syenites and limestone. In places the observable veining of ultrabasic by leuco-syenite complicates the anomaly. Further masses of ultrabasic rocks held in syenite to the west have been proved by excavation.

Map 3 (back of thesis) is an attempt to produce a structural picture

of the Allt Cathair Bhàn area, bringing together exposural and geophysical evidence. The dips suggested were deduced by comparison of observed anomalies with the curves calculated in the previous sections.

The base of the ultrabasic body must in most cases be at least 2.5 times the outcrop width, except possibly at its southern end.

Bibliography to Chapter 3.

FISHER, R.A., 1953. Dispersion on a sphere. Proc. Roy. Soc. Lond. Ser.A., v.217, pp.295-305.

PHEMISTER, J., 1926. in 'The Geology of Strath Oykell and Lower Loch Shin.' Mem. Geol. Surv. Scotland. (Explanation of sheet 102).

RUNCORN, S.K., et al., 1960. in 'Methods and Techniques in Geophysics.' Interscience Publishers, Inc.

HEILAND, C.A., 1940. "Geophysical Exploration", Prentice-Hall, New York.

Appendix to Chapter 3.

Note on the Loch Borralan Complex.

During the course of the field magnetometer survey a number of additional traverses were made across parts of the Loch Borralan intrusion. Two traverses, at the localities shown on fig. 3.9, showed magnetic anomalies strikingly similar to those of Allt Cathair Bhàn, Loch Ailsh, both in shape and magnitude. (One is shown on fig. 3.9; the other was closely similar). The maximum of the anomaly corresponds closely to the contact of the intrusion postulated by Shand (1910, see bibliography of Chapter 1). The nearest exposures observed are Durness Limestone, to the south, and basic syenites to the north. The anomaly strikes directly towards the basic rocks of Bad na h'Achlaise (cromaltites). According to Shand, however, cromaltite does not contain magnetite. Nonetheless magnetite bearing rocks undoubtedly occur in the area described. By analogy with the L. Ailsh magnetic rocks they are probably steeply dipping, and, further, appear to occupy the same position between limestone and syenite as do the Loch Ailsh pyroxenites. A comparable zone of irregular anomalies is also seen on the side of the main anomaly nearest the syenite.

The field evidence of laccolithic form for the L. Borralan complex would seem to be tenuous. This data does not support the hypothesis. Further work could yield valuable information on the field relations of these unusual rocks.

Fig. 3.9.

Magnetic data on the Loch Borralan intrusion.

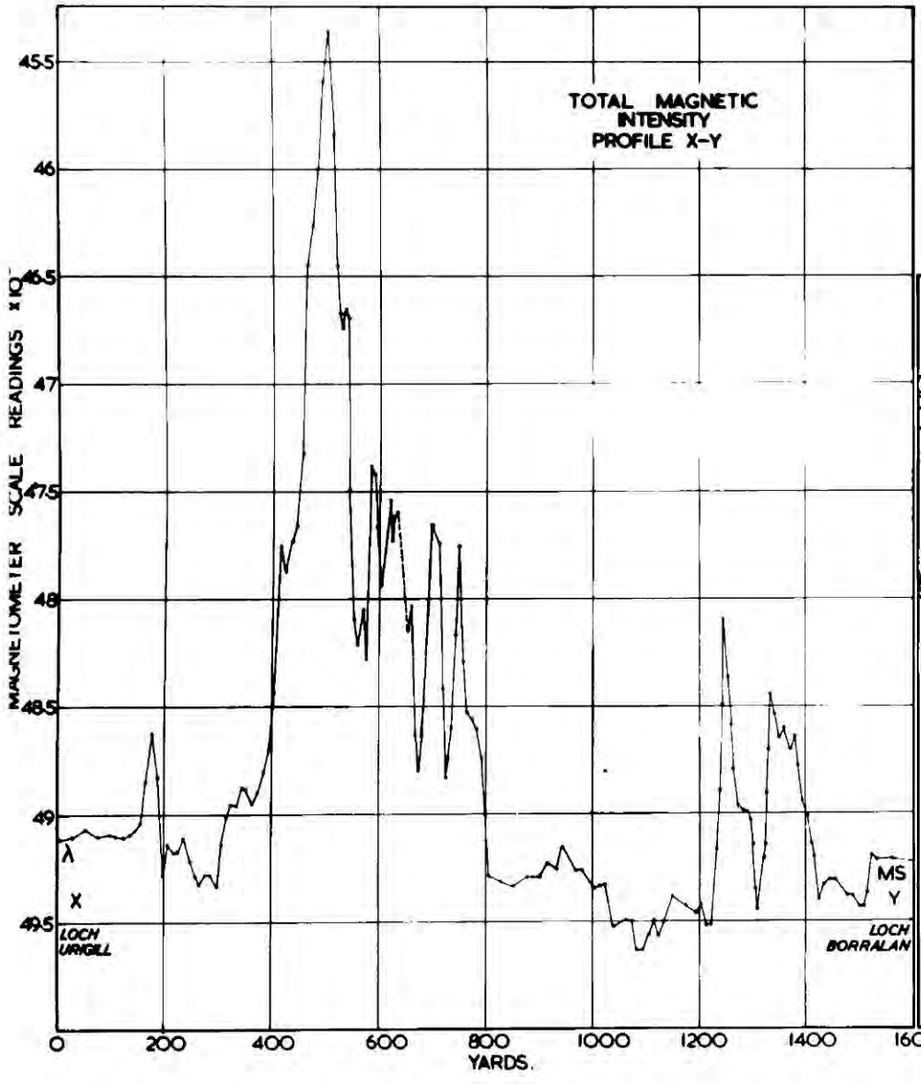

λ Durness limestone.
a^2 Pipe rock.
a^1 Basal quartzite.
A Lewisian.
QS Quartz syenite.
TZ Transition zone.
MS Melanite syenoids, Augite syenoids.

LOCH BORRALAN COMPLEX.
MAGNETIC DATA.

Profiles. Peat (totally obscured.).

SKETCH MAP OF S.W. OF INTRUSION SHOWING GEOLOGY, LOCATION OF PROFILES, AND STRIKE OF ANOMALY

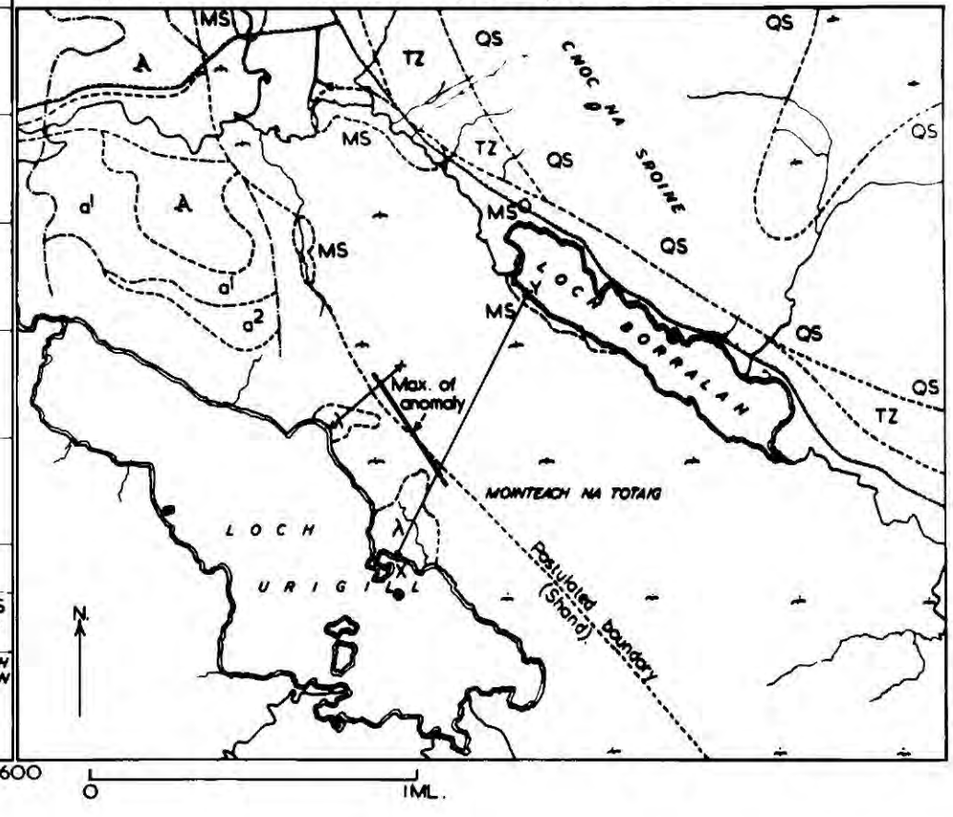

CHAPTER 4.

GENERAL PETROGRAPHY.

Contents:

b) Technique.

c) Data.

d) Conclusions.

Section 8. General conclusions.

Appendix. Technique for determination of b and a sin β of clino-pyroxenes.

General introduction.

Phemister, in his 1926 account of the L. Ailsh mass, gives a full account of the petrography of the main rock types represented, and also mentions a number of unusual forms. This account does not attempt to duplicate his descriptions, but to reassess the inter-relations of the rock types in the light of the revised structural picture developed in Chapters 2 and 3.

For the purpose of these descriptions a sub-division of the rock types will be made, following Phemister (1926) in a general way. The purpose of this chapter is to establish which of these distinctions is real, on petrographic grounds, or whether, as is suggested by the revised structural picture developed in the preceding chapters, a common origin is shared between a number of the rock types.

The following broad sub-divisions will be considered:

(1) Leucocratic syenites.

(2) Rocks produced near contacts between syenite and xenolithic sedimentary material.

(3) Basic and ultrabasic types xenolithic in the leuco-syenite. The "shonkinites" and "basic knots" of Phemister (1926).

(4) Sròn Sgàile rocks.

(5) The ultrabasic rocks of Cathair Bhàn.

The leucocratic rocks were investigated largely through their alkali feldspars which are fully described in Chapter 5. In this chapter notes on the major mafic constituents only are given.

Minor veins and the various dykes within the mass will not be described except in cases where they are considered to throw light on relations of the massive rocks.

The localities of all specimens mentioned in the text are shown as fig. 4.1.

Section 1.

Leucocratic syenites.

a) General statement.

The leucocratic syenites have previously been sub-divided into two main groups, S1 and S2, and the later S3. S1 and S2 are early syenites perhaps artificially sub-divided on the basis of location, but proving to differ in terms of the nature of the potassium phases of their perthites, (see Chapter 5), and in the type of mafic minerals present. The marginal forms of S2, in the Black Rock Burn, and at the top of the Metamorphic Burn, are characterized by a strikingly pleochroic (purple-turquoise-yellow) amphibole, sometimes together with a pyroxene and dark mica. In the central area of S2 a green pyroxene is more typical, although amphibole is sometimes present. S1 on the other hand characteristically carries either a dark green or a colourless mica, with both coexisting in some cases. The pyroxene is often rather pale green in colour. S3 has normally very little mafic material which may be either a green pyroxene, the purple amphibole, a colourless mica or sometimes opaque

Fig.4.1.

Outline map of intrusion showing localities and rock types of specimens described in the text of Chapter 4.

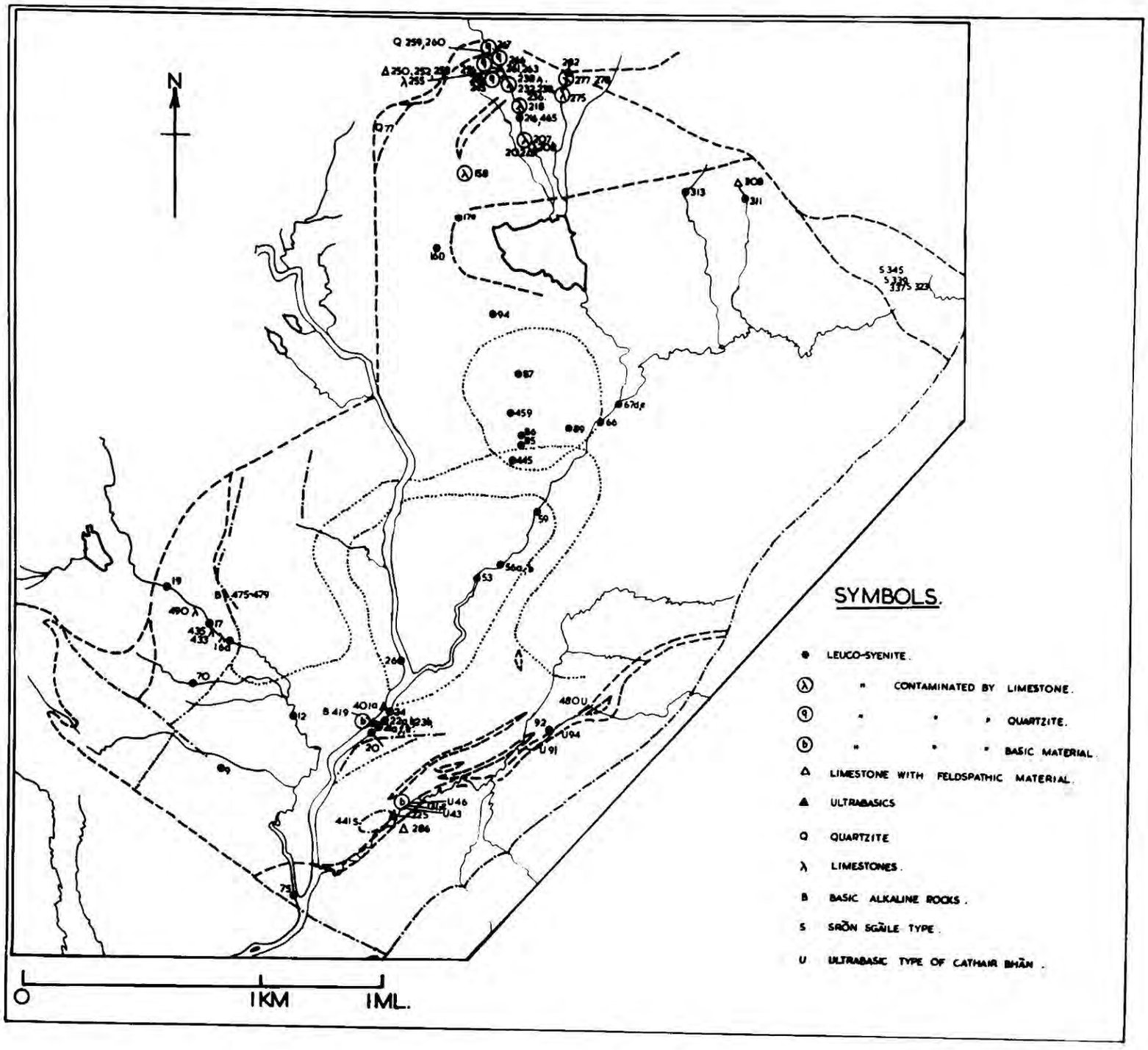
N
SYMBOLS.
LEUCO-SYENITE.
CONTAMINATED BY LIMESTONE.
QUARTZITE.
BASIC MATERIAL.
LIMESTONE WITH FELDSPATHIC MATERIAL.
ULTRABASICS
Q QUARTZITE
λ LIMESTONES.
B BASIC ALKALINE ROCKS.
S SRÒN SGAILE TYPE.
U ULTRABASIC TYPE OF CATHAIR BHÀN.
O
1KM
1ML.

material alone. The melanite bearing varieties of the South Top, Sail an Ruathair, carry a very dark green pyroxene. Diagram 4.2 summarizes the distribution of the chief mafic constituents of the leucosyenites.

b) Modal data.

A number of modal analyses were made by point counting thin sections, initially to test whether this was an adequate method for differentiating S1/2 from S3 in cases where some doubt had arisen. S1 is frequently rather coarse and often exhibits a strong lamination which makes straightforward point counting inapplicable. S2, however, is usually not as coarse and is usually unlaminated. The modal analyses completed, however, show some overlap between thin sections of S1/2 and S3 rocks. The data are presented as table 4.1, and plotted as figure 4.3.

At least 2000 points were counted for each thin section. All the rocks shown were chosen as being uncrushed examples, since crushing is seen to lead to reduction of mafics to strings of opaque material, and is often associated with the introduction of quartz.

c) Variation in content of mafic constituents.

S3 is normally a most leucocratic rock, except in its melanite bearing variety when the total mafic constituents are at least equal to S1/2. When the rock has acquired considerable S2 material, to develop the xenocrystic relationship described in Chapter 2, the mafic content also increases, showing that the whole of the immediately pre-existing S2 rocks have been broken up and mixed with S3 material. Since mixed rocks of this type appear to represent a considerable portion of the exposed rocks, and bearing in mind the factors rendering the point counting method inapplicable, modal data are inadequate to differentiate

Fig.4.2.

Outline map of intrusion summarizing the distribution of the chief mafic minerals in leuco-syenites of which thin sections showed fresh mafic material.

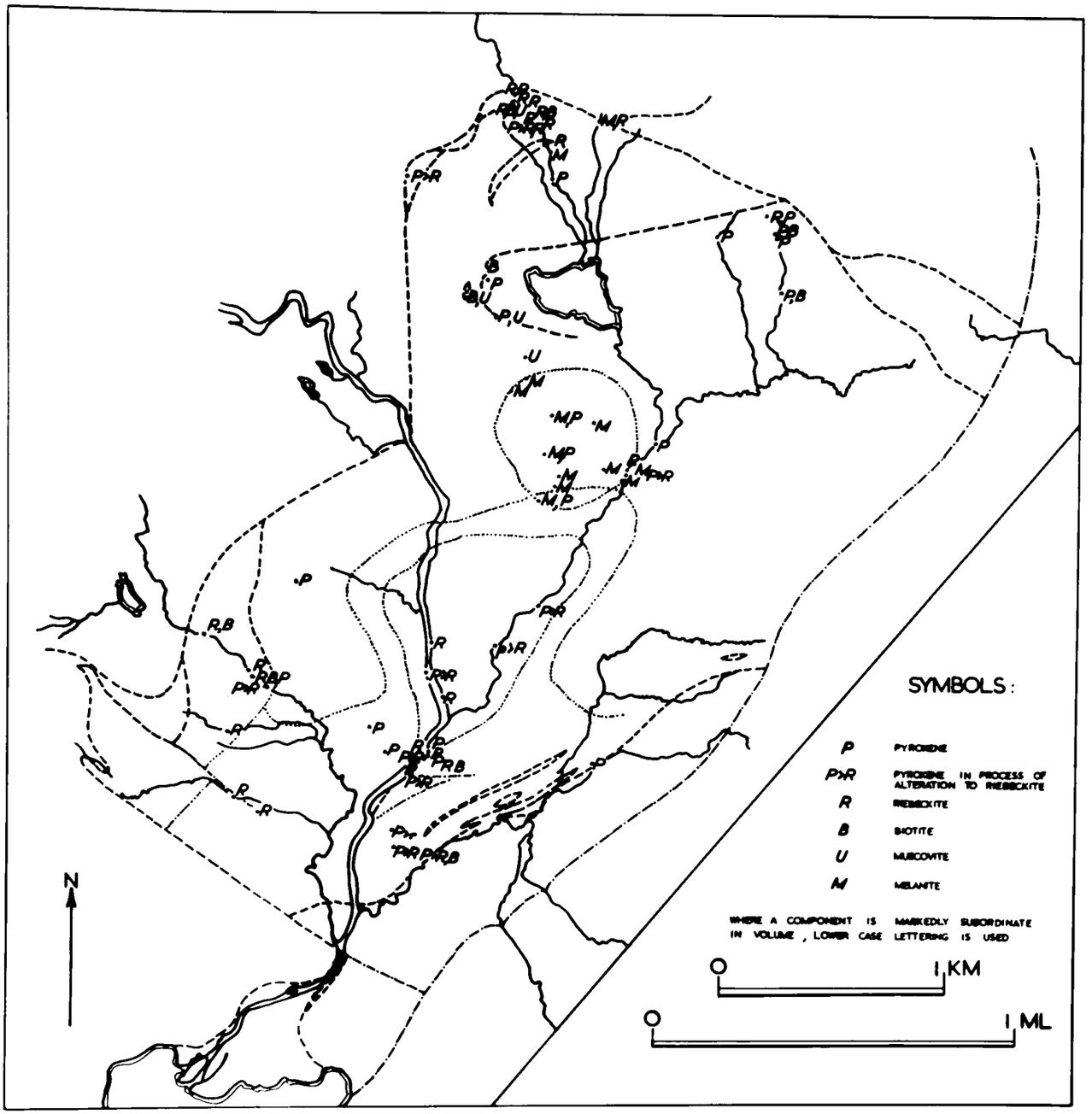
SYMBOLS :
P PYROXENE
P>R PYROXENE IN PROCESS OF ALTERATION TO RIEBECKITE
R RIEBECKITE
B BIOTITE
U MUSCOVITE
M MELANITE
WHERE A COMPONENT IS MARKEDLY SUBORDINATE IN VOLUME, LOWER CASE LETTERING IS USED
1 KM
1 ML
N

Fig.4.3.

Modal analyses of leuco-syenites.

Triangular diagram of total feldspar-quartz-total mafics , as volume percentages.

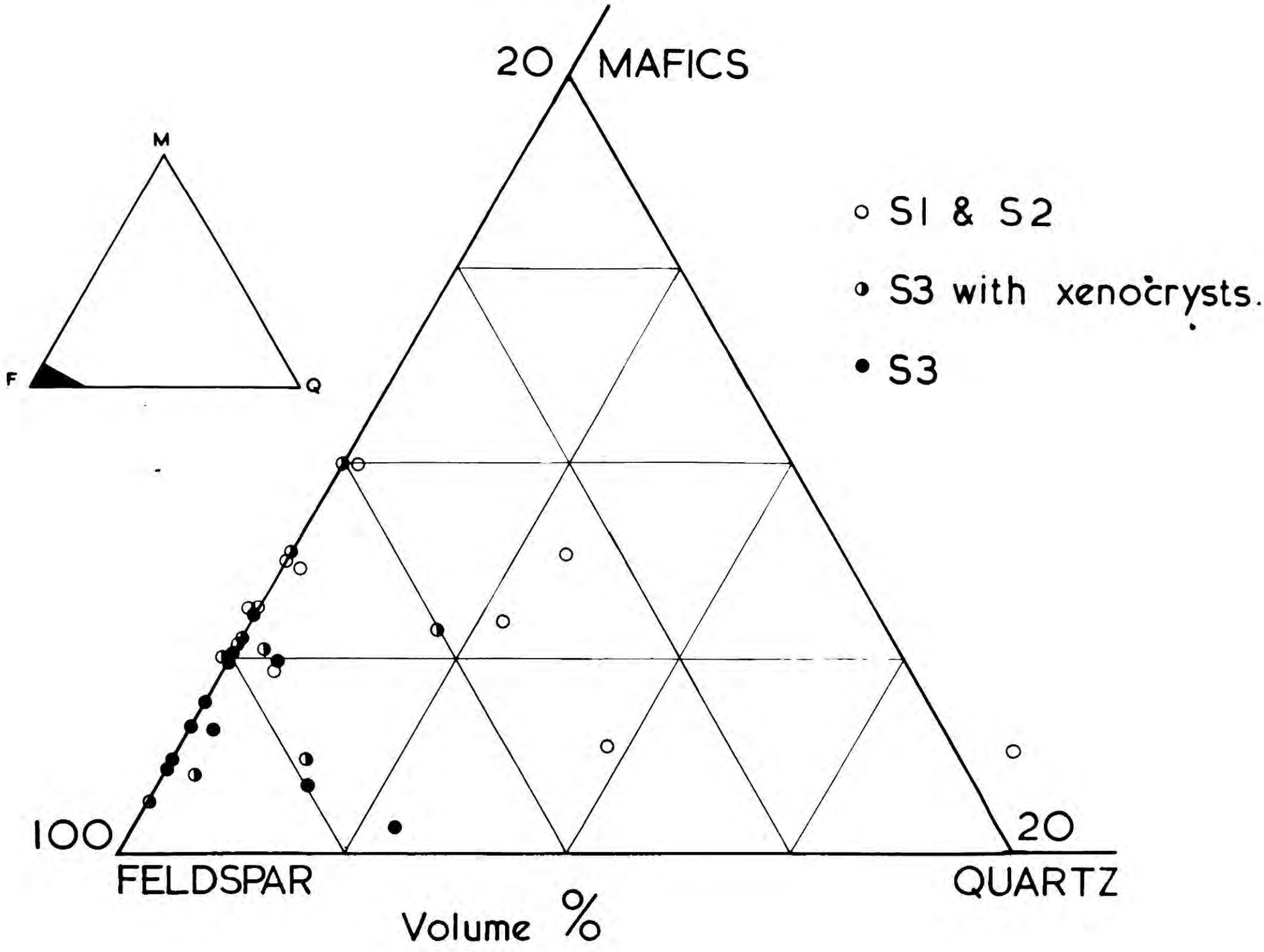
20
MAFICS
M
F
Q
○ S1 & S2
◑ S3 with xenocrysts.
● S3
100
FELDSPAR
20
QUARTZ
Volume %

Table 4.1.

Modal analyses of leucocratic syenites. (Vol. per cent.).

N.B. 'p' = mineral present.

Generation	Specimen No.	Feldspar	Quartz	Pyroxene	Amphibole	Biotite	Muscovite	Melanite	Sphene	Apatite	Opaques	Calcite	Zircon	Others	N.B.
S1	311	89.6	-	7.3	-	0.1	-	-	1.0	0.6	1.4	-	-	-	
	313	82.3	-	15.2	-	0.2	-	-	0.6	0.4	1.4	-	-	-	Foliated.
S2	17	93.0	-	-	5.6	p	-	-	0.1	p	0.6	0.7	-	-	
	19	92.5	-	-	5.8	p	-	-	p	-	1.7	-	-	-	
	26	88.9	5.1	-	2.6	-	-	-	p	-	3.5	-	-	p+	+Tourmaline.
	53	86.8	4.2	(7.8)		p	-	-	p	p	1.1	-	-	-	
	56b	92.4	0.4	5.1	1.0	p	-	-	0.9	p	0.3	-	-	-	Possibly some subordinate S3 Material.
	59	78.6	18.8	-	2.6	-	-	-	-	-	0.5	p	-	-	
	70	91.4	-	-	7.4	p	-	-	0.6	-	0.5	p	-	-	
	92	87.7	9.5	2.7	-	-	-	-	p	p	0.1	-	-	-	
	24	89.9	-	9.3	0.2	-	-	-	0.4	-	0.2	-	-	-	
S3 with xenocrysts	12	94.9	p	(3.1)		-	-	-	p	-	2.0	-	p	-	
	16a	90.7	4.4	4.5	0.2	-	-	-	p	-	0.2	p	p	-	
	20	91.6	p	0.8	2.2	-	-	-	0.8	p	0.2	-	-	-	
	22a	94.5	p	(5.5)		-	-	-	-	-	0.3	-	-	-	
	23b	92.8	-	-	3.8	-	-	-	p	p	1.2	2.3	-	-	
S3	21f	97.5	-	1.3	0.5	-	-	-	0.3	-	0.4	-	-	-	
	22b	97.2	-	(2.4)		-	-	-	-	-	-	0.4	-	-	
	66	98.2	-	0.2	0.2	p	-	-	p	-	1.4	-	-	-	
	67d	97.4	-	2.3	0.1	-	-	-	0.1	0.1	-	-	-	-	
	67e	98.5	-	p	p	-	-	-	p	p	1.5	-	-	-	
	94	97.0	-	-	0.2	-	1.6	-	p	-	1.2	-	p	-	
Melanite bearing S3	85	92.7	p	-	-	-	-	5.7	-	-	2.5	-	p	-	
	87	94.3	-	0.3	-	-	p	3.8	0.4	-	1.3	-	-	-	
	89	97.4	-	0.3	-	-	-	1.9	p	-	0.4	-	p	-	
	459	90.9	-	5.3	-	-	-	1.9	0.2	-	1.6	-	p	-	
	216	86.7	-	-	-	-	1.5	7.8	0.1	-	-	-	-	3.6+	+Colourless, isotropic zeolite (?)

the rock types.

d) Variation in quartz content.

Leuco-syenites in which quartz is present which can with certainty be said to be original, are comparatively rare, the majority of rocks being quartz free. The crushing frequently observed is often associated with quartz veining, and it is sometimes difficult to ascertain whether quartz is original or introduced. In the table of modal data the quartz volume percentages quoted are for quartz judged to be an original constituent of the rock; i.e. quartz interstitial to or sometimes irregularly intergrown with the feldspar, rather than present in aggregates of grains, or as veinlets.

Original quartz cannot usually be seen in hand specimen, and thus it is not possible to map areas of quartz-bearing syenite in the field. The most marked concentration of quartz-bearing types is in the S2 of the area around the confluence of the River Oykel and the Allt Sail an Ruathair. Quartz is rarely found in non-xenocryst bearing S3, but is abundant in xenocryst-rich varieties, suggesting that quartz too was contributed by the earlier rock.

e) Contamination by country rock.

In the foregoing remarks discussion has been restricted to minerals in associations that show no evidence of their being derived by reaction with country rock, and are therefore true products of crystallization of the alkaline magma. However, in the Metamorphic Burn area and elsewhere clear examples of incorporation of mafic minerals at contacts with, in particular, limestone, are to be seen. Quartz may also be incorporated from xenolithic Cambrian quartzites. This form of contamination, which was recognized by Phemister (1926, pp.95-102), will be

dealt with in separate sections.

f) Minerals of the leuco-syenites.

(i) Pyroxenes.

A pleochroic apple green pyroxene is especially well developed in the S2 of rocks of the central area. Attempts to find the unit cell dimensions b and a sin β by the X-ray technique outlined as the appendix to this chapter, were only partially successful. The diffractometer peaks believed to represent the relevant reflections were ill defined but appeared to bring the cell parameters into positions between those of aegirine and those of the soda-free diopsidic pyroxenes measured. In the absence of analytical data it is not possible to specify their position in the aegirine-augite series.

(ii) Amphiboles.

No special work was carried out on the numerous amphiboles of the intrusion. The characteristic purple amphibole of the leuco-syenites will be referred to as riebeckite on the same grounds as Phemister (1926, p.34). It is present as an alteration of pyroxene, or in some cases, apparently as an original mineral. Fig. 4.4 shows this amphibole in development along fractures in, and rimming, a pale green pyroxene core, the amphibole being again rimmed by a darker green pyroxene. This is in an xenocryst bearing variety of S3, and suggests that this stage of alteration of pyroxene to amphibole preceded the incorporation of the S2 material in S3.

(iii) Melanite.

A golden brown garnet occurs in two different settings in the mass. In the massive syenite of the South Top of Sail an Ruathair a garnet is present over a nearly circular area with a vertical thickness

Fig.4.4.

Photomicrograph (Specimen 63) showing a zoned pyroxene in a xenocryst bearing variety of S3, riebeckite having developed around and within the inner zone of pyroxene before its incorporation into S3, when a darker pyroxene formed outside the riebeckite. (Crossed nichols, X70).

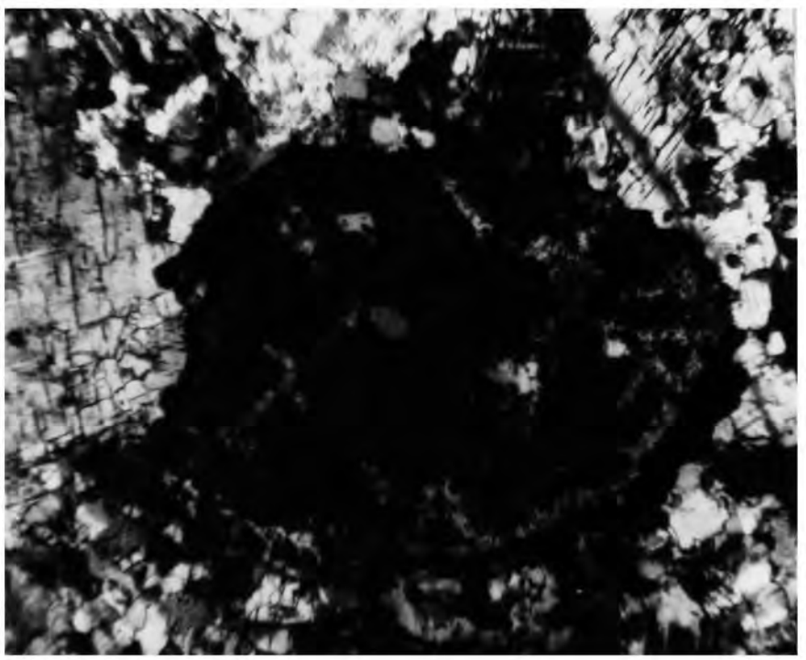

of at least 550 feet. In the Metamorphic Burn a white feldspathic type contains an abundance of small garnets. The Sail an Ruathair garnets are frequently intergrown with sphene and aegirine, (Fig. 4.5a) and are homogeneous in colouring. The rock from near-by limestone in the metamorphic burn contains only colour-zoned garnets as dark minerals, the cores being a deeper brown than the rims (Fig. 4.5b). The apparent association of this rock with a limestone mass perhaps suggests that this rock should be considered in section 2, with contaminated rocks. A colourless isotropic zeolite with colourless micaceous inclusions was believed by Phemister (1926) to represent pseudomorphs after a feldspathoid. Another example of brown garnet at the horizon of limestone xenoliths was found at the top of the Burn east of the Metamorphic Burn (Specimen 282, Fig. 4.5c). Here a mass of colour zoned granules is aggregated with opaque material. In the S2 area at the base of the South Top of Sail an Ruathair in the Allt Sail anRuathair a feldspathic dyke was found carrying skeletal garnets (Fig. 4.5d, Specimen 56a).

The unit cell edge of a specimen from the South Top of Sail an Ruathair (89) and another from the Metamorphic Burn (216), were determined from X-ray diffractometer traces, and are compared below (Table 4.2) to examples of andradite and schorlomite, quoted by Deer, Howie and Zussman (1962).

The large cell dimensions of the Loch Ailsh specimens show that they are true members of the melanite-schorlomite series, and comparison with the specimens quoted from Deer, Howie and Zussman (1962) shows that they lie approximately midway between their andradite and schorlomite examples. Determinative data relating composition to cell size does not exist for this range.

Fig.4.5.

Examples of different occurences of melanite.

A: Intergrown with aegirine and sphene, spec. 87., S.Top, Sail an Ruathair. The dark mass at the top is aegirine, the angular portion at the bottom, sphene. (Ord. light, X25).

B: Colour zoned melanite, rock 216, Metamorphic Burn. The large hexagonal grain has a darker brown core. (Ord. light, X40).

C: Granular melanite and ores. Stream E. of Metamorphic Burn. Spec. 282. (Ord. light, X40).

D: Skeletal melanite, dyke in S2, Central Area. Spec. 56a. A euhedral sphene and perthite lamellae can also be seen. (Ord. light, X25).

A

B

C

D

Table 4.2.

Cell dimensions of Melanite Garnets.

Specimen No.	Locality	a (Å)	Appearance
89	Base of South Top, Sail an Ruathair.	12.055	Golden brown in thin section.
216	Metamorphic Burn, 4' from Limestone.	12.037	Colour-zoned. Deep brown cores.
(4)	In metamorphosed andesite, Cotil Bay, Jersey. *	11.996	Chestnut brown. Massive.
(10)	Oberbergen. *	12.104	Black, well crystallized.

Mol. per cent. end members:

	(4)*	(10)*
Almandine	5.5	2.4
Andradite	78.5	93.7
Grossular	12.3	-
Pyrope	0.1	3.1
Spessartine	3.6	0.8
	ANDRADITE	SCHORLOMITE

* From Deer, Howie and Zussman, 1962. Vol.1, Table 15.

Section 2.

Rocks produced near contacts between leuco-syenite and country rocks.

a) Introduction.

In this section rocks are described which broadly fall into three main groups.

Sub-section (b): Predominantly leuco-syenite with included material clearly derived from xenolithic country rock-"contaminated" syenites.

(c) Country rock with some material derived from the intruding leuco-syenites.

(d) Contact metamorphosed country rocks.

This section is included before that on the mafic feldspathic types of the River Oykel and the Black Rock Burn, because in the cases considered here there can be no doubt as to the origin of the basic material. In the following section remarkably similar rocks are described for which a totally different origin has previously been invoked (Phemister, 1926).

b) Contaminated leuco-syenites.

Examples of rocks falling into this category are found at numerous localities in the Metamorphic Burn, and throughout the xenolith rich northern side of Coire Sail an Ruathair. The rocks described always demonstrably margin, or are closely associated with xenolithic sediments. On fig. 2.5 an attempt is made to show these rocks in the Metamorphic Burn, but their irregular and gradational nature of necessity makes recognition of all examples in the field difficult, and in fact they may be more widespread than indicated. To underline the essentially irregular and inhomogeneous nature of these types a series of photographs of entire thin sections are given, together with brief descriptions in

Fig.4.6. ABOVE

Photograph of entire thin section, presented in negative form. (Ord. light, X5).

Specimen 207, base of Metamorphic burn.

Leuco-syenite margining a limestone xenolith encloses coarse well-formed, green pyroxenes, and euhedral sphene. (Far left).

Fig.4.6.BELOW

Photograph of entire thin section, presented in negative form. (Ord. light, X5).

Specimen 21e, Falls, R.Oykel.

Leuco-syenite margining a basic xenolith encloses similar well- formed green pyroxenes , as well as fine ragged grains.

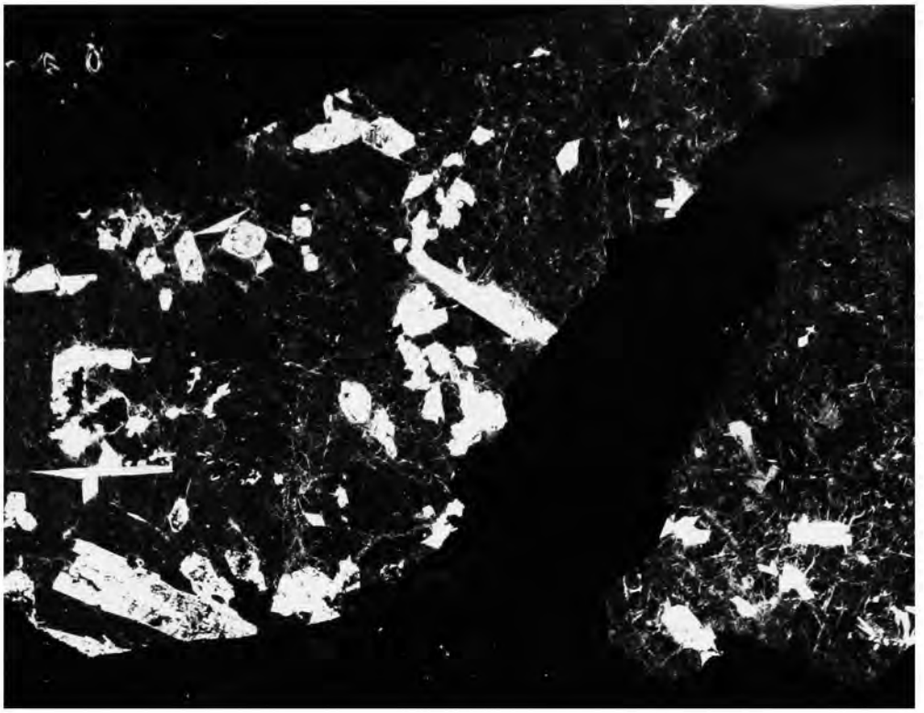

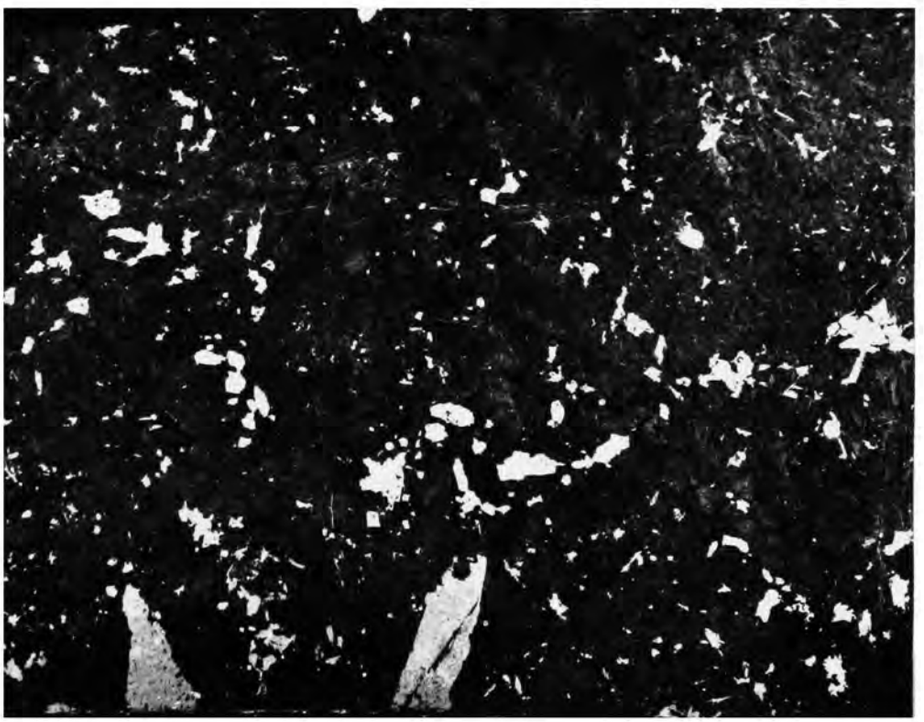

Fig.4.7.

Photographs of entire thin sections.(Presented in negative form.) Ord. light; X5.

ABOVE: Specimen 218, Metamorphic Burn. Mica-amphibole basic clot in leucosyenite.

BELOW: Specimen 238, Metamorphic Burn. Pyroxene -mica -amphibole basic string in leuco-syenite.

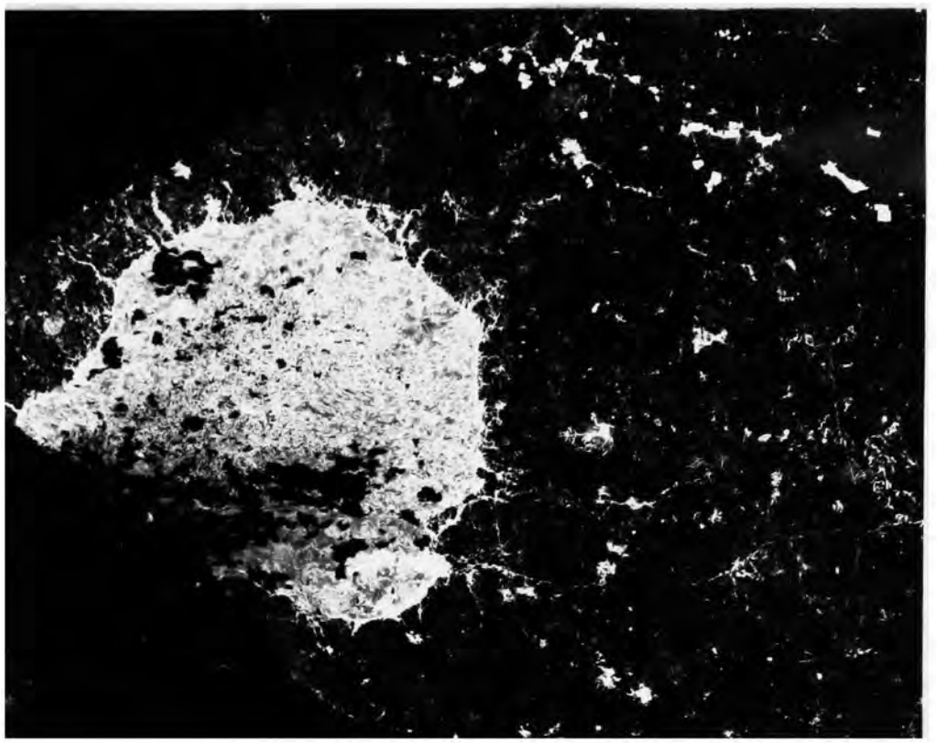

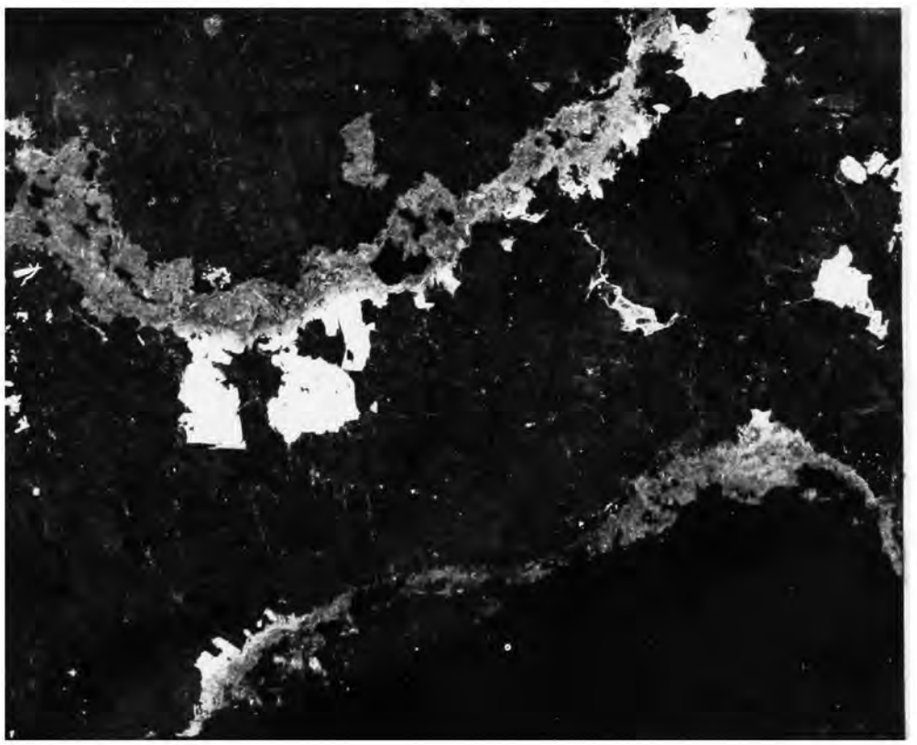

the text following (Figs. 4.6; 4.7; 4.8).

(i) Fig. 4.6 (above). Specimen 207, Base of Metamorphic Burn.

Most of the hand specimen is pale brown S3, but immediately adjacent to a micaceous and diopsidic Durness limestone xenolith, coarse pyroxenes and sphene are enclosed in the feldspathic material. The pyroxene is often euhedral or partially corroded by the normal coarsely perthitic alkali feldspar. This type dies out into normal leuco-syenite (right of picture) at a distance of about 2 cms. from the massive marble xenolith.

For comparison a rather similar texture is illustrated (Fig. 4.6, below) from a rock margining a basic xenolith in the Oykel falls area. Fine twinning can be discerned in the pyroxene. Similar fine lamellae are sometimes developed in specimens from diopside marbles.

(ii) Fig. 4.7 (above). Specimen 218, Metamorphic Burn (see Fig. 2.5 for detail of locality).

At the top right of the photograph euhedral magnetite can be seen in a ragged string. The somewhat angular light area is a crosssection of a small equidimensional mafic inclusion. The pale material forming the outer part of this clot is largely a felted mass of yellow-green mica, and presents sharp faces to the enclosing feldspar. The grey centre of the clot consists of a finer textured purple amphibole, with a little green mica, and patches of calcite.

(iii) Fig. 4.7 (below). Specimen 238, Metamorphic Burn (see Fig. 2.5 for detail of locality).

In this case the basic material is included as ragged edged bands. Such a band runs across the top left of the photograph. The lowest part, appearing white on the photograph, is deep green pyroxene, which is in contact above with an amphibole with the violet-turquoise-straw

yellow pleochroism common in the mass. This in turn becomes gradually colourless and gives way, in the centre of the medium grey band, to a greenish yellow mica. Between the mica and the feldspathic material is a further narrow zone of very pale blue amphibole.

In numerous other rocks from the Metamorphic Burn occur small aggregated includions of mafic minerals of the types described. Such contamination, as demonstrated, can give rise to clots, strings or disseminated inclusions of mafic material in an otherwise normal feldspathic matrix.

(iv) Fig. 4.8. Specimens 277, 278, top of stream ⅛ mile E. of Metamorphic Burn.

These two specimens come from a basic mass about 2' x 3' in outcrop, and exhibit features reminiscent both of the types described above, and of the more homogeneous basic rocks xenolithic in the southern part of the intrusion.

The inhomogeneous nature of both rocks is shown by fig. 4.8. The general textural relations of mafic minerals to enclosing feldspar has exact counterparts in the basic xenoliths of the southern part of the mass. Yet the irregular distribution of mafics, the concentration of pyroxene into one area, of mica into another, is strikingly like the textures described in the foregoing sub-sections.

Specimens demonstrating the enclosure of basic material originating from limestone xenoliths, either as single crystals or as aggregates of crystals, may be encountered at numerous localities throughout Coire Sail an Ruathair.

(v) Specimens 231-236, 238A. Metamorphic Burn. ("Lower Hybrid" of Fig. 2.5).

This is a rock which the writer considers must be described in this section because of its obvious affinities with other contaminated rocks.

Fig.4.8.

Photographs of entire thin sections presented in negative form. (Ord. light, X5).

ABOVE: Specimen 277, stream 1/8 ml. E. of Metamorphic Burn. Margin of xenolith.

BELOW: Specimen 278, central portion of same xenolith.

In both photographs the green pyroxene appears white, mica is medium grey, and feldspar dark. Note that in the upper photograph, part, (centre,top) is micaceous, part pyroxenic, whilst in the lower photograph they are intergrown in ragged aggregates.

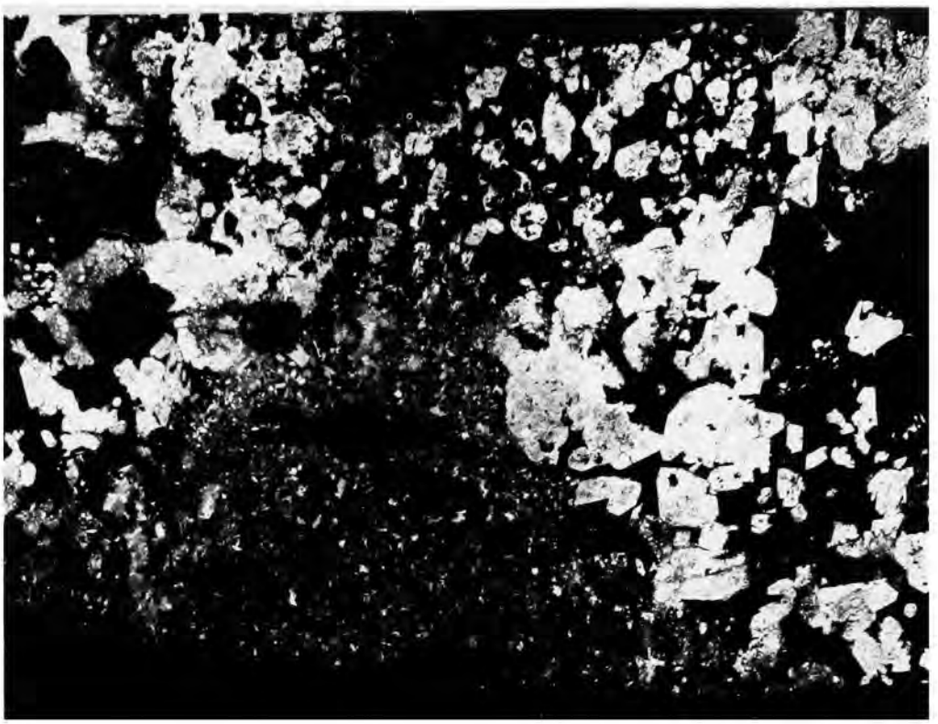

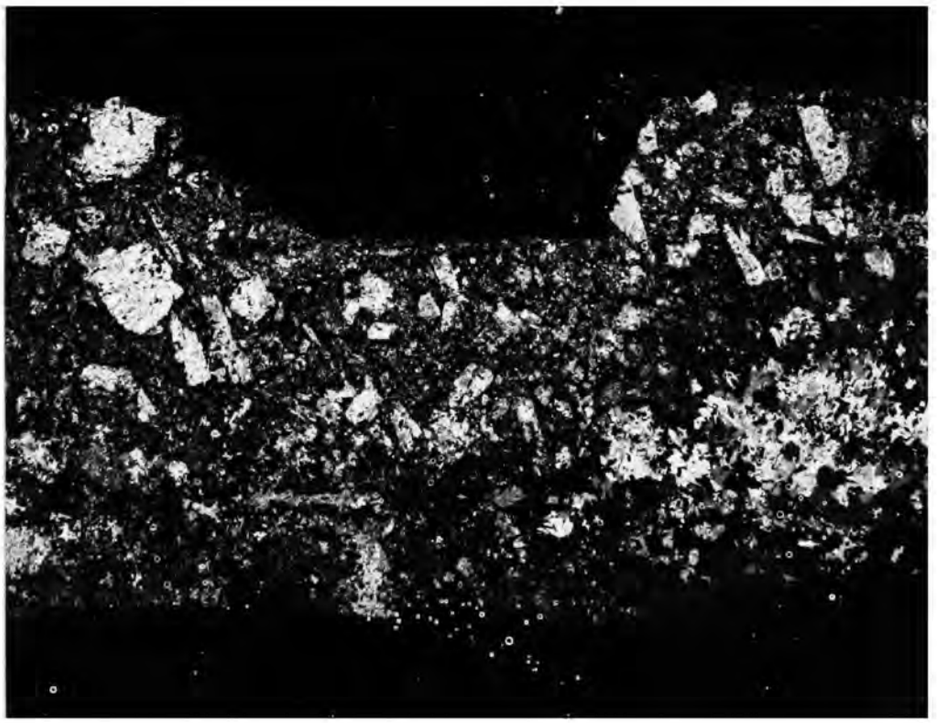

It appears to correspond to the lower of the "shonkinites" reported in the Metamorphic Burn by Phemister (1926), although it is difficult to be certain, as basic alkaline types seem much more common in this series of exposures than his table (op.cit. p.77) would suggest. The rock is massive, not associated with indisputable calc-silicate rocks, and has a strong foliation imparted by alignment of the mafic constituents. (The dip of this foliation is shown on Fig. 2.5). The feldspathic part of the rock is pinkish in colour but the conspicuous mafic constituents impart an overall greenish tinge. The rock is strikingly similar to specimens from the southern part of the mass, with which it was grouped by Phemister (1926). On the other hand there is also a similarity to specimen 278, described previously, and some of the available specimens, 238A and 235, exhibit the sort of inhomogeneity described for rocks 238 and 277. Irregular mafic rich strings of mica, pyroxene and purple amphibole occur. The variable texture of parts of this rock is comparable to rocks which have arisen by contamination of leuco-syenite by country rock. It is included within the horizon of limestone xenoliths. Both these factors, and other considerations to be described below, lead the writer to propose that this rock is a product of contamination of syenite, rather than a differentiate thereof.

(vi) Modifications to leuco-syenite at contacts with quartzite.

The examples of contamination described above concern syenite-limestone contacts. In the upper part of the Metamorphic Burn, syenite intrudes quartzite. Some specimens of syenite from this area show unusually high quartz contents. Rock 266 contains at least 20 per cent. (by volume) of quarts in patches interstitial to the feldspar, not in veins as the case with those rocks which have quartz introduced with the

crushing. It seems likely that some adoption of quartz from the quartzite has taken place.

Another abnormal type of syenite produced at contacts with quartzite is represented by specimens 245, 248, 256, 261, 263, 267 from the Metamorphic Burn (see Fig. 2.5). Whilst most of the specimens come from the horizon of the Pipe-rock, 245 and 248 come from the quartzitic horizon believed to represent the Serpulite Grit in part. This type appears to correspond to the "fine grained shonkinite" of Phemister (1926, p.57), although it is uncertain which of the examples found by the writer corresponds exactly to his example. Specimen 256 differs from the others in that it appears to be associated with micaceous and pyroxenic rocks to be described in Section 2(c). It is probably produced by reaction with a siliceous part of the Fucoid Bed, the pyroxenic and micaceous types corresponding to dolomitic horizons. In hand specimen they are fine grained dark green or grey rocks, although in specimens 245, 248 and 261 coarse pink feldspars may be seen. 256 and 263 both have some pink feldspathic veining.

In thin section the specimens are characterized by a fine grained feldspar matrix of irregular grains, sometimes perthitic, and sometimes representing discreet grains of albite and potassium feldspar. Irregular quartz grains of similar size are sometimes present. Specimens 245, 248, 261 all carry porphyritic feldspars up to 5 mm. in length, with highly corroded margins and cloudy centres. These would appear to represent S1/2 xenocrysts held in a chilled S3 matrix. Set in this matrix are fine granular pale green pyroxenes and green-yellow mica either as individuals or as aggregates. Specimen 263 has mainly fine ($\pm$ 0.05 mm.) biotites arranged roughly parallel, with occasional areas

in which both feldspar and dark minerals are coarser grained, and in which strings of comparatively coarse pale green diopsides occur. Sphene is abundant in these rocks.

c) Metamorphosed country rock with additional material derived from syenite.

There will, of necessity, be a continuous gradation between rocks of the types described in this sub-section and those described in sub-sections (a) and (c). Description of specific examples of the rock types involved will be made.

(i) Specimen 202. Base of Metamorphic Burn.

A description of contamination of the leuco-syenite around this xenolith has been given previously (specimen 201). The specimen considered here, rather than illustrating the contamination of a leuco-syenite with a small amount of basic material, shows the results of invasion of a metamorphosed limestone xenolith by feldspathic material. Part of the thin section has not been invaded by feldspathic material, and in this part of the slide coarse ($\pm$ 2 mm.) blades of pale yellow-green mica are set in, and sometimes enclose, rounded, granular, colourless diopsides. Sometimes the mica is absent, and the rock consists of a close textured mass of fine ($\pm$ 0.2 mm.) equigranular diopside. This texture is characteristic of the diopsidic metamorphosed limestone xenoliths, and is illustrated (specimen 308) in fig. 4.9(a). This zone grades into a rock consisting of the same rounded pyroxenes, now pale green with darker green margins, set with cloudy interstitial feldspars. The coarse mica is absent, but mica is represented now more strongly but similarly coloured, in occasional groups or strings. A feature particularly worthy of note is the retention, in the feldspathic parts, of rounded granular aggregates of diopside with the characteristic close

equigranular texture described. The enclosure of one of these areas in feldspathic material is illustrated as figure 4.9(b). The feldspathic part of this rock is strikingly similar to specimen 435, which comes from the basic xenolith rich part of the Black Rock Burn. The diopsidic aggregates have a close similarity with the diopsidic aggregates observed in other basic rocks from the southern part of the mass and considered to represent a synneusis texture by Phemister (1926). Fig. 4.9(c) shows this texture in specimen 438, and this close similarity will be commented upon in later sections.

(ii) Specimens 250, 252, 258. Metamorphic Burn. "Upper Hybrid" of fig. 2.5.

These specimens are associated in part with rock 256 which was described in the foregoing section. Rock 255 is a wholly micaceous type and will be described in the next section. Rock 252 is a type apparently transitional between the fine grained type represented by 256, and the coarse type represented by 250 and 258. The association of the latter rocks with the micaceous type, 255, and their close textural similarity in their more mafic parts to the diopside marbles of elsewhere, suggests that the feldspar bearing types are derivatives, in part, of metamorphosed limestone. From their position in the otherwise undisturbed "stratigraphy" of the Metamorphic Burn, it seems likely that they represent the feldspathized equivalents of metamorphosed dolomitic bands in the Fucoid Bed.

Rocks 258 and 250 are closely similar. Apple green but only slightly pleochroic equidimensional pyroxenes up to 2 mm. in length, but often less than 0.1 mm., are sometimes held separately in a feldspathic matrix, or are bunched together in the granular aggregates described as characteristic of diopside marbles. The cell dimensions b and a sin β of this pyroxene show it to be close to diopside, despite its strong colouration

Fig.4.9.

A: Typical granular texture of diopside-rock.
(Spec. 308., Metamorphic Burn. Ord. light, X40.)

B: Rounded mass of colourless diopside broken from massive diopside rock and enclosed in feldspathic material. The darker rim is pale green in colour, the centre colourless. Other individual pyroxenes are also pale green in colour , held in the feldspathic part.(Spec. 202, Metamorphic Burn. Ord.light. X40.)

C: Diopside aggregate in a basic type from the Black Rock Burn. Note the granular aggregates of pyroxene, and the overall rounded shape of the pyroxene rich area.
(Spec. 438, Ord. light. x25.)

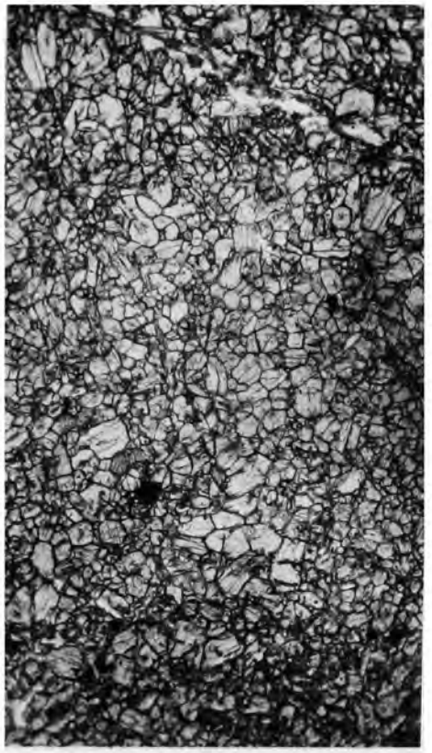

A

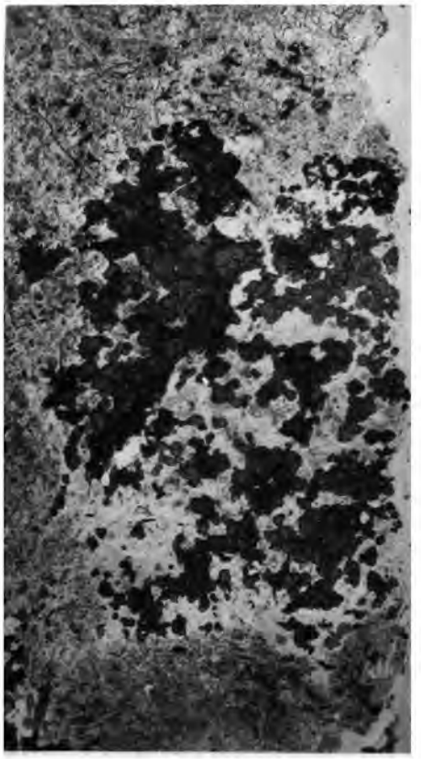

C

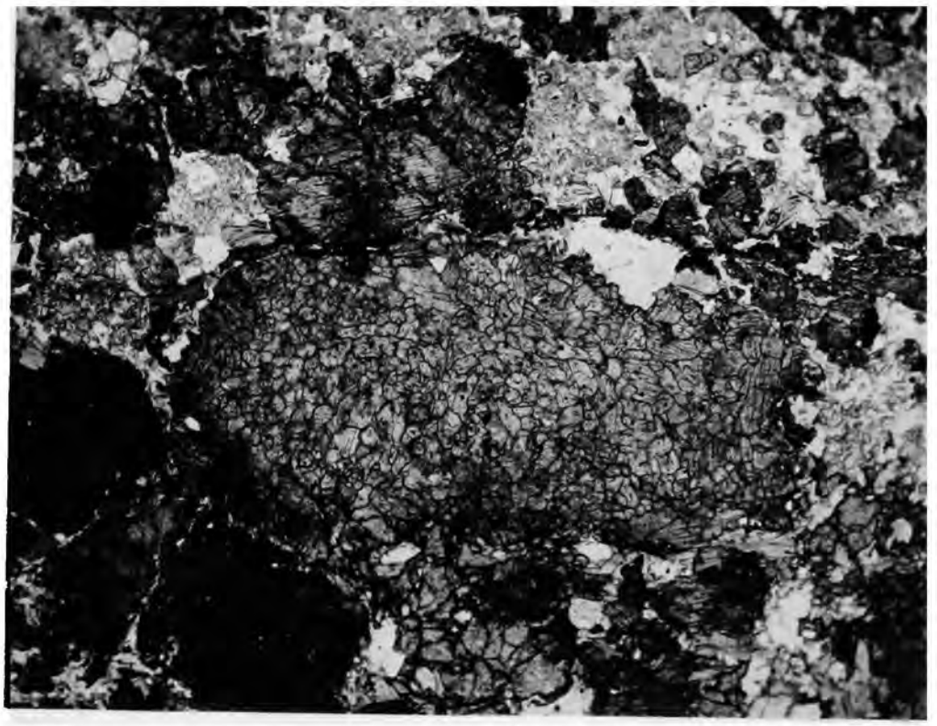

B

(see Section 7). The feldspars are of comparable size to the pyroxenes, and fill interstices between the coarse pyroxenes or are moulded on the finer pyroxene aggregates. The feldspar may be either perthitic, or, rare in the Loch Ailsh mass, be non-perthitic microcline with well developed cross-hatched twinning.

In rock 250 perfect euhedral crystals of an almost colourless but very faintly pleochroic (pale pink to pale blue) amphibole are set amongst the pyroxene. Fractures in 258 contain calcite, rare quartz, and fibrous blue pleochroic amphibole, together with tiny flecks of greenish mica. These rocks have exact parallels with pyroxenic parts of the xenolithic basic types from the southern part of the intrusion. Table 4.3 gives comparative modal data, and fig. 4.10 compares the textures of rocks from these two environments.

Rock 252 also has exact counterparts in the southern part of the intrusion. It consists of a felted mass of green mica (up to 0.5 mm. in length) and pale blue colourless amphibole blades. There are numerous granules of colourless pyroxene, and occasional patches of ore and carbonate. Fine interstitial feldspars are sometimes perthitic, and sometimes are non-perthitic well twinned albite. Comparison is drawn in table 4.3 between this rock and 16e, an ultramafic type from the Black Rock Burn.

d) Contact metamorphosed country rocks.

The previous sections have been devoted to rocks in which material has been contributed (by a mechanical mixing) by the leuco-syenites and country rock. Because in many respects parts of rocks falling into these categories resemble and preserve the textures of the parent sediment, a brief résumé of especially relevant features of the rock types

Table 4.3.

Modal Analyses of Basic Types from the southern part of the Intrusion, and similar rocks from the Metamorphic Burn.

(Vol. per cent.).

Spec. No.	Feld-spar	Quartz	Pyro-xene	Amphi-bole	Bio-tite	Ores	Apa-tite	Sphene	Cal-cite	Others
21c	78.8	-	12.2	-	8.3	0.1	0.3	0.3	-	-
21a	10.4	p	84.8	1.4	0.1	p	p	p	3.2	-
258	17.0	p	74.8	5.0	0.2	p	p	p	3.0	-
16e	9.3	-	39.7	-	50.5	p	p	p	0.5	-
252	4.4	-	(34.2)		56.3	p	0.6	0.4	4.2	-

p= present.

Type and Locality.

21c - Normal basic xenolithic type, Oykel Falls.

21a - Ultramafic 'clot' in above.

258 - Pyroxene-feldspar rock associated with lst xenolith, Metamorphic Burn.

16e - Micaceous ultramafic type, Black Rock Burn.

252 - Micaceous basic type, Metamorphic Burn.

Fig.4.10.

Photomicrographs. (Ord. light. X40.)

ABOVE: Rock 250. Pyroxene-feldspar rock associated with calc-silicate types, Metamorphic Burn.

BELOW: Rock 408. Pyroxene-feldspar rock. Part of intermediate xenolith from the falls , R. Oykel.

Note the irregular distribution of the pyroxene and its tendency to exist as aggregates of equidimensional grains. Compare this texture to that shown in Fig. 4.9.

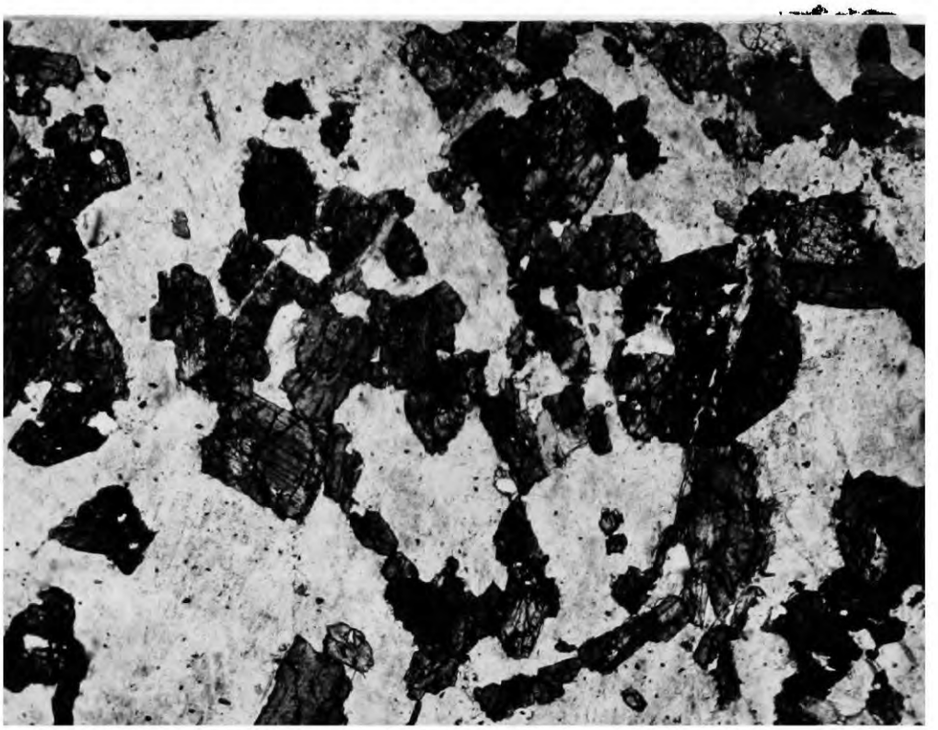

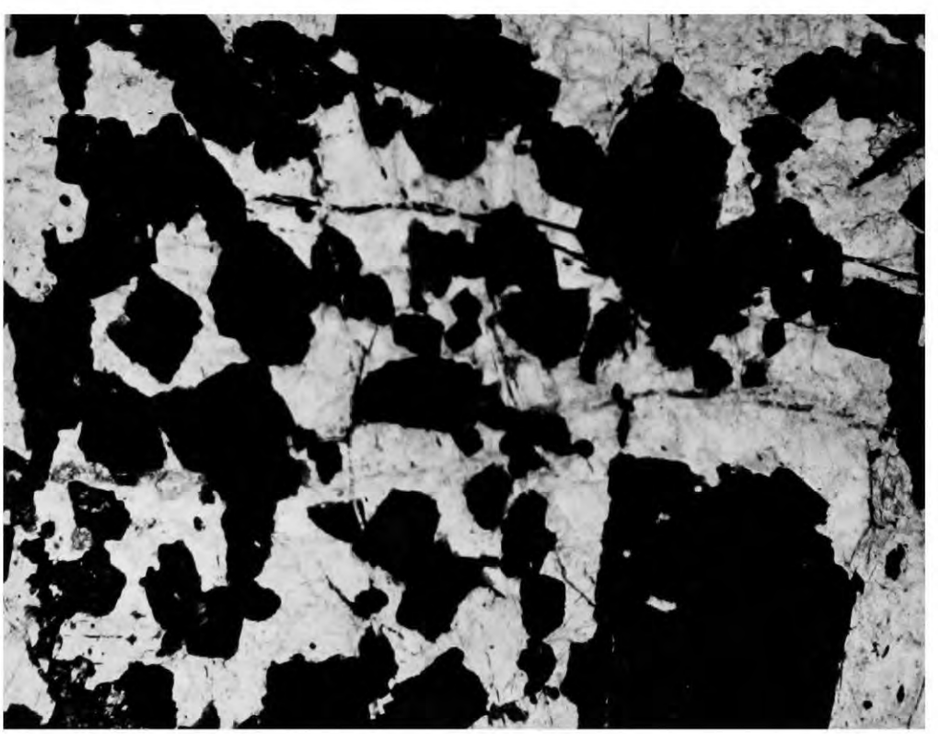

produced by thermal metamorphism (and metasomatism, as opposed to the mechanical mixing described before) of the sediments is given.

Phemister (1926, p.92) described the types of metamorphic rocks produced. Localities at which such rocks were found in this study are shown on the main map (Map 1).

Contact metamorphism of the Pipe Rock.

Numerous xenoliths from this horizon occur at the top of the Metamorphic Burn. Earlier in this Chapter (section 2(b)) basic syenites margining these xenoliths were described. The quartzites themselves are baked to a splintery glassy rock, often white in colour but sometimes adopting a pale greenish tinge. Unlike the specimens described by Phemister (1926, p.92) several of the specimens found by the writer show a development of metamorphic minerals.

Rock 260 is glassy and pale green in hand specimen, with numerous pinkish streaks. In thin section the green colouration is found to be caused by the presence of well formed if somewhat blunted tabular crystals of a pale green pyroxene, individual grains being up to 4 mm. in length. The matrix is of recrystallized quartz. There is a tendency for the pyroxene to occur in fine grained parts of the matrix. It is always associated with numerous apatite prisms, and rounded aggregates of this mineral occur throughout the rock. A very pale bluish amphibole also occurs in ragged skeletal patches, enclosing quartz.

The coarse pyroxene-apatite association in this rock is most unusual. Sometimes the corroded pyroxenes show evidence of breakage, whilst the quartz matrix has recrystallized around them. This perhaps suggests that the pyroxene was introduced into a quartzitic matrix which was able to flow. Certainly these pyroxenes do not in any way resemble the tiny

granular diopsides scattered regularly throughout the metamorphosed carbonate bearing quartzites, which are more commonly found, particularly at the Serpulite Grit horizon.

Metamorphism of limestones.

All the types of metamorphosed limestones described by Phemister (1926, p.92 et seq.) have been found by the writer, the diopside rich type being by far the most abundant with varying development of the micaceous variety, often grading into the pyroxenic type. The diopside xenoliths have a particularly characteristic granular texture (fig. 4.9a) with masses of slightly rounded equidimensional grains in a close packed mosaic. In rock 202 a rounded mass of this type of diopside mosaic was shown breaking away from the massive diopside of the remainder of the section, and being enclosed in feldspathic material (Fig. 4.9b). Numerous other rocks (250, (Fig. 4.10a), 258, 277) show the retention of the diopside hornfels texture in rocks in which feldspathic material has entered.

The hybrid types described are thus characterized by mafic minerals present as aggregates set in the feldspathic matrix. There will be a close similarity between a texture developed in this fashion and the so-called "synneusis" texture described by Phemister (1926, p.57). In the process envisaged by the writer, and illustrated in fig. 4.9, the basic aggregates are in a process of destruction on invasion of the feldspathic material. In the process envisaged by Phemister surface tension was supposed to cause the mafic minerals, crystallizing from the magma, to draw together into the rounded heaps. In the present writer's process, the basic aggregates are relics of a hornfels texture and have not crystallized from the alkaline magma. Although the textural

affinities of pyroxenic types have been considered, the development of mica, commonly intergrown with the pyroxene, has been described in the metamorphic rocks. Comparison of the basic rock types found in the southern part of the mass will be made in Section 3.

Sedimentary xenoliths in the Black Rock Burn.

Three types were found xenolithic in the leuco-syenite of the Black Rock Burn for which a sedimentary origin cannot be doubted. The field relations of these types are described in Chapter 2, section 6.

In thin section rock 490 consists entirely of recrystallized quartz and carbonate, the latter usually rather fine grained whilst the quartz is found in coarse grained lenses, with rims of finer grained material. In hand specimens irregular lenses of dark mica may be seen.

There can be no doubt that this rock is a siliceous limestone in which thermal metamorphism has produced only a limited development of mica. Similar recrystallized rocks with little mineralogical change are found as xenoliths in Coire Sail and massively all along the eastern margin of the mass.

Rock 433 also consists largely of calcite, but a colourless mica is also present in small flakes. Apatite, opaque material and very occasional feldspar grains are also seen. Some of the carbonate is secondary since the feldspars are very cloudy and corroded.

Rock 435 has been compared previously to rock 202, the edge of a limestone xenolith from the Metamorphic Burn. It consists largely of pale diopside in the characteristic granular mosaic, with bands of small feldspars and occasional green biotites.

Section 3.

Basic and ultrabasic types xenolithic in the syenite.

a) General statement.

In this section basic rocks, usually as small xenoliths but sometimes massive, will be described from the Black Rock Burn, from the southern shoulder of Black Rock, the River Oykel around the waterfall west of Cathair Bhàn, and the south-eastern base of the Cathair Bhàn ridge.

Instantly striking in this group as a whole is the variability and inhomogeneity of the rocks visible on a broad scale in hand specimen, and also being apparent in thin section. In the field it may be observed (Figs. 2.7, 2.8, 2.9, 2.10) that the intermediate basic types sometimes have sharp contacts against syenite but sometimes grade into it. They enclose ultramafic fragments, which are themselves sharply or gradationally bounded against intermediate material, and may abut against leucosyenite.

Rather artificially the rocks can be divided into three groups:

1) Feldspar-pyroxene rocks, grading into pyroxenites.

2) Ultramafic mica-rich and sometimes amphibole bearing types.

3) Feldspar-mica-pyroxene rocks, the percentage of mafics being variable between the extremes of (1) and (2).

Even over the short distance of a thin section a transition between any of these groups may take place, mica free areas and pyroxene free areas often grading into one another.

Some comparative modal data are given in table 4.3 (21e, 21a, 16e).

b) Feldspar-pyroxene rocks and related pyroxenites.

Pyroxenite occurs in this group as ultrabasic patches in the more normal intermediate types. In rock 21a the pyroxene is a bright apple green (but has cell dimensions rather close to diopside, whilst those of specimen 225 depart a little from those of the more common colourless diopsides of the mass - see section 7), and occurs as individual crystals up to 5 mm. in length or as a finer grained granular mosaic. There is occasional development of blue amphibole along fractures, and abundant small brown sphenes. The rocks mentioned have at least 80 per cent. of pyroxene, the remainder being largely perthitic feldspar moulded on the euhedral pyroxenes.

At the margins of such ultrabasic types against leuco-syenite, intermediate feldspar-pyroxene types are found, the pyroxenes occurring as individual euhedral crystals or as granular aggregates (21e, 131).

There is a striking similarity between such rocks and mafic types from the Metamorphic Burn, which may be traced into rocks with clear affinities with metamorphosed limestone. Fig. 4.10 compares two such rocks, 408 and 250. The cell dimensions of the pyroxenes are almost identical (see Section 7).

c) Ultramafic mica-rich and sometimes amphibole bearing types.

This type also forms some of the conspicuous ultramafic sharply-bounded patches in the intermediate rocks, and is also present as ill-defined areas in these types. Feldspar is subordinate to the mafic constituents and occurs as irregular interstitial grains or as small aggregates. The remainder of the rock consists of chains of green mica blades enclosing granular aggregates of colourless pyroxene and sometimes individual pyroxenes up to 3 mm. in length. Specimen 401A has a

generally similar texture but consists exclusively of a felted mass of very pale blue to colourless amphibole. The striking similarity between this rock and rock 252 from the Metamorphic Burn has been mentioned (this chapter, section 2,b).

d) Feldspar-mica-pyroxene rocks (common intermediate types). Black Rock Burn and R. Oykel.

These rocks are the characteristic and most widespread type of basic inclusion in the leuco-syenites of the Black Rock Burn, Black Rock, Oykel Falls and Cathair Bhàn areas. The ratio of feldspar to mafics is very variable even in a single thin section, parts of which may tend towards either the pyroxenic or the micaceous varieties described above. Within a few millimetres a thin section may show a change from a rock in which euhedral coarse pyroxenes are set in a feldspathic matrix, through one in which aggregates of pyroxene and mica are intergrown, to a type in which ragged strings and patches of green mica occur, with only rare pyroxene granules. Other areas of the section may be free of mafic minerals and consist of what appears to be normal perthitic feldspar as seen in the leuco-syenites. There is a tendency for the feldspars in the more mafic areas to be rather coarsely exsolved and to show well developed although still narrow albite twin lamellae. Sometimes individual grains of albite are present and in some cases an intergrowth of discreet potassium and sodium-feldspar grains form the matrix of the rock.

The most abundant rock type in the group, however, consists of aggregated granular diopside (see Section 7) and a greenish yellow mica, forming ultramafic 'clots' in the feldspathic matrix. This was described as a synneusis texture by Phemister (1926). In preceding passages, (Section 2,d), development of identical aggregates was described. Rather

than representing the results of growth by clotting together of mafic material as suggested by Phemister, the writer suggests (by analogy with the undoubted cases illustrated) that they represent the incorporated remnants of a texture derived from a metamorphosed limestone parent (see Fig. 4.9, 4.9c representing a rock in the group here considered).

In some cases a pale blue amphibole replaces the pyroxene (419, 479) which in others is accompanied by ragged masses of epidote (475).

The rocks from the base of the cliff on the south side of Black Rock (475, 476, 478 and 479) are strongly sheared, and the mafics are then drawn out into elongate strings of mica and granules of epidote. There is also much secondary calcite.

Base of south-east flank of Cathair Bhàn ridge.

Most of the specimens from this area are in the advanced stage of crushing described above. Rock 221, however, shows no signs of mechanical breakdown and is closely similar to Sron Sgaile rocks of type '4' - '"sieve-mica"-hornblende-feldspar rocks.'

Section 4.

Sròn Sgàile Rocks.

The rocks making up this group largely outcrop in the low broken cliff on the southern face of the spur of Meall an Aonaich known as Sròn Sgàile. Their structural relations remain enigmatic as indeed do the reasons for their mineralogical differences. The only texturally similar rock found elsewhere in the intrusion was that from the Cathair Bhàn area mentioned in the preceding paragraph. Chemically, as illustrated by fig. 4.13, they lie perfectly along the compositional trend of the other L. Ailsh types and are comparable to members of the basic and ultrabasic xenolithic types.

Localities of rocks from Sròn Sgàile of which thin sections were cut are shown on fig. 4.11. Phemister (1926) observed that there was a transition upwards into less basic rocks, and that the transition was through a mixed zone. In this a clear banding expressed by differential weathering (see Fig. 2.6, above) was believed to correspond to the complex mixing of more mafic and leucocratic varieties. The writer's observations suggest that this is a shear zone, since the irregular transition can be shown to take place over a much wider belt than is expressed in the observed banding. Further, thin sections of rocks from the banded zone show obvious evidence of mechanical breakdown which is not generally observed in the Sròn Sgàile rocks.

In this study the rocks were divided into four groups on the basis of mineral content and the textural relations of the mica. The distribution of these types is shown on Fig. 4.11.

Type 1. Ultramafic biotite-pyroxene rock.

One example only of this type was found, at the lowest and most easterly exposure on the hill.

Fig.4.11.

Sketch of Sròn Sgàile (side view, from the south), showing localities of sectioned specimens and the rock types into which they fall.

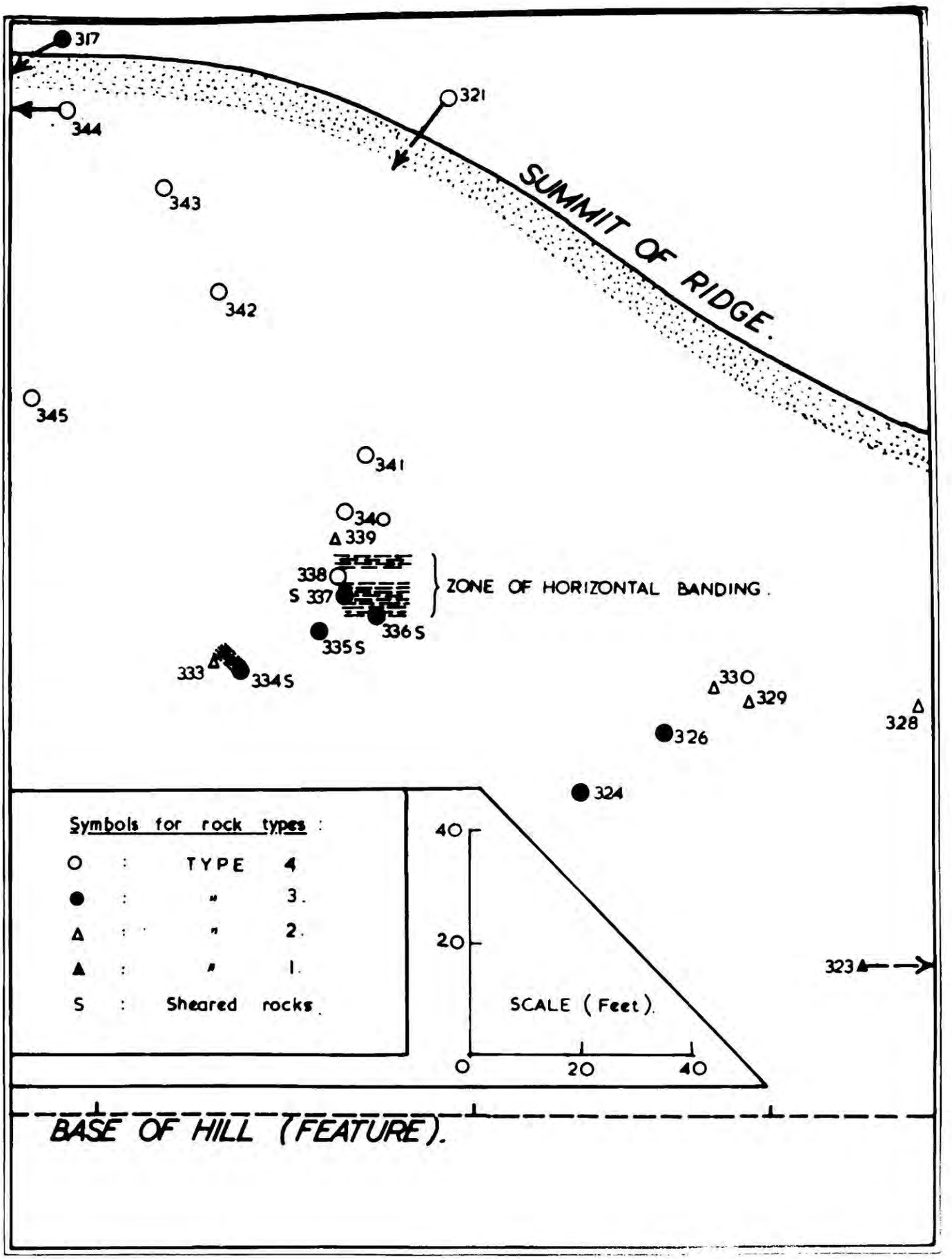
317
321
344
343
342
345
341
340
339
338
S 337
336 S
335 S
333
334 S
330
329
328
326
324
323
SUMMIT OF RIDGE.
ZONE OF HORIZONTAL BANDING.
Symbols for rock types :
O : TYPE 4
● : " 3.
Δ : " 2.
▲ : " 1.
S : Sheared rocks.
40
20
0
20
40
SCALE (Feet).
BASE OF HILL (FEATURE).

The rock contains abundant rather rounded, sometimes close packed colourless diopsides, often with a greenish rim. Sometimes they occur in lenticular aggregates, but more usually appear as stout (± 1 mm. in length) tablets, often rimmed by a green mica, which also occurs as ragged grains enclosing pyroxene. There are also a number of angular areas filled with a colourless amphibole which appear to be pseudomorphs after an unknown mineral. Feldspar occurs as rare interstitial grains, and usually appears to be albite. There are rare grains of quartz.

Type 2. Biotite-hornblende rock.

These rocks consist almost exclusively of a mass of pale green to pale greenish yellow pleochroic hornblende, intergrown with a dark greenish brown to straw yellow pleochroic mica. The interstitial feldspar, which is crowded with tiny colourless grains of high relief, is sometimes well twinned albite, and sometimes appears to be slightly perthitic. Occasional grains of a bright yellow member of the epidote group are present.

Type 3. Feldspar-hornblende rock.

These rocks are a rather more feldspathic variety of type 2; the division made for the purposes of fig. 4.11 was visual only and thus by no means precise. Mica is comparatively rare and occurs as small ragged grains. The pale green amphibole is frequently well formed, and has pale cores and darker green rims. The feldspar is somewhat more coarse grained (+ 0.5 mm.) and individual albite, microcline (with well developed cross-hatched twinning) and perthitic grains are present.

Type 4. 'Sieve-mica'-feldspar-hornblende rock.

This type is generally similar to type 3, but exhibits a characteristic development of mica which makes it at once recognizable. Individual

dark green micas up to 1 cm. in length are always present, and they present characteristic ragged outlines to the feldspar and hornblende, which they also enclose poikilitically (Fig. 4.12). Colourless rounded pyroxenes are also present in some specimens.

General comments on the Sròn Sgàile rocks.

The distribution of these rock types is shown on fig. 4.11. Phemister's observation of a general upward transition to more leucocratic material is born out, and the mixing of types demonstrated. Texturally type 4 rocks have a counterpart in rock 221 from the Cathair Bhàn area. Clearly these rocks have chemical affinities (see Fig. 4.13) with the intermediate rocks of the mass, but their characteristic mineralogy and texture perhaps suggest recrystallization at some stage in their history. Possibly this is in some way related to their nearness to the eastern margin of the mass (bearing in mind the location of 221). Their derivation remains largely a mystery, however, but their chemical affinities undoubtedly suggest a common origin with the basic hybrid types of other parts of the intrusion.

Fig.4.12.

Photomicrograph,(ord. light X25), of "seive" type mica , appearing black , enclosing hornblende, feldspar and occasional pyroxene in the upper rock of Srôn Sgàile.

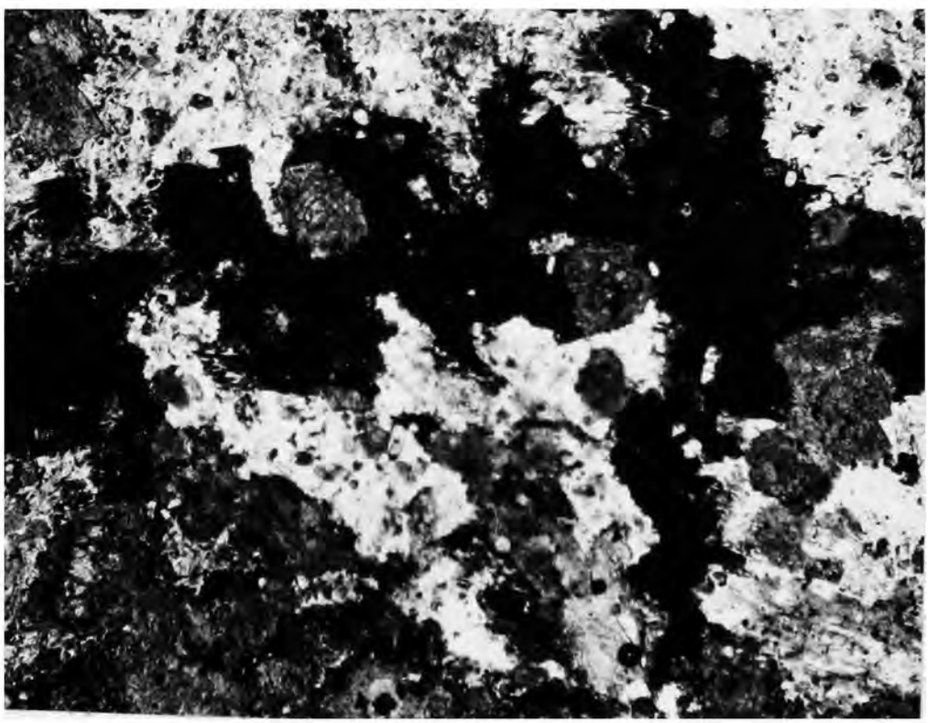

Section 5.

Ultrabasic rocks of Cathair Bhàn.

This suite of rocks gives rise to the magnetic anomalies described in Chapter 3. They were demonstrated to be a steeply inclined sheet margining the syenite where it adjoins limestone, and always following the observed margin of the intrusion.

Modal data are tabulated in table 4.4. It will be observed that feldspar is rare, and in two cases only was judged to be an original mineral; in all other cases it was in veins, and the sections moded were chosen to be free of late additional material.

No constructive additions can be made to the thin section descriptions of Phemister (1926).

Feldspathic veins in the basic rock can be seen breaking off pyroxenes in the manner described previously for the hybrid rocks of the Metamorphic Burn. The pyroxene rimming such veins is converted to a pale green form, the green colour diminishing in intensity away from the contact even in a single crystal.

Other rocks of the Cathair Bhan area.

In the exposures to the E. of the special types of pyroxenites and hornblendites described above are found normal diopside hornfelses and forsterite marbles, demonstrating that the limestone is in the position it occupied at the time of intrusion of the leuco-syenite, rather than being related to syenite by a thrust. An excavation in the slope to the east of Allt Cathair Bhàn, about halfway between the limestone exposures and the stream, revealed a buried scree in which fragments of metamorphosed limestone types were found, and included one example (286) of a fine grained feldspathic vein cutting diopside rock, and incorporating

Table 4.4.

Modal Analyses of Ultrabasic Rocks of the Allt Cathair Bhàn.

(Vol. per cent.).

Spec. No.	Px.	Am.	Bi.	Opaques	Sph.	Ap.	Fsp. (orig.)	Fsp. (Vn.)	Calcite
43	84.4	3.7	0.6	4.2	0.9	0.4	0.5	5.4	0.1
46	68.3	12.6	7.3	11.6	0.2	-	-	-	-
132	75.5	4.1	10.6	8.8	0.7	0.3	-	-	-
91(1)	49.6	4.8	38.3	1.9	1.1	3.4	-	-	0.9
91(2)	42.4	3.9	43.6	4.7	0.5	4.8	-	-	0.1
94b(2)	35.9	1.0	49.6	0.4	0.4	2.7	-	-	-
M22	49.8	1.2	36.3	6.0	3.4	2.9	-	0.5	-
M25	43.1	-	47.0	3.6	1.1	4.7	-	-	0.5
480	-	61.4	11.8	8.5	1.5	2.0	0.4	0.5	8.8

N.B. Additional modal information (opaque minerals only) is given in Table 3.2.

diopside grains in the manner described from the Metamorphic Burn area. Thus feldspathic veining extends beyond the Allt Cathair Bhan ultrabasic types, into the more normal calc-silicate rocks to the east.

The syenitic body seen cutting limestone of the south bank of the Black Rock Burn close to its junction with the R. Oykel, is seen in thin section to consist of a very fine grained feldspathic matrix in which are set corroded perthitic crystals up to 2 mm. in length. This rock is similar to some of the minor intrusives observed within the leuco-syenites and is believed to represent a member of the Assynt suite of dykes intrusive into the limestone.

Section 6.

Chemistry of the Loch Ailsh Rocks.

Fig. 4.13 was plotted (using the analyses tabulated in Phemister (1926)), largely to demonstrate the affinities of the various Loch Ailsh rocks, and in particular the position of Sròn Sgàile types in the range represented.

The composition of the S3 example approximates to the composition determined for the feldspars (see Chapter 5), since the rock is almost monomineralic. The remaining rocks lie on a close approximation to a straight line approaching the SiO_2-(CaO, MgO, FeO, Fe_2O_3, TiO_2) sideline.

The ratio CaO:MgO reveals a sudden and distinct change of magnitude between the leuco-syenites and the more basic types. The actual amount of CaO + MgO in these rocks is much higher than the leuco-syenite, but the ratio CaO:MgO approximates to that of diopside, the most abundant mafic constituent of the basic types. Note also the position of the example (F) of siliceous dolomite from the Fucoid Bed. The plot suggests

Fig.4.13.

Triangular diagram illustrating the range of compositions of L.Ailsh rocks , with some additional data on Cambrian sediments. In addition to weight per cent of the elements quoted the ratio of CaO:MgO (weight per cent) is also shown, using a line normal to the SiO_2-(K_2O+ Na_2O + Al_2O_3) sidelime as abscissa.

The rock names used are those of Phemister (1926) from whom the analyses of the L.Ailsh rocks are taken.

The two examples of Cambrian sediments are from Knox (1941).

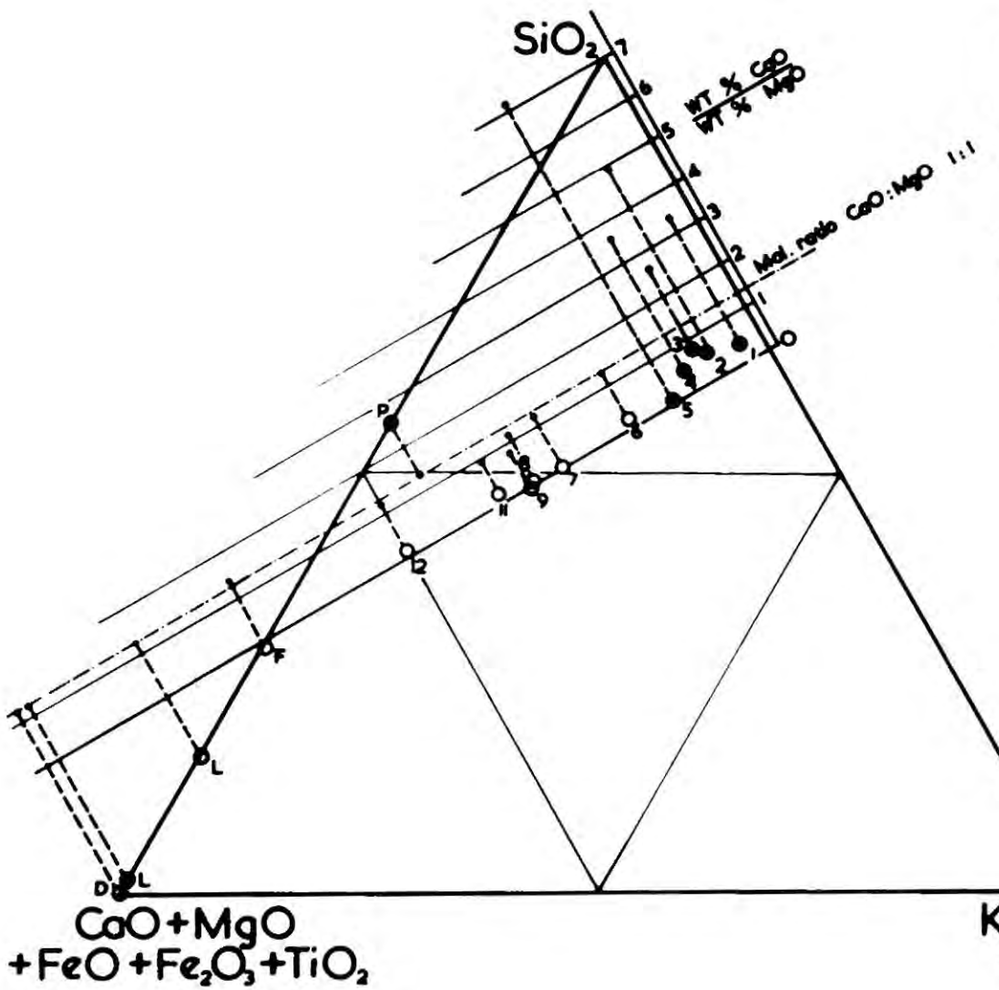

Leucocrates.

1. PERTHOSITE. (S 3)
2. PULASKITE. (S 2)
3. AEGIRINE - MELANITE - SYENITE. (S 3+MEL.)
4. RIEBECKITE PULASKITE. (S 2)
5. MELANITE SY. OF METAMORPHIC BURN. (S 3)

Melanocrates.

6. SPOTTED 'BASIC KNOT.'
7. EPIDIORITIC ROCK. (UPPER SRÒN SGÀILE)
8. DARK 'BASIC KNOT.'
9. FINE GRAINED SHONKINITE.
11. EPIDIORITIC HORNBLENDITE. (LOWER SRÒN SGÀILE)
12. BIOTITE - PYROXENITE.

F. FUCOID BED DOLOMITIC BAND
L. DURNESS LIMESTONE
D. IDEAL DOLOMITE
P. DIOPSIDE.

a sharp discontinuity between the basic types and the leuco-syenites, a break attributable largely to the presence of diopsidic pyroxene. The writer believes that this diopsidic material rather than being a differentiate of the alkaline magma, is an addition derived from metamorphosed siliceous limestones.

Section 7.

Pyroxenes from the complex.

a) Introduction.

The observation has been made previously in this chapter that normally colourless pyroxenes, whether undoubtedly from metamorphosed limestone or from the more obscure Allt Cathair Bhàn pyroxenites, were converted to a green variety of pyroxene around syenitic veins. Some pyroxenes from the pyroxenic clots in the Black Rock Burn and R. Oykel basic types, and some from the Metamorphic Burn, connected with rocks of metamorphosed limestone type, are a bright green, in the former case quite as intensly coloured as the aegirine-augites (see later) from the leuco-syenites. It thus seemed worthwhile to try to establish whether this change in colour was linked to major changes in composition, and whether, in fact, a range of pyroxenes in the diopside-aegirine series was present.

b) Technique.

Pyroxenes were separated from ten rocks by magnetic separator. Smear mounts for the diffractometer were made and the position of the 600, 060, 150 and 510 reflections established. Using a method suggested by Mr. W.G. Hancock (Geology Dept., Durham University), the cell parameters b and a sin β could be calculated. These dimensions are used by

Brown (1960), to define compositions in the system $CaMgSi_2O_6$-$CaFeSi_2O_6$-$Mg_2Si_2O_6$-$Fe_2Si_2O_6$. Details of the method of calculation and of the diffractometer settings used are given in an appendix.

The cell dimensions of aegirine and some members of the aegirine-augite series fall outside the range defined by the trapezium (Fig. 4.14), increase in soda leading to a decrease in both b and a sin β throughout the series, (Yagai, 1958, quoted in Deer, Howie and Zussman, 1962). The parameters measured could not in any case give an unambiguous measure of the sodium content, but it was hoped would suggest whether a gradual trend of sodium enrichment exists, and possibly allow estimates of composition of sodium free specimens.

c) Data.

The results obtained are tabulated in table 4.5 and plotted on fig. 4.14. Also indicated on this diagram are the b and a sin β dimensions of aegirine (after Deer, Howie and Zussman). The compositions quoted at the corners of the trapezium cannot strictly be taken at face value as the amount of sodium, in particular, which may be present is not known. The diagram should indicate composition satisfactorily, however, for the colourless pyroxenes of the metamorphosed limestone xenoliths.

Specimens which depart from the main group and are thus probably soda bearing are shown by solid circles; both specimens are bright green in colour, and it is interesting to note that of the remainder, 250 and 21a are also intensly coloured. Both lie on the side of the main group towards specimens 225 and 25.

The diffractometer patterns of 25 and 16a (not shown as measurement was impossible) were characteristically different from the other specimens in that the relevant reflections were ill defined and had different relative

Table 4.5.

Cell dimensions b and a sin β of Loch Ailsh clinopyroxenes.

(Å)

Spec. No.	Locality	Rock Type	b	a sin β	Remarks*	
272	Burn ½ mile E. of Metamorphic Burn.	Metamorphosed limestone xeno.	8.928	9.384	Very pale yellow-green.	
240	Metamorphic Burn.	"	8.931	9.390	Colourless.	
312	E. side of Coire Sail an Ruathair.	"	8.922	9.378	"	
91	Allt Cathair Bhàn.	Biotite-pyroxenite.	8.916	9.384	"	
21c	Falls, R. Oykel.	Intermediate xenolith.	8.931	9.384	V. pale green.	
250	Metamorphic Burn.	Syenite-meta-limestone hybrid.	8.922	9.375	Bright yellowish green.	
21a	Falls, R. Oykel.	Ultramafic incl. in 21c.	8.922	9.369	Intense pleochroic apple-green.	
225	Allt Cathair Bhàn.	U.B. veined by syenite, W. of main U.B. mass.	8.898	9.322	"	(1)
25	Above falls, R. Oykel.	S2.	8.886	9.298	"	(2)
16a	Black Rock Burn.	S2	not measurable.		"	(2)

N.B. (1) X-ray pattern of intermediate type.

(2) X-ray pattern with characteristic poorly defined reflections, rendering 16a impossible to measure.

* Colour as seen in thin section.

Fig.4.14.

Cell parameters b and a sin β of nine pyroxenes plotted on the diagram of Brown (1960).Open circles are for specimens which appear to be soda-free or low in soda, and the cell dimensions thus may be used as an indicator of composition. The solid circles appear to deviate from the bulk of the specimens and trend towards the value of aegirine (from Deer, Howie, and Zussman , 1962) and are probably soda bearing. The diagram cannot therefore be used as an indicator of composition for these specimens.

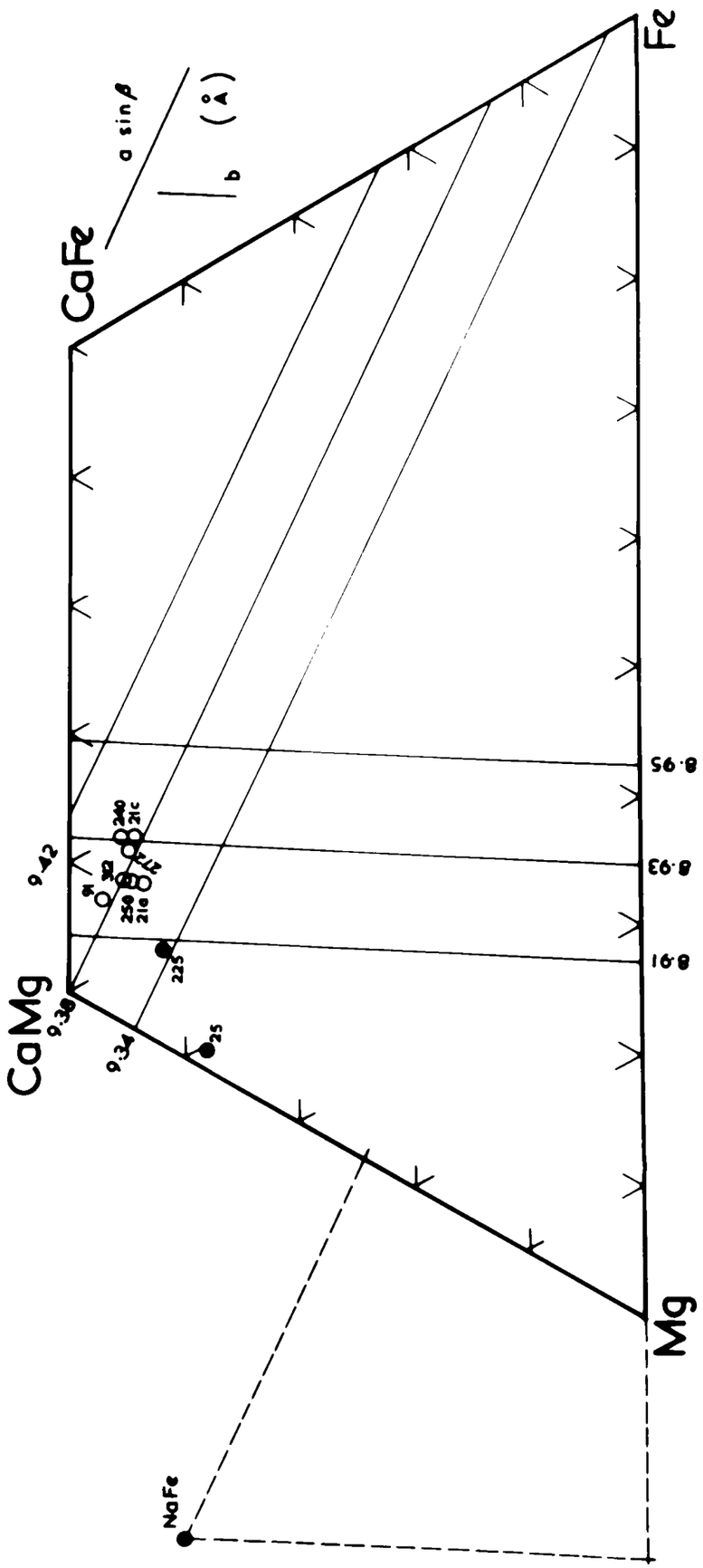
Fe
CaFe
a sinβ
b (Å)
8.95
8.93
8.91
9.42
9.38
9.34
CaMg
Mg
NaFe
225
25
240
21c
250
21a

intensities, allowing these specimens to be differentiated at a glance from the main group. The chart of 225 appeared to lie somewhere between the two types, and indeed plotted in an intermediate position.

d) Conclusions.

The specimens from the ultrabasic rocks, basic xenoliths and metamorphosed limestones with the exception of 225, all fall close together near the diopside corner of the trapezium, and lie around the junction of the diopside, salite and augite fields of Poldervaart and Hess (1951). The other specimens are tending towards the lattice dimensions of aegirine although one could not, on the basis of these parameters alone, differentiate them from endiopside.

The conclusion seems justified that the development of green rims against feldspathic material is a reflection of the adoption of soda, but the green colour of a pyroxene may become intense without appreciable change in the lattice parameters b and a sin β .

Since rock 225 is very similar to 21a but has lattice parameters deviating towards aegirine, it seems likely that this rock alone represents a stage in the metasomatic adoption of soda by diopsidic pyroxenes to give aegirine-augites. Clearly the conditions for this to occur must be very special, since pyroxenes in highly feldspathic rocks such as 250 and 21c are nonetheless close in composition to the diopsides of massive, non-feldspathic diopside hornfels xenoliths. The close grouping of the basic alkaline specimens should be noted. A sharp discontinuity thus exists between the pyroxene of the leuco-syenites and those of the remaining rocks. The cell dimensions of the pyroxenes of the basic alkaline types and the Allt Cathair Bhàn ultrabasics are identical with those of metamorphosed limestone xenoliths, and except in one special case (225) show no

gradation towards those of the leuco-syenites.

Section 8.

General Conclusions.

During this discussion of certain features of the petrography of these rocks a number of significant parallels have been drawn. It has been pointed out that there is a striking similarity between certain rock types produced by contamination of leuco-syenite by material originating from the metamorphism of limestone, and the xenolithic basic alkaline rocks of the southern part of the mass. The origin proposed by the writer for these latter types is based on consideration of the following salient observations:

(i) Definite examples of limestone have been found amongst the basic xenoliths of the Black Rock Burn.

(ii) There can be no doubt that effectively identical types are found at the limestone xenolith horizon in the Metamorphic Burn, and in certain cases can be traced into metamorphosed limestones.

(iii) The group as a whole has great variability.

(iv) The aggregated texture (the synneusis texture of Phemister) of the mafic materials in the basic types is also developed when metamorphosed limestone is broken up and incorporated into leuco-syenite.

(v) There is a discontinuity of composition (Ca:Mg) between the basic and ultrabasic types and the leuco-syenites.

(vi) Pyroxenes of basic alkaline xenoliths, ultrabasic types and metamorphosed limestone xenoliths are identical.

There are thus spatial, textural and chemical relationships between the basic alkaline xenoliths and metamorphosed limestone, and it is

believed that the evidence presented suggests that the former type are the result of incorporation of metamorphosed limestone into feldspathic material, in a largely mechanical fashion. (The aggregate texture and similarity of composition of pyroxenes suggest this).

The Allt Cathair Bhàn ultrabasics are believed to have a similar origin. They are a natural extreme of the trend shown by progressive basification of leuco-syenite, and their position at the contact of the leuco-syenite against limestone has been proved (Chapter 3).

Conversion of dolomite to diopside-mica assemblages (with the adoption of potash from the syenite) and subsequent incorporation of this material into the invading alkaline magma, gave rise to types reflecting the universal variety observed in the metamorphic rocks. Sometimes individual crystals are incorporated, sometimes aggregates retaining the textural features of the parent metamorphosed dolomite. Thus a continuous gradation exists from the leuco-syenite with rare additional mafic material, to the ultrabasic pyroxenic or micaceous types. Since the basic material is xenolithic in the leuco-syenite, contacts may be sharp, where the mixing of alkaline and basic material took place at an earlier pulse of intrusion than that now enclosing the xenolith, or gradational, when the mixing is taking place in situ.

The writer does not consider that the spatial, textural and chemical relationships of these rocks are compatible with an origin as differentiates of the alkaline magma. The term 'hybrid' has been adopted and used elsewhere in the text to cover these rocks produced by mixing of metamorphic and igneous material in varying proportions.

Bibliography to Chapter 4.

BROWN, G.M. (1960). The effect of ion substitution on the unit cell dimensions of the common clinopyroxenes. Amer. Min., vol.45, p.15.

DEER, W.A., HOWIE, R.A. and ZUSSMAN, J. (1962). "Rock-Forming Minerals." Longmans.

KNOX, J. (1941). "Dolomite and Brucite Marble in the Scottish Highlands." Supplement No.2. Geol. Surv. of Great Britain, War-time pamphlet No.6.

PHEMISTER, J. (1926). in 'The Geology of Strath Oykell and Lower L. Shin.' Mem. Geol. Surv., Scotland.

POLDERVAART, A. and HESS, H.H. (1951). Pyroxenes in the crystallization of basaltic magma. Journ. Geol., vol.59, p.472.

Appendix to Chapter 4.

X-ray technique for determination of b and a sin β of clinopyroxenes.

(Suggested by Mr. W.G. Hancock, Durham University Geology Department).

Basis of Method.

Brown uses the cell dimensions b and a sin β for compositions in the CaMgFe triangle.

These are most easily calculated using reflections with h = l = 0, for b and k = l = 0 for a sin β , since the general formula for monoclinic crystals is:

$$\frac{1}{d^2_{hkl}} = \frac{h^2}{a^2 \sin^2\beta} + \frac{l^2}{c^2 \sin^2\beta} + \frac{2hl\cos\beta}{ac\sin^2\beta} + \frac{k^2}{b^2}$$

so that, for a reflection 0k0 :

$$\frac{1}{d^2_{0k0}} = \frac{k^2}{b^2} \quad ; \quad b = k d_{0k0} . \qquad (i)$$

and for a reflection h00 :

$$\frac{1}{d^2_{h00}} = \frac{h^2}{a^2 \sin^2\beta} \quad ; \quad a \sin\beta = h d_{h00} . \qquad (ii)$$

The only suitable reflections in practice are 600 and 060. The indexing of the reflections and possible mistakes in measurement can be checked (but their accuracy not increased) by use of the nearby 150 and 510 reflections, in which case:

For 150 :

$$b = \frac{5}{\sqrt{\left(\frac{1}{d_{150}} + \frac{1}{a\sin\beta}\right)\left(\frac{1}{d_{150}} - \frac{1}{a\sin\beta}\right)}} \qquad (iii)$$

and for 510 :

$$a \sin\beta = \frac{5}{\sqrt{\left(\frac{1}{d_{510}} + \frac{1}{b}\right)\left(\frac{1}{d_{510}} - \frac{1}{b}\right)}} \qquad (iv)$$

X-ray technique.

Smear mounts with silicon internal standard were used.

Instrument settings were:

Radiation: CuKα at 40 kV 20 mA, Ni filter; slits 4° - 0.2 - 4°.

Scanning speed: ⅛°/min.

Chart speed: 200 mm/hr.

Rate Meter: 4, Time constant: 8.

Pulse height discriminator used at attenuation 4, amplitude 302, channel width 4.

Silicon reflections 220 at 47.302° 2θ and 311 at 56.122° 2θ were used as standard peaks.

CHAPTER 5.

THE ALKALI FELDSPARS.

Contents:

c) Nature of the potash phase.

d) Obliquity of the potash phase.

6) Single crystal X-ray data.

a) General data.

b) S1-S3 contact relationships.

Section 2. Discussion.

7) Crystallization temperatures.

8) Subsolidus history.

a) Early stages of exsolution.

b) Late stages of exsolution and ordering of Al and Si.

A) Local coarsening of the perthitic intergrowth.

B) Variations in the nature of the potash phase.

c) Effects observed at contacts. Contrast between xenocrysts and host rock.

d) Persistence of orthoclase.

e) Limited diffusion of volatiles.

f) Variable structure of orthoclase.

g) Variable obliquity of microcline phases.

Bibliography.

Appendices.

1) Diffractometer settings.

2) Details of diffractometer patterns between 20° and 33°.

3) Separation of perthites into phases.

4) Potash enrichment.

5) Orientation of alkali feldspar specimens for single crystal X-ray oscillation photographs.

6) Detailed description of single-crystal photographs.

7) Heating experiments.

Abstract.

The alkali feldspars of the intrusion are described in terms of their appearance in thin section, optic axial angle, bulk composition and X-ray powder and single crystal properties.

They are shown to be low-albite-microcline and low-albite-orthoclase perthites in the compositional range Or_{27} to Or_{41}. Early phases of the intrusion differ fundamentally from the later in the relative proportions of monoclinic and triclinic material present in the potassium phase. There is a suggestion of a systematic distribution of microcline obliquities throughout the mass.

Very little modification of early feldspars was found at contacts between syenites, and xenocrysts preserve higher temperature features than host material.

Compositions of the feldspars are discussed in the light of experimental knowledge of liquidus-solidus relations in the Ab-Or-An system and minimum crystallization temperatures suggested. The variation observed in the nature of the potash phase and in the form of the perthites is not thought to depend primarily on the Caledonian thrusting but probably on the concentration of volatiles during the cooling of the rock. The apparent metastable preservation of orthoclase bearing forms is discussed and a possible mechanism suggested.

Introduction.

The leucocratic syenites of Loch Ailsh consist predominantly of perthites which exhibit a considerable variety of forms. The occurrence of a range of perthites showing varying coarseness of exsolution from fine blebs to coarse patches or even discreet grains was noted by Phemister (1926, p.25), who commented that segregation of perthite into

its components was common in rocks that have recrystallized, either as a result of deformation or because of the presence of hot solutions. His early observation of the significance of the exsolution process in the formation of the common textures of the acid and alkaline igneous rocks was quoted by Tuttle (1952) in his important discussion of the origin of the contrasting mineralogy of the extrusive and plutonic salic rocks. Furthermore there are in the L. Ailsh mass several distinguishable generations of syenites whose feldspars have obvious differences both in hand specimen and in thin section. The contact relationships between the different rock types are well established and contacts with country rock, as massive xenoliths or protrusions, are present in the Metamorphic Burn area.

Thus it seemed that a detailed investigation of the alkali feldspars of these rocks could yield valuable information on both the relationships between the syenites themselves and on the behaviour of a suite of perthites of several types. The work was greatly facilitated by the extreme leucocratic nature of the rocks, and absence of plagioclase as a separate phase rendering lengthy separation procedures unnecessary.

A locality map of feldspars described is shown together with specimen numbers as quoted in brackets throughout the text, (Fig. 5.1).

A number of abbreviations of common terms will be used in the text as tabulated below:

Ab : ALBITE.

Or : ORTHOCLASE, used generally for the potassium feldspar molecule. When a low temperature monoclinic potassium feldspar is specifically implied the term "orthoclase" will be quoted in full.

Mi : MICROCLINE.

Fig.5.1.

Outline map of the intrusion showing localities of rocks from which feldspars have been described, with specimen numbers as used in the text.

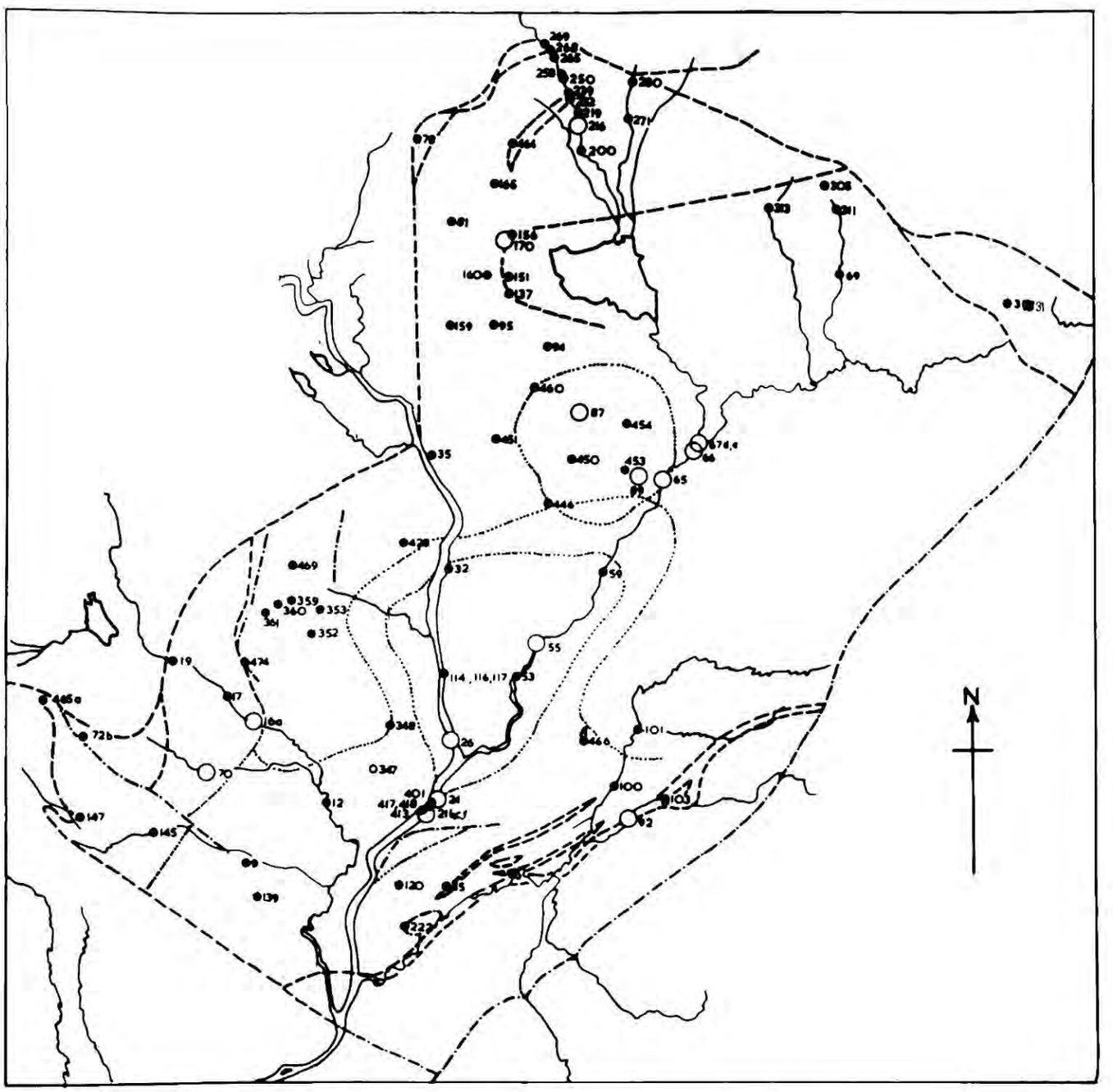
N
O Analysed Specimen.
• X-Rayed Specimen.
O
1 KM.
1 ML

Na-feldspar, Na-phase : Sodium rich feldspar or sodium rich phase of perthite.

K-feldspar, K-phase : Potassium rich feldspar or potassium rich phase of perthite.

An : ANORTHITE.

Q : QUARTZ.

N.B. All X-ray data is for CuKα radiation.

Section 1.

Techniques and Data.

Appearance of the feldspars in hand specimen and thin section.

1) Hand specimen.

In hand specimen feldspars from the early syenites S1 and S2 tend to be pink or reddish brown in colour whilst those of the later syenite, S3, have a grey or grey-brown colouration. This allows contacts between the rock types to be clearly visible and further makes it possible to recognize xenocrysts of S1 and S2 where they are held in S3. At the western contact of S1 on the North Top of Sail an Ruathair, where the rock is strongly laminated, crystals often exceed 2.0 cm. in length, in contrast to the intruding S3 in which feldspars rarely exceed 0.5 cm. in length and are usually much less. Rarely throughout the mass do S3 feldspars approach 1 cm. in length; for the most part half this value is more typical.

Material in contact with massive quartzite xenoliths in the Metamorphic Burn are is often chilled to a fine greenish-grey rock in which individual crystals cannot be seen, although in some cases coarse pink xenocrysts are present.

2) Thin section.

Adequate description of the form of perthites in thin section is difficult and thus a series of photomicrographs is shown which attempt to cover the range of types and coarseness of exsolution that may be found in these rocks (Figs. 5.2-3). It is difficult to generalize about the variation exhibited but a few points can be made.

(1) Feldspars from S1.

The finest scale of exsolution seen is in rock 313, a red laminated type from the northern side of Coire Sail an Ruathair. In this rock the

Fig.5.2. Photomicrographs:

A: Fine scale of exsolution in Sl of Coire Sail an Ruathair. Specimen 313. (Crossed nichols, X40.)

B: The same grain at higher magnification. (Crossed nichols, X200.)

C: Normal fine Sl perthite. The K-phase in the right-hand grain (of the twinned pair) appears pale. Note the pale lines of complete exsolution running more or less straight across both crystals at various angles. These are presumedto follow fractures.(Specimen 160, crossed nichols, X 65.)

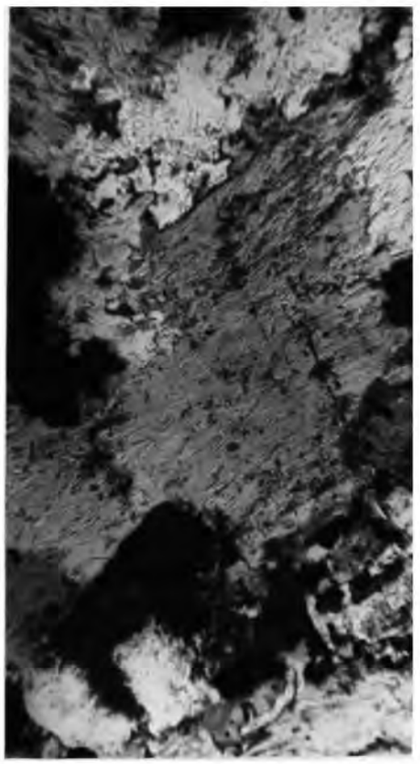

A

B

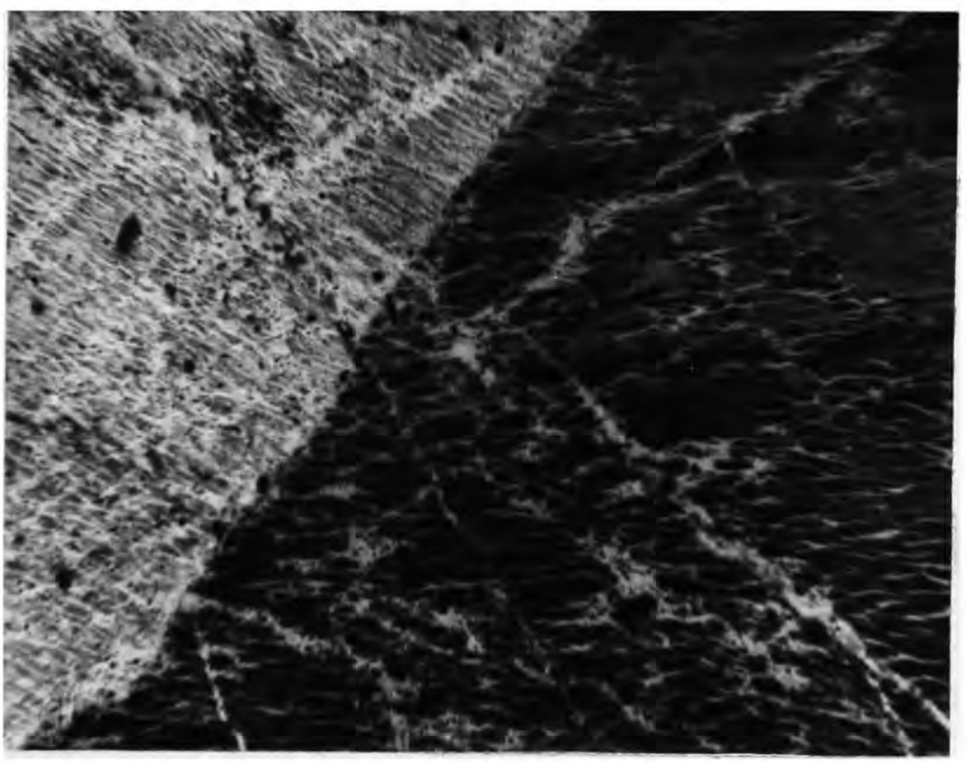

C

K-feldspar is seen as spindles or fine veins in the Na-feldspar host. The diameter of these spindles may be as little as 2 μ. In sections with 'c' approximately vertical the perthite is barely visible as a vague crenulation. General fineness of veins or spindles and vague, hazy extinction are typical of S1 rocks, but there is a tendency in some specimens to develop areas of greater coarseness around which the fine lamellae are not seen. Where coarsening of perthite occurs it is always in the form of the development of irregular patches or blebs around which the fine perthite has disappeared. In individual thin sections the basic fine lamellae tend to be of more or less constant dimensions (although often coarser towards the margins of crystals, or in zones parallel to the crystal edges) with areas on which the development of the bleb type has been superimposed. Within the more coarsely exsolved rocks of S1, Ab and pericline twinning can be discerned on a fine scale in the Na-phase. The K-phase was found to show microcline type Ab-pericline twinning only rarely in three specimens (160, 311, 305) classed with this syenite. Even bearing in mind the difficulty of discerning this type of twinning in the more finely exsolved rocks, and the comparative rarity of ideally orientated specimens ($\pm$ normal to 001) this style of twinning is much more rarely seen in the S1 rocks, an observation consistent with X-ray data on the nature of the K-phase in this syenite. There is complete absence of twinning, at least on a scale visible optically, in the K- or Na-phases of many specimens, although single crystal X-ray photographs universally show an Ab twinned Na-phase (Fig. 5.2a, b, c).

(2) <u>S2 rocks</u>.

In general these rocks are similar to S1, but considerable development of "bleb" types is seen. It is worth noting that the finest and most regular perthite seen in this generation is in those rocks, in the

central area, which have unaltered pyroxene as the mafic constituent rather than riebeckite or mica, either as a primary mineral or rimming pyroxene. Microcline type twinning is frequently observed in the K-phase of these feldspars (Fig. 5.3a).

(3) S3 rocks.

Perthites in the S3 rocks, including the melanite bearing varieties, are very regular in form and similar to the more regular types of S2. Characteristically the K-phase occurs as elongate sinuous veins. ± 25 would be a typical figure for the width of these veins although there is some variation. In suitably orientated sections Mi-type twinning can frequently be seen. Carlsbad twinning, giving a "herring bone" effect is often observed. Fine Ab twinning is usually visible in the Na-phase (Fig. 5.3b).

(4) Local variations in the type of perthite.

(a) Metamorphic Burn.

All specimens from the Metamorphic Burn area, including those from the stream exposures ⅛ ml. to the east and on to the shoulders of the North Top of Sail an Ruathair, irrespective of rock type, show extreme coarsening of scale of exsolution. The now coarsely Ab twinned Na-phase encloses large irregular areas of K-feldspar often up to 1 mm. in width and typically in excess of 0.25 mm. The polysynthetic twinning of the Na-phase is much more coarsely developed in both the Ab and pericline directions and striking chequer effects are produced. Mi-type of twinning of the K-phase can easily be discerned in appropriately orientated sections (Fig. 5.3c).

(b) Central area.

A tendency for similar coarsening to be developed is also characteristic of the quartz bearing varieties of S2 in the central area

Fig.5.3.

Photomicrographs. All crossed nichols, X25.

A: Fine patch or 'bleb' type of exsolution, K-phase dark. Specimen 70, S2.

B: Typical S3 exsolution, with a 'herring bone' twin effect. Specimen 21f, S3.

C: Ultra-coarse exsolution, typical of the Metamorphic Burn area. K-phase black. Mi-type twinning can be discerned in the larger patches. Specimen 268, S3 with xenocrysts.

D: Areas of coarse albite in a quartz rich type from the central area, rimmed by perthite. Specimen 59, S2.

A

B

C

D

around the confluence of the R. Oykel and the Allt Sail an Ruathair. The tendency here is not so well marked as in the Metamorphic Burn area. An extreme type (59) seems to be exsolved to a stage when central portions of crystals are non-perthitic Ab, the edges of crystals being coarsely perthitic. This type of zoning is very irregular and every gradation is observed in the section. This rock has 19 per cent. (by volume) of modal quartz, the highest observed at L. Ailsh, with the exception of contaminated material from the Metamorphic Burn (Fig. 5.3d).

(5) Zoned or 'mantled' feldspars.

(a) Feldspars with plagioclase cores and perthitic rims.

Rare crystals with albite-oligoclase cores which appear to be the result of original crystallization occur near the exposures of ultrabasic rock in the upper part of Allt Cathair Bhan (92). Here the Ab cores are regular and angular in form and the rimming perthite is rather fine. Chemical analysis of these feldspars shows them to be unusually sodic and this would appear to be original compositional zoning. By no means all crystals in the rock show this feature.

(b) Feldspars with concentric zones of clouding.

A more common form of zonation is exhibited by some S1-S2 feldspars (9, as xenocrysts) as concentric zones of clouding generally following crystal margins. Usually in perthites the K-feldspar is turbid whilst the Ab is clear. In the zoned type described the clouding crosses the perthite lamellae, which are fine veins (Fig. 5.4a). This suggests that this is a zonation imposed during growth as a homogeneous feldspar. It is very clearly brought out in slightly weathered examples, when it may be seen in hand specimen.

Fig.5.4.

Photomicrographs:

A: Concentric zones of clouding (dark) cutting across perthite lamellae (faintly visible running from top right to bottom left). Xenocryst in S3, Black Rock Burn. Specimen 9. (Ord. light, X 20.)

B: Coarsely exsolved margin to finely exsolved xenocryst (left) in S3 of the Black Rock. Specimen 359., (crossed nichols, X 60.).

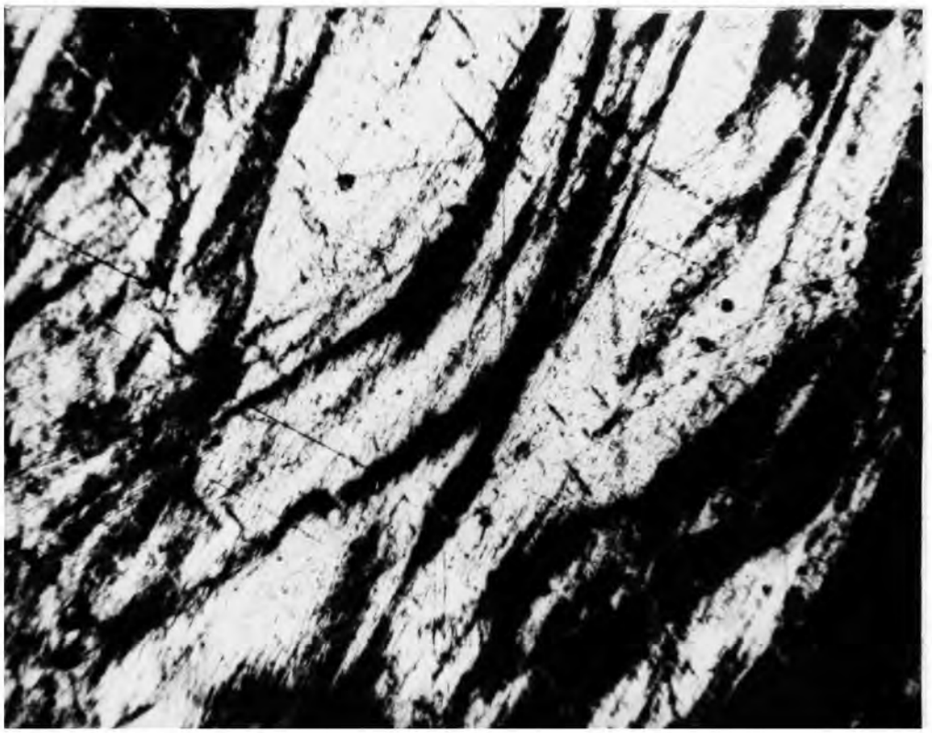

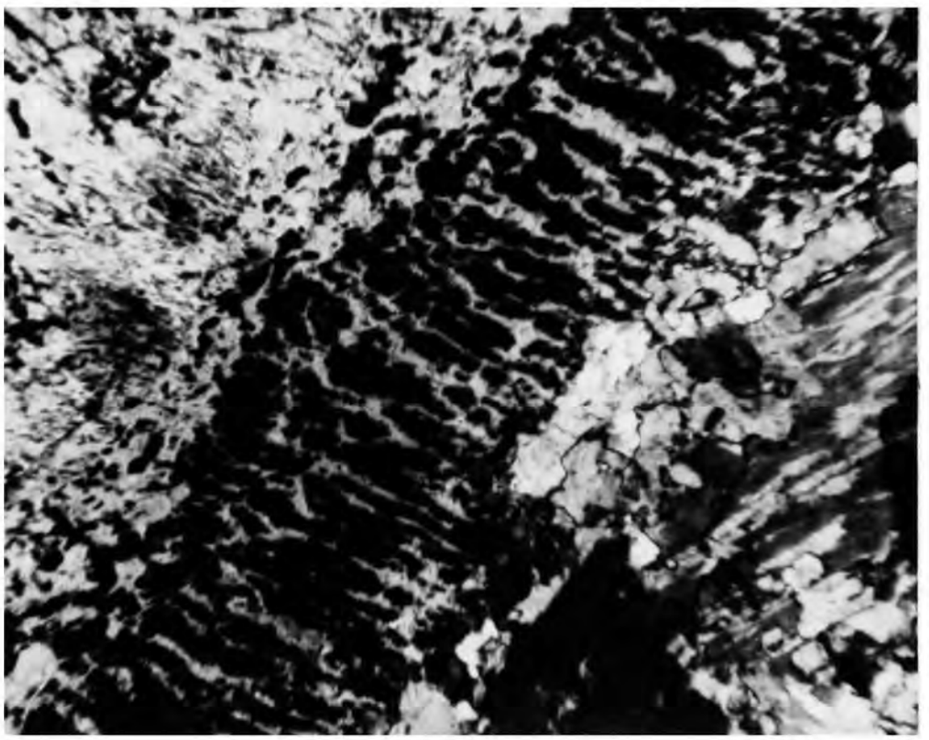

(6) Contrast between xenocrysts and host.

Where S1-S2 xenocrysts are held in an S3 matrix they may be identified in thin section because they are frequently of large size and retain a faint pink clouding. Rather remarkably many of these xenocrysts have preserved their finely exsolved silky perthitic centres (348, 9, 16a, 359). In a marginal zone of the order of 0.5 mm. wide the perthite is often coarser and equal in coarseness to the enclosing S3 (Fig. 5.4b). Even in the otherwise unusually coarsely exsolved rocks of the Metamorphic Burn area xenocrysts sometimes show areas of finer perthite (206), whilst becoming coarsely exsolved in other areas of the same crystal.

(7) S1-S3 contact relationships, North Top, Sail an Ruathair.

At this locality S1 crystals may be seen broken across (137). The finer S1 perthite and the shadowey extinction is preserved up to the contact although at this locality the contrast in perthite coarseness between S1 and S3 is not striking. A slight amount of crushing (tectonic) is also in evidence at this contact but it does not in general mask the intrusive contact relationship and is easily identified.

(8) Effects undoubtedly attributable to stress during the thrust movements.

A discussion of the importance of the Caledonian thrusting in governing the overall features of these perthites will be made after all the data has been presented. The particular textures described here are those connected with obvious cataclastic fracturing of the rock and associated effects. It is commonly observed that along cracks in crystals coarse twinning develops (Fig. 5.5a) the feldspar immediately beside the crack being non-perthitic Na-feldspar. Similar bands of highly exsolved and coarsely twinned feldspar can extend across crystals without obvious fractures but presumably in areas of strain. The same

effect sometimes only extends to developing a plane through the crystal in which the perthite lamellae broaden. A series of photomicrographs showing stages in mechanical breakdown of a leuco-syenite are given as fig. 5.7.

(9) Crystal margins.

A striking feature of thin sections of feldspars from L. Ailsh is the universal occurrence of sutured margins or 'swapped rims' (Voll, 1960) between crystals. Frequently this reaches a point when an irregular narrow belt of one feldspar is completely enclosed in a neighbouring feldspar (Photo 5.5b). Sometimes this stage has not been reached and an irregular lobate suturing has developed. In the photomicrograph (Photo 5.5b) it can be seen that the lobes of one feldspar have adopted an elongation in the same direction as the perthite lamellae of the host crystal, whilst maintaining the crystallographic orientation of the parent as shown by the conformity of the Ab twin lamellae. Phemister (1926) suggested that these interdigitating areas between crystals were the result of crystallization of the last dregs of the magma in continuity with adjacent crystals.

Voll (1960) discusses the development of such rims, and shows that they may develop in the solid state, even between randomly orientated adjacent grains. Stress and interstitial fluids would undoubtedly flux this type of boundary migration. It is worth noting that "swapped rims" are not found in the undisturbed Ben Loyal complex (B.C. King, 1942).

Sometimes it can be seen that the material associated with these sutured rims is coarsely Ab twinned, and the Ab rims frequently recorded around perthitic alkali feldspars are often observed here. Broad rims and even discreet grains of Ab are particularly well seen in the specimens

Fig.5.5.

Photomicrographs;

A: Exsolution and coarse twinning of albite induced by strain. Specimen 474, crossed nichols, X100.

B: "Swapped rims". Note that the "swapped" portions of the darker crystal on the left adopt the elongation of the perthite lammelae of the host feldspar (pale) whilst maintaining the orientation of the albite twinning of the parent. Specimen 26., crossed nichols, X 50.

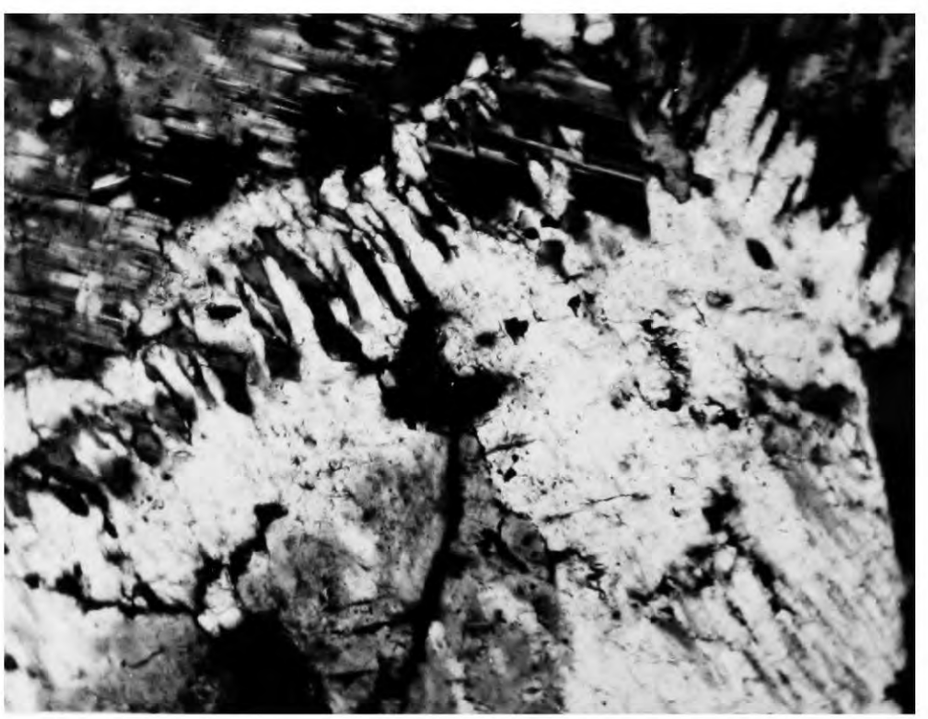

from the quartz syenites of the central area (59, 52b) where it is often concentrated around the interstitial grains of quartz.

(10) Two feldspar rocks.

All the textures described previously concern individual crystals with both K and Na feldspars coexisting within the boundaries of a single morphological unit. Some of the leucocratic veins and small dykes in the basic rocks consist of a finely interlocking mass of discreet K and Na feldspar grains (103, 418, 326) or in some cases perthitic material is present either (326) as coarse crystals enclosed in the fine two-feldspar matrix (xenocrysts?) or (418) apparently grading through areas of coarse lobate types of perthite from more normally perthitic feldspars. The latter rock carries a considerable amount of coarse muscovite.

Very similar in appearance to the latter is the texture exhibited by a mass of riebeckite and biotite-bearing S2 from the Oykel falls area (413). Here again the normal blebby S2 perthite gives way to a fine granular intergrowth of rounded discreet K and Na feldspar grains (fig. 5.6a). Identical effects can be seen in perthosites from the Black Rock (352, 360, 361). In 352 an intermediate type seems to be seen with the development of broad marginal Ab to perthitic crystals, which in places has segregated into discreet rounded blebs with distinct interfaces between grains (fig. 5.6b).

Fig.5.6.

Photomicrographs. Both crossed nichols, X 40.

A: "Two-feldspar texture." Granular mass of discreet Ab and Mi grains. Specimen 413.

B: Lobate rims of Ab to perthitic grains. A stage in the development of the "two-feldspar texture"

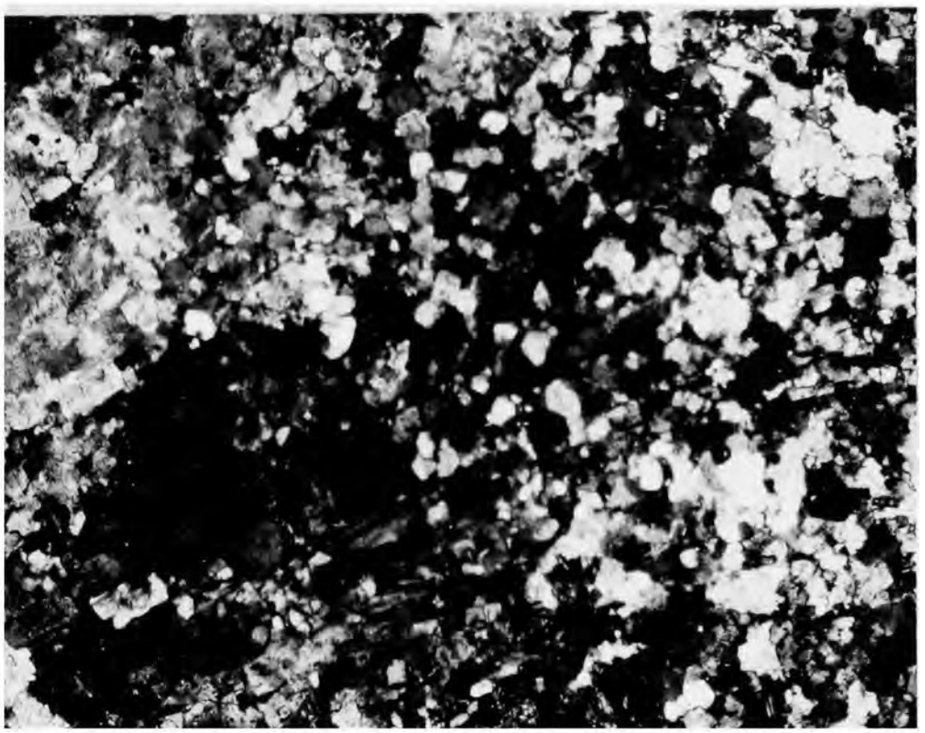

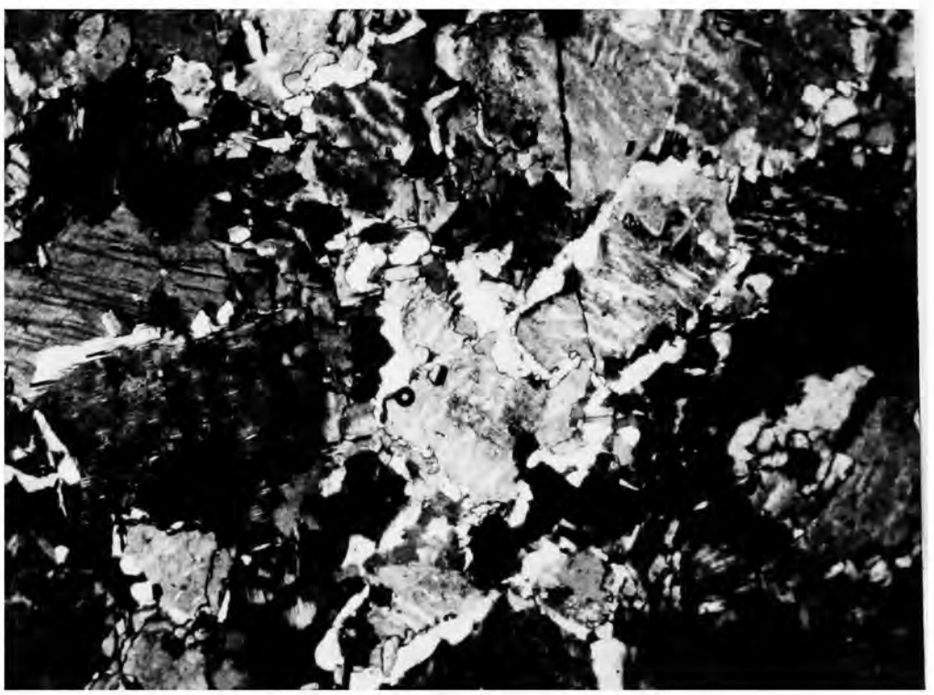
P

Fig.5.7.

Photomicrographs.

A: "Mortar gneiss" stage of breakdown. Specimen 116

B: Complete mylonitization. Specimen 72a.
Both crossed nichols. X40.

C: Microcline type twinning developed in a crushed rock. Specimen 113. Crossed nichols, X 80.

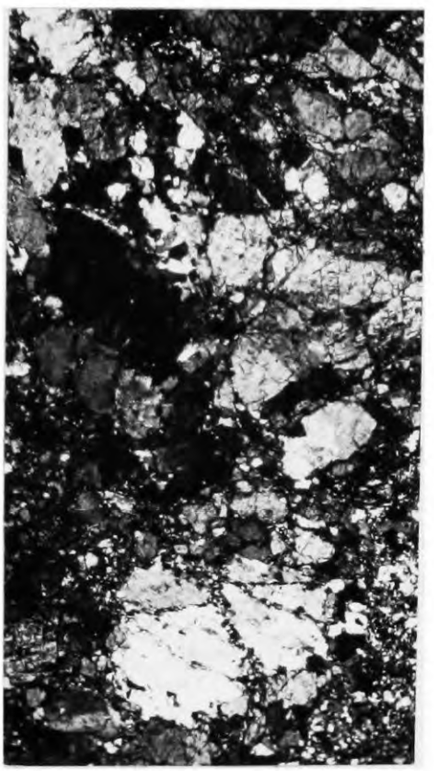

A

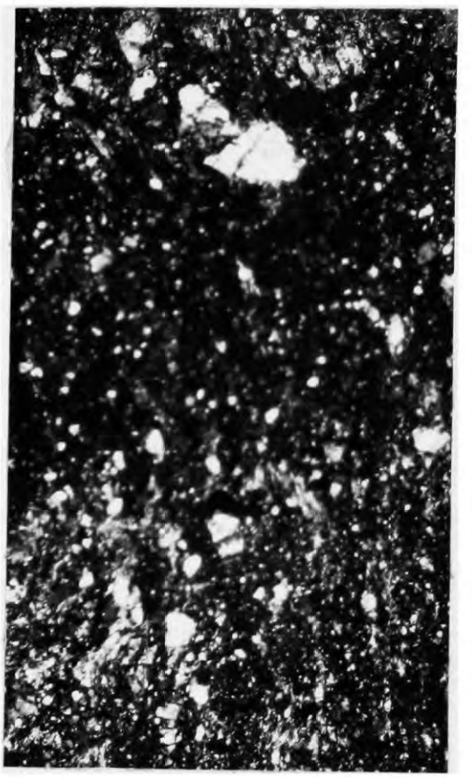

B

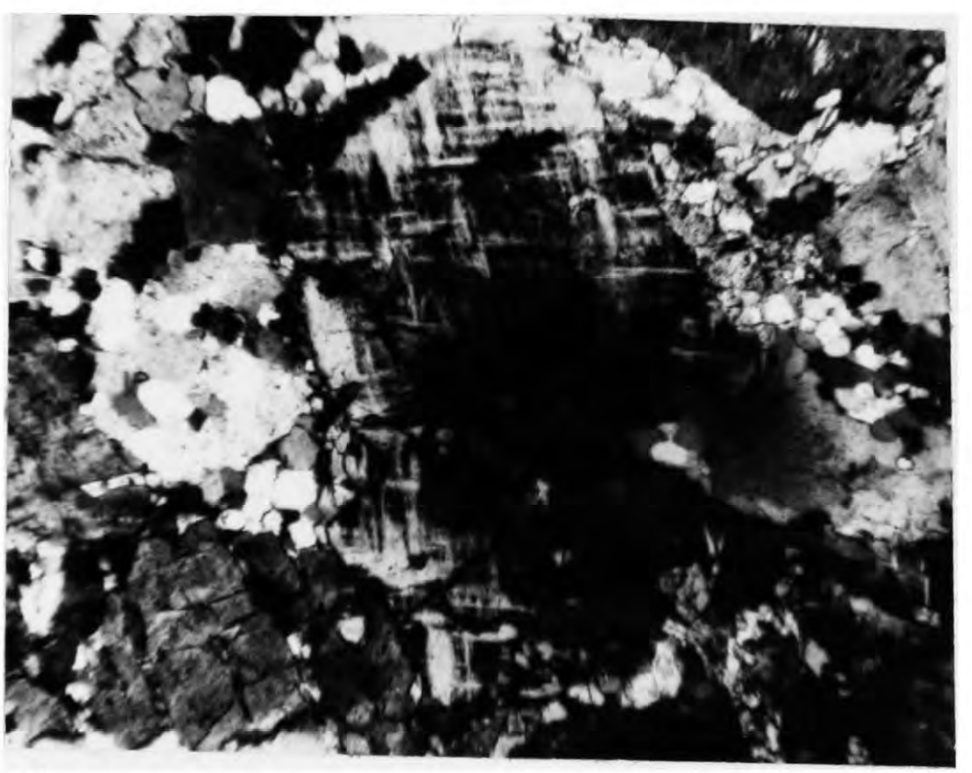

C

3) Bulk composition.

Pure alkali feldspar fractions for analysis were obtained by crushing and magnetic separation.

Na_2O, K_2O and CaO were determined by the flame photometer using sodium oxalate, potassium nitrate and calcium chloride for calibration. The standard Na-feldspar (American Bureau of Standards spec. 99) was used as a check. For Na_2O and K_2O the results were reproducible to $\pm$ 0.16 wt.% in the amount present; for the small amount of CaO present the results were reproducible to $\pm$ 0.05 wt.%. All the values quoted in table 1 are means of two determinations except for 401X and 401M of which less than 0.5 grm. was available.

Some of the specimens contained quartz and thus the total alkalis fall far short of 100%. The bulk of the powders definitely did not contain quartz but nevertheless all the analyses total considerably less than the maximum. This far exceeds the observed difference in duplicated analyses and would appear to be genuine. Presence of BaO could possibly account for some of this discrepancy and further, microscopic evidence shows brown turbidity and sometimes numerous fine needles of an unknown mineral aligned along the cleavage directions of the host feldspar. Perhaps the combined effect of these impurities and presence of BaO and SrO would account for the apparent deficiency of alkalis.

The results are plotted on figs. 5.8A and 5.8B, and as table 5.1.

In diagram 3b it can be seen that the S1 rock has the most sodic feldspars, S2 intermediate values and S3 the most potassic, although the range of the analyses is not great and further work might no doubt show overlap.Despite some doubt as to the accuracy of the determinations of the xenocrysts (401X) and matrix (401M) drilled from an xenocrystic

Fig.5.8.

ABOVE: Bulk compositions of all (14) analyzed L.Ailsh feldspars plotted on the Ab-An -Or liquidus surface at 5000 bars H_2O pressure as determined by Yoder et al,(1957), and the frequency contours of feldspar compositions for all rocks in Washington's tables with more than 80 per cent. modal Ab+Or+Q as shown by Tuttle and Bowen. (1958).

BELOW: Detail of the compositional range covered showing the trend towards potash enrichment in later phases of the intrusion.

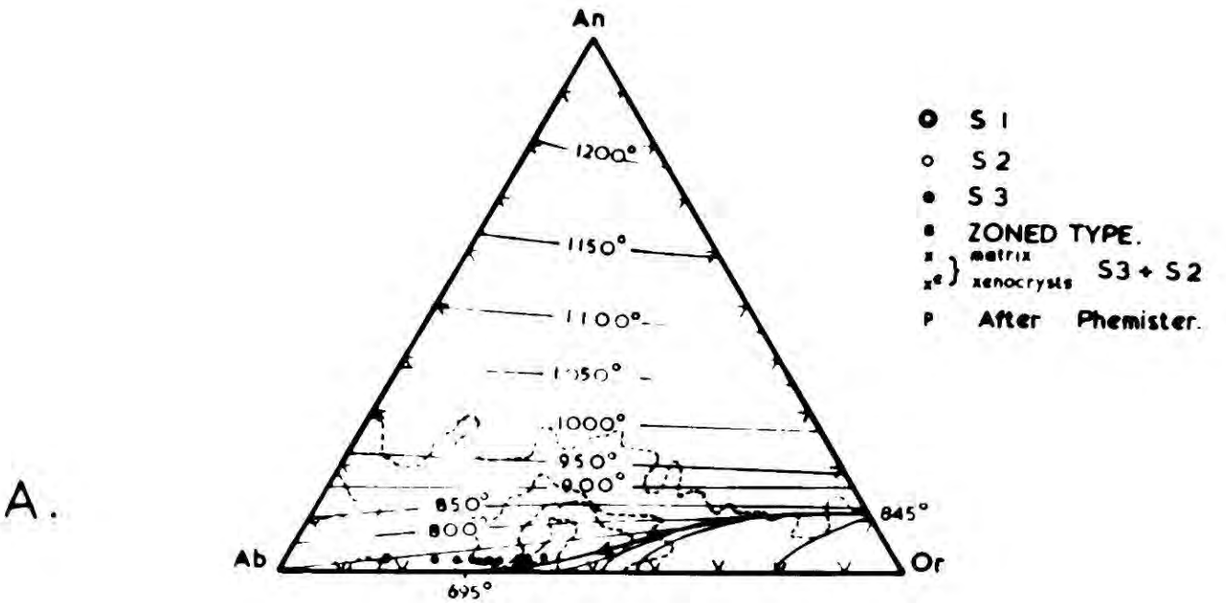
An
1200°
1150°
1100°
1050°
1000°
950°
900°
850°
800°
845°
Ab
Or
695°
S 1
S 2
S 3
ZONED TYPE.
matrix
xenocrysts
S3 + S2
After Phemister.

A.

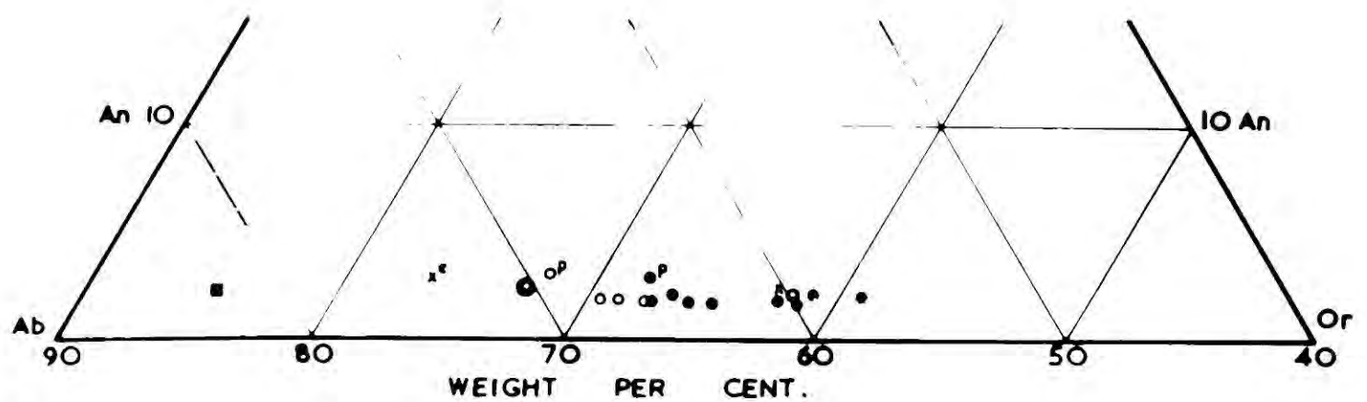
An 10
10 An
Ab
Or
90
80
70
60
50
40
WEIGHT PER CENT.

B.

Table 5.1.

Bulk compositions of L. Ailah Alkali Feldspars.

Spec. No.	Rock* type	Na_2O	K_2O	CaO	Total % observed	Ab Recalc. to 100.	Or	An	N.B.
			Wt. %						
170	S1	7.84	4.33	0.47	94.19	70.4	27.2	2.4	
26	S2	7.35	4.75	0.36	92.03	67.5	30.5	2.0	Q present
70	S2	7.49	4.99	0.36	94.63	66.9	31.2	1.9	
24	S2	7.30	5.10	0.35	93.63	65.9	32.2	1.9	
21b	S3	7.30	5.20	0.35	94.22	65.5	32.7	1.9	
89	S3+m	7.38	5.44	0.39	96.51	64.7	33.4	2.0	
67d	S3	7.20	5.46	0.35	94.91	64.1	34.0	1.8	
65	S3+m	7.08	5.60	0.33	94.53	63.3	35.0	1.7	
21f	S3	6.86	6.10	0.34	95.77	60.6	37.7	1.8	Mica-zeolite(?) inter-growths
66	S3	6.76	6.21	0.33	95.53	59.8	38.5	1.7	
216	S3+λm	6.15	6.28	0.40	91.14	57.0	40.8	2.2	
55	S2,Cr	5.26	4.80	0.29	74.30	59.8	38.2	1.9	Much Q
16a	S3+S2	6.17	5.80	0.38	88.37	59.0	38.8	2.1	Q
92	Mantled type	6.90	1.80	0.30	70.47	82.8	15.1	2.1	Much Q
401X	(S2)	8.53	3.85	0.55	97.63	73.9	23.3	2.8	One determination only
401M	(S3)	6.75	6.03	0.45	94.98	60.1	37.6	2.4	

* symbols, see appendix.

central area rock the incorporated xenocrysts would seem to be significantly more sodic than the host S3 material.

The only exception to this apparent series is specimen 55, which is a slightly crushed rock of S2 type. X-ray diffractometer traces for related but more deformed rocks from the central area of the mass (114, 116) show very strong K-phase peaks and very weak Na-phase reflections, the reverse of the arrangement normally seen in feldspars from L. Ailsh. The uncrushed equivalent (117) 1 metre from (116) shows normal peak intensity ratios. Thus it seems that in this area at least, late stage potash enrichment has occurred localized within the crush belts. There is also considerable quartz veining associated with this zone.

The analyses given in the table were for rocks selected as having escaped crushing and it would seem from the narrow range and series into which they fall, and to their relationships to the liquidus surface in the ternary Ab-Or-An system (see discussion), that they do in fact represent true values for the original bulk compositions of the feldspars (with the exception mentioned of spec. 55). No other major anomalies in bulk composition can be seen by inspection of other diffractometer charts, although small variations would not be detected in this way since no special precautions were taken to make peak intensities a precise measurement.

4) Optic axial angle.

2V was measured on thin sections of a number of rocks using a five-axis universal stage. Measurement was made only when both optic axes were accessible. For the most part the fineness of the perthite lamellae was too great to allow estimates of 2V for the components either conoscopically or by the extinction method. Thus the conoscopic method

was used to obtain an overall figure. The isogyres produced were rather diffuse but reproducibility was very good. The results are given in table 5.2.

The range of 2V's thus obtained on a section depends on a number of independent factors:

a) Different volumes of Na and K phases within the field of the objective giving an interference figure biased towards one or other component.

b) Different degrees of Al and Si ordering within the feldspar phases - in practice in these feldspars variation in the K-phase, all the Na-phases being close to low Ab.

c) Crystal distortion, either due to lattice strains imposed by the coexistence of two feldspar phases with different lattice parameters, or as a result of overall disturbance of the rock during movements at intrusion or during later tectonism.

Fig. 5.9 (below) shows the range and mean of 2V's from sections of rocks from which feldspars have been analysed plotted on the diagram of Tuttle (1952) slightly modified by Emeleus and Smith (1959). In some cases the perthite was coarse enough to measure each phase separately (by the extinction method) and no distinction has been made with specimens measured in this way.

Fig. 5.9 (above) is the same diagram as the above with a distorted solvus, as shown by MacKenzie (1959, etc), plotted on it. The three 2V/composition plots on it are means of all 2V's for each generation plotted against the mean feldspar composition for each generation. Since all the Na-phases are low Ab tie lines may be drawn from low albite through the three points to project on the solvus. The diagram thus

Fig.5.9.

BELOW: Range,(as shown by the length of the vertical lines) and means, (as shown by dots) of optic axial angles of feldspars in thin sections of rocks of which the feldspars were analyzed, plottedon the diagram of Tuttle (1952) slightly modified by Emeleus and Smith, (1959).

ABOVE: Mean 2V and mean compositions of all examples of S1,S2 and S3 respectively plotted on the same diagram with the distorted solvus as used by Mackenzie, (1959) superimposed. The projection of a line through low albite and these points onto the solvus reflects the general tendency towards development of microcline as shown by the X-ray data.

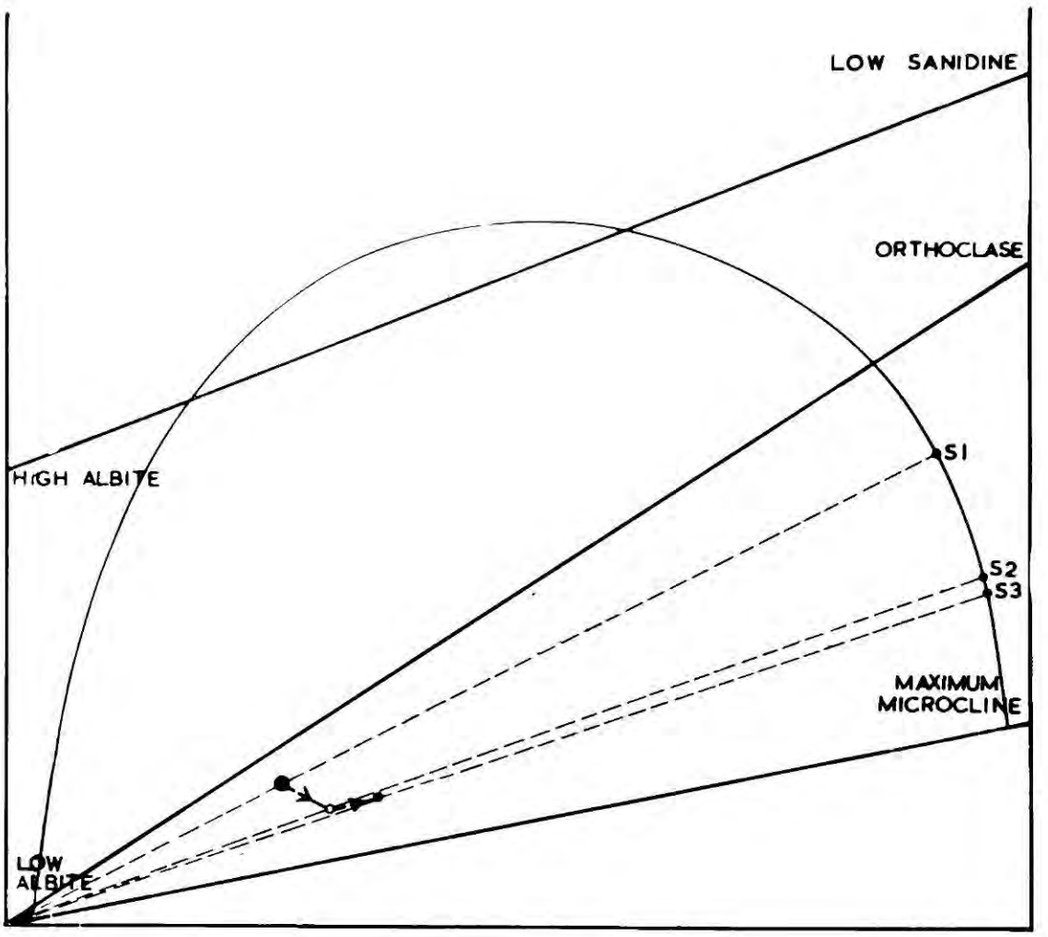
LOW SANIDINE
ORTHOCLASE
HIGH ALBITE
S1
S2
S3
MAXIMUM MICROCLINE
LOW ALBITE

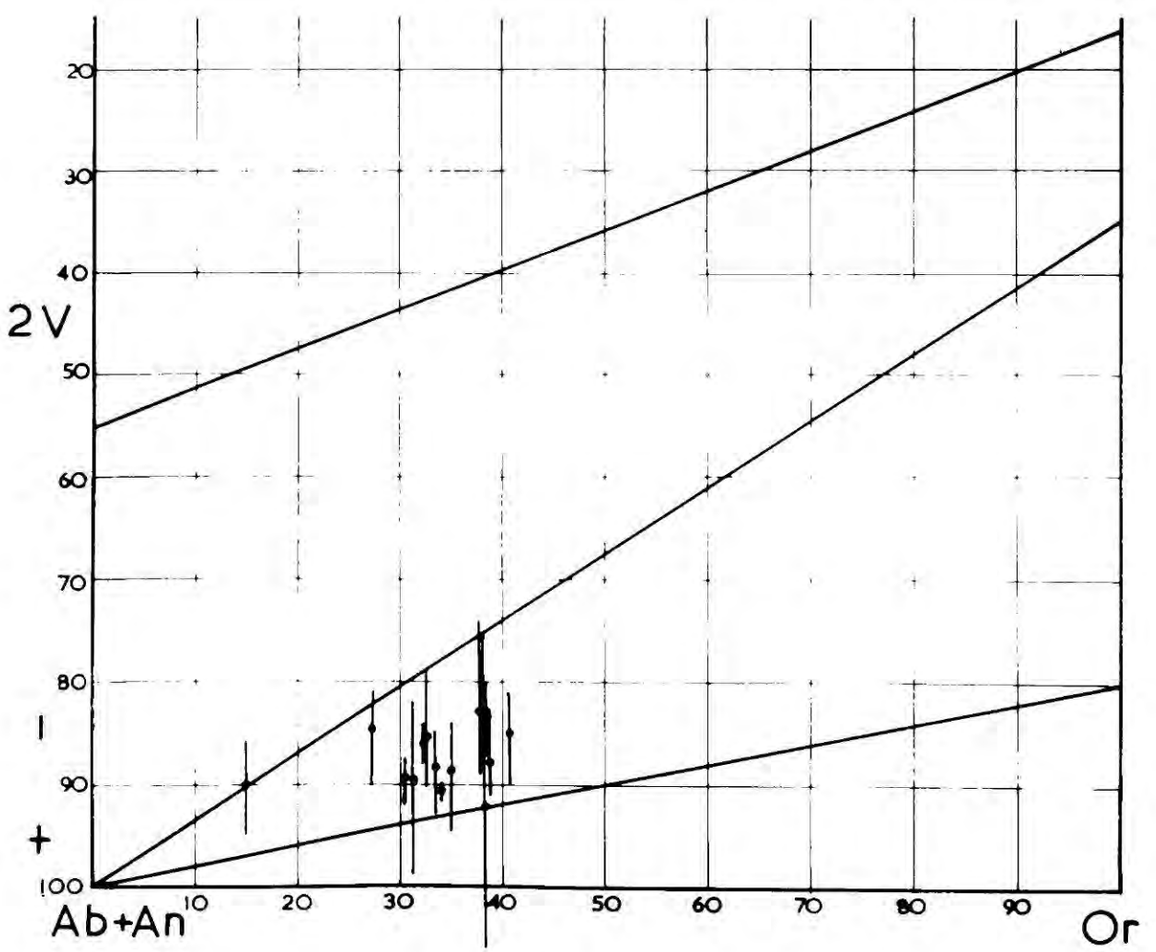
2V
20
30
40
50
60
70
80
90
100
I
+
Ab+An
10
20
30
40
50
60
70
80
90
Or

Table 5.2.

Optic Axial Angles of L. Ailsh feldspars.

Specimen	Rock generation	Or content	Mean 2V	Range of 2V	No.of meas.	N.B.
170	S1	27.2	85	90 - 81	5	
311			87	91 - 84	8	
313			85	87 - 83	4	
70		31	90	99 - 83	6	
219			90	93 - 87	2	
269			88	94 - 80	8	Coarse perthite
265			91	105*-87	5	V. coarse perthite * Discreet Ab areas
19	S2		92	94 - 90	5	
17			91	93 - 88	3	
55		38	92	107*-75	17	V. coarse perthite *for Ab patches
24		32	86	88 - 84	6	
26		30	90	92 - 88	6	
53			90	92 - 89	5	
92		15	90	95 - 86	8	
16a	S2 M X	39	88	91 - 83	5	Matrix.
			87	95 - 78	25	Includes xenocryst measured in detail to show zoning. (No significant variation)
9	S_3^+		87	91 - 85	9	
66		39	83	88 - 80	3	
89		33	89	93 - 85	7	
21f		38	83	89 - 74	8	
87			89	93 - 84	9	
216	S3	41	85	90 - 81	6	
65		35	89	95 - 84	8	
21b		33	86	91 - 79	7	
67d		34	91	92 - 90	5	
94			89	93 - 83	8	
67e			87	93 - 82	8	
418	V1 Veins.		100	109*-91	7	Non-perthitic Ab grains*
417	V2		85	93 - 79	7	
222	V		88	95 - 84	7	
103	V		88	105*-70	9	Non-perthitic Ab grains*

suggests that the K-phase of S1 rocks is substantially orthoclase whilst S2 and S3 carry highly oblique microcline.

5) X-ray diffractometry.

a) Technique.

X-ray diffractometer measurements were made using a Philips wide angle diffractometer. CuKα radiation was used throughout and all 2θ values are quoted for this radiation. Whenever possible pressed mounts were used since these gave more comparable results particularly in cases where the general shape of peaks was considered. All data quoted are the means of at least one pair of measurements. The charts were measured by taking the mid-point $^2/_3$ up the limbs of symmetrical peaks, or in cases where the peak showed significant assymmetry, the top of the peak. Measurement of the estimated peak positions was made to $\pm$ 0.005° 2θ using a vernier. Details of the instrument settings are given in an appendix (Appendix No.1).

Because of the feldspathic nature of most of the rocks separation was unnecessary and adequate feldspar traces indistinguishable from those of separated feldspars were obtained from crushed whole rocks. Quartz produced the only non-feldspar reflections and can easily be distinguished.

Reflections were indexed using the 2θ tables of Smith (1956) and Goldsmith and Laves (1954a). (See Appendix No.2).

b) Measurement of obliquity.

A series of characteristic scans from 2θ 20° to 2θ 33° are shown in the appendix together with a diagram illustrating the overlapping of peaks of the two phases present (Figs. 5.19 and 5.20). The most important data that can be obtained from diffractometer patterns is of the nature of the potassium phase as shown by the splitting of certain single

reflections in monoclinic K-feldspars in to doublets in triclinic K-feldspars. Doublets which have been used previously for this measurement ('obliquity' - MacKenzie, or 'triclinicity' - Laves) are 111/1$\bar{1}$1, 130/1$\bar{3}$0 and 131/1$\bar{3}$1. In sodic perthites these comparatively weak K-phase reflections are masked completely or in part by the strong Na-phase reflections. Of the doublets mentioned above 131/1$\bar{3}$1alone offered a feasible means of estimating obliquity. As shown in fig. 5.10, No.6, the 131 reflection of the microcline doublet is clearly resolved at high obliquity. The 1$\bar{3}$1 reflection, however, is completely masked by low albite 1$\bar{3}$1. Since direct measurement of the separation of 131/1$\bar{3}$1 was not possible it seemed that measurement of half the doublet - i.e. the movement of 131 alone - might be a usable indicator of obliquity relative to a suitable standard peak. Data supplied by Dr. W.S. MacKenzie (personal communication) on the 2θ positions of the 131/1$\bar{3}$1 peaks for some of the microclines described in his 1954 paper (see table in appendix) show that the doublet splits more or less symmetrically about a mean position of 2θ 29.87° (compare Laves, 1954, figure of 29.80° for 131 sanidine which may or may not be comparable). As a reference peak the 02$\bar{2}$ reflection of albite was chosen. It is possible that this peak is affected by Ab 04$\bar{1}$. Dr. MacKenzie suspects that 02$\bar{2}$ is in fact the strongest reflection and the peak is always found to be sharp. The advantages of using 02$\bar{2}$ as a reference peak are:

a) It is close enough to Mi 131 to permit direct measurement and to cut down time taken by the instrument in making the pattern.

b) It is more or less stationary in the series from low to high albite, any movement due to changes in thermal state or composition of this phase being easily determined by consideration of the position of Ab 131.

A possible check for this method, by separating the perthite into its components, is described in an appendix.

c) Nature of the potash phase.

In fig. 5.10 six different types of reflections in the region of 2θ 29° - 33° are shown. Oblquity is only measurable on patterns of types 5 and 6. Possibly more important is the nature of the potash phase as shown by the forms of the 131/$1\bar{3}1$reflections. For the six patterns shown the interpretation would seem to be:

1) K-phase monoclinic in entirety.

2) K-phase mainly monoclinic but also contains some material of intermediate and high obliquity.

3) and 4). Both monoclinic and triclinic material present in quantity giving very broad and ill defined peaks with no really measurable values.

5) K-phase predominantly microcline of high obliquity but undoubtedly intermediate and possibly monoclinic material present.

6) K-phase entirely microcline of high obliquity.

Naturally there are intermediates possible but these patterns were found to be characteristic of different rock types within the mass.

On fig. 5.11 peak types as defined in fig. 5.10 are plotted against their locality in the intrusion for S1 and S2 rocks only, since S3 was found, without exception, to be of type 6. The category into which a given trace was placed was judged simply by comparison with fig. 5.10 and is thus by no means a precise quantity. S1 rocks within the main mass in Coire Sail gave patterns of types 1 to 4 - i.e. the K-feldspar is predominantly orthoclase (see 2V data) - but at its margins (219, 69) the reflections are of group 5. Rocks classed as S2 can be seen to show patterns 5 or 6, except for two crushed rocks on the shoulder of Coire na

Fig.5.10.

Parts of diffractometer patterns between 29° (2θ CuKα) and 31.5° to show six types of 131-131 reflections indicating the variable nature of the K- phase of these feldspars.

The series is generally similar to the ill-named "Random Disorder" series of Christie. (1962, in Norsk Geologisk Tidsskrift, Bind 42,2.)

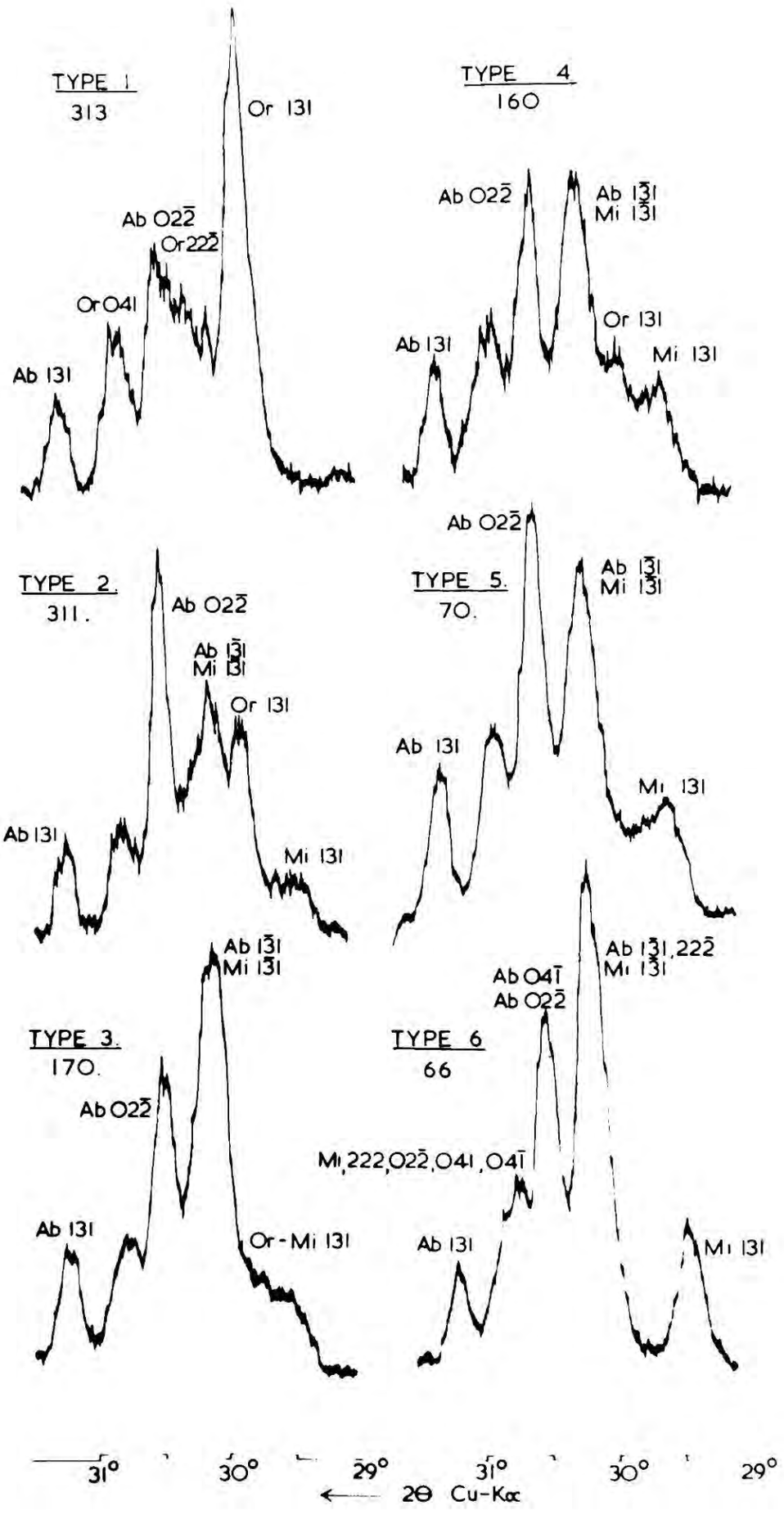
TYPE 1
313
Or 131
Ab 02$\bar{2}$
Or 22$\bar{2}$
Or 041
Ab 131
TYPE 4
160
Ab 02$\bar{2}$
Ab 1$\bar{3}$1
Mi 1$\bar{3}$1
Or 131
Ab 131
Mi 131
TYPE 2.
311.
Ab 02$\bar{2}$
Ab 1$\bar{3}$1
Mi 1$\bar{3}$1
Or 131
Ab 131
Mi 131
TYPE 5.
70.
Ab 02$\bar{2}$
Ab 1$\bar{3}$1
Mi 1$\bar{3}$1
Ab 131
Mi 131
TYPE 3.
170.
Ab 1$\bar{3}$1
Mi 1$\bar{3}$1
Ab 02$\bar{2}$
Ab 131
Or-Mi 131
TYPE 6
66
Ab 04$\bar{1}$
Ab 02$\bar{2}$
Ab 1$\bar{3}$1, 22$\bar{2}$
Mi 131
Mi, 222, 02$\bar{2}$, 041, 04$\bar{1}$
Ab 131
Mi 131
31°
30°
29°
31°
30°
29°
← 2θ Cu-Kα

Fig.5.11.

Map showing distribution of 131-1$\bar{3}$1reflection types as defined by fig. 5.10. S3 rocks are universally of type 6., and are thus omitted from the diagram.

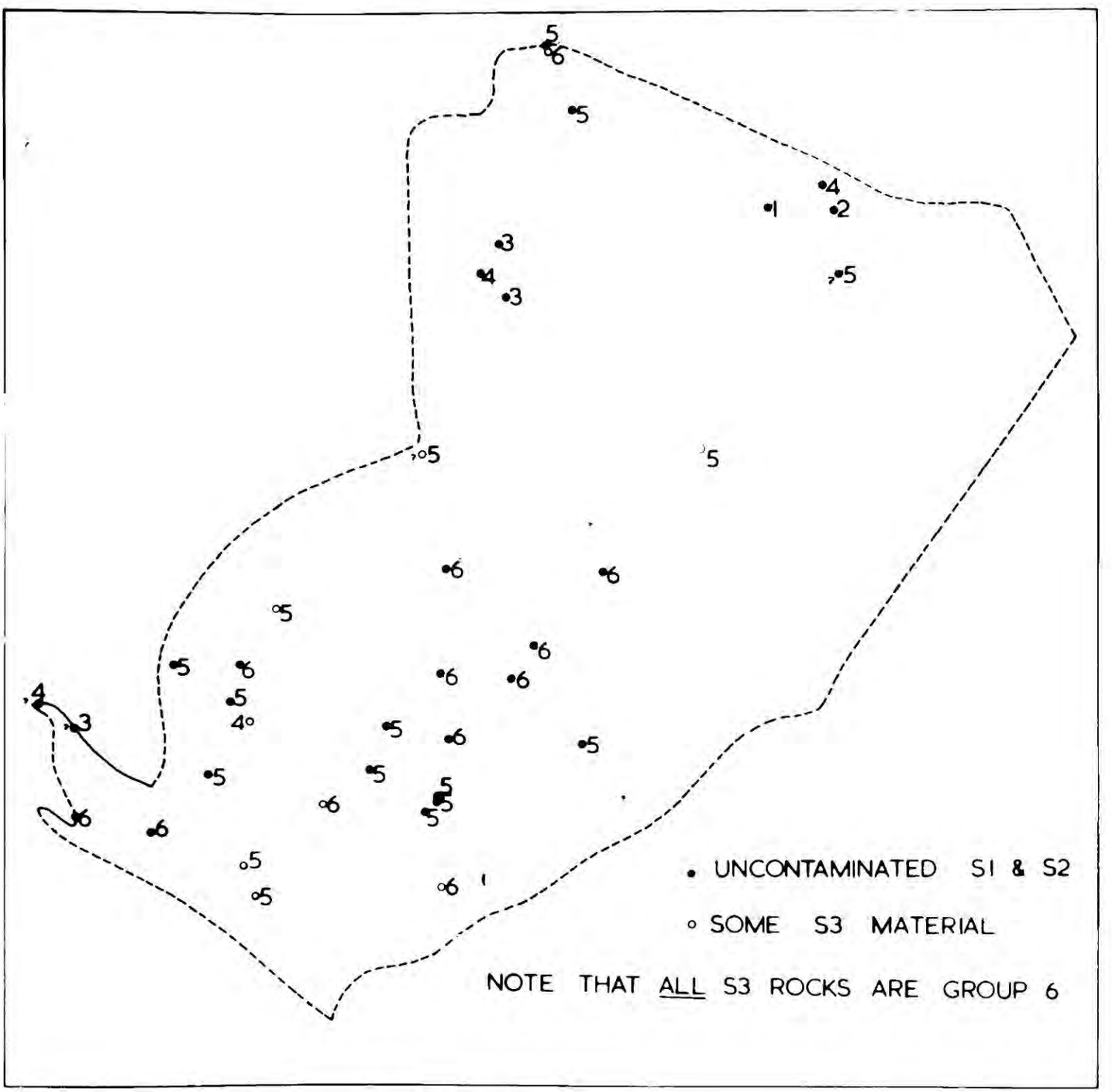
• UNCONTAMINATED S1 & S2
∘ SOME S3 MATERIAL
NOTE THAT ALL S3 ROCKS ARE GROUP 6

Mang and rock 16a which has an additional reflection at 29.8° and has been classed with group 4. Patterns of group 5 are very frequent in the rocks of the SW area of the mass.

This rough classification of the rocks on the basis of the nature of their potassium phase shows that the rocks from S1 to S3 form a series with increasing development of microcline. This was roughly indicated by the 2V measurements. Furthermore it can be seen that the pattern is preserved even when the S1 or S2 rock is close to contact with S3, or when it is being invaded by S3 to produce an xenocrystic variety of S3. Material drilled out of S1 (137) right up to within less than 0.5 cm. of the contact with S3 maintained its type 3 pattern, whilst the invading S3 gave normal type 6 reflections. Xenocrysts drilled from an xenocrystic rock (401) from the central zone showed a type 5 pattern in contrast to the type 6 of the matrix. The significance of the preservation of these features which was also noted in a different form in terms of the contrasted appearance of the perthite in thin section will be discussed later. The origin of the two group 3 and 4 specimens on Sgonnan Beag is not clear but they are very strongly crushed. Normally the effect of strain would be to assist ordering and this is in fact seen in the case of rocks 114, 116, etc., which appear to have higher obliquities than the uncrushed rock nearby. Complete crushing with subsequent recrystallization might, however, lead to development of metastable higher temperature forms. It is not impossible that the types 3 and 4 patterns of specimens 72b and 465a, on Sgonnan Beag, both extremely highly crushed, originate in this way. (See Smith, 1962, in Norsk Geologisk Tidsskrift, Bind 42).

From this aspect of the diffractometer work it can be seen that S1

and S2 might well better be regarded as parts of a single intrusion disrupted by S3. Nevertheless, with this in mind, it is convenient to differentiate S1 as those rocks, in Coire Sail an Ruathair, having a predominantly monoclinic potash feldspar component.

d) Obliquity of the potash phase.

As described above, the obliquity of the microcline phase of the feldspars was determined using the separation of Ab $02\bar{2}$ and Mi 131. On fig. 5.12 the values of 2θAb 131 - Ab $02\bar{2}$, and 2θAb $02\bar{2}$ - Mi 131 are plotted against the separation of the $\bar{2}01$ reflections of the respective phases from the 101 reflection of $KBrO_3$ as an internal standard. This latter difference was originally thought to be a method of determining the composition of the unmixed phases of perthites but numerous workers (Laves, 1952; Coombs, 1954, etc.) found that some perthites gave values outside the limits set by pure Na and K-feldspar. Smith (1961) has demonstrated that this effect is due to lattice strain between the unmixed components in their attempts to provide a good fit along the perthite composition planes. Fig. 5.12 shows that numerous values for the L. Ailsh feldspars are indeed outside the limits of the pure components, particularly in the Na-phase. The diagram is shown primarily for two points:

a) The values of Ab 131 - Ab $02\bar{2}$ with one exception (313) are scattered tightly about the position found by Smith (1956) for low albite (Amelia). The unusual values for 313 are probably genuine and this is the only rock with an entirely monoclinic K-phase. (See also single crystal data for this rock). The mean value of 2θ Ab 131 - 2θ Ab $02\bar{2}$ for the L. Ailsh feldspars is 0.722 as compared to Smith's figure for low albite of 0.73. This does suggest that the $02\bar{2}$ peak is a

Fig.5.12.

Diagram showing distribution of 2Θ values of 52 feldspars for which both 2Θ (Fsp $\bar{2}01$-$KBrO_3$ 101) and 2Θ (Ab $02\bar{2}$-Fsp 131) were measured, plotted against the published limits of the pure end members and the theoretical position of the potassium rich limb of the solvus as drawn by Mackenzie (1961), distorted to fit these coordinates.

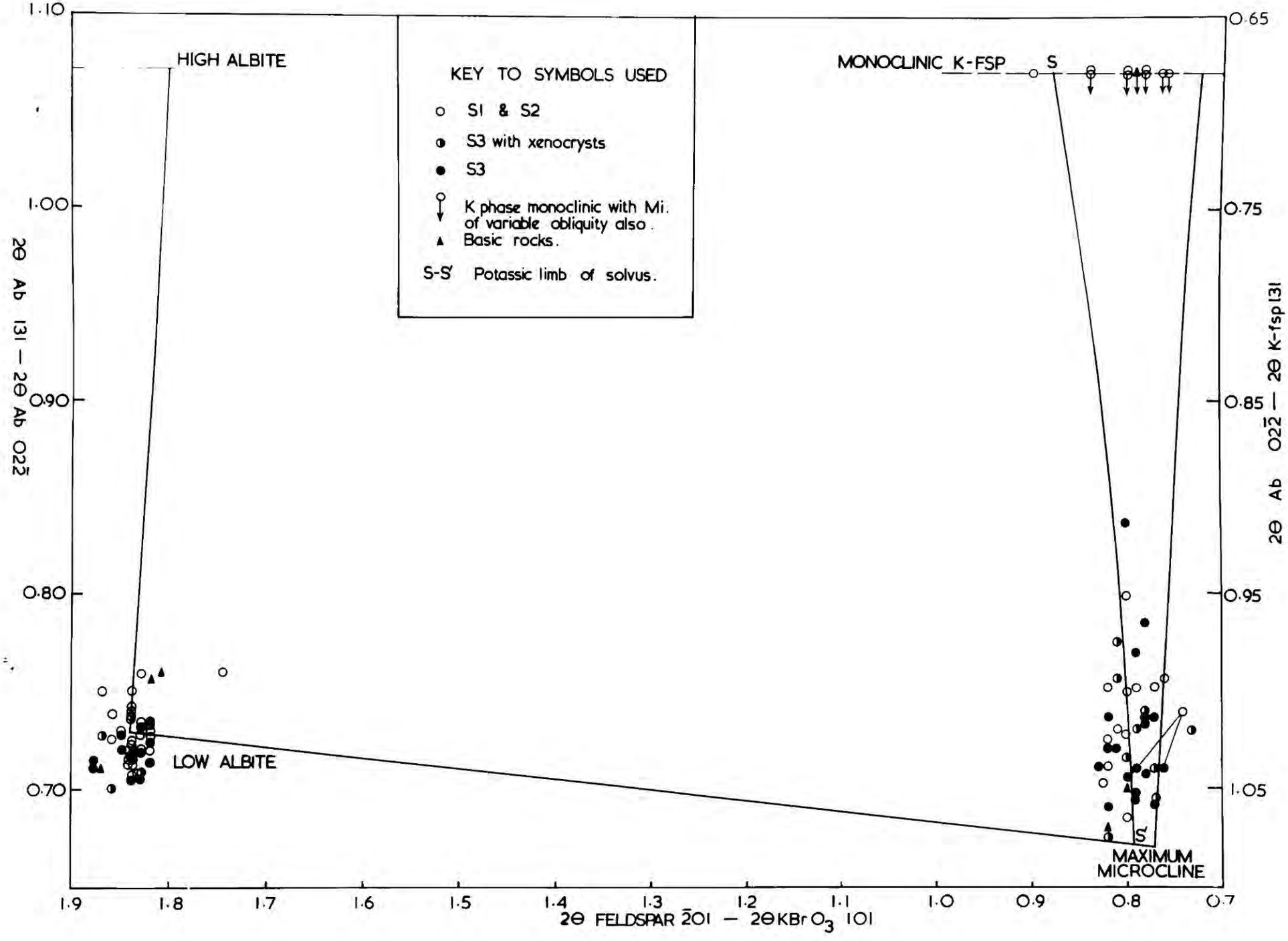
HIGH ALBITE
KEY TO SYMBOLS USED
S1 & S2
S3 with xenocrysts
S3
K phase monoclinic with Mi. of variable obliquity also.
Basic rocks.
S-S' Potassic limb of solvus.
MONOCLINIC K-FSP
S
LOW ALBITE
S'
MAXIMUM MICROCLINE
2θ Ab 131 − 2θ Ab 022̄
2θ Ab 022̄ − 2θ K-fsp 131
2θ FELDSPAR 2̄01 − 2θ KBrO3 101
1.10
1.00
0.90
0.80
0.70
0.65
0.75
0.85
0.95
1.05
1.9
1.8
1.7
1.6
1.5
1.4
1.3
1.2
1.1
1.0
0.9
0.8
0.7

reliable datum for measurement of movement of K-131.

b) In comparison with the Ab side of the diagram there is a very real scatter of points at the Or side. All the rocks of groups 1 to 4 are shown plotted as monoclinic although microcline is present in all except 313. The form of these peaks does not make an estimate of maximum obliquity for the triclinic components of these K-phases possible although high obliquity would seem to be indicated. All S2 and S3 rocks have values of moderate to high obliquities. There is no systematic difference between S1 and S2 rocks.

Fig. 5.13 shows the variation of obliquity over the L. Ailsh mass. The figures quoted are obliquities expressed as percentages of the maximum observed at L. Ailsh, which must be very close to Maximum Microcline (see Appendix). Note that the values of $\Delta\ 2\theta$ Ab $02\bar{2}$/ K 131 quoted on fig. 5.12 are larger than theoretically possible from Smith's and MacKenzie's figures. This is thought to be due to partial resolution of Ab $02\bar{2}$ and $04\bar{1}$ at the slow (⅛°/min.) scanning speed used here, since scans made at Smith's settings give good agreement (see appendix). From the map it can be seen that a simple contouring is possible, with few exceptions, and that there is quite a strong tendency for high values in the N.W. corner and low values in the S.W. area of the mass. The possible significance of these measurements will be discussed later.

6) Single crystal X-ray data.

a) General data.

Single crystal X-ray oscillation photographs were taken of about forty selected feldspar cleavage fragments. Only a dozen gave satisfactory photographs for measurement using the technique of Smith and MacKenzie (1955), since the majority showed elongation of the reflections

Fig.5.13.

Map showing the regional variation of obliquity of feldspars with a triclinic K-phase.

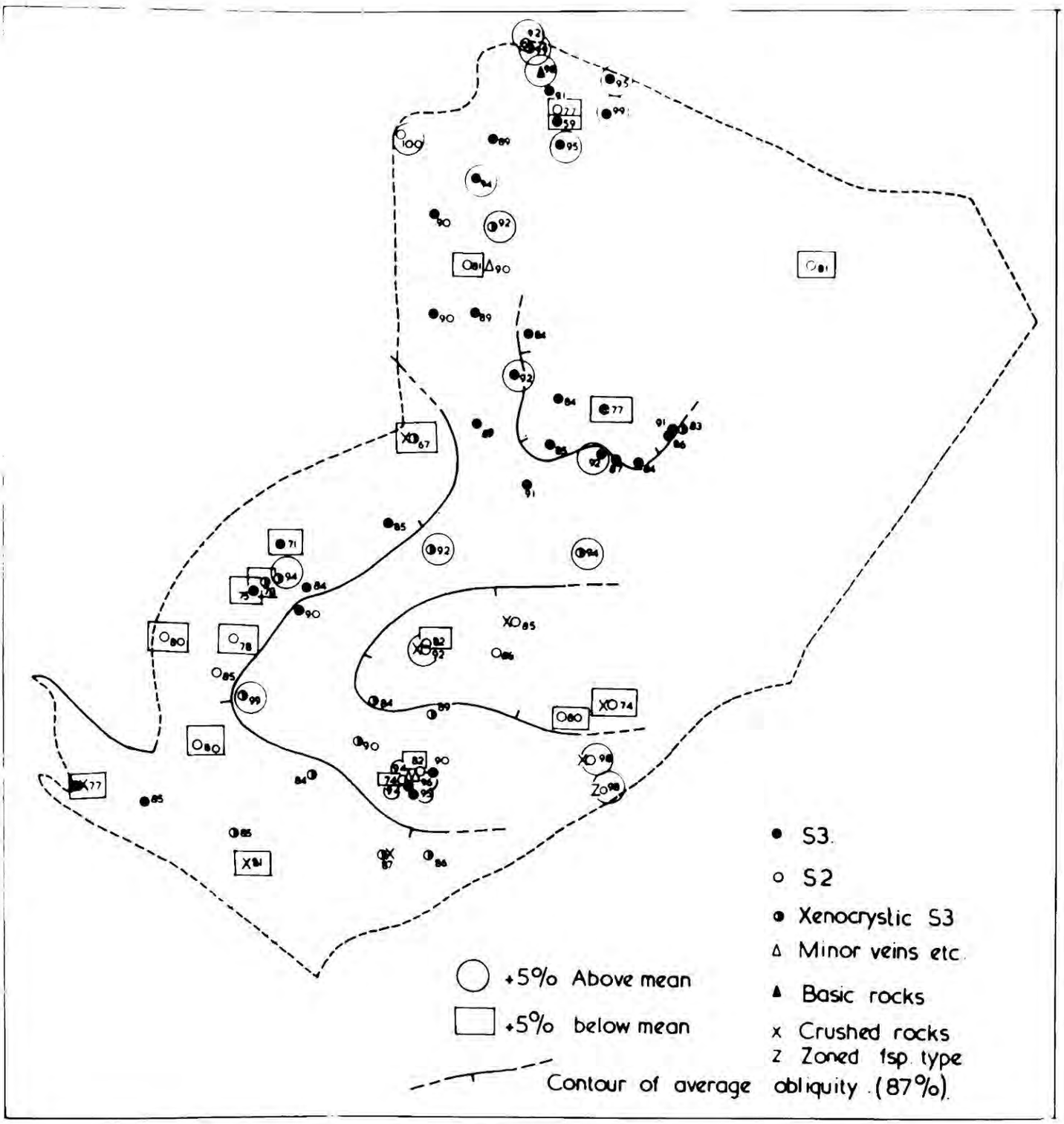
S3.
S2
Xenocrystic S3
Minor veins etc.
Basic rocks
Crushed rocks
Zoned fsp. type
+5% Above mean
+5% below mean
Contour of average obliquity (87%)

along lines of constant θ indicating disorientation. This is particularly clear in fragments from rocks which have obviously been crushed and is certainly partly connected to the thrusting these rocks have undergone, although such smearing of reflections is reported in other plutons (e.g. Dartmoor Granite) which have not been severely affected by tectonism, and may be the result of stresses at a late stage of intrusion.

Table 5.3 gives details of the interpretable photographs, together with the reciprocal lattice angles α^* and γ^* of the Na-phases which are plotted on diagram 5.14.These are all calculated from Ab twinning. Pericline twinning of the Na-phase is seen weakly in three specimens, where it occurs in the 'M' type of relation to the albite twinning (Smith and MacKenzie, 1958) indicating original unmixing of a monoclinic Na-phase which twinned on inversion to a triclinic Na-phase. (See diagram and photographs in appendix).

The K-phase reflections when triclinic appear to be twinned in the 'diagonal association' (MacKenzie, 1954) often close to the position of Ab twinning.

As shown in diagram 5.14 the values of α^* and γ^* fall very close to the published figures of low albite with the sole exception of 313 which has $\gamma^* = 89°31'$. The powder pattern of this rock was also anomalous and the distinctive form of the perthite was described previously. This is the only rock found in which all the K-phase is monoclinic. MacKenzie (1959, 1955) ascribes deviations of this type to solid solution of potassium and calcium, an observation consistent with the less highly exsolved and ordered nature of feldspars from this rock.

b) <u>S1-S3 contact relations</u>.

It was suggested above that features of S1 and S2 rocks were persisting when they were in contact with S3 as massive rocks, or even when they were

Fig.5.14.

Reciprocal lattice parameters α^* and γ^* of the Na-phases of twelve feldspar cleavage fragments determined from single crystal X-ray oscillation photographs by the method of Smith and Mackenzie, (1955), plotted on their diagram showing the range of these values in the alkali feldspars.

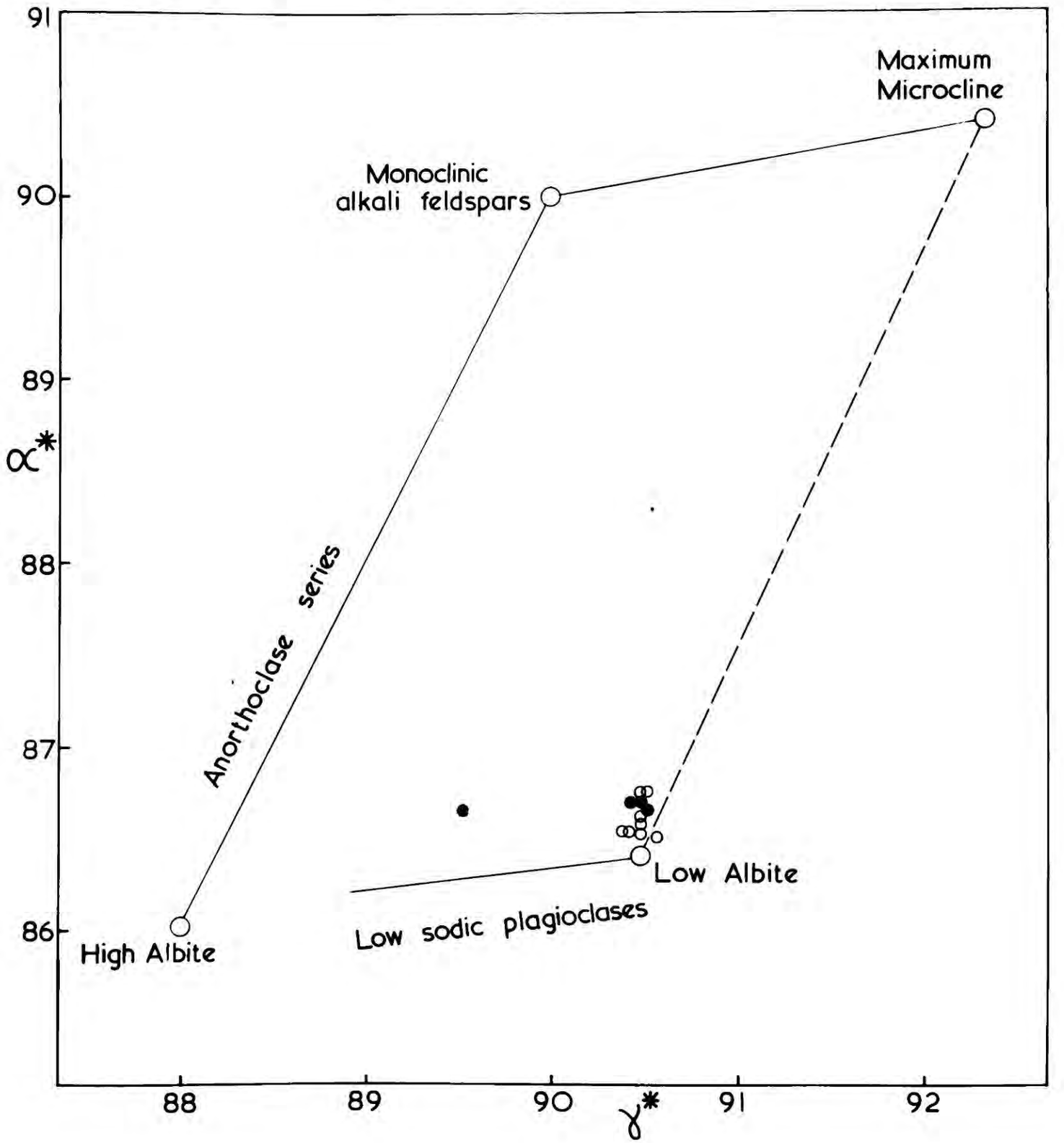
91
90
89
88
87
86
α*
Maximum
Microcline
Monoclinic
alkali feldspars
Anorthoclase series
Low Albite
Low sodic plagioclases
High Albite
88
89
90
91
92
γ*

Table 5.3.

Summary of Data from Single Crystal X-ray Photographs.

Specimen	Bulk composition (Or% - rock)	Rock generation	Na-phase Ab	Twinning Pc	Reciprocal lattice ∠s α^*	γ^*	K-phase
170	27	S1	x		86°39'	90°31'	M
313	-	S1	x		86°30'	89°31'	M
137F	-	S1	x		86°42'	90°25'	M±
137A	-	S1	x		86°42'	90°29'	M
(137B)	-	S1	x		-	-	T(Diag?)
(137P1)	-	S1	x		-	-	T(")
(137P3)	-	S1	x		-	-	T(")
219A	-	S1 or 2	x		86°30'	90°34'	T Diag. ± Ab
(219B)	-	S1 or 2	x		-	-	T? Diag.?
311B	-	S1	x	x	86°32'	90°25'	T Diag.± Ab
26A	31	S2	x		86°34'	90°29'	(")
53X	-	S2	x		86°45'	90°31'	(")
(117)	-	S2	x		-	-	(")
(269)	-	S2	x		-	-	(")
(70)	31	S2	x		-	-	("?)
67d	34	S3	x	x	86°31'	90°29'	T Diag.
216	41	S3	x	x	86°32'	90°23'	T Diag.
66	38	S3	x		86°45'	90°29'	T.Diag.± Ab
137D	-	S3	x		86°37'	90°29'	± Ab
250	-	Microcline rich perthite from basic rock.	x		-	-	Ab

Photographs showing excessive constant θ smearing:

137B1; 137B3; 137P2; 305; 311A; 116 A & B; 19; 137E; 219C; 92.

M = monoclinic. T = triclinic. Diag. = Diagonal association.

fragmented and included as xenocrysts. An attempt was thus made to see whether xenocrysts could be distinguished from their host rock by their single crystal X-ray patterns, and whether any changes could be detected at contacts.

a) A number of xenocrysts of S1 (recognizable by their red colour) were picked from S3 in the neighbourhood of the S1 contacts on Sail an Ruathair North Top. All fragments photographed from the massive S1 in this area possessed single untwinned monoclinic K-phases (although the diffractometer results suggested that triclinic material was also present) but all the xenocrysts tried showed extreme smearing of reflections indicating disorientation and appeared to have two potash phases which may well have both been triclinic although the constant θ smearing precluded positive identification.

b) A series of cleavage fragments were taken across a contact on a large hand specimen (137). The appearance of the 242 reflections for a series of fragments across the contact are sketched in diagram 5.15. As can be seen, untwinned monoclinic K-phases persist up to less than 2 cms. from the contact. Nearer to the contact smearing of reflections becomes acute but the K-phase reflections are resolved into pairs. The centres of these smeared reflections appear to lie at a small angle to the row lines suggesting triclinic phases in a diagonal association although it is not possible to be sure. The invading S3 right up to the contact retains its characteristic pattern with some disorientation, so that the appearance of the reflections is very similar to that of the S1 rock.

Fig.5.15.

Sketches of the 242 reflections on oscillation photographs of a series of specimens taken across the S1–S3 contact on the North Top, Sail an Ruathair.

N.B.

M: Monoclinic K-phase.
T: Triclinic K-phase.
A: Albite twinned Na-phase.

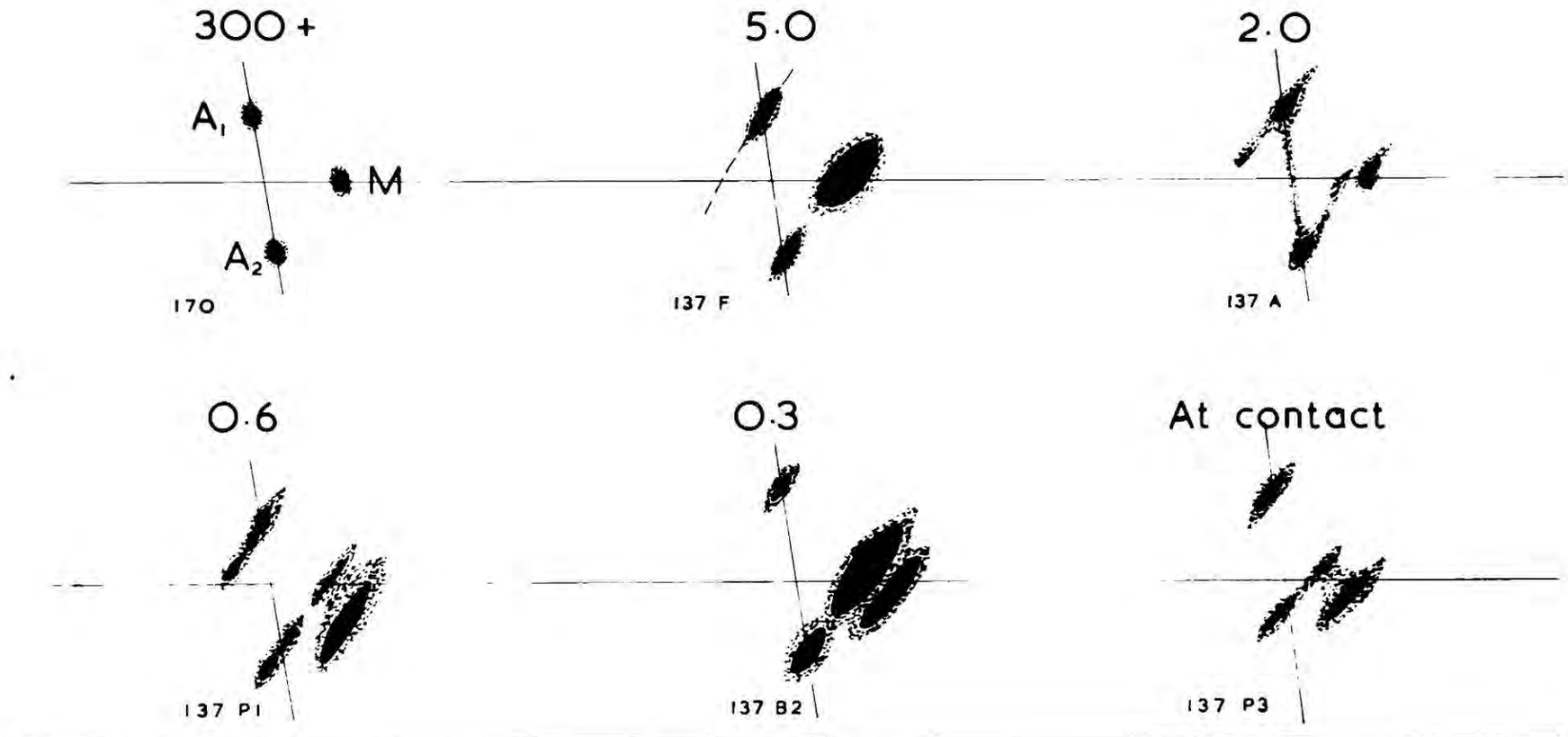

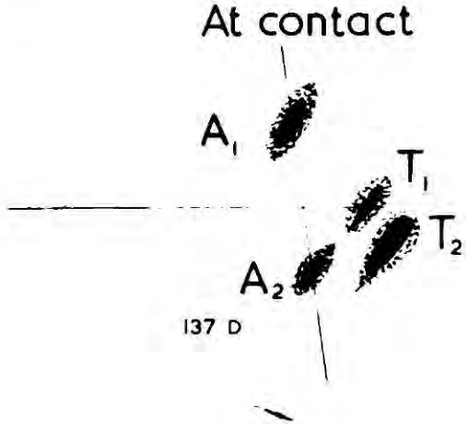

S 3.

Distances from contact in cms.

Reflection shown is 242.

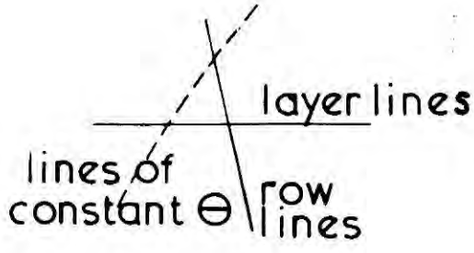

Section 2.

DISCUSSION.

7) Crystallization temperatures.

None of the features which have been described can give us direct information about the temperature of crystallization of these feldspars from a melt. Using the experimentally known relationships in the feldspars it is possible to suggest upper and lower limits for the crystallization of the Loch Ailsh feldspars by considering their bulk composition and the observation that they have exsolved stably along a solvus like that shown on the phase diagram (fig. 5.16).

In figure 5.8(a) the range of composition of L. Ailsh feldspars is plotted on the Ab-Or-An liquidus surface at 5000 bars water vapour pressure as determined by Yoder et al. (1957). Also shown are the contours of distribution of all analysed rocks in Washington's Tables (1269) that carry 80 per cent. or more normative Ab + Or + Q, after Bowen and Tuttle (1958). The tendency of the successive syenites to be relatively more potassic thus brings the composition of the feldspars (which, particularly in the case of the perthosites, is close to the composition of the whole rock) towards the low temperature trough determined in this system. None of the analysed feldspars lies on the potassic side of the cotectic line. (Potash metasomatism has accompanied crushing in places, however - see appendix 4).

The bulk composition of these analysed feldspars is thus completely in accord with crystallization in equilibrium with a melt, the later phases of intrusion tending towards a minimum melting composition. There is no reason to believe that the perthites owe themselves to any form of replacive process, as postulated by King (1942) for the Cnoc nan Cuilean

mass. Exception to this is made only in the case of the crushed, potassium enriched rocks of the central area (114, 116), where redistribution of alkalis, probably connected to the quarts veining accompanying the crushing, has taken place.

Because of lack of knowledge of the vapour pressures at the time of crystallization, the ternary diagram of Yoder et al. cannot be used as a direct indicator of temperature of crystallization. A minimum temperature-maximum pressure may be deduced from the observation that the feldspars crystallized above the top of the solvus. In the dry system $NaAlSi_3O_8$-$KAlSi_3O_8$ (calcium free) exsolution should commence at about 660° for the most potassic L. Ailsh feldspar (using the solvus shown on MacKenzie's 1961 diagram). Two factors will tend to put the inception of exsolution at a higher temperature:

a) The small and more or less constant An content.

b) Pressure of water vapour and other volatiles.

The degree to which the small An content will raise the solvus is not known accurately since it depends on the location of the intersection of the solvus with the solidus in the Or-Ab-An-temp. prism, which is only roughly known and has been deduced largely from geological evidence. To get a general estimate of the relationship between Ca content and immiscibility the line shown by Bowen and Tuttle (1958, p.132), showing the bulk composition of a large number of analysed feldspars, can be taken to represent the intersection of solvus with solidus in the dry Ab-Or-An system. The nearness of the limit of the immiscibility field to the Ab-Or sideline shows that calcium will have a profound effect in raising the exsolution temperature. Making the assumption that in the Ab-Or rich portion of the diagram the solvus-solidus intersection will

be at about 1200°C it can be calculated that in a general way the presence of only 1 per cent. of An could raise the solvus as much as 40°C. The effect of Ca may not be directly proportional to its concentration since the solvus may be dome-shaped or the cross section normal to the Ab-Or face of the prism between the top of the solvus on this face and the intersection of the solvus with the solidus could be convex or concave upwards. It is usually shown to be convex and making allowance for this effect it seems safe to conclude that the 1.5 to 2 per cent. An in the L. Ailsh feldspars could raise the solvus by something up to about 100°C.

In addition water vapour pressure will have a small effect on the position of the solvus. Yoder, Stewart and Smith (1957) concluded that the solvus was elevated by about 14°C. per 1000 bars and that the solidus intersected the solvus at 5000 bars in the Ab-Or system. Actually, even at this high pressure inspection of the diagram of Yoder et al. (1957, p.208) shows that feldspars to the sodic side of the ternary minimum will still crystallize as homogeneous sanidines but 5000 bars is very close to the pressure at which immiscibility will extend also the sodic side of the minimum. Calcium would raise the immiscibility break so that two feldspars would crystallize well below this pressure. It should be noted that the relationship between solidus and pressure is not linear and that initially small increases in pressure have a large effect which falls off at higher pressures. In the absence of knowledge of the slope of the solidus in the ternary Ab-Or-An system we can only suggest that a pressure of about 2000 bars is the maximum before intersection will occur, with the Ca contents considered. This corresponds to a temperature of about 780°C.

The ternary projection of Yoder et al. at 5000 bars shows that if

pressure had remained constant the temperature interval over which these feldspars would have crystallized is small - about 50°C.

In summary the range of feldspars at Loch Ailsh crystallized as homogeneous sodic sanidines in the temperature range of 1200°C. (normal pressure) to about 800°C. at 2000 bars (p, H_2O), and at constant pressure would have crystallized over a narrow temperature range of about 50°C.

8) Subsolidus history.

a) Early stages of exsolution.

From the foregoing section it was suggested that the L. Ailsh feldspars crystallized at above about 800°C. at less than 2000 bars pressure. From MacKenzie's 1961 phase diagram (fig. 5.16) it will be seen that feldspars in the compositional range considered will strike the solvus very nearly at its highest point and will commence exsolution over a very narrow range of temperature. The figures given as minimum crystallization temperatures are the maximum values at which exsolution will commence - 800°C. at 2000 bars but in the absence of volatiles at about 750°C. At this temperature the feldspar will have monoclinic symmetry and the primary stage of exsolution will be to give a perthite consisting of potassium and sodium rich sanidines. (The nomenclature of MacKenzie and Smith is used throughout. It differs somewhat from that of Laves, particularly over anorthoclase and the modifications of albite). Evidence that the sodium phase was monoclinic is given by the single crystal X-ray data showing albite and pericline twinning in the 'M' type relationship of Smith and MacKenzie (1958). This type of twinning is supposed to develop on inversion of the soda-sanidine phase to an anorthoclase phase as represented by the point S on the phase diagram (fig. 5.16). Because of lack of knowledge of the shape of the

Fig.5.16.

Phase diagram(stable)of the alkali feldspars (Ca-free) as suggested by Mackenzie and Smith (1961), with some additions to show the courses followed by an S1 and an S3 feldspar, and the final forms attained.

At the point's' the 'M'-type twinning of the previously monoclinic Na-phase develops.

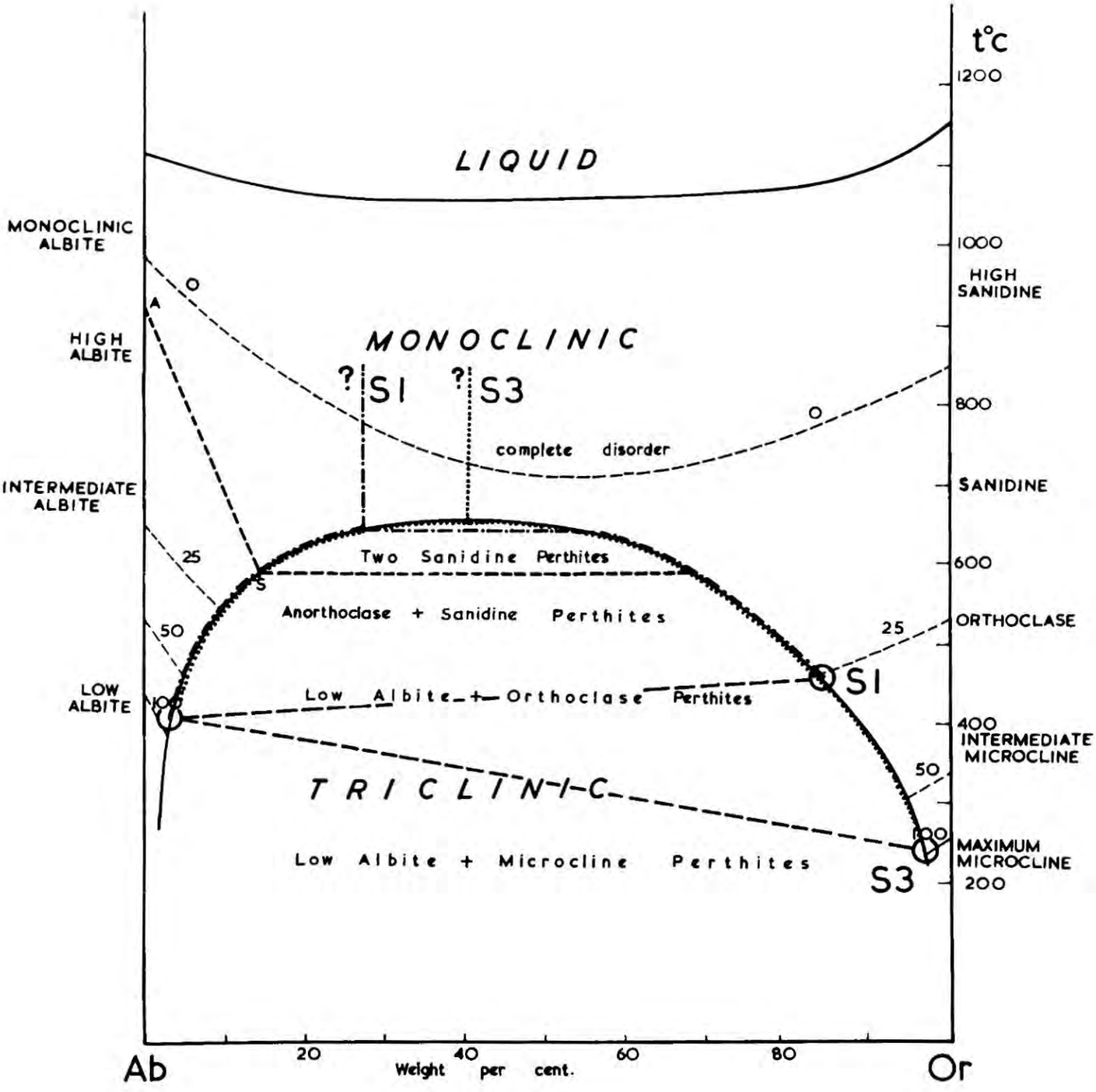
t°c
1200
LIQUID
MONOCLINIC ALBITE
1000
HIGH SANIDINE
HIGH ALBITE
MONOCLINIC
?
S1
?
S3
800
complete disorder
INTERMEDIATE ALBITE
SANIDINE
600
Two Sanidine Perthites
25
Anorthoclase + Sanidine Perthites
ORTHOCLASE
50
25
S1
LOW ALBITE
Low Albite + Orthoclase Perthites
400
INTERMEDIATE MICROCLINE
50
TRICLINIC
MAXIMUM MICROCLINE
Low Albite + Microcline Perthites
S3
200
Ab
20
40
60
80
Or
Weight per cent.

Fig.5.17.

Two current versions of the "stable" phase diagram for the alkali feldspars.

ABOVE: Mackenzie and Smith, 1961.

BELOW: Laves, 1960.

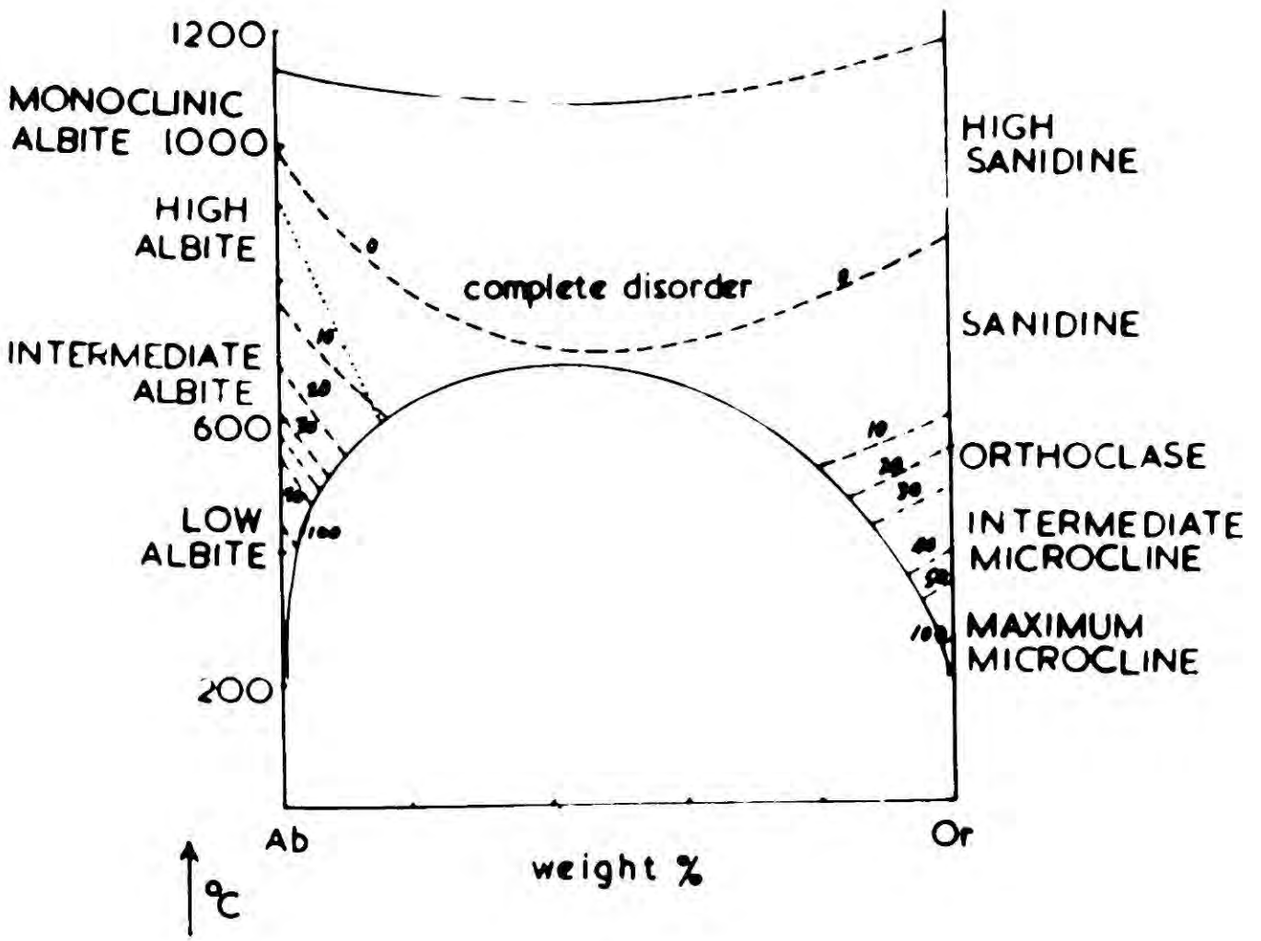
1200
MONOCLINIC
ALBITE 1000
HIGH
ALBITE
INTERMEDIATE
ALBITE
600
LOW
ALBITE
200
complete disorder
HIGH
SANIDINE
SANIDINE
ORTHOCLASE
INTERMEDIATE
MICROCLINE
MAXIMUM
MICROCLINE
Ab
Or
weight %
°C

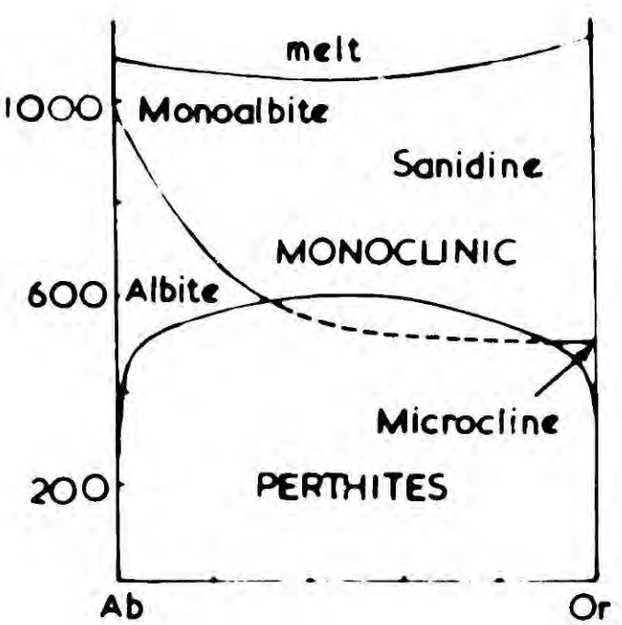
melt
1000
Monoalbite
Sanidine
MONOCLINIC
600
Albite
Microcline
200
PERTHITES
Ab
Or

solvus 'tunnel' in the Ab-Or-An-temp. prism and of the shape of the sanidine-anorthoclase displacive transformation in this projection (Smith and MacKenzie, 1958) exact prediction of the temperature at which this inversion occurred cannot be made. Smith and MacKenzie describe the cooling history of a feldspar of comparable composition (1958, p.881-2) and the single crystal X-ray photograph is very similar to that obtained for a number of Loch Ailsh specimens, but exsolution (and ordering) has not proceeded so far. It must be remembered that the effective shape of the solvus for a feldspar cooled quickly enough to prevent the achievement of Al/Si ordering will differ from that of a slowly cooled feldspar in which ordering is in equilibrium at a given temperature. A further complication arises from Laves' suggestion that the diffusive monoclinic-triclinic transition may occur at a higher temperature than the displacive one under equilibrium conditions. (In other words, the feldspar becomes triclinic by movement of Al and Si atoms from lattice site to lattice site as against the displacive transformation which entails only change in lattice geometry appropriate to Na, K, and Ca ratios and occurs more or less instantaneously at the appropriate temperature). The two phase diagrams are shown in fig. 5.17. In the absence of experimental data to support Laves' contention it seems that the experimentally determined displacive boundary is most safely used whilst realizing that if Laves is right the 'M' type of twinning may have developed at a higher temperature than the point 3 (fig. 5.16) would suggest (modified by Ca and pH_2O).

The observation that the Na-phase was monoclinic at an early stage in its history is further evidence that the present bulk composition of the feldspars is that at which they crystallized and that there has been no addition of soda at least below the temperature of the monoclinic-

triclinic displacive inversion of the soda-phase at some temperature above 600°C.

b) Late stages of exsolution and ordering of Al/Si.

Discussion of the origins of the features now seen in these feldspars demands consideration on the one hand of features which seem to be related to the cooling history and volatile content of the rocks, and on the other of features impressed by the Caledonian thrusting. Phemister (1926, p.25) suggests that the very existence of these feldspars as perthites is an effect of the tectonism and of the hot solutions which he believed permeated the syenite after its consolidation. The effect of local concentrations of volatiles in the late stages of the cooling of the intrusion is of undoubted importance in development of the range of textures seen, as is stress in promoting features described previously.

When stress has been important in developing the textures of the rock the effects are localized in planes, usually, but not necessarily, mappable as thrust planes of varying degrees of intensity. Ultimately, with extreme fracturing mylonites are developed. There is a good parallel with the Adirondack syenitic rocks described by Buddington (1939). The bulk of the Loch Ailsh rocks are very similar in texture to his rare undeformed massive syenites from the Diana complex (op.cit. p.282) and textures like those of his Mortar Gneiss (op.cit. p.283) and Syenite Mylonite (op.cit. p.287) are occasionally seen at L. Ailsh (Fig. 5.7a, b). Recrystallization of initially perthitic rocks to give two-feldspar types has been mentioned. At L. Ailsh, however, in contrast to the Adirondacks, extreme cataclasis is exceptional and most rocks seem to preserve original magmatic textures. Other features of the feldspars seem to vary either over large areas of the mass or from rock type to rock

type. These features will be discussed in turn and suggestions made of possible origins and modifications by the thrust movements.

(A) Local coarsening of the perthitic intergrowth.

As described on p. 137 all the rocks in the N.W. corner of the mass show extreme coarsening of the perthitic texture and of the polysynthetic twinning. Another locality at which this type of coarsening of perthitic textures takes place is in the quartz bearing varieties in the central area. It is possible that this is an effect of stress and the development of coarsely twinned non-perthitic types under stress has been described in Section 1. However, if stress has been important at these localities it has had a more widespread effect than elsewhere in the mass. Thrust planes do occur in the central area, but not more commonly than elsewhere, and they are rare in the Metamorphic Burn, which appears to contain an undisturbed succession of Cambrian xenoliths or protrusions. It seems likely that this effect is due to local concentration of volatiles able to act as fluxes to the exsolution process. Concentration of water in marginal and apophysal regions of plutons is often invoked and would seem to be a reasonable suggestion for the clearly marginal and probably apophysal Metamorphic Burn area. Apophysal and marginal development of microcline rather than orthoclase has been noted in granitic rocks in France (Caillere and Kraut, 1960) and bearing in mind the general interdependence of exsolution and ordering of Al/Si, might be comparable. Microcline from the Metamorphic Burn area has the highest obliquity observed in the L. Ailsh mass.

(B) Variation in the nature of the potash phase.

As is illustrated in fig. 5.10, specimens of L. Ailsh rocks show every gradation from a K-phase which is monoclinic (i.e. orthoclase in the

sense accepted by MacKenzie), to a triclinic one with the maximum departure from monoclinic symmetry. The range that this represents in terms of the current phase diagram is shown on fig. 5.12. Obliquity as measured by separation of the 131 - $1\bar{3}1$ reflections is not necessarily linearly related to distant ordering but this assumption is made for the diagram. The diagram does not show clearly, however, the fact that all but one of the specimens plotted as mainly monoclinic also contain triclinic material, and that many of those plotted as triclinic probably contain monoclinic material.

The type of pattern as classified by fig. 5.10 was found to be characteristic of different rock units in the mass. In fig. 5.11 the variation is plotted on a locality map. The mode of transformation from orthoclase to microcline-bearing rocks is such that parts of a specimen are monoclinic and parts triclinic, of high obliquity. Since obliquity is related to distant ordering of Al and Si, and ordering is ideally dependent on temperature, it follows that these rocks are not in strict thermal equilibrium even over short distances. It has been suggested (Smith and MacKenzie, 1961) that "orthoclase differs so little in stability from microcline that once formed it would persist indefinitely unless other factors (than temperature), the most likely one being stress, provide additional activation energy for the conversion to microcline." The existence of rocks giving 131 reflections of types 1 to 5 (fig. 5.10) implies that this "activation energy" has been available only through limited volumes of the rock and raises an important question as to whether the nature of the K-phase is not simply dependent on different degrees of deformation of different portions of the mass, connected with the Caledonian thrusting.

Two observations would seem to discount this possibility. Firstly,

the patterns are characteristic of different rock types, and all S3 rocks have highly oblique microcline with no intermediate material. This distribution would not be expected if the development of microcline was solely due to the thrusting. Secondly, it has been mentioned that these patterns are maintained right up to contacts, (S1/S3 on North Top, Sail an Ruathair, 137), and when the early crystals are present as xenocrysts (401X, etc.). This second observation is conclusive evidence indicating that the basic causes of the features observed were impressed during the intrusive and cooling history of the rocks. The apparent 'metastable' preservation of the higher temperature forms on intrusion of the second magma will be discussed later.

We must, therefore, look for a process which, in the post-consolidational history of the mass, allows this general arrangement to develop:

Early intrusion.
- S1: Predominantly orthoclase with variable development of microcline in coexistence with dominant orthoclase.
- S2: Microcline developed mainly, but monoclinic material is probably present in many cases.

S3: The entire K-phase is microcline of high obliquity.

The lack of effect of the later intrusion on the xenocrysts and at massive contacts indicates that cooling rate alone is not adequate to explain the differences, and in any case, if cooling rate was the only agent of importance S1 and S2 should have constant potash phase properties over long distances, rather than the short range variations observed. Differences in cooling rate may have been important in

determining whether S1 was overall a more "quenched" rock than S3, but other factors must have played a critical part.

The most likely suggestion is that the differences reflect variations in water content of the consolidating magma. On this basis, S1, when wholly monoclinic, would represent the driest portion of the magma, and S3 would be the last and wettest phase of the intrusion. It is likely that water, although generally distributed according to the thermal gradients within the rock mass, would be locally concentrated and preferentially channelled through lines of weakness in the recently consolidated rock, and thus with some reservations outlined below the uneven but roughly systematic development of microcline in S1-S2 is explained. S3 would, in contrast, be considerably wetter, and the critical volume of water required to allow the orthoclase-microcline transformation to go to completion would everywhere be present. Local concentration of volatiles has been invoked as a primary factor in governing structural state in more rapidly cooled rocks (Emeleus and Smith (1959)), and a possible catalytic mechanism has been described by Donnay, Wyart and Sabatier(1960).

However, further considerations given below indicate that complications to this simple picture arise. A mechanism is required whereby the early (i.e. above-solvus) cooling history of the feldspars modifies their later behaviour and this possibility will be discussed in the following sections.

c) Effects observed at contacts. Contrast between xenocrysts and host rock.

As described on pages 159 and 164 the S1 rock on the North Top of Sail an Ruathair preserves its predominantly monoclinic potash phase almost to the contact with the invading S3 with a highly oblique potash

phase. Very close (± 2 cm.) to the contact single crystals from A1 show severe straining and the apparent development of a triclinic K-phase, the twins probably being in a diagonal association. Although the diffractometer patterns indicated the presence of triclinic material in S1 away from the contact it was not detected in single crystal photographs and the common development of a triclinic K-phase, together with disorientation, near the contact would seem to be a genuine effect. The association with constant θ smearing suggests that the forceful intrusion of S3 may be responsible, in straining the outer crystals of the more or less rigidly held S1, and eventual breakage is evidenced by the occasional red xenocrysts found held in S3. Stress will have promoted the development of microcline from orthoclase. The diagonal twin association could conceivably be related to stressing, which could modify the directions in which the ordering domains present in orthoclase could enlarge and thus be recognizable as microcline twins.

Contrast between xenocrystic and host feldspars has been described. Sometimes coarsely perthitic rims can be seen around otherwise finely perthitic centres. The xenocrysts also appear to be more sodic and to yield type 5 (fig. 5.10) X-ray reflections.

There seem to be two possibilities for the development of these rims. Either they are the result of overgrowth of S3 on to an S2 core, and the S3 material was different in some way (see below) sufficient to allow it to exsolve, and order, more than the S2 nucleus, or the rims are the result of limited diffusion of water from S3 assisting the exsolution of S2 material, or fluxes were able to penetrate the crystal lattice only to the depth of an initial S3 overgrowth. Some specimens (348) seem to have included grains of feldspar, pyroxene and sphene in the coarsely exsolved rim material only, the fine core having

no inclusions, which might suggest overgrowth, but it is not possible to be certain on this point. Nevertheless the existence of these apparently less exsolved cores and the persistence of orthoclase up to the S1 contact raises an important question as to the mechanism of the apparent 'metastable' persistence of orthoclase under conditions in which microcline is forming.

d) Persistence of orthoclase.

If the processes involved in this discussion went rapidly to equilibrium with temperature and were not appreciably affected by fluxes, we could interpret the lack of any 'metamorphic' effect of the later syenite on the earlier in terms of its temperature of intrusion being below the temperature equivalent to the structural state represented by the earlier syenite. This would imply a temperature of intrusion of S3 of below 500°C (a little above allowing for the effect of calcium, and using MacKenzie's tentative stable phase diagram) and certainly well within the range at which two feldspars would crystallize, thus requiring that S3 be intruded in a semi-solid state. (We know that it crystallized as a homogeneous one-feldspar rock). There is no suggestion that S3 was intruded in any such fashion and in fact it has an unusually even grained texture, there are only rare indications of a foliation, and no indication of crystal breakage in a flowing matrix. It is necessary therefore to consider whey S1/S2 feldspars are fundamentally different from S3 even though we can be sure that, at contacts and when intimately mixed as xenocrysts, they have had the same cooling history, from the temperature of intrusion of S3, as a magma, down to normal temperatures.

The nature of orthoclase is at present not fully understood and

currently there are three schools of thought. The most radical, of Ferguson, Trail and Taylor (1958), based on the hypothesis that electrostatic neutrality is the primary structure determining factor in the feldspars, holds that the ideal stable form of $KAlSi_3O_8$ is monoclinic in symmetry. This hypothesis seems to be contrary to the common occurrence of microcline in those rocks which have been annealed for the longest periods and is criticized on these and crystal structural grounds by MacKenzie and Smith (1961, 1959). These latter authors believe that orthoclase has a structure that is stable or nearly so at some intermediate temperature. They agree that it may consist of triclinic ordered domains, as stressed by Laves, who considers this a good reason for the persistence of orthoclase. He believes (discussion in Smith and MacKenzie, 1961) that the common occurrence of orthoclase is because of its finely twinned state and the difficulty of increasing the domain size (to the state when it is recognized as microcline twinning) which requires the "recrystallization" of domains twinned in a "left-hand" sense if they are to enlarge a "right-hand" domain and vice-versa.

A number of authors (Marmo, 1959; Smith and MacKenzie, 1961) have recognized the problem posed by certain rocks in which orthoclase seems to persist even when microcline is growing. Marmo quotes the case of microcline-bearing aplitic dykes cutting orthoclase granites and concludes that "once orthoclase has been formed it seems to be as stable as microcline at low temperatures." MacKenzie and Smith, invoking their phase diagram with lines of iso-order-disorder sloping steeply downwards towards the solvus, consider this to be a reflection of appreciable ("at least 10 per cent.") Na in the orthoclase whereas "the

microcline is likely to be nearly pure K-feldspar." The Na-bearing orthoclase can be in equilibrium at certain temperatures with Na-free microclines.

The Loch Ailsh feldspars seem to show a similar problem in a different light for it appears that the orthoclase bearing and microcline bearing perthites must have cooled together through the temperature range in which exsolution and the bulk of the ordering process took place. Since the K-feldspar considered here is a phase in perthitic intergrowth the arguments of MacKenzie and Smith do not seem to apply.

From the phase diagram, fig. 5.16, it can be seen that exsolution would commence over a very narrow temperature range since the compositions encompassed by S1 and S3 are only Or_{27} to Or_{41}. The difference between two feldspars of these bulk compositions exsolving side by side assuming they are both in equilibrium at a given temperature will be simply in the different volumes of Na-rich and K-rich material present. The compositions of the two K-phases at specific temperatures should be the same and under the same conditions of cooling rate and in the presence of the same fluxes there would seem to be no apparent reason why S1 feldspars should not develop highly oblique microcline as has S3. Rock 313, the only specimen with wholly monoclinic K-phase, has 2θ values appropriate for a K-phase with at least 10% Na in solid solution. The highly oblique microcline K-phases of S3 have $\bar{2}01$ spacings indicative of almost pure K-feldspar. Since perthites of any bulk composition may contain a triclinic potash phase the bulk composition of the perthites cannot be a controlling factor here. Two possible sources for the effects described will thus be discussed.

e) Limited diffusion of volatiles.

As proposed on page 180 the variations within S1/S2, and the overall difference of S3 may well be connected to volatile content during the late stages of consolidation and cooling of the rock. The later S3 is taken to be wetter than S1. In the absence of other factors the preservation of S1 and S2 features at contacts with S3 and as xenocrysts cores requires that water must have been unable to diffuse far into the coarser early crystal centres. The coarsely perthitic rims on the xenocrysts might therefore be either more highly exsolved than original S1 material, or S3 overgrowth which has been the limit of diffusion of the volatile material. The rims are of the same order of width and coarseness of exsolution as the enclosing material and if volatiles have been important only very limited lattice diffusion is implied after S1 and S3 had come into contact (less than about 0.5 mm.). Alteration of the mafic minerals in S1 on the North Top of Sail an Ruathair, does suggest that volatiles from S3 were mobile and that dispersion could occur over far greater distances at least between crystal interfaces. If limited lattice diffusion has been important in preserving the xenocryst cores it is remarkable how short is the range through which it might occur particularly bearing in mind the low cooling rate implied by the highly oblique microcline in the later material. Coarsely exsolved rims like those seen on the S2 xenocrysts are not found at the S1/S3 contacts where the stresses imposed by the second intrusion seem to have provided activation energy for the development of microcline. It is thus difficult to see how the early forms could have resisted following the structural patterns developed by the later forms, if the effects of fluxes active at temperatures below that represented by the thermal state of the S1 rocks were of great importance.

It does not seem impossible, however, that the earlier cooling history of the feldspars might be important in determining the ease with which they could transform from orthoclase to microcline, and a tentative mechanism by which this could arise is suggested below.

f) Variable structure of orthoclase.

Orthoclase is generally agreed to be a partially ordered form and MacKenzie and Smith (1961), Hafner and Laves (1957), and Barth (1959) have discussed the way in which Al and Si may be distributed between the four slightly different Al or Si/O tetrahedra in the K-feldspar structure. If these are designated a_1, a_2, b_1, b_2, in the disordered state (high sanidine) Al/Al + Si in each of these sites is 0.25 and in the fully ordered (maximum microcline) condition Al/Al + Si in $a_1 a_2 b_1$, is 0 and in b_2, 1. There are various paths which may be followed between these two extremes (see diagram 5.18 for summary), Barth proposing that orthoclase might have 0, 0, 0.5, 0.5 Al in the respective sites. The other workers point out that the intermediate microcline for which a structure determination was made by Bailey and Taylor (1955) had values of 0.05, 0.07, 0.25, 0.58 in the four tetrahedra which implies that a feldspar which had achieved Barth's ideal structure would have to regain Al in the a_1 and a_2 sites. MacKenzie and Smith thus suggest values of about 0.15, 0.15, 0.35, and 0.35 for orthoclase but consider that considerable latitude is possible.

The possibility of variable atomic arrangements for orthoclase does suggest a mechanism by which certain orthoclases, once formed, could persist under conditions in which other orthoclases would be continuing the ordering process to give microclines. The proposition is that under certain rates of cooling and in presence or absence of suitable fluxes some feldspars (at Loch Ailsh those of S1) might be able to reach a condition in which more Al was in the 'b' tetrahedra than was ideal for

Fig.5.18.

Diagram illustrating known and hypothetical arrangements possible of Al and Si in lattice sites in the high-sanidine -maximum microcline series, and the possibility of different paths being followed by two feldspars having different thermal histories above the temperature of the inception of recognizable triclinic symmetry.

The representations of high-sanidine and maximum microcline are theoretical ideals not necessarily ever achieved.

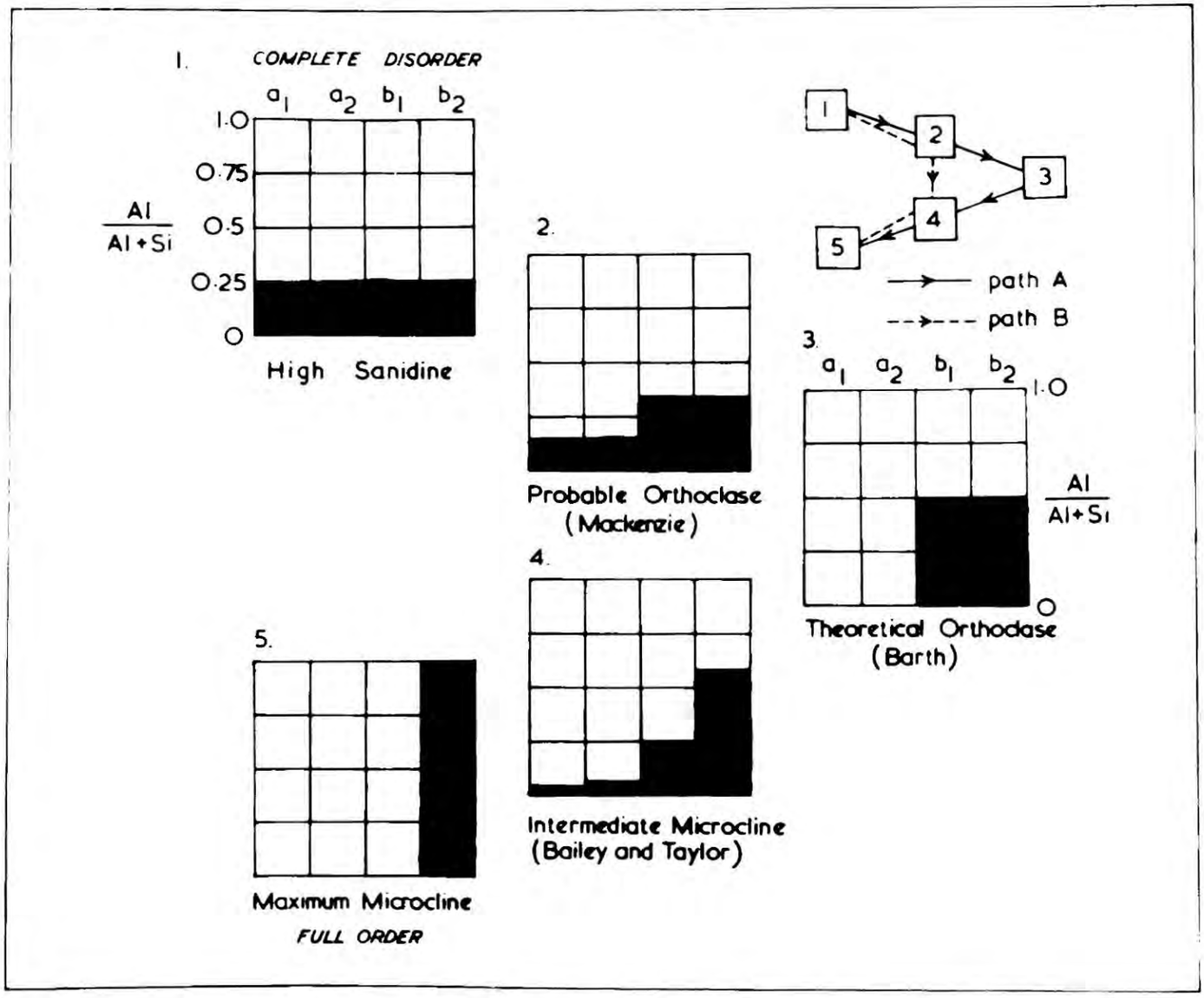
1. COMPLETE DISORDER
a_1 a_2 b_1 b_2
1·0
0·75
0·5
0·25
0
Al / Al+Si
High Sanidine
2.
Probable Orthoclase
(Mackenzie)
4.
Intermediate Microcline
(Bailey and Taylor)
5.
Maximum Microcline
FULL ORDER
1
2
3
4
5
path A
path B
3.
a_1 a_2 b_1 b_2
1·0
0
Al / Al+Si
Theoretical Orthoclase
(Barth)

attainment of the microcline condition. Such a feldspar would require additional activation energy to allow loss of Al to 'a' tetrahedra before further relative gain of Al to b_2 could take place. Other conditions might give rise to a feldspar which would be able to transform directly to microcline from an orthoclase with some Al still in the a_1a_2 tetrahedra (S3 feldspars). Considerable latitude is possible - in fact all that is required is that the activation energy required to transform the orthoclase of the S1/S2 feldspars is greater than that of the S3 feldspars. Additional activation energy could be provided by later stressing or the catalytic action of water, which allows for some of the variation observed in the S1/S2 rocks. A very diagrammatic representation of the situation is given as fig. 5.18.

This suggestion does require that even though the S1 crystals were homogenized by the S3 intrusion, the basic Al/Si distribution attained prior to the intrusion of S3 was not destroyed. This is a possibility bearing in mind the ease with which homogenization but not sanidinization may be achieved, particularly at the near solvus temperatures envisaged.

Possibly also the inability of the S1-2 orthoclase to follow the host feldspars in adoption of the microcline state is better envisaged in terms of the shape and size of the domains of ordered structure which have attained triclinic symmetry in a 'left' or 'right-hand' sense relative to their neighbours. If the early cooling history of S1 developed ordering domains which 'changed sense' over shorter distances than the enclosing S3, cooled at a more optimum rate, the S3 would be able to develop the large triclinic domains necessary for the recognition of the microcline form, whilst the S1 could not overcome the barrier made by the need to reverse the sense of one of each pair of adjacent

ordering domains. The small S1 domains (the fruits perhaps of quicker cooling or lack of volatile fluxes early in their cooling history) would not be destroyed by enclosure in the S3 magma particularly if this was at a low temperature, just above the solvus.

These tentative suggestions, in summary, are that rate of cooling and volatile action in the temperature range above that at which orthoclase is a stable form, may determine the ease with which microcline is formed as cooling proceeds. Since it appears that exsolution and ordering and size of exsolved units are generally if not precisely inter-related, it follows that the fine style of exsolution could be preserved in the xenocryst cores. Although these ideas are thoroughly speculative they are suggestions of possible sorts of solutions to a problem which cannot, as far as can be seen, be solved in terms of mechanisms previously invoked.

g) Variable obliquity of the microcline phases.

There is some indication (fig.513) of a systematic distribution of obliquity values for feldspars with a triclinic K-phase. This variation is partly connected to rock type - e.g. S1/S2 rocks (219) (269) in the Metamorphic Burn have low obliquities, S2 rocks from the mixed zone around the Oykel falls have lower obliquities than the enclosing S3, as do xenocrysts from (401). (See tie lines on fig.5.2). On the other hand it partly transcends the boundaries of the rock types - e.g. across the S3/S2 contact to the E. of Black Rock. An explanation of this apparent contradiction may lie with the fact that the S2 on the shoulder of Black Rock is a massive rock and whatever the controlling factor for determination of obliquity, it also applied to the invading S3. Wherever obliquities of S2 and S3 in contact apparently differ it may imply that

the S2 material has been moved from the environment which originally determined the obliquity into an environment which determined the different obliquity of the intruding S3.

Confidence in the finer points of the variation as described above is not great, since the variation is small. There seems to be little doubt, however, that values in the Black Rock - Sgonnan Beag area are significantly lower than normal whilst values in the Metamorphic Burn area tend to be higher than the mean. The one low figure for S3 rocks in the Metamorphic Burn (Rock 216, obliquity 59%) is from a melanite and feldspathoid pseudomorph (?) bearing form only 1' from a contact with a massive limestone xenolith or protrusion. This rock is not as coarsely perthitic in section as the bulk of the Metamorphic Burn rocks and it is possible that some form of quenching (perhaps only removal of volatiles) is operative here. Otherwise the bulk of the Metamorphic Burn rocks are very coarsely exsolved and polysynthetically twinned, an observation in keeping with the high obliquity.

The meaning of the other variations in obliquity is not known. Variation in obliquity with position in plutons has been described elsewhere but its meaning is not at present understood. The suggestion in the Metamorphic Burn area is that concentration of volatiles able to act as fluxes to the exsolution process is important. This area would seem to be best interpreted as a region where syenite is interleaving with massive tongues of sediment, perhaps near the roof of the intrusion. The apparent diminution of obliquity near the contacts in the Black Rock area would imply that this contact was not similar to the Metamorphic Burn. Taking the Black Rock and South Top of Sail an Ruathair together it would seem that obliquity is tending to diminish upwards, an observation

inconsistent with the Metamorphic Burn area.

More observations and a greater knowledge of the factors controlling the later stages of the ordering process are necessary before apparently systematic variations like that observed here can be interpreted. It might then provide a useful technique in zoning acid and alkaline plutons. A study of less disturbed rocks would clearly offer the best approach.

Bibliography to Chapter 5.

For a concise summary of present knowledge of the alkali feldspars, together with discussion with authors of conflicting views, the reader is recommended to the following two papers:

SMITH, J.V. and MacKENZIE, W.S., 1961. Atomic, chemical, and physical factors that control the stability of alkali feldspars. Instituto "Lucas Mallada". C.S.I.C. (Espana) Cursillos y Conferencias. Fasc VIII, pp.35-52.

MacKENZIE, W.S. and SMITH, J.V., 1961. Experimental and geological evidence for the stability of alkali feldspars. As above, pp.53-69.

and other papers in the same publication.

Further recent views on all aspects of feldspars are given in:
Norsk Geologisk Tidsskrift, Bind 42, 2 (Halvbind). (Feldspar volume).1962.

General Bibliography.

BAILEY, S.W. and TAYLOR, W.H., 1955. The structure of a triclinic potassium feldspar. Acta Cryst., 8, 621-632.

BARTH, T.F.W., 1959. The interelations of the structural variants of the potash feldspars. Zeit. Krist., 112, 263-274.

BROWN, W.L., 1960. Lattice changes in heat treated plagioclases - the existence of monalbite at room temperature. Zeit. Krist., 113, 297-329.

BUDDINGTON, A.F., 1939. Adirondack igneous rocks and their metamorphism. Geol. Soc. Am. Memoir, 7.

CAILLERE, S. and KRAUT, F., 1960. Sur la repartition des feldspaths potassiques dans les roches eruptives et metamorphiques de la region d'Avalon. Bull. Soc. franc. Min. Crist., 83, 21-23.

COOMBS, D.S., 1954. Ferriferous orthoclase from Madagascar. Miner. Mag., 30, 409-427.

DONNAY, G. and DONNAY, J.D.H., 1952. The symmetry change in the high-temperature alkali-feldspar series. Am. Jour. Sci., Bowen Volume, 115-132.

DONNAY, G., WYART, J. and SABATIER, G., 1960. The Catalytic Nature of high-low feldspar transformations. Carnegie Institution of Washington. Annual report of the Director of the Geophysical Laboratory, 1959-1960, pp.173-175.

EMELEUS, C.H. and SMITH, J.V., 1959. The Alkali Feldspars, VI. Sanidine and orthoclase perthites from the Slieve Gullion area, Northern Ireland. Amer. Min., 44, 1187-1209.

FERGUSON, R.B., TRAILL, R.J. andTAYLOR, W.H., 1959. Charge balance and the stability of alkali feldspars. A discussion. Acta Cryst., 12, 716-718.

FERGUSON, R.B., TRAILL, R.J. and TAYLOR, W.H., 1958. The crystal structures of low temperature and high temperature albite. Acta Cryst., 11, 331-348.

GOLDSMITH, J.R. and LAVES, F., 1954a. The microcline-sanidine stability relations. Geochim. Cosmochim. Acta, 5, 1-19.

GOLDSMITH, J.R. and LAVES, F., 1954b. Potassium feldspars structurally intermediate between microcline and sanidine. Geochim. Cosmochim. Acta, 5, 100-118.

HAFNER, St. and LAVES, F., 1957. Ordnung/Unordnung und ultrarot absorption II. Variation der Lage und Intensitat einiger Absorptionen von Feldspaten. Zeit. f. Krist., 109, 204-225.

KING, B.C., 1942. The Cnoc nan Cuilean area of the Ben Loyal igneous complex. Quart. Journ. Geol. Soc., 1942, 98, pp.147-185.

LAVES, F., 1952. Phase relations of the alkali feldspars, I and II. Journal of Geology, 60, 436-450 and 549-574.

LAVES, F., 1960. Al-Si-Verteilungen, Phasen-Transformations und Namen der Alkali feldspate. Zeit. f. Krist., 113, 265-296.

MacKENZIE, W.S., 1954. The orthoclase-microcline inversion. Miner. Mag. XXX, No.225, pp.354-366.

MacKENZIE, W.S., 1952. The effect of temperature on the symmetry of high-temperature soda-rich feldspars. Am. Jour. Sci., Bowen Vol., pp.319-342.

MacKENZIE, W.S. and SMITH, J.V., 1961. (See page 191).

MacKENZIE, W.S. and SMITH, J.V., 1959. Charge balance and the stability of alkali feldspars. Acta Cryst., 12, 73.

MARMO, V., 1959. On the stability of potash feldspars. Bull. Comm. Geol. Finlande, 29, 133-137.

ORVILLE, P.M., 1958. Feldspar investigations. Carnegie Institution of Washington. Annual report of the Director of the Geophysical Laboratory. 1957-1958. pp.206-209.

READ, H.H., PHEMISTER, J. et al., 1926. Geology of Strath Oykell and Lower Loch Shin. Geological Survey, Scotland, 1926.

SCHNEIDER, T.R., 1957. Rontgenographische und optische untersuchung der Umwandlung Albit-Analbit-Monalbit. Zeit. Krist., 109, 245-271.

SMITH, J.V. and MacKENZIE, W.S., 1955. The Alkali Feldspars I. Orthoclase microperthites. Am. Min., 40, 707-732.

SMITH, J.V. and MACKENZIE, W.S., 1955. The Alkali Feldspars II. A simple X-ray technique for the study of alkali feldspars. Am. Min., 40, 733-747.

SMITH, J.V. and MacKENZIE, W.S., 1958. The Alkali Feldspars IV. The cooling history of high temperature sodium-rich feldspars. Am. Min., 43, 872-889.

SMITH, J.V. and MacKENZIE, W.S., 1959. The Alkali Feldspars V. The nature of orthoclase and microcline perthites and observations concerning the polymorphism of potassium feldspar. Am. Min., 44, 1169-1186.

SMITH, J.V., 1956. The powder patterns and lattice parameters of plagioclase feldspars. I. The soda-rich plagioclases. Miner. Mag., 31, 47-68.

SMITH, J.V., 1961. Explanation of strain and orientation effects in perthites. Am. Min., 46, pp.1489-1493.

SMITH, J.V., 1962. in Norske Geologiske Tiddskrift. (See above).

TUTTLE, O.F., 1952b. Origin of the contrasting mineralogy of extrusive and plutonic salic rocks. Jour. Geology, 60, pp.107-124.

TUTTLE, O.F. and BOWEN, N.L., 1958. Origin of granite in the light of experimental studies in the system $NaAlSi_3O_8$-$KAlSi_3O_8$-SiO_2-H_2O. Geol. Soc. Amer. Memoir, 74.

VOLL, G., 1960. New work on petrofabrics. Liverpool and Manchester Geol. Journ. 2, pp.521-525.

YODER, H.S., STEWART, D.B. and SMITH, J.R., 1957. Ternary feldspars. Carnegie Institution of Washington. Annual report of the Director of the Geophysical Laboratory, 1956-1957. pp.206-214.

APPENDICES TO CHAPTER 5.

1) Diffractometer Settings.

Diffractometer instrument settings used were:

For measurement of scans from 20° to 33° 2θ (CuKα): scanning speed ¼°/min., chart speed 400 mm/hr., rate meter 4, time constant 8. Slits 1° - .1° - 1°, at 40 kV 20 mA. The 2θ values quoted for this range (Table 5.6) are for specimens scanned six times, i.e. three times in each direction using the oscillating device. Only the fully resolved single reflections or the most important combined reflections, shown underlined in this table, are the means of six measurements. For measurement of 2θ $\bar{2}01$ feldspar - 2θ 101 $KBrO_3$ the same settings were employed, the goniometer being oscillated between 19.5° and 22.5°. $KBrO_3$ or a quartz powder were used as an internal standard where appropriate (Q masks K-phase $\bar{2}01$ reflection and $KBrO_3$, K-feldspar 131, among others).

For measurement of the Ab 131, Ab $02\bar{2}$, and Mi 131 reflections, to improve resolution of the region between Mi 131 and Ab/Mi $1\bar{3}1$ the slower scanning speed of ⅛°/min. was employed together with a rate-meter setting of 2. At least one complete oscillation was made for each record, between 29° and 32°.

2) Details of diffractometer patterns between 20° and 33° 2θ.

A series of typical charts is shown in figs. 5.19, 20. 2θ values for a pair of L. Ailsh feldspars are given (six measurements) in table 5.6 together with the 2θ values for pure forms of $KAlSi_3O_8$ and $NaAlSi_3O_8$ as determined by previous workers for comparison (Tables 5.5 and 5.4).

In addition Dr. W.S. MacKenzie supplied unpublished 2θ values for three microclines of varying obliquity from his 1954 paper. These were:

Table 5.7.

	131	$1\bar{3}1$	Separation
Blue Mountain microcline:	29.455	30.240	0.785
Spencer E.:	29.670	30.055	0.385
Spencer U.:	29.740	29.990	0.250

The separation observed for Blue Mountain microcline is very close

Fig.5.19.

Diagrammatic representation of diffractometer charts between 21° and 33° 2θ., showing overlapping of peaks for the individual phases. Intensities are drawn with roughly the same relative magnitude as observed at L.Ailsh.

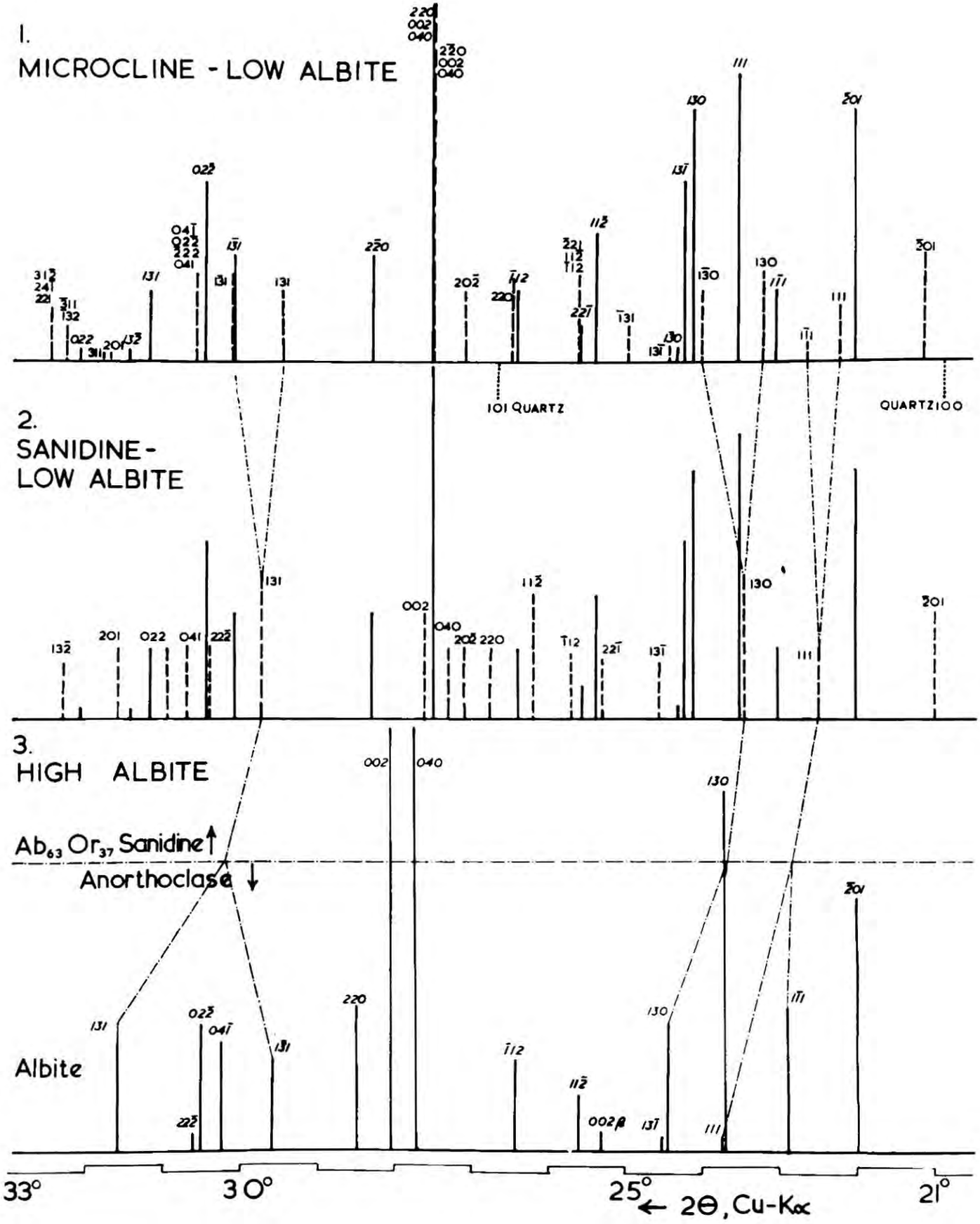
1.
MICROCLINE - LOW ALBITE
101 QUARTZ
QUARTZ100
2.
SANIDINE-
LOW ALBITE
3.
HIGH ALBITE
Ab63 Or37 Sanidine
Anorthoclase
Albite
33°
30°
25°
21°
← 2θ, Cu-Kα

Fig.5.20.

Copies of diffractometer traces from 21° to 33° of feldspars showing varying proportions of monoclinic to triclinic material in the K-phase. (66) has a K-phase of highly oblique microcline alone, whilst (313) , at the other end of the range, has exclusively monoclinic K-feldspar.

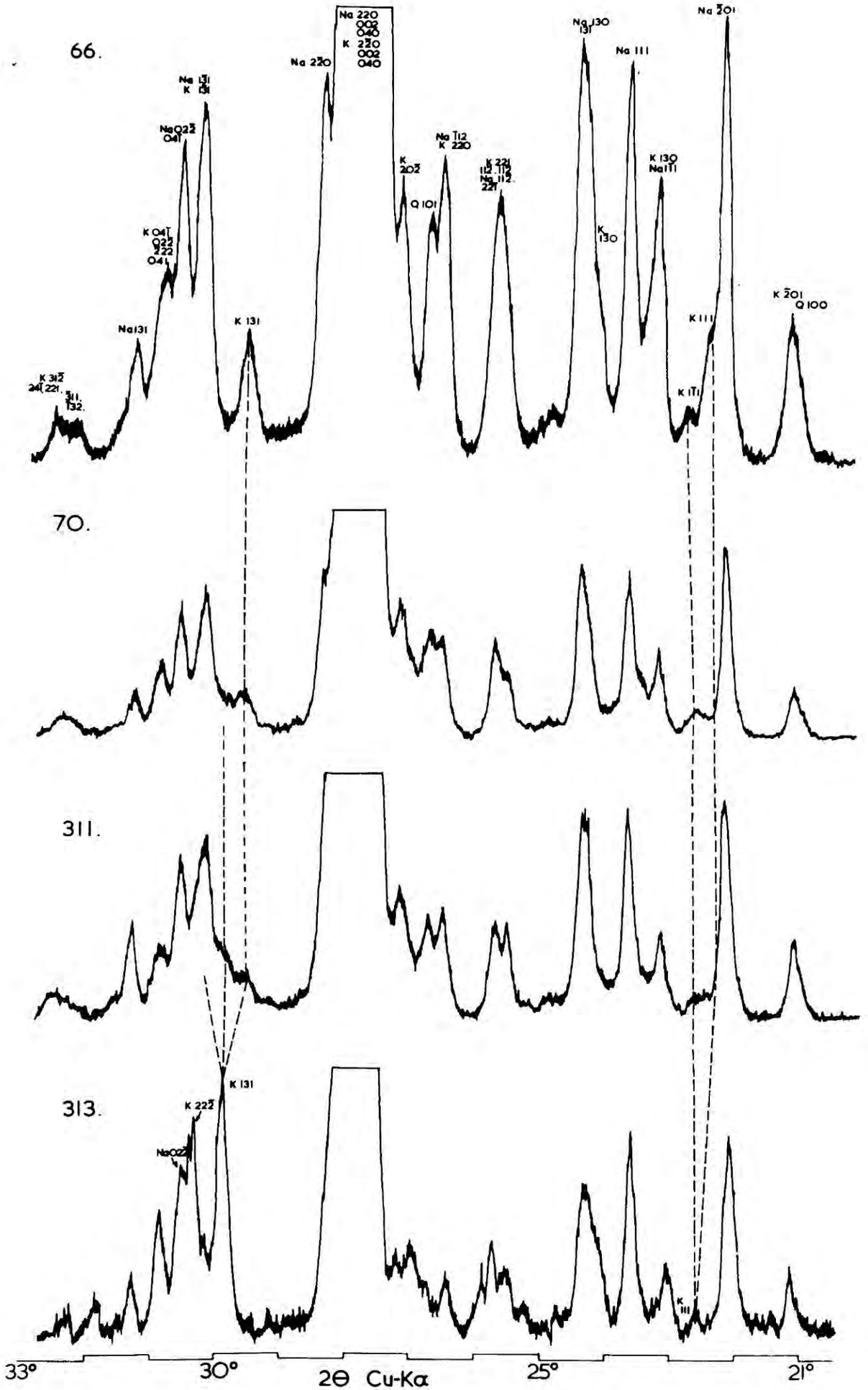
66.
70.
311.
313.
Na 220
002
040
K 220
002
040
Na 131
K 131
Na 220
Na 022
041
K 041
022
222
041
Na 131
K 131
K 202
Q 101
Na 112
K 220
K 221
112 111
Na 112
221
Na 130
131
K 130
Na 111
K 130
Na111
Na 201
K 111
K 111
K 201
Q 100
K 313
241 221
311
132
K 131
K 222
Na 022
K 111
33°
30°
2θ Cu-Kα
25°
21°

Table 5.4.

X-ray powder data of monoclinic and triclinic $KAlSi_3O_8$ between 2θ (CuKα) 20° & 31°.

hkl	2θ calc.	2θ obs.	q	hkl	2θ calc.	2θ obs.	q
$\bar{2}01$	21.05	21.14	6	$\bar{2}01$	20.945	20.945	8R
111	22.25	22.34	3	111	22.54	22.525	3R
$1\bar{1}1$	22.66	22.66	1-	200	22.98	22.92-22.99	1R
200	23.03			130	23.485	23.475	10R
130	23.21	23.21	5	$13\bar{1}$	24.565	24.57	4R
$1\bar{3}0$	24.0	24.0	4	$22\bar{1}$	25.05	25.035	3R
$13\bar{1}$	24.32	24.48	1-	$11\bar{2}$	25.76	25.755	8R
$22\bar{1}$	24.81			220	26.79	26.785	9R
$\bar{1}31$	24.95	24.91	2	$20\bar{2}$	27.13	27.13	9R
$11\bar{2}$	25.52			040	27.35	27.35	6R
$\bar{2}21$	25.66	25.64	5	002	27.66	27.655	10R
$\bar{1}12$	25.66			131	29.795	29.80	8R
220	26.43	26.48	5	$22\bar{2}$	30.43	30.465	1
$20\bar{2}$	27.06	27.1	4	041	30.73	30.73	2
$2\bar{2}0$	27.36			022	30.93	30.92	1
002	27.43	27.46	10				
040	27.5						
131	29.49	29.52	4				
$22\bar{2}$	30.2	30.15	5				
$1\bar{3}1$	30.26						
022	30.7						
041	30.7	30.6	5				
$02\bar{2}$	30.85						
$04\bar{1}$	30.90						

Microcline

(Laves, 1954a, converted to CuKα).

Sanidine (Artificial)

(Donnay and Donnay, 1952).

Table 5.5.

X-ray powder data of high and low $NaAlSi_3O_8$, between 2θ 20° and 32° (CuK_α).

hkl	2θ calc.	2θ obs.	q	hkl	2θ calc.	2θ obs.	q
$\bar{2}01$	22.055	22.057	60	$\bar{2}01$	21.995	22.0	60
$1\bar{1}1$	23.07	23.071	20	$1\bar{1}1$	22.905	22.915	40
111	23.54	23.538	85	$1\bar{3}0$	23.715	23.73	100
130	24.155	24.155	70	111	23.75		
$13\bar{1}$	24.27	24.306	50	130	24.47	24.46	35
$1\bar{3}0$	24.335			$13\bar{1}$	24.54		
002β		25.185	5	002β		25.35	5
$11\bar{2}$	25.40	25.392	35	$11\bar{2}$	25.635	25.63	15
$22\bar{1}$	25.565	25.57	5	$\bar{1}12$	26.46	26.445	25
$\bar{1}12$	26.418	26.418	20	$2\bar{2}0$	27.66		
002	27.92	27.915	360	040	27.79	27.785	160
040	27.99			$20\bar{2}$	27.805		
220	28.12			002	28.095	28.095	360
$2\bar{2}0$	28.325	28.325	30	220	28.535	28.525	40
$1\bar{3}1$	30.145	30.148	30	$1\bar{3}1$	29.62	29.62	25
$22\bar{2}$	30.225			$04\bar{1}$	30.305	30.295	30
$02\bar{2}$	30.51	30.48	50	$02\bar{2}$	30.52	30.54	35
$04\bar{1}$	30.54			$22\bar{2}$	30.655	30.65	5?
131	31.23	31.21	20	131	31.595	31.61	35

Low albite (Amelia) — Heated Amelia albite

Smith (1956).

Table 5.6.

2θ values of two feldspars from L. Ailsh, 20° to 32° 2θ CuKα.

Phase	hkl	2θ obs.	q	Phase	hkl	2θ obs.	q
K	$\bar{2}01$	20.97	3R	K	$\bar{2}01$	21.095	1R
Na	$\bar{2}01$	22.032	7R	Na	$\bar{2}01$	21.950	3R
K	111	22.24	1	Na	$1\bar{1}1$	22.95	1
K	$1\bar{1}1$	22.58	1	Na	111	23.508	3R
K	130	23.05	4	Na	$130, 13\bar{1}$	24.2	3
Na	$1\bar{1}1$			Na	$22\bar{1}$	25.5 to	1
Na	111	23.519	10R	K	$11\bar{2}$	25.65	
K	$1\bar{3}0$			Na	$\bar{1}12$	26.4	1
Na	130	24.28	9	K	220	26.9 to	1
Na	$13\bar{1}$				$20\bar{2}$	27.15	1
K	$13\bar{1}$	24.78	<1	K	220		
K	$\bar{1}31$	24.91	<1		002		
K	$22\bar{1}$				040		
	112			Na	$2\bar{2}0$	27.7	10+
	$11\bar{2}$	25.52	5		002		
Na	$11\bar{2}$				040		
	$22\bar{1}$			K	131	29.805	5R
Na	$\bar{1}12$	26.40	7	Na	$1\bar{3}1$	30.15	1
K	220			?	?	30.26	3
K	$20\bar{2}$	27.04	4	Na	$02\bar{2}$	30.43	3
Na	220				$04\bar{1}$		
	002			K	$22\bar{2}$		
	040			K	041	30.75	2
K	$2\bar{2}0$	27.7	10+		022		
	002			Na	131	31.198	1R
	040						
Na	$2\bar{2}0$	27.31					
K	131	29.443	2R				
Na,K	$1\bar{3}1$	30.152	6				
Na	$04\bar{1}$	30.48	7				
	022						
K	$04\bar{1}, 022$	30.71	3				
	$\bar{2}22, 041$						
Na	131	31.199	2				

Specimen 16a

Specimen 313

Fig.5.21.

Plot of 2θ values for 131 and $1\bar{3}1$ reflections of a series of microclines determined by Dr.W.S.Mackenzie, together with three L.Ailsh feldspars, 313, 216, and 16a.

B: Blue Mountain microcline.

E: Spencer E.

U: Spencer U.

D: Artificial $KAlSi_3O_8$ (Donnay and Donnay)

'k' is the measurement assumed for calculation of percentage obliquity at L.Ailsh, rather than k+ ac, c being the extrapolated position of orthoclase 131 from Mackenzie's figures.('a' is the 131 position determined from the monoclinic K-phase of specimen 313.)

to Laves' Maximum Microcline and was used by MacKenzie to establish lattice parameters appropriate for this material. The 2θ values above were used to establish whether the doublet concerned (131/1$\bar{3}$1) split symmetrically about the single 131 peak reflection of a monoclinic K-feldspar. Diagram 5.21 shows the relation found; the 131/1$\bar{3}$1 doublet divides linearly about an extrapolated 'monoclinic 131' position at about 29.87°.

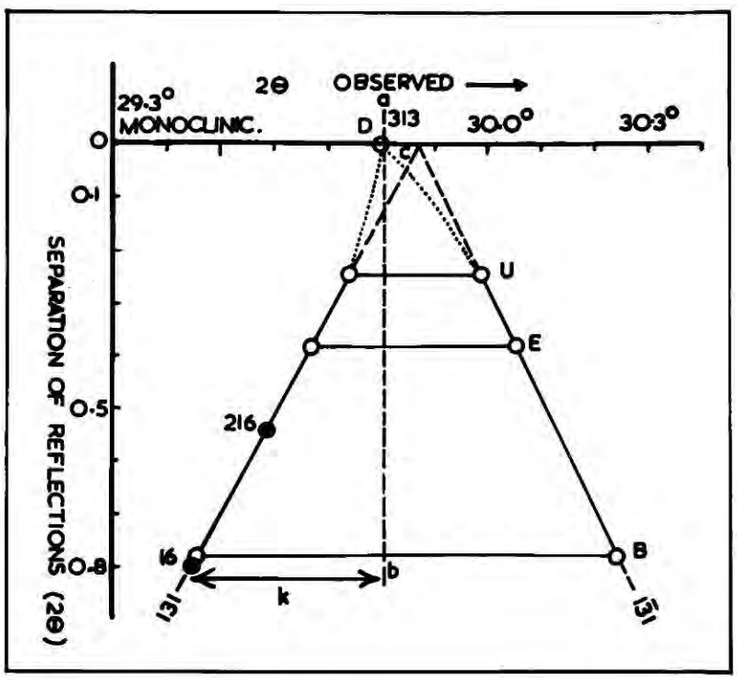

Donnay and Donnay give the 131 reflection for monoclinic $KAlSi_3O_8$ at 29.80°, or applying the correction to their figures suggested by Smith (1956), at 29.825°. The 131 position found for the monoclinic potash phase of specimen 313 was 29.805° but it must be remembered that this figure is not strictly comparable with that of the above workers since it certainly contains appreciable Na in solid solution. The effect of Na or the position of the 131 reflection of monoclinic potash feldspar is to increase its 2θ value, however (see Donnay and Donnay, 1952, $Ab_{61}Or_{39}$ 131 at 30.14°), so there is some uncertainty in the significance of this value for sp. 313. It was, however, used as the datum of "zero obliquity" in the construction of figure 5.12 and also in construction of fig. 5.13. Fig. 5.21 shows that if Donnay and Donnay's and MacKenzie's 2θ values are strictly comparable at low Δ 2θ values

the movement of $1\bar{3}1$ relative to any fixed datum does not necessarily bear a straight line relationship to the corresponding movement of 131, but this relation holds at high $\Delta\ 2\theta$ values within the range found. Because percentage obliquities are calculated on the basis that the line ab (diagram 5.21) is 0 obliquity - i.e. 131 orthoclase is at 29.8) and this line does not intersect 0 obliquity at c, we get low values of % obliquity for all but obliquity = 100% relative to the $131/1\bar{3}1$ doublet were it measured, as is ideal, direct. The quoted figures should not therefore be used for comparison with other areas but are valuable relative to one another.

There is good agreement between values of obliquity determined using Ab $02\bar{2}$ and that deduced from the position of 131 relative to a standard, e.g. (216), obliquity with $02\bar{2}$ as datum 59%, position of 131 peak with quartz standard 29.585°, equivalent obliquity from fig. 5.21, 61%.

It will be seen also that certain high obliquity values exceeded (i.e. had lower 2θ values) the position of $1\bar{3}1$ of MacKenzie's Maximum Microcline, thus:

Blue Mountain microcline	:	29.455°
Loch Ailsh 268	:	29.447°
Loch Ailsh 16a	:	29.443°

In the absence of direct measurement of the separation of the $131\text{-}1\bar{3}1$ doublet it is not certain that this does indicate the existence of microclines of higher obliquity than previously recorded.

A further complication arose when it was discovered that the separation of Ab $02\bar{2}$ and microcline 131 measured at low scanning speeds (½°/min. and rate meter 2), gave consistently higher values of separation than those measured at ¼°/min. and R.M. 4. The figures plotted on fig. 7 are those obtained at the low scanning speed which was adopted for improved resolution especially of the region between K 131 and $1\bar{3}1$. Calculation of the maximum value of $\Delta 2\theta$ Ab $02\bar{2}$ - 2θ Mi 131 to be expected using Smith's low albite 2θ values and MacKenzie's microcline 2θ values showed that this was exceeded by L. Ailsh feldspars in numerous cases. Measurement at the higher scanning speed used by Smith (and presumably MacKenzie) gave much better agreement. It is believed that the slow scanning speed allowed partial resolution of the datum peak into the reflections $02\bar{2}$ and $04\bar{1}$. This may be a major source of scatter but the relative values obtained should be valid since all plotted

measurements were made at the same instrument settings.

Symbols used in the tables of X-ray data.

Rock types:

1 = S1.	2 = S2.
3 = S3.	3m = Melanite bearing S3.
3/ m = Melanite bearing S3 in Metamorphic Burn.	
Z = Zoned or mantled variety.	V = Minor dyke or vein.
Cr = Crushed rock.	B = Feldspars from basic rocks.

Where a rock is mixed - e.g. S2 xenocrysts in S3, the material in greatest amount (simply judged very roughly by eye in the hand specimen) is placed first, thus: '2 + 3'. If the admixed material is small in quantity the prefix 'r' is used. Thus: '2+ r3'.

Table 5.8.

Table of Important X-ray Data for Loch Ailsh Alkali Feldspars.

(All 2θ are means of at least two measurements, except those marked *. Radiation CuKα. For symbols of rock type, see above).

Spec. No.	Rock Generation	(2θKfsp $\bar{2}01$)-(2θKBrO$_3$ 101)	(2θNafsp $\bar{2}01$)-(2θKBrO$_3$ 101)	131/$1\bar{3}1$ peak type (Fig.5.10)	(2θNafsp $02\bar{2}$)-(2θKfsp 131)	(2θNafsp 131)-(2θNafsp $02\bar{2}$)	Obl. %	N.B.
66	3	0.81	1.84	6	1.030	0.705	88	
170	1	0.80	1.83	3	-	0.720	-	
89	3m	0.82	1.82	6	1.030	0.735*	88	
21f	3	0.79	1.82	6	1.055	0.713	94	
87	3m	0.82	1.83	6	1.013	0.705	84	
216	3(m	0.80	1.83	6	0.913	0.723	59	Mi 131 peak strongly assymetric. Obliq. measured at top.
65	3m	0.78	1.83	6	1.013	0.730	84	
21b	3?Cr	0.77	1.85	6	1.060	0.710	95	
24	2+3	0.79	1.83	5	1.020	0.708	85	
70	2	0.80	1.84	5	1.000	0.713	80	
55	2Cr	0.80	1.83	6	1.023	0.708	86	
67d	3+2	0.77	1.84	5	1.013	0.718	83	
16a	3+2	0.82	1.86	4	1.075	0.700	99	
94	3	0.78	1.83	6	1.017	0.730	84	
26	2+3	0.80	1.84	6	1.035	0.735	89	
92	2Z	-	1.84	6	1.070	0.713	98	V.strong Na-phase refl.
418	2V	0.79	1.82	6	1.055	0.740	94	
417	3V	0.80	1.85	6	1.065*	0.720*	96	
219	2	0.79	1.83	5	0.998	0.733	80	
311	1	0.80	1.83	2	-	0.760*	-	
72b	2?Cr	0.76	1.83	3	-	0.730*	-	
269	2	0.83	1.84	5	1.048	0.723	92	
465a	2?Cr	0.76	1.84	4	-	0.74*	-	
250	B	0.82	1.87	5	-	-	94	
232	B	0.79	1.82	3	-	0.76*	-	

Table 5.8 cont.

21c	B	0.80	1.81	4	1.050*	0.76	-	K 131 v. irreg. but ± type 4.
1370	1	0.78	1.82	3	-	0.73*	-	
200	3+r2	0.82	1.88	6	1.060	0.715	95	
239	3+r2	0.83	1.88	6	1.045	0.710	91	
53	2	0.82	1.86	6	1.025	0.738	86	
67e	3	0.78	1.83	6	1.043	0.720	91	
9	2+3	0.73	1.83	5	1.020	0.720	85	
19	2	0.82	1.83	5	0.998	0.728	80	
17	2	0.81	1.84	5	1.020	0.743	85	
305	1	0.84	1.87	4	-	0.750*	-	
313	1	0.89	1.75	1	-	0.76*	0	V. sharp strong K 131 refl.
117	2+3	0.78	1.84	6	1.010	0.715	82	
116	2+3Cr	Masked by quartz	Not present	6	-	-	90	Crushed K_2O enriched. % obl.from sep. of 131/1$\bar{3}$1 Mi peaks.
114	2+3Cr			6	-	-	94	
469	3	0.78	1.82	6	0.965	0.725	71	
413	2	0.81	1.84	5	0.975	0.738	74	
361	3	0.79	1.85	6	0.980	0.728	75	
466	2	0.77	1.83	5	0.998	0.720	80	
360	3+2	0.81	1.87	5	0.993	0.728	78	
331	V	not present	1.84	-	-	0.75*	-	Albite rich vein.
359	3+2	0.77	1.84	6	1.055	0.715	94	
474	2	0.76	1.82	6	0.993	0.733	78	
352	3+r2	0.79	1.84	6	1.040	0.720	90	
347	2c3	0.77	1.82	5	1.040	0.715	90	
35	2?Cr	0.80	1.86	5	0.950	0.725	67	
353	3	+	+	6	1.013	0.743	84	
151	V	0.81	1.85	6	1.040	0.730	90	
280	3+r2	+	+	6	1.060	0.720	95	
401X	2	0.74	1.84	5	1.010*	0.725*	82	
401Ma	3	0.80	1.84	6	1.045*	0.740*	91	
401Mb	3	0.76	1.84	6	1.040*	0.705*	90	
271	3	+	+	6	1.073	0.708	99	
268	3+2	+	+	6	1.075	0.718	99	

Table 5.8 cont.

459	3m	+	+	6	1.020	0.743	85	
120	3+2Cr	+	+	6	1.030	0.723	87	
428	3	+	+	6	1.023	0.733	85	
139	?Cr	+	+	5	1.005	0.728	81	
147	2+3Cr	+	+	6	0.988	0.723	77	
100	2Cr	+	+	6	1.068	0.707	97	
101	2Cr	+	+	6	0.975	0.703	74	
59	2+3	+	+	6	1.058	0.723	94	
32	2+3	+	+	6	1.050	0.700	92	
45	2+3	+	+	6	1.023	0.723	86	
446	3	+	+	6	1.043	0.718	91	
454	3m	+	+	6	0.990	0.718	77	
451	3m	+	+	6	1.035	0.718	89	
464	3	+	+	6	1.033	0.710	88	
348	2+3	+	+	5	1.015	0.730	84	
156	3+1	+	+	6	1.048	0.710	92	
12	3+2	+	+	6	1.015	0.720	84	
95	3	+	+	6	1.033	0.730	88	
453	3m	+	+	?6	1.048	0.730	92	Has peak at 29.8° due to contamination by minor vein).
69	?	+	+	5	1.005	0.760	81	Fine fairly mafic type of unknown affinities.
145	3+r2	+	+	6	1.020	0.720	85	
159	3	+	+	6	1.038	0.723	90	
78	3?	+	+	6	1.080	0.710	100	
460	3m	+	+	6	1.048	0.715	92	
81	3m	+	+	6	1.038	0.713	90	
160	1	+	+	4	-	0.730*	-	
258	B	+	+	5	1.05*	0.720*	94	
137A	3	0.78	1.85	6	+	+	-	
B	3	+	+	6	+	+	-	
C	1	0.84	1.84	3	-	0.72*	-	
D	1	+	+	4	-	0.72*	-	

+ : Present but not measured.

- : Not present or possible to be measured.

3) Separation of perthites into phases.

As a possible solution to the problem of indirect measurement of obliquity an attempt was made to separate the albite and microcline phases of a perthite having a K-phase of high obliquity. The feldspar was ground to pass 300 mesh and dried. Mixtures of bromoform and benzene were used and the suspension centrifuged. If two fractions did not form bromoform or benzene appropriately was added a small drop at a time into the centrifuge tubes and the suspension again centrifuged briefly. When two distinct fractions formed the light portion was filtered off, dried and X-rayed. A series of portions of the X-ray charts in the 29° - 32° region at three different stages in the fractionation process are shown in fig. 5.22 together with scans from 20° to 32° of powders before and after separation. The technique is clearly quite a feasible method of study for such perthites. Dr. W.S. MacKenzie, who suggested the method, has separated nepheline from feldspar in artificial mixtures down to 2μ in grain size - not pure separations but concentrations of the one mineral so that its X-ray pattern is resolved. Further development of the technique was precluded because of lack of time and further it will be seen that even after four separations some Ab inevitably remains so that uncertainty as to the true position of microcline $1\bar{3}1$ still persists. Thus the method did not seem to offer a certain method of obliquity measurement, with particular difficulty in the more finely exsolved specimens.

4) Potash Enrichment.

The absence of albite lines in diffractometer charts of certain rocks was mentioned in Section 1 as associated with crushing. Charts showing this effect are shown on fig. 5.23. Specimen 117 is the uncrushed central S2 type and 116 the crushed and quartz veined material about 1 m. away.

5) Orientation of alkali feldspars for single crystal X-ray oscillation photographs.

The technique used is that of Smith and MacKenzie (1955), in their standard orientation, i.e. with the 'b' crystallographic axis of the grain vertical and the X-ray beam to 001 in the centre of a 15° oscillation. However, the method of setting the crystal on the fibre in this orientation is, of course, not described by them, and the

Fig.5.22.

Diagram illustrating the removal of albite from perthites subjected to repeated centrifuging in heavy liquids of closely controlled specific gravity.

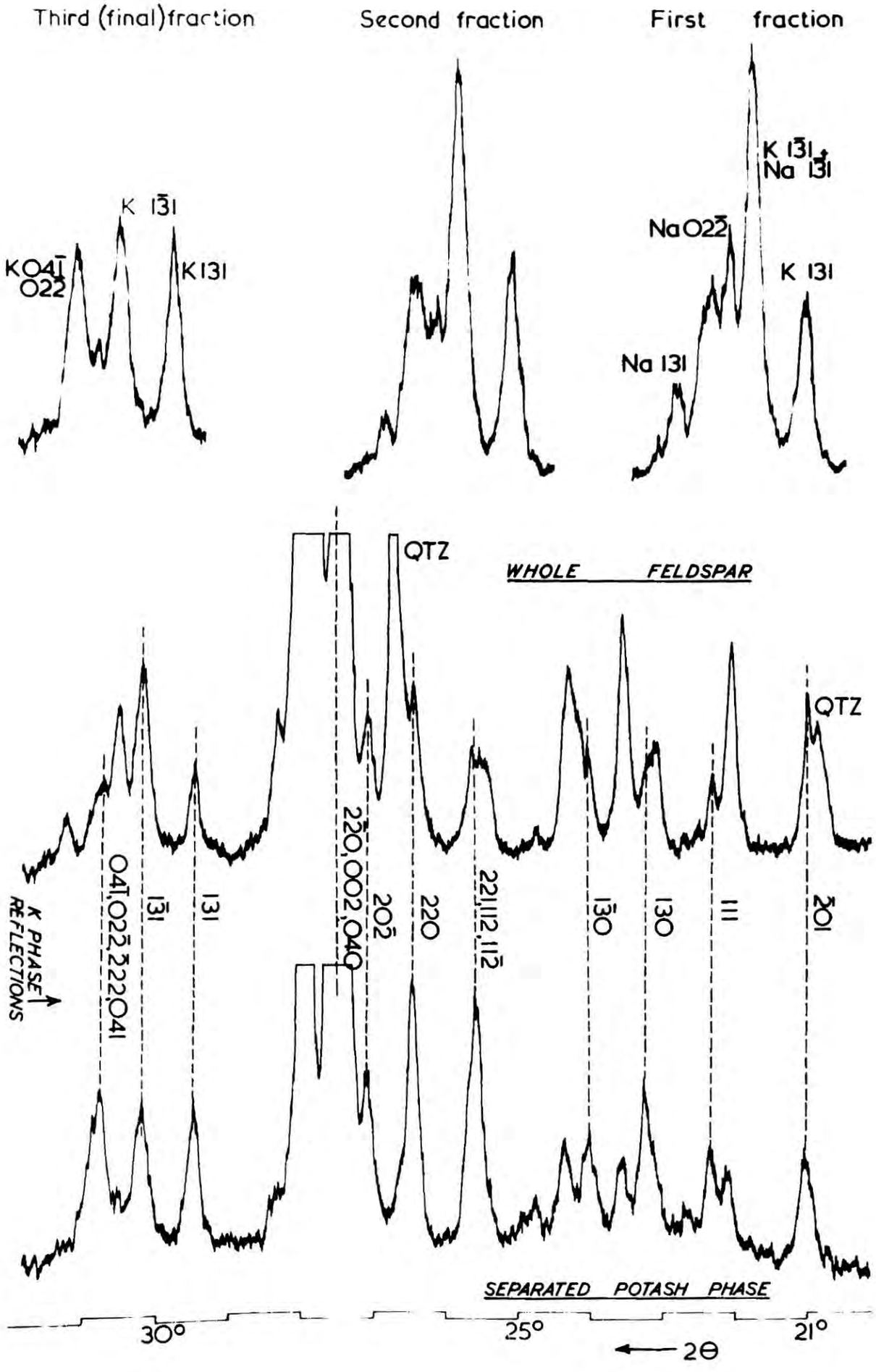
Third (final) fraction
Second fraction
First fraction
K 1̄31
K041, 022
K131
K 131, Na 131
Na022̄
K 131
Na 131
QTZ
WHOLE FELDSPAR
QTZ
K PHASE REFLECTIONS
041, 022̄, 222, 041
1̄31
131
220, 002, 040
202̄
220
221, 112, 112̄
1̄30
130
111
201̄
SEPARATED POTASH PHASE
30°
25°
21°
2Θ

Fig.5.23.

Diffractometer patterns demonstrating the potash enrichment along crush-belts in the central area of the mass. 117 and 116 are whole rocks about 1m. apart. Ab peaks are very weak in 116, from near the centre of the crush belt.

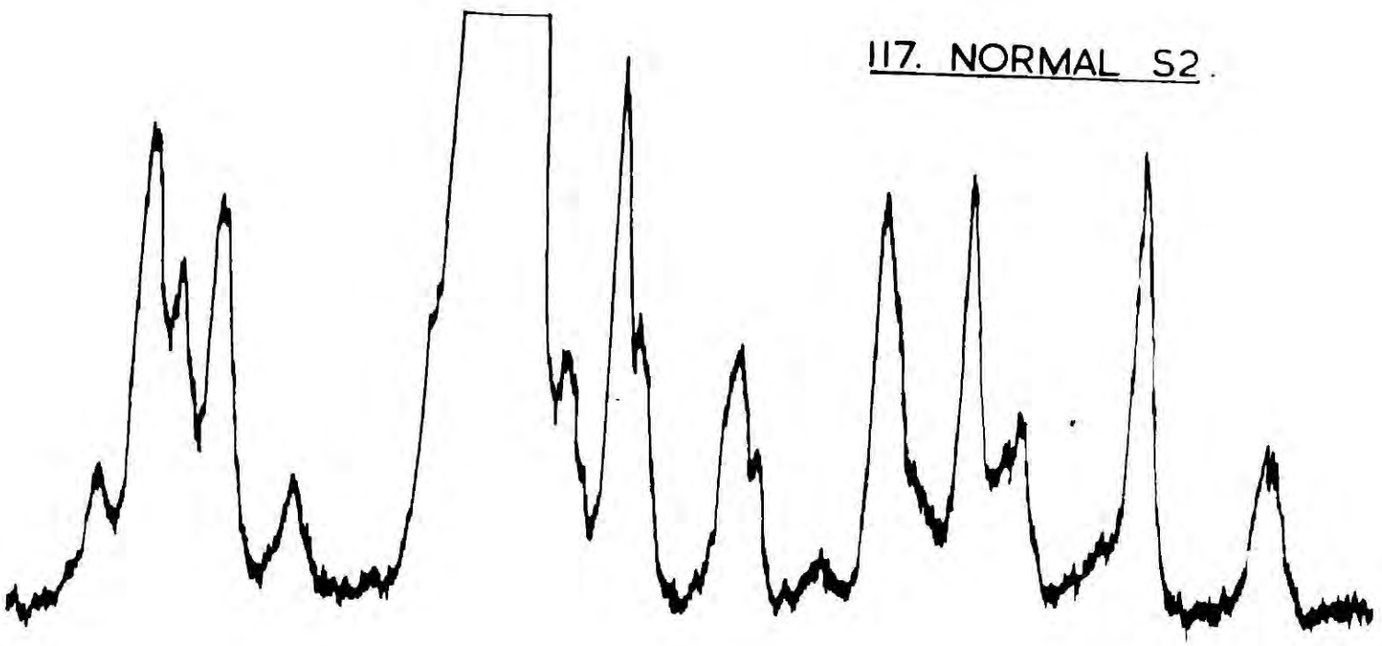

117. NORMAL S2.

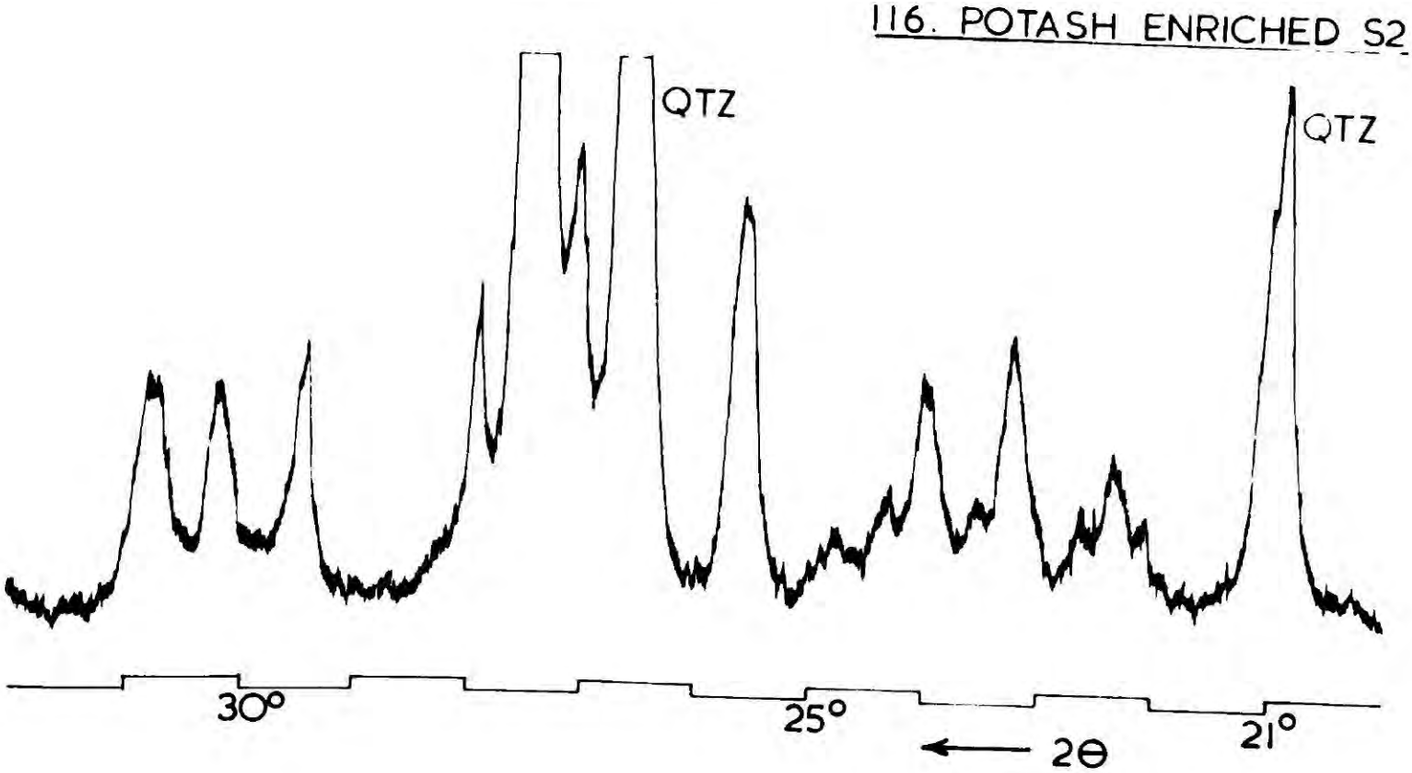

116. POTASH ENRICHED S2

comparative unfamiliarity of the technique would seem to make a more detailed description of this part of the process worth while. (For orientation see fig. 5.24).

Procedure.

(1) Select a cleavage fragment c. 0.1 mm. - 0.3 mm. in largest dimension, showing reasonable cleavage faces.

(2) Usually such a fragment will lie on its 001 cleavage which is perfect in the feldspars. To check the identity of the cleavage note:

(a) Flash figure or something near it should be obtained, since 001 is app. // to the optic axial plane, in low temp. feldspars.

(b) Where present Ab and pericline twinning are normal to 001.

(3) When such a fragment has been obtained 'b' must be determined and set vertically. In such a grain, which should be roughly rectangular, we have to choose between 'a' and 'b'. To determine which note:

(a) 010 is usually the better of the two cleavages, normal to the microscope stage.

(b) Ab twins are // 010, normal to 100.

(c) Pc twins are // 100, normal to 010.

(d) Note that if the external morphology of the grain can be seen, even if it is triclinic, the section of the crystal as seen when correctly orientated and viewed from the same direction as the X-ray beam, should approximate to a rectangle, since:

ORTHOCLASE :	$\alpha = 90^\circ$	$\beta = 116^\circ 3'$	$\gamma = 90^\circ$
MICROCLINE:	$\alpha = 89^\circ 19'$	$\beta = 115^\circ 50'$	$\gamma = 92^\circ 10'$
ALBITE :	$\alpha = 94^\circ 31'$	$\beta = 116^\circ 38'$	$\gamma = 87^\circ 1'$

(Values from Winchell, Pt.2, 1946).

If, however, 'a' has by accident been set vertical the angle will then also be vertical and end view of the crystal will not be a rectangle but will deviate from 90° by 25° app. Since even sodic perthites tend to retain the external monoclinic morphology of their higher temperature forms, this can be a useful way of recognizing the correct cleavage.

(4) The grain may now be mounted on the glass fibre and set with 001(?) vertical and 010(?) horizontal, by means of the microscope on the single crystal camera. This may be done with considerable accuracy, so that if a picture is now taken the general layout of a photograph similar to those shown here and in the literature should be obtained. If so the crystal need only be set so that the zero layer line is horizontal by

the normal x-ray setting procedure. The most easily made mistake in the process is confusion of 'a' and 'b'; if 'a' has been set vertically clear layer lines should be seen, all the spots being roughly in layer lines without the groupings of spots on close, somewhat offset layer lines commonly seen on photographs of crystals in the standard orientation. In such a case (i.e. 'a' vert.):

$2h_1$ = 11.2 mm. app.

$2h_2$ = 23.6 mm. app.

and the crystal must be removed from the fibre and reset at 90° to the original position.

6) Detailed description of single crystal X-ray photographs.

A series of reproductions of single crystal photographs are given together with the individual descriptions below, and sketches of detail of certain groups of reflections.

313 (Fig. 5.24, above). Coire Sail, S1.

Ab twinned Na-phase with single well defined reflection from a monoclinic K-phase. There is a certain amount of material in a disorientated position in this photograph, probably due to a small detached fragment lying on the major cleavage fragment.

311(B) (Fig. 5.25). Coire Sail, S1.

There is slight strain disorientation in this photograph. A strong Ab twinned Na-phase (AA) shows weak pericline twin reflections (PP) between the Ab twin reflections. These are in the position known as the 'M' type relation by MacKenzie indicative of exsolution as a monoclinic Na-phase. The somewhat diffuse pair of triclinic K-phase reflections appear to lie off the row lines - i.e. in a 'diagonal association'.

26 (Fig. 5.25). Central Area, S2.

A strong pair of Ab twinned Na-phase reflections with two diagonally associated K-phase reflections close to the position for Ab twinning.

67d (Fig. 5.26). Central Area S3.

Considerable disorientation is apparent in this photograph. Weak pericline twinned reflections of the Na-phase in the 'M'-type association visible between the stronger Ab twinned spots. The K-phase is probably in a diagonal association near Ab twinning.

92 (Fig. 5.26). Zoned type.

Shows extreme smearing along lines of constant θ indicating

Fig.5.24.BELOW.

Sketch showing the arrangement of units of idealized feldspar cleavage fragment, orientated for single crystal oscillation photograph, with the 'b' axis vertical and the X-ray beam parallel to 'c' in the centre of a 15° oscillation.

Figs.5.24.(ABOVE)., 5.25.,5.26.

Reproductions of single crystal X-ray oscillation photographs of five L.Ailsh feldspars in the standard orientation of Smith and Mackenzie. A key to the interpretation of the groups of reflections is sketched in the corners of each example.

A: Albite twinned Na-phase.

P: Pericline twinned Na-phase.

T: Triclinic K-phase.

M: Monoclinic K-phase.

Detailed descriptions are given in the text.

N.B. It was found difficult to reproduce adequately the weaker reflections, and thus the K-phase reflections of 26, the K-phase and pericline twinned Na-phase of 311., and the pericline twinned Na-phase of67d have been touched into the reproductions in ink.

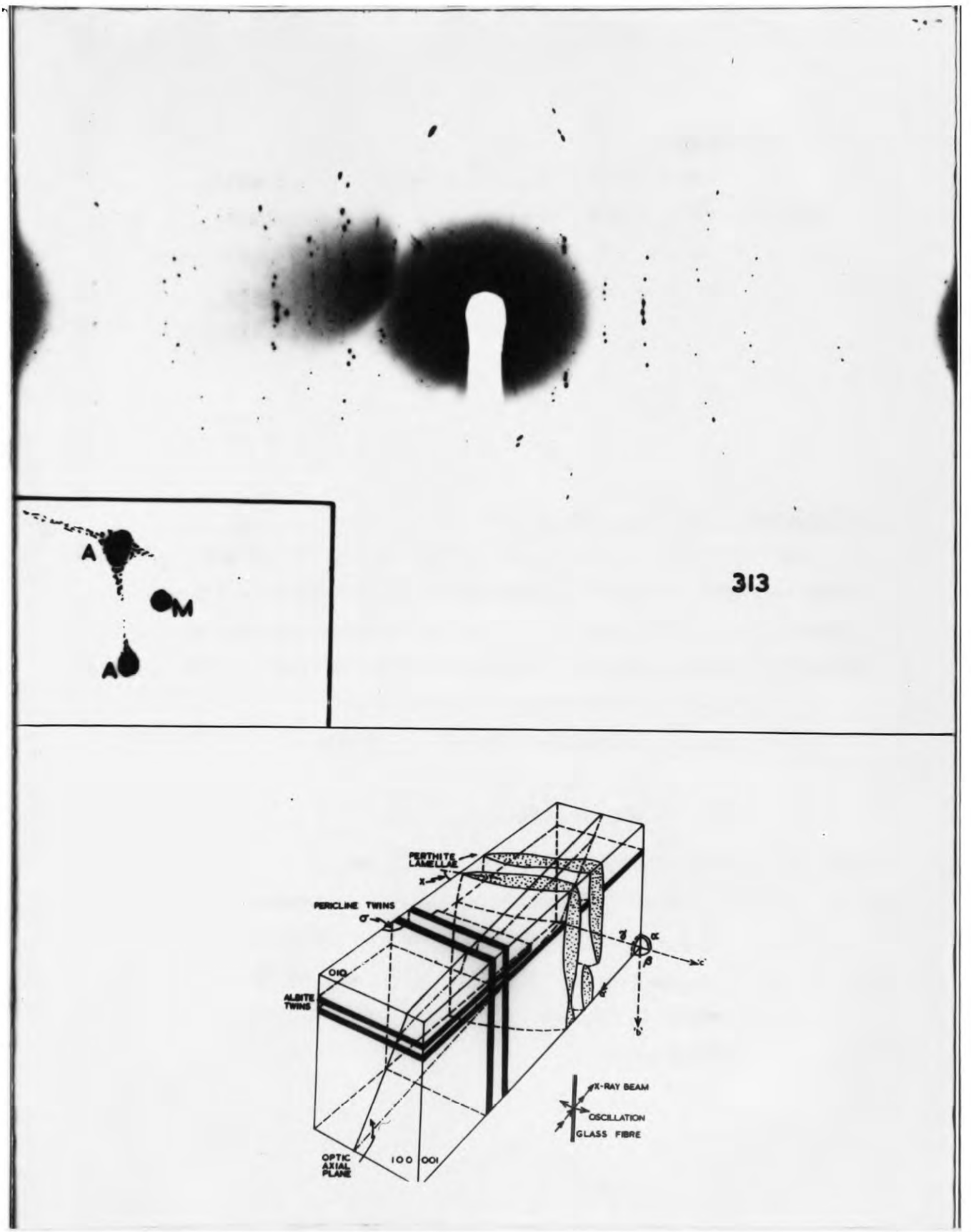
A
M
A0
313
PERTHITE LAMELLAE
PERICLINE TWINS
ALBITE TWINS
010
OPTIC AXIAL PLANE
100
001
X-RAY BEAM
OSCILLATION
GLASS FIBRE

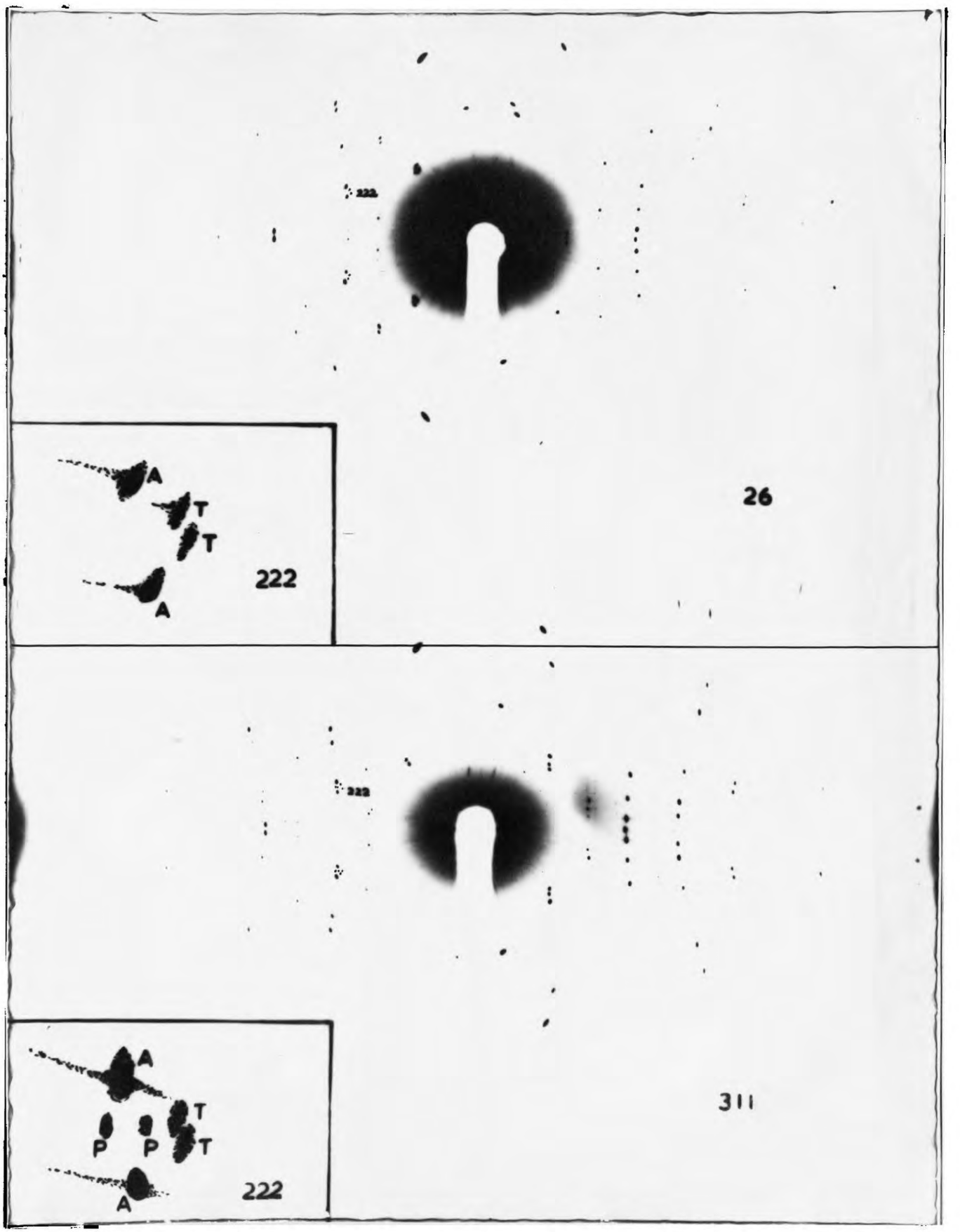
222
26
A
T
T
A
222
222
311
A
T
P
P
T
A
222

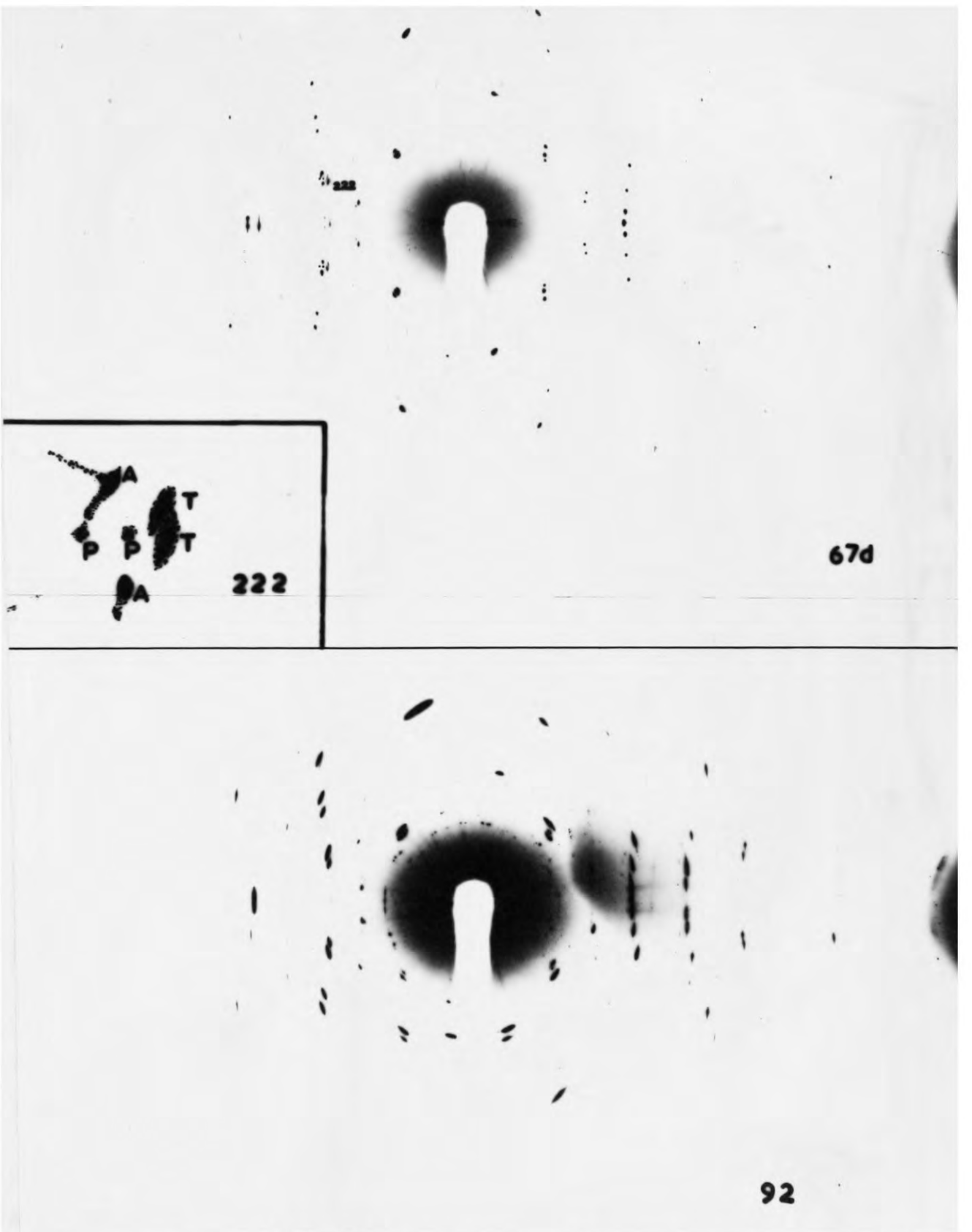
222
A
T
P
P
T
A
222
67d
92

disorientation in this case connected to the deformation of this partially crushed rock. Very commonly seen, to a lesser degree, throughout L. Ailsh rocks.

7) Heating Experiments.

Introduction.

Many different workers have experimented with the behaviour of different feldspars on heating, their results at times apparently conflicting. It seemed worth while to try heating a number of the Loch Ailsh feldspars and determining their response to different heating periods. The method could also provide a check on the wet analyses.

Technique.

The powdered samples were heated in a tube furnace at 1040°C ± 10°C in small platinum crucibles, open, standing in larger outer platinum crucibles which allowed easy withdrawal of the sample after the required heating period. For the homogenization/time data the crucibles were removed, a small sample taken out, and the remainder replaced. A control sample not subjected to this succession of rapid quenchings but continuously heated for 15 hours gave 2θ values closely comparable to a discontinuously heated specimen. No special precautions were taken to ensure rapid quenching, the crucibles being allowed to cool to room temperature standing on an asbestos sheet, which they did in a few minutes.

X-ray diffractometer charts were made as soon as possible after removing the powders from the oven. Smear mounts were used because of the small amount of material available.

Data.

The figures in brackets in table 5.9 are of doubtful accuracy or significance since they represent merely the most obvious peaks in a diffuse pair of reflections as the $\bar{2}01$ reflections of the two phases become one.

The form of the $\bar{2}01$ peaks is shown in diagram 5.27. For some reason the mode of change from two to one reflection is different in specimen 170 from the more potassic specimens 66 and 216. In the latter the Na-phase reflection becomes smaller and eventually appears as a shoulder on the more intense K-phase peak at lower 2θ. 170 on the other hand shows the opposite behaviour, the Na reflection always being

Table 5.9.

Table of 2θ ($\bar{2}01$ Fsp.)-(101 $KBrO_3$) at various heating times.

Specimen:	170		66		216	
Time(hrs.)	K Δ2θ	Na	K Δ2θ	Na	K Δ2θ	Na
Natural	0.80	1.83	0.81	1.84	0.80	1.83
0.5	(1.31)	(1.745)	(1.10)	(1.78)	(1.33)	(1.71)
1.0	-	-	(1.23)	(1.78)	(1.24)	(1.77)
2.0	(1.295)	(1.765)	(1.25)	(1.75)	(1.29)	(1.70)
4.0	1.685		(1.32)	(1.725)	(1.315)	(1.76)
8.0	1.595		(1.35)	(1.61)	1.33	
15.0	-		-		1.355	
25.0	1.600		-		1.415	
42.0	1.573		1.425		-	
66.0	1.59		1.435		-	
96.0	1.60		1.44		-	
132.0	-		-		1.45	
1485.0	1.555		1.44		-	

Specimen:	21b		24	
Natural	0.77	1.85	0.79	1.85
1,485.0	1.49		1.48	

Fig.5.27.

Change in the form of the $\bar{2}01$ reflections of three feldspars after different periods of heating.

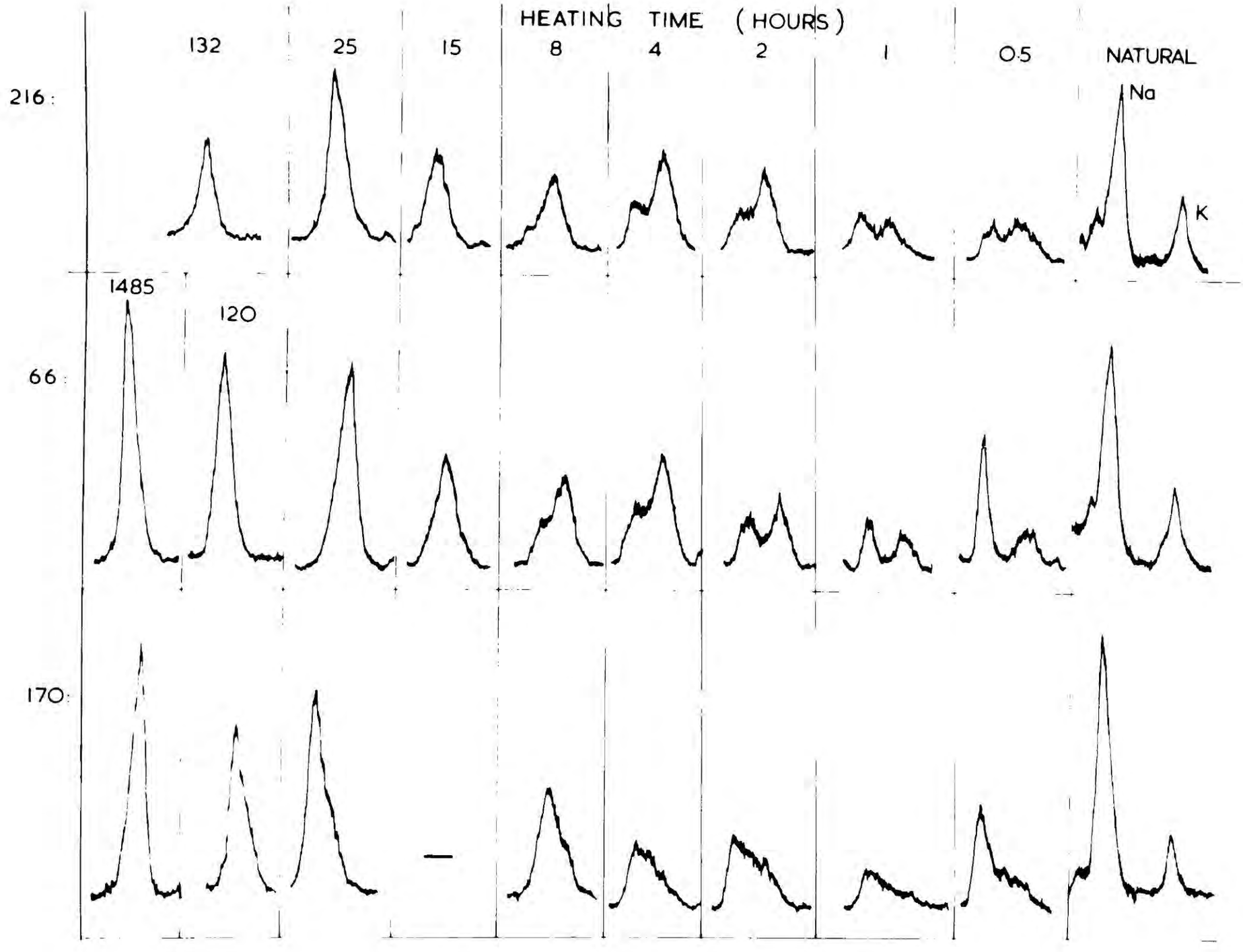
HEATING TIME (HOURS)
132
25
15
8
4
2
1
0.5
NATURAL
Na
K
216
1485
120
66
170

dominant. Diagram 5.28a shows the movement of the $\bar{2}01$ reflection against time and this difference in homogenization behaviour is reflected in the continuous plot of $\bar{2}01$ of 170 from higher 2θ values whilst the $\bar{2}01$ spacing of 66 and 216 is continuous from lower 2θ values.

The $\bar{2}01$ spacing of homogenized feldspars offers a method of determining bulk composition, to which there are a number of uncertainties attached. Fig. 5.28b shows the difference in 2θ of the feldspar $\bar{2}01$ reflection and 101 $KBrO_3$ of four feldspars heated for two months at 1040°C plotted against bulk composition as determined by flame photometry. The line determined for high temperature feldspars by Orville (1958) is shown together with the relative position of $\bar{2}01$ for a series of triclinic potash rich feldspars into which Na had been introduced by ion exchange (Orville, 1960). 2θ $\bar{2}01$ for low albite is also shown. Fit to the line for high feldspars is rather poor (the X-ray values being about 5% high for $NaAlSi_3O_8$) but the fit to a line for low feldspars made by projecting the ordered feldspar line of Orville to the position for low albite would be rather better.

This underlines the chief uncertainty of this method for determination of bulk composition in that the $\bar{2}01$ spacing is also dependent on the order-disorder of the Al-Si framework and between the composition/$\bar{2}01$ curves for the most ordered and disordered forms there will be an infinite number of possibilities. These cover a 5% compositional range. A lengthy period of heating does not necessarily imply that the structure is fully high - several workers report persistence of the low forms even after lengthy heating periods, (Rao, Nesbitt, etc.). If the flame photometer analyses are correct it would seem that the structures of these feldspars are not fully high even after two months' heating on the basis of the $\bar{2}01$ spacing.

Evidence to the contrary seems to come from the form of the diffractometer patterns at higher 2θ angles. The change in the form of the diffractometer patterns between 20° and 32° are shown in fig. 5.29. Indexing was carried out using the tables of Donnay and Donnay, 1952. They gave 2θ values for high temp. feldspars of composition $Ab_{61}Or_{39}$ and $Ab_{71}Or_{29}$. The agreement with their figures is good except for the reflection $13\bar{1}$ which does not appear on the L. Ailsh traces.

The compositions available in the L. Ailsh analysed specimens range from Or_{27} to Or_{41} which encompasses the composition Or_{37} at which

Fig.5.28.

ABOVE: Graph showing the rate of change of position of the $\bar{2}01$ reflections of three L.Ailsh feldspars with different heating periods.

BELOW: (2θ feldspar $\bar{2}01$)-($2\theta KBrO_3 101$) for four feldspars heated for two months plotted against analyzed bulk composition. The lines determined by Orville(1958 and 1960) are shown.

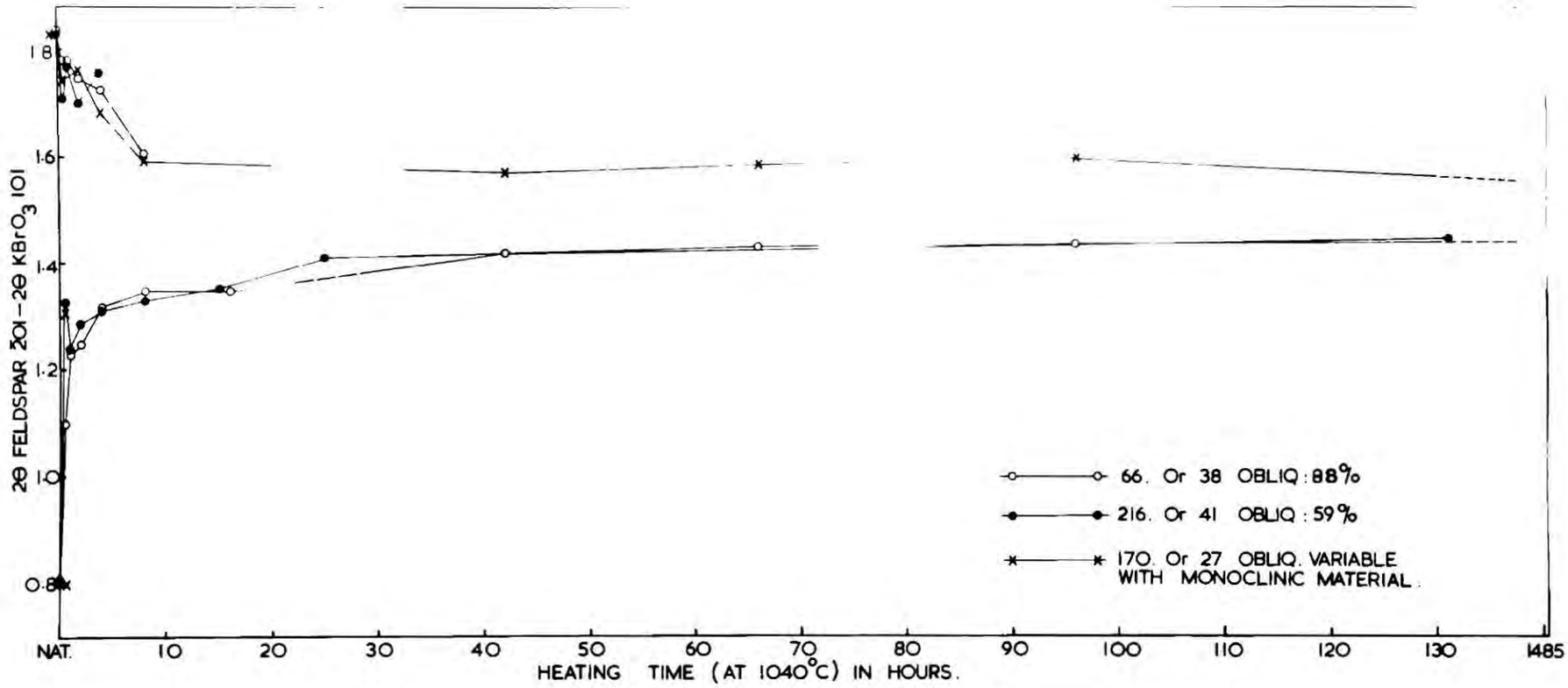
2θ FELDSPAR $\bar{2}01$ – 2θ $KBrO_3$ 101
1·8
1·6
1·4
1·2
1·0
0·8
NAT.
10
20
30
40
50
60
70
80
90
100
110
120
130
1485
HEATING TIME (AT 1040°C) IN HOURS.
66. Or 38 OBLIQ : 88%
216. Or 41 OBLIQ : 59%
170. Or 27 OBLIQ. VARIABLE WITH MONOCLINIC MATERIAL.

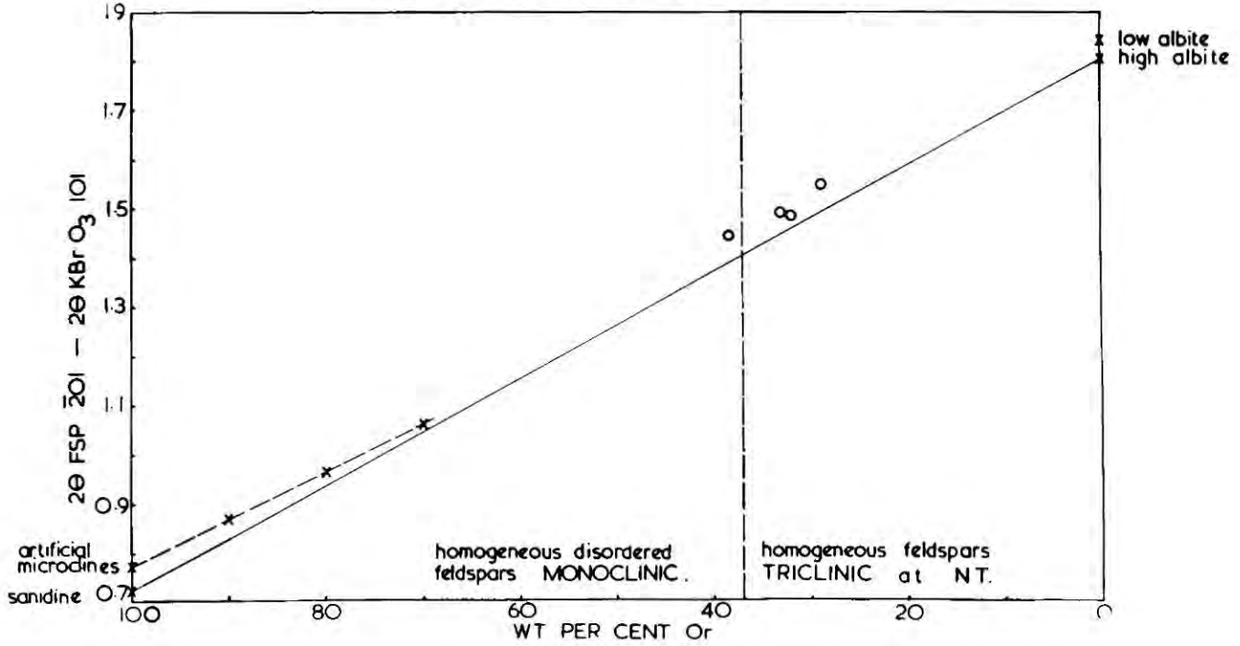
2θ FSP $\bar{2}01$ – 2θ $KBr\,O_3$ 101
1·9
1·7
1·5
1·3
1·1
0·9
0·7
low albite
high albite
artificial microclines
sanidine
homogeneous disordered feldspars MONOCLINIC.
homogeneous feldspars TRICLINIC at N.T.
100
80
60
40
20
0
WT PER CENT Or

Fig.5.29.

Change in form of diffractometer patterns between 20° and 32° 2θ for two feldspars, 170 and 66., after different heating periods.

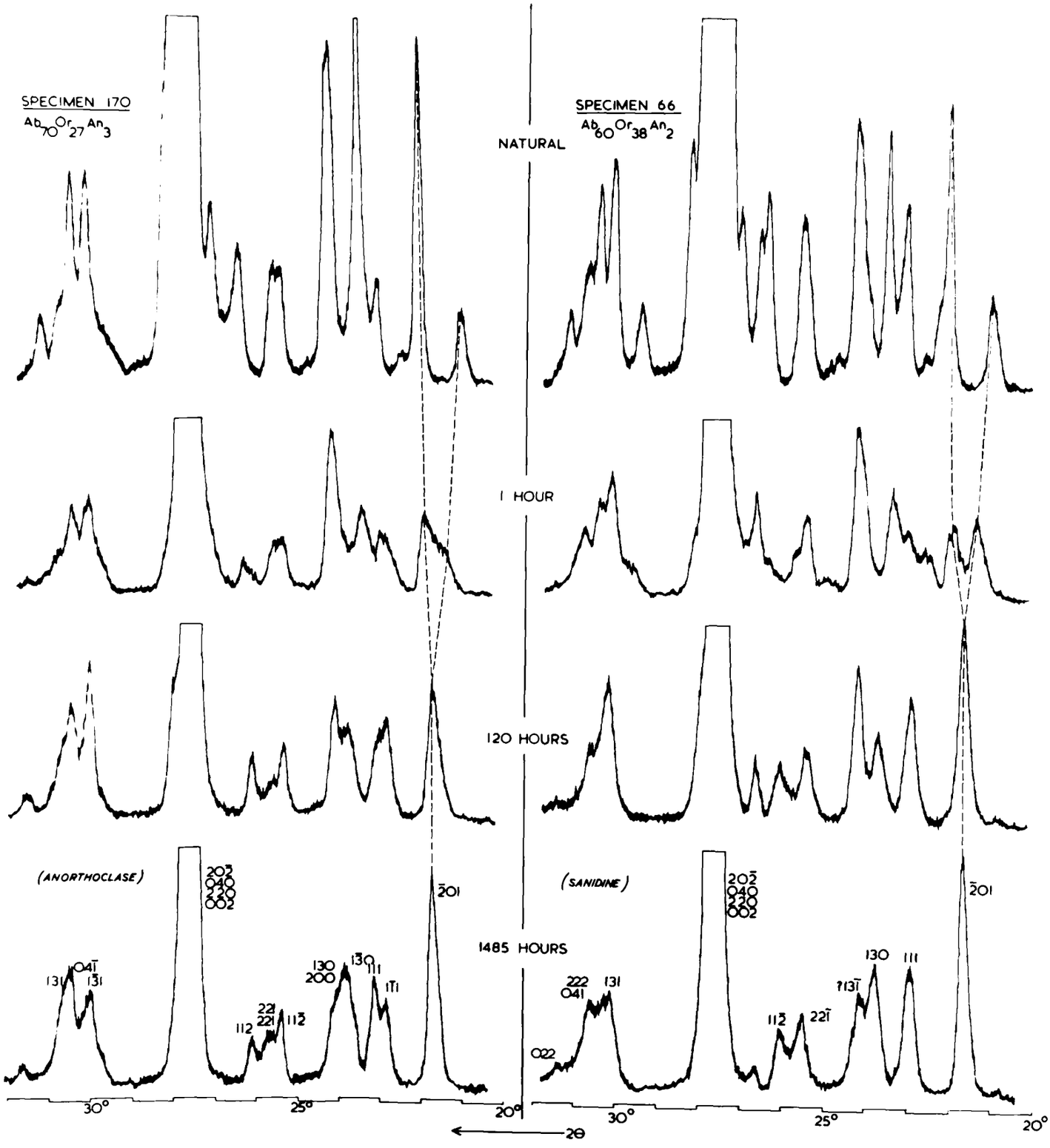
SPECIMEN 170
$Ab_{70}Or_{27}An_3$
SPECIMEN 66
$Ab_{60}Or_{38}An_2$
NATURAL
1 HOUR
120 HOURS
1485 HOURS
(ANORTHOCLASE)
(SANIDINE)
$20\bar{3}$ 040 220 002
$\bar{2}01$
$04\bar{1}$
131
$13\bar{1}$
112
221
$22\bar{1}$
$11\bar{2}$
130
200
$1\bar{3}0$
111
$1\bar{1}1$
022
222
041
$?13\bar{1}$
$22\bar{1}$
30°
25°
20°
2θ

disordered feldspars (at room temperature) begin to deviate from monoclinic symmetry with increasing Na content. MacKenzie (1952) used the splitting of the 111/1$\bar{1}$1 doublet to trace the change in composition of this symmetry change with temperature and Donnay and Donnay (1952) give figures for 111/1$\bar{1}$1 at room temperature.

In fig. 5.30 (above) the 111 and 1$\bar{1}$1 reflections are shown for the four L. Ailsh feldspars heated for a long period. The development of a doublet as soda content increases is clear. Specimen 21b is not resolved into two reflections as is specimen 24 which has very similar composition. This may imply that the chemical analysis is in error, although it can be seen that the peak has a rather lower height - breadth ratio than specimen 66 which might suggest a small departure from monoclinic symmetry. The other specimens all show excellent agreement with Donnay and Donnay's data shown in fig. 5.30 (below). This X-ray method appears to give values consistently high in Or (by 2% app. - compare the 20$\bar{1}$ method which gave values high in Ab). The effect of the small amount of Ca in the L. Ailsh specimens must be remembered, however.

The observations of Schneider (1957) and Brown (1960) that the displacive sanidine-anorthoclase transformation may not be strictly non-quenchable and that protracted heating may allow the preservation of the high forms (e.g. monoclinic albite) at room temperature are not apparent here, the composition at which the displacive inversion occurs fitting well that established by MacKenzie and Donnay and Donnay within the limited amount of experimental work attempted by the writer.

Discussion.

The conflicting evidence of two X-ray methods of determining bulk composition with each other and with the figures determined by wet methods suggests that the X-ray techniques are poor substitutes for flame photometer determinations of feldspar compositions. The differing responses of feldspars to heat treatment and the long heating time necessary before the X-ray patterns cease to change, coupled with the complication discovered by Schneider all seem to make the X-ray methods unsuitable, although Schneider's observations may not be so important in practice since fit with natural specimens and with heated specimens such as this small number of L. Ailsh specimens seems to be good as far as the

Fig. 5. 30.

ABOVE: Detail of the 111 and $1\bar{1}1$ reflections of four feldspars heated at 1040° for two months together with their bulk compositions.

BELOW: 2Θ values of 111 and $1\bar{1}1$ reflections of the same four heated specimens plotted against composition and compared to the 2Θ values of Donnay and Donnay (1952) determined on artificial specimens.

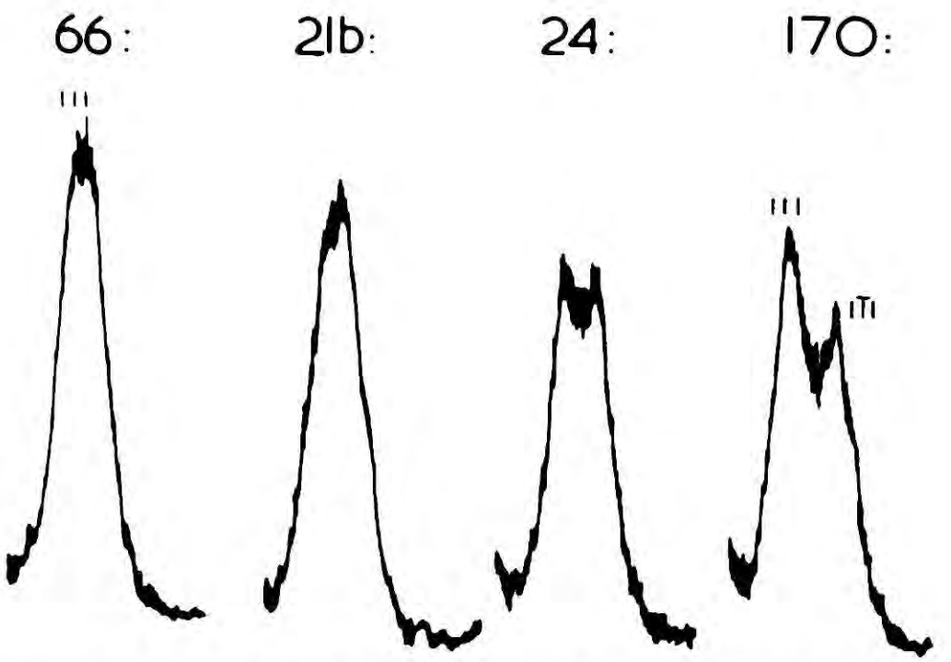

	60	65·5	66	70·5 Ab.
wt.%	1·5	2	2	2·5 An.
	38·5	32·5	32	27 Or.

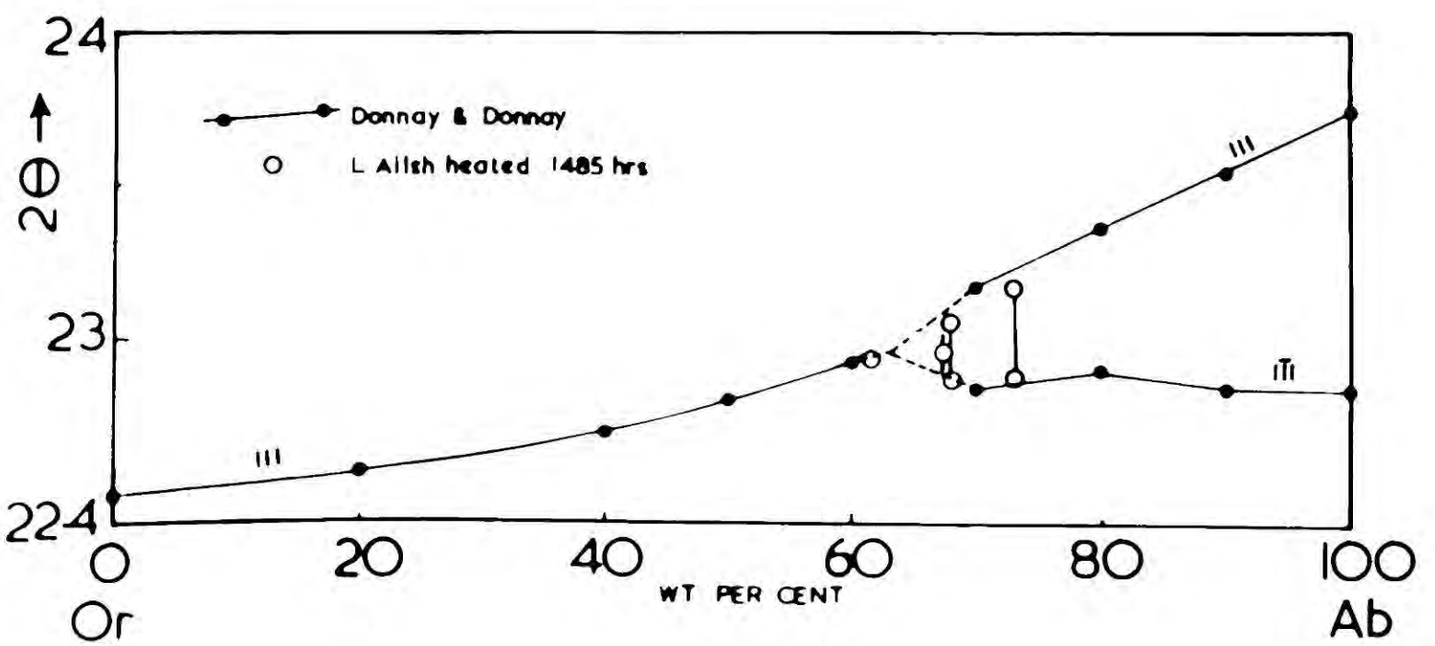

111/1$\bar{1}$1 reflections are concerned.

The initial rate of homogenization as seen by movement of the 20$\bar{1}$ reflections, is high. The reason for the different behaviour of the $\bar{2}$01 reflections (Fig. 5.27) is not known. It could be related to the bulk composition in which case the change in behaviour must come very close to the composition (Or_{37}) of the sanidine-anorthoclase displacive transformation at room temperature, or to the top of the solvus or it could be due to the initial differences in thermal states as shown by the nature of the K-phases. Further experimental work is clearly required.

Table 5.10.

Data for fig. 5.30 (below).

	Donnay and Donnay (1952)			Loch Ailsh			
	2θ			%	2θ		
Ab%	111	1$\bar{1}$1	Specimen	Ab+An	111	1$\bar{1}$1
0	22.5					
20	22.57					
40	22.70					
50	22.80					
60	22.92		66	61.5	22.935	-
65	22.94		21b	67.5	22.955	-
66	22.95	22.84	24	68	23.055	22.865
70	23.17	22.84	170	73	23.17	22.87
80	23.36	22.80				
90	23.54	22.84				
100	23.74	22.84				

On the diagram the inception of triclinic symmetry is taken at Ab_{63}, the figure determined by MacKenzie, and Donnay and Donnay's values in this region are omitted.

Table ..11.

2θ Values for Hea... ...ch Ailsh Feldspars.

(Heated 1485 hrs. at 1040°C).
(Compare with Donnay and Donnay, 1952).

hkl	2θ obs.	q	hkl	2θ obs.	q
$\bar{2}01$	21.755	6	$\bar{2}01$	21.685	6
$1\bar{1}1$	22.87	2	$1\bar{1}1$	22.865	2
111	23.17	2	111	23.055	
$1\bar{3}0$			$1\bar{3}0$	23.755	
200	23.7 to 24.25	3	200	to	3
130			130	24.105	
$22\bar{1}$	25.54	1	$22\bar{1}$	25.435	1
$2\bar{2}\bar{1}$			$2\bar{2}\bar{1}$		
$11\bar{2}$	to		$11\bar{2}$	to	
$1\bar{1}\bar{2}$	26.18	1	$1\bar{1}\bar{2}$	26.075	1
040			040		
202			202		
002	27.7	10+	002	27.625	10+
220			220		
$1\bar{3}1$	30.07	2	$1\bar{3}1$	29.835	2
$04\bar{1}$	30.55	3	$04\bar{1}$	30.075	2
131			131	30.535	2

Specimen 170

(Ab + An 73, Or 27)

Specimen 24

(Ab + An 68, Or 32)

Table 5.11 cont.

hkl	2θ	q
$\bar{2}01$	21.695	5
111, $1\bar{1}1$	22.955	3
$1\bar{3}0$, 200, 130	23.76 and 24.205	3
$22\bar{1}$, $2\bar{2}\bar{1}$, $11\bar{2}$, $1\bar{1}\bar{2}$	25.435	1
	26.1	<1
040, $20\bar{2}$, 002, 220	27.645	10+
$1\bar{3}1$	30.155	2
$04\bar{1}$, 131?	30.585	

Specimen 21b

(Ab + An 67, Or 33).

hkl	2θ	q
$\bar{2}01$	21.645	6
111	22.935	3
130	23.785	3
200	24.12	3
$22\bar{1}$, $11\bar{2}$	25.495	1?
$1\bar{1}\bar{2}$	26.05	1?
040, $20\bar{2}$, 002, 220	27.74	10+
131, $22\bar{2}$, 041, 021	30.15 to 30.65	3

Specimen 66

(Ab + An 61.5, Or 38.5).

CHAPTER 6.

GENERAL CONCLUSIONS.

Contents:

Introduction.

In this chapter an attempt is made to summarize the more important conclusions arrived at in previous chapters and to present some sort of coherent picture of the genesis and structural relationships of the rock types. There will, of necessity, be a certain amount of repetition of points made in previous chapters.

Section 1.

Structure of the Mass.

A) General considerations.

In this section data from Chapters 2 and 3 must be brought together. The following generalizations can be made:

(a) There are at least two generations of leucocratic syenite, and at their contacts the earlier (designated S1 and S2) is enclosed in the later (S3) both as xenoliths, and, when broken down, as xenocrysts.

This relationship can be demonstrated around all the S1/2-S3 contacts. The later syenite also veins the earlier for a considerable distance from the contact. Occasionally large xenoliths of S1/2 are held in S3 at a substantial distance from the main mass, and xenocryst bearing types of S3 make up a substantial area of the mass.

(b) S3 always overlies S1 or S2, the former having a demonstrably domal form on Sail an Ruathair North Top, and the latter also having an undulating top in the R. Oykel-Black Rock Burn areas.

(c) In the southern part of the mass a zone of variable basic alkaline rocks occurs xenolithically near the junction of S2 and S 3(see fig. 2.13) and occurs in diminishing amount downwards into S2, and not up into S3. The xenolithic masses contain two generations of feldspathic veins.

(d) The largely xenocryst bearing S3 of the Metamorphic Burn contains frequent xenoliths of an undisturbed Cambrian succession from the Pipe Rock to some distance into the limestone. Limestone xenoliths occur at numerous other localities in Coire Sail an Ruathair. They have also been found in the Black Rock Burn.

(e) The biotite-pyroxenites and hornblendites exposed in the Allt Cathair Bhan area are a steeply inclined sheet, veined by leuco-syenite and occur along the contact between syenite and Durness limestone. To the east the limestone is metamorphosed to calc-silicate rocks exactly comparable with those to the north, into which feldspathic veins also extend. To the west, lenses of Cathair Bhàn-type pyroxenites are held in the syenite.

(f) Within this leuco-syenite-pyroxenite belt occur rocks like those of the Sròn Sgàile mass. This rock is most basic in its most easterly

and lowest extension, but has no large magnetic anomaly associated with it.

(g) The melanite bearing syenite in the centre of the intrusion carries S2 xenocrysts in part, but its angular relationships to the surrounding syenites are obscure.

(h) The broad contact relationship of syenite to country rock remains obscure. In the Cathair Bhàn area the contact is vertical or steeply inclined away from the intrusion. On Sgonnan Beag it appears to be partially a thrusted contact, but may otherwise be steep. On the north side of Black Rock, the contact can be traced in a general way down to the Oykel and is roughly vertical. On the opposite side of the valley, on the Sail an Ruathair ridge, it is at a low angle. In the Metamorphic Burn the syenite tongues into sediment. In general, however, it seems that the intrusion can best be represented by a simple, stock-like body, extending to unknown depth.

B) Conclusions; discussion of sections.

On the basis of the considerations outlined above two sections are appended to Map 1. Thrusts are omitted unless the presence of some definite structural feature has been established by the thrusting.

The basic alkaline types are seen to form a discontinuous roof to the undulating surface of S2. The form of the melanite bearing body of the S. Top, Sail an Ruathair, has been intentionally left obscure since the question of whether it owes its melanite to processes taking place below (and thus could be a plug) or to contamination from above, is not resolved.

S1 and S2 are shown in forming a continuous mass at depth; the feldspar data suggests that they have true differences in cooling history which may imply an intrusive relationship to one another, but they could

merely be different facies of the same intrusion.

S3 forms a comparatively thin sheet above S1/2 but the depth to the base of the earlier portions of the intrusion cannot be predicted.

The Allt Cathair Bhàn ultrabasic rocks are shown to be a steeply inclined or vertical sheet veined by syenite, extending to the top of the quartzite, although masses within the syenite may have deeper bases if stoping has occurred, and this is indicated on Section AA'.

Section 2.

Petrogenesis.

a) Leuco-syenites.

Little that has an observational basis can be added to previous ideas of the derivation of the alkaline magma responsible for the main rocks of the intrusion, or, for that matter, the other alkaline masses of the N.W. Highlands. Any hypothesis pertaining to the rocks of any one of these intrusions must take into account relationships observed in the other alkaline plutons, as well as the extensive suite of minor alkaline intrusions present throughout the district. It can hardly be doubted that such a suite of otherwise unusual rocks, of approximately the same age, had, if not a common source at depth, at least closely comparable environments for their development.

The main leuco-syenites were intruded already differentiated into two, if not three, phases. If the assimilation of limestone and consequent desilication of an acid magma type led to the alkaline nature of the rocks, the process of assimilation has been singularly complete and implies an elaborate system of circulation and differentiation at depth, to give rise to the alkaline plutons and the very widespread alkaline dykes.

The writer can thus only echo the statement of Phemister (1926) that: "the alkaline character of the Loch Ailsh mass is original and independent of its contiguity to dolomite." No deductions can be made from the observed rocks of the probable petrogenic process at depth, except to observe that the vast bulk of the rock of the mass has a composition approximating to and trending towards the minimum melting composition in the system $KAlSi_3O_8$-$NaAlSi_3O_8$. Since this composition corresponds very closely to the bulk composition of the rock of the mass as a whole (the basic types being contaminated rocks) some sort of liquid-crystal differentiation process leading to a feldspathic residuum at the minimum of the alkali feldspar system is implied.

From the data obtained from the feldspars it was deduced that the feldspathic rocks must have been intruded at less than 2000 bars water vapour pressure (corresponding to a depth of about 7.5 kms.) and at more than 800°C. If pressure remained constant throughout the crystallization interval the leuco-syenites must have begun crystallization over a narrow range of temperature of about 50°C, S3 being the last and lowest temperature type to crystallize.

The evidence from the subsolvus variation seen in the feldspars is that S3 was wetter than S2 and in turn S1. All rocks in the apophysal Metamorphic Burn region show evidence for concentration of volatiles.

The feldspars present a problem in themselves, however, since the S1/2 feldspars incorporated in S3 preserve the features they adopted during the cooling history of S1/2 rather than adopting (as might be expected) the crystal structure of the feldspars of the enclosing S3.

The origin of the melanite in some of the varieties of S3 remains obscure. There is no doubt that melanite is produced near xenolithic

limestone in the Metamorphic Burn area. The melanite of the South Top, Sail an Ruathair, appears to have only a slightly different cell size, but lacks the colour zoning of the Metamorphic Burn examples. It is also associated with dark aegirine and sphene.

The lack of colour zonation could be attributed to prolonged heating and thus homogenization of the types in the massive syenite. However, if they had developed as a result of contamination of the syenite by limestone material the distribution has been singularly even, and there is no sign of concentration towards the top as might be expected if the melanite was sinking into the syenite from a roof of limestone. The melanite at this locality is in fact further from any signs of contamination than any other part of the mass, and represents the thickest vertical section of syenite seen.

Most of the evidence points to the melanite having originated at depth, but one cannot hazard a mechanism by which this might have occurred, unless by analogy with the development at limestone contacts, it involves the presence of carbonatite at depth.

If this is so then the pipe hypothesis of Phemister (1926) is correct and it could be a feeder for the whole of S3.

Most of the features of the perthites described are independent of the Caledonian deformation, but certain special features can be ascribed to this period of the history of the mass. Potassium metasomatism has been described in crush belts.

b) Basic alkaline types (Hybrids).

In the Metamorphic Burn, rocks identical with the basic alkaline types occurring in the R. Oykel are found and all stages between calc-silicate rocks obviously originating from the metamorphism of limestone,

feldspathized derivatives, and contaminated leuco-syenites are seen.

The discovery of limestone xenoliths in the Black Rock Burn at the horizon of basic alkaline xenoliths lends support to the hypothesis that this suite of basic rocks represents a mixture of material of syenitic and metamorphosed-limestone origin.

The "synneusis" texture of Phemister (1926), rather than demonstrating the development of diopsidic clots by a process of aggregation under surface tension forces, illustrates stages in the breakdown of the granular texture so characteristic of diopside rocks originating from the metamorphism of limestone. Certain cell dimensions of pyroxenes from both metamorphosed limestone and the basic types are identical.

The basic rocks in the southern part of the mass were demonstrated to form a discontinuous roof zone on S2. They can now be seen to represent the partially assimilated remains of the contact metamorphic rocks produced when S2 was intruded into the limestone.

c) Ultrabasic rocks of Cathair Bhàn.

The ultrabasic mass of Cathair Bhàn is a steep sheet between syenite and limestone (the latter metamorphosed to diopside and forsterite marbles). Two possibilities exist; either it is an intrusive dyke or it is a skarn assemblage.

The latter is undoubtedly suggested by the structural setting, the way the ultrabasic rocks follow exactly the syenite-limestone boundary and the presence of ultrabasic pods within the leuco-syenites.

Diagram 4.13 illustrates that chemically its composition lies rather close to that of an impure dolomite from the Fucoid Bed. Adoption of alkalis, alumina and iron is required to develop the present composition. All these constituents could be contributed by the intrusion.

If it is an intrusive mass it has no affinities whatever with other rocks of the intrusion since the hybrid origin of the basic xenoliths has been demonstrated. It is unclear which syenite is in contact with the ultrabasic sheet, but at least in part it appears to be S1/S2. The ultrabasic rocks would thus be the earliest phase of the intrusion. It thus seems unlikely that the massive leuco-syenite should have been intruded only to the W. of the sheet, and that only feldspathic veins extend through the sheet and into the limestone.

It appears therefore that both the structural and chemical evidence points to these rocks as being a reaction skarn walling the syenite at its steep contact with limestone. Perhaps the different nature of the Allt Cathair Bhàn rocks and the basic hybrid types is related to the walling relationship of the former and the roofing relationship of the latter.

d) Sròn Sgàile rocks.

These rocks are believed to represent a facies of the hybrids intermediate both spatially and mineralogically between the Cathair Bhàn types and the Oykel - Black Rock Burn types. The pyroxene rich part of the Sròn Sgàile mass is its lowest and most easterly extension, but the absence of a large magnetic anomaly shows that the Cathair Bhàn types do not connect with it. It must be observed that the Sròn Sgàile rocks lie at the level of limestone xenoliths in S1 which outcrop to the west.

Section 3.

Summary of the Igneous History of the Mass.

1) Development by an undefined process at depth of a very feldspathic magma, and differentiation into a somewhat more sodic and mafic phase (S1/2) and a somewhat more potassic and ultra-leucocratic phase (S3).

2) Intrusion of S1 and S2, either representing different facies of

a single intrusion or two intrusions with S1 presumably the earlier. The intrusion took place upwards into the lower part of the Durness limestone only, and limestone fragments are held as xenoliths in both rocks. Contamination of syenite with calc-silicate material near the top of the intrusion produced intermediate and basic hybrid rocks. A thick reaction skarn was produced along the eastern margin of the intrusion.

3) A late phase of this intrusion produced the early veinlets observed in the Oykel and Black Rock Burn hybrid rocks.

4) Intrusion, largely roofing S1/2, of the exceedingly leucocratic differentiate, S3. This veined S1 and S2, and caught up xenoliths, sometimes as substantial screens, and xenocrysts, from the earlier rocks. Limestone xenoliths and resultant hybrid types were incorporated. The S3 material, often with considerable xenocrystic S1-2 material,veined the pre-existing hybrids of the Black Rock and R. Oykel, and also the ultrabasic Cathair Bhàn rocks.

It is possible that the latest part of the S3 intrusion contained melanite developed at depth, and if this is the case the S3 intrusion was largely injected through a pipe below the South Top, Sail an Ruathair.

5) Injection of minor intrusions (not described; some may pre-date S3).

6) Injection of quartz veins.

7) Potash metasomatism along crush belts during or subsequent to the Caledonian orogeny.

Mode of emplacement and form of the body.

It will be seen from Map 1 that there is a tendency, both in Coire Sail an Ruathair and in the Black Rock Burn for limestone xenoliths to be held at topographic levels well below outcrops of quartzite on the

surrounding hills. It suggests that stoping took place and that xenoliths were able to sink into the intruding magma.

The relationship of S3 to S1/2 suggests that it was intruded as a sheet between S1 and S2 and the present top of the intrusion. The Metamorphic Burn area may be near to the roof of the intrusion.

No data can be suggested as to the depth of the base of S1/S2, since the geophysical data are not critical enough to allow an estimate of depth to base beyond very shallow depths and in any case it would be expected that the magnetic skarn rocks would have their base at the top of the quartzite and would not extend to the base of the intrusion. The possibility that the base of the Allt Cathair Bhàn ultrabasic rocks is nearer the surface at their southern end was mentioned in Chapter 3, section 3.

Although a stock-like mass has been postulated this is largely on the grounds that some contacts appear to be steep, and no suggestion of a base is ever seen. A shallow cylindrical form cannot be discounted.

Bibliography to Chapter 6.

PHEMISTER, J., 1926. in 'The Geology of Strath Oykel and Lower L. Shin.' Mem. Geol. Surv. Scotland. (Explanation of sheet 102).

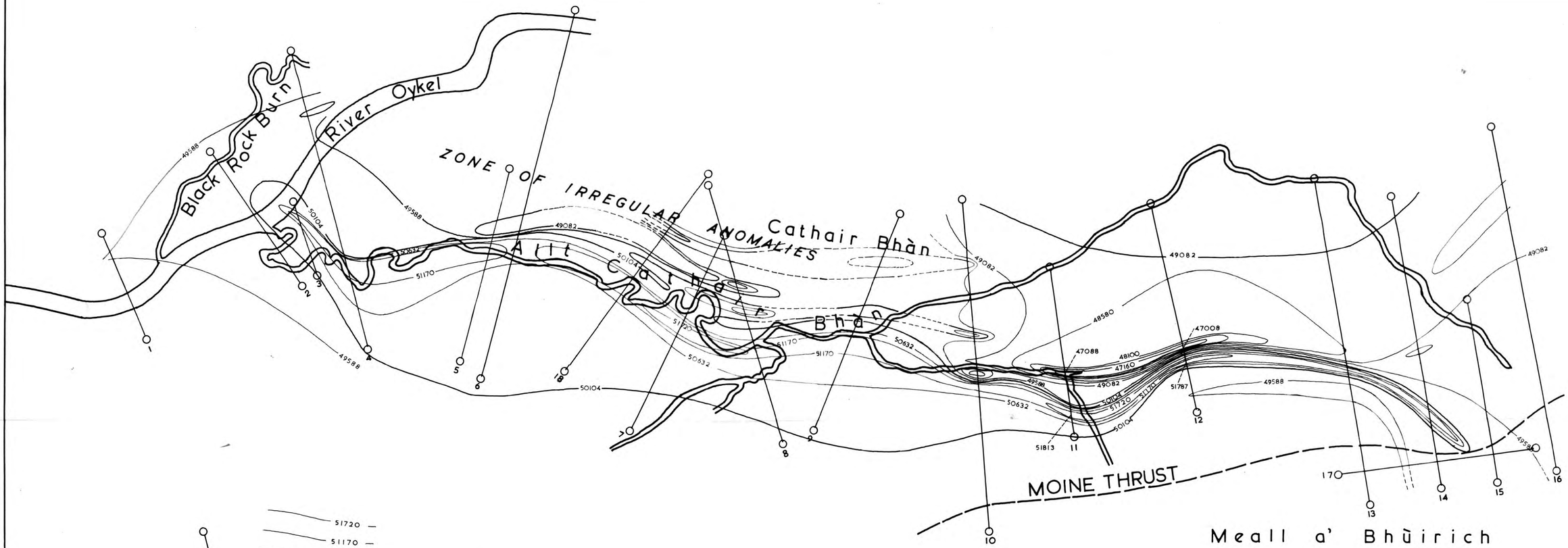

Profiles

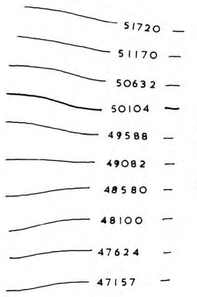

Contour interval 500
magnetometer scale units
plotted as GAMMA equivalent

N

ALLT CATHAIR BHÀN
TOTAL MAGNETIC INTENSITY.

1 GAMMA = 10^{-5} OERSTED

0 MILES 1/4

0 500 1000
METRES

I. PARSONS, 1963.

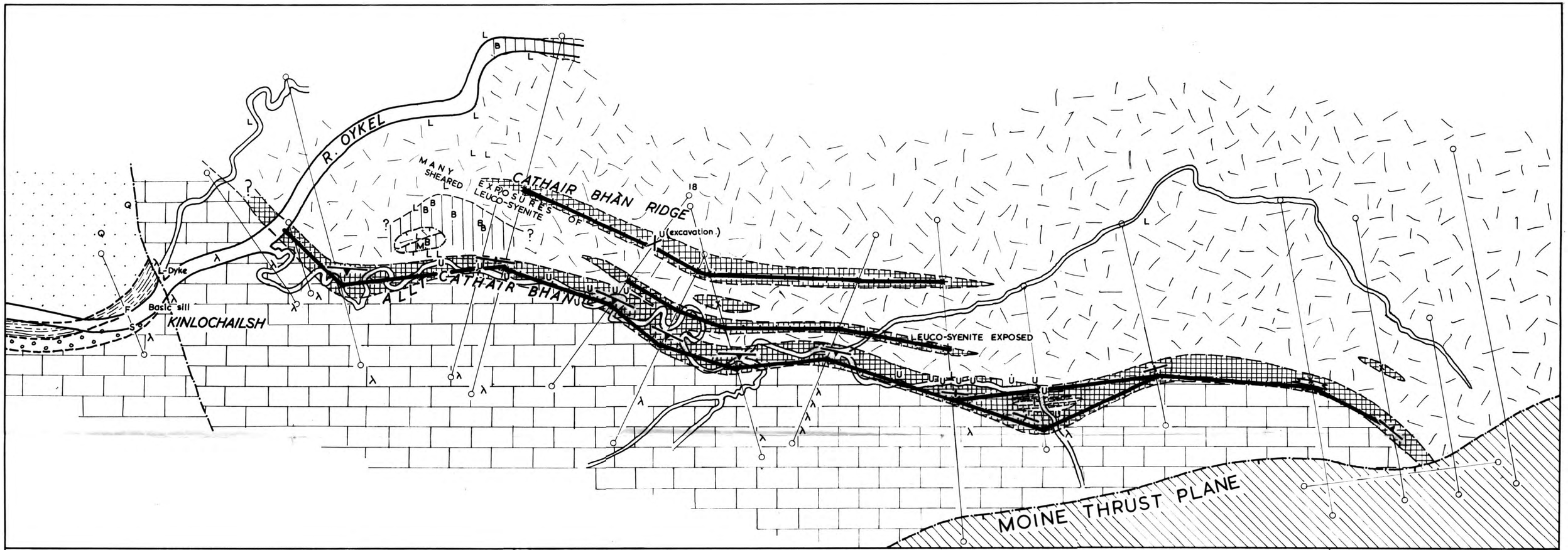

Profiles.

Line joining maxima of magnetic anomalies.

Leuco-syenite. (L).

Basic syenites. (B).

Ultrabasics. (U).

Durness limestone. (λ).

Serpulite grit. (S).

Fucoid bed. (F).

Quartzite. (Q).

Moine.

M = Mylonite.

MLS. 1/4

KMS. 1/2

Symbols for rock types indicate exposures.

GEOLOGICAL MAP OF ALLT CATHAIR BHÀN AREA DERIVED FROM EXPOSURES AND MAGNETIC DATA.

Ultrabasic body vertical.

" " steeply dipping.

I. PARSONS, 1963.

GEOLOGY OF THE LOCH AILSH COMPLEX

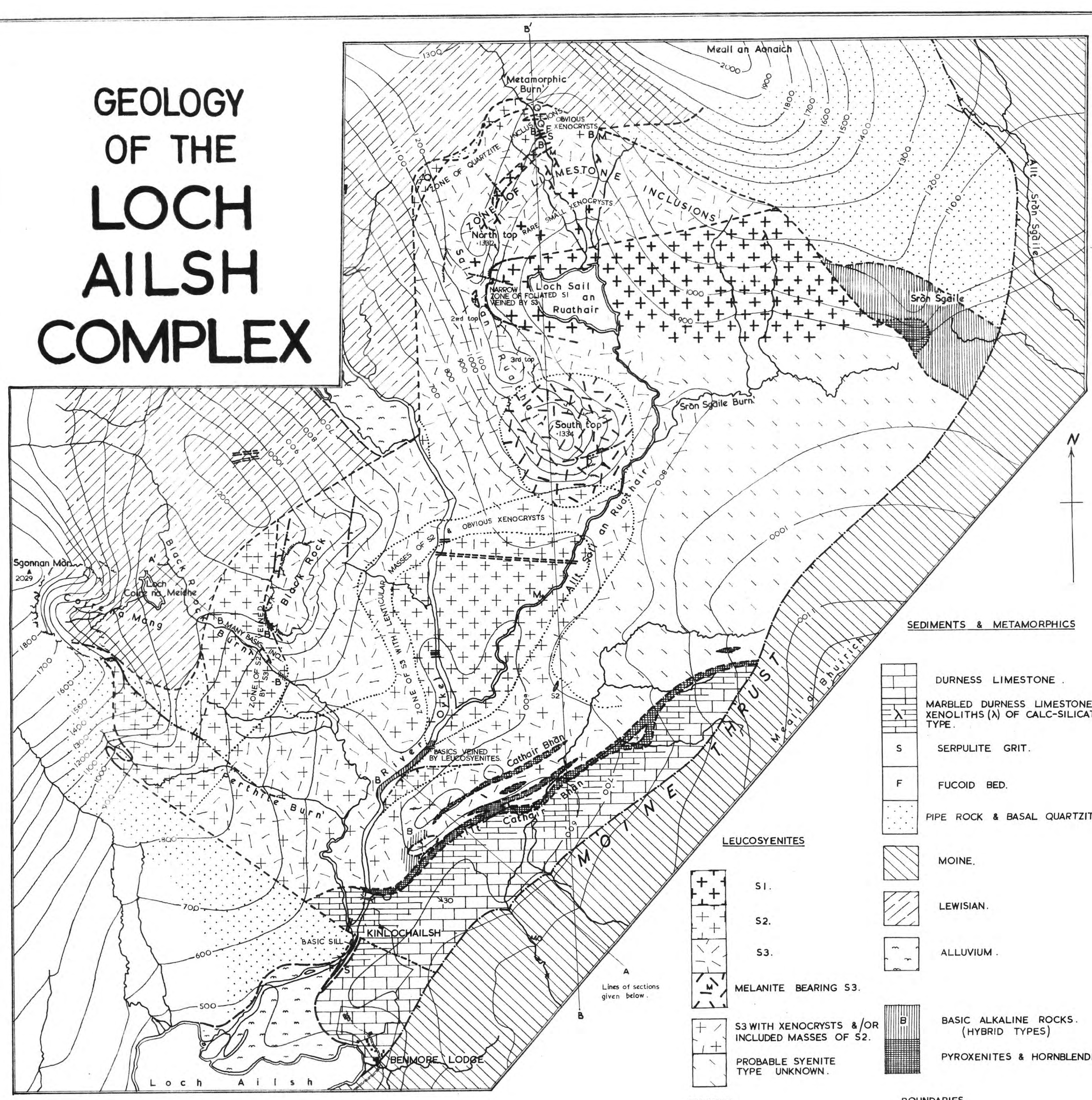

I. PARSONS, 1963